

FLUX ENHANCEMENT USING FLOW DESTABILIZATION IN CAPILLARY MEMBRANE ULTRAFILTRATION

Jacobus Petrus Botes



Thesis presented in partial fulfilment of the requirements for the degree of Master of Chemical Engineering at the University of Stellenbosch.

Study Leaders:

S. M. Bradshaw

E. P. Jacobs

December 2000

Declaration

I, the undersigned, hereby declare that the work contained in this thesis is my own original work and has not previously in its entirety or in part been submitted at any university for a degree.

Summary

The aim of the thesis was to investigate the use of flow destabilization methods, combined with permeate backflushing (B/F) or on their own, on flux recovery and maintenance in capillary UF membrane systems under cross-flow (XF) and dead-end (DE) operating conditions. Various hydraulic and mechanical methods have been used to remove the accumulated cake layer and improve steady state process flux. Permeate backflushing (B/F) is the most widely used but the drawbacks are loss of product and extensive down-time. In a pilot plant study for ultrafiltration of surface waters containing high NOM, turbidity and cation loads, the use of flow destabilization, or feed flow reversal (FFR) combined with cross-flow B/F was able to improve the normalised flux by 10.7 ± 3.4 %, compared with 3.2 ± 1.6 % improvement for B/F without FFR. When a second B/F included FFR, the flux improvement was 7.0 ± 2.0 % compared with 4.3 ± 2.5 % for a B/F without FFR. The hypothesis was proposed that the flow destabilization caused slight lifting of the oriented cake layer, while the cross-flow B/F was able to sweep the lifted cake out of the lumen. If the flow destabilization may be effected by a simple but effective and low-cost method, and if this flow destabilization may be combined with reverse flow for short durations, the "lift-and-sweep" approach will be the ideal method of maintaining process flux and increasing membrane life. Such a flow destabilization method, now named "reverse-pressure pulsing" (R/P), was developed. The method involves circulation of feed water in a recycle loop for 2 s to gain momentum, followed by closure of a fast-action valve upstream of the modules. The momentum of the water in the concentrate loop carries it into an air-filled feed accumulator, while concentrate and reverse-flow permeate (which also lifts the fouling layer) are discharged to the atmosphere using the recycle pump for 15 s. When the valve opens again, the air in the accumulator forces the water under pressure through the membrane lumens, causing a pressure pulse and flow perturbations that lift, shift and break up the fouling layer. During 3 such "lift-and-sweep" events, the cake is lifted and the debris is swept out of the lumen. Experimental results for uninterrupted dead-end filtration at a UF pilot plant using R/P only on a severely fouled membrane, indicated that the R/P increased the flux by 18.4 % and decreased the dP by 8.2 % over a 7.2 h period. The method is effective in removing the cake layer intermittently and no long-term flux decline occurred for a period of 555 h since the previous chemical cleaning.

Opsomming

Die doel van die tesis was om die gebruik van vloeï-destabiliserings metodes, alleen of gekombineer met permeaat-terugwas, op vloed-herwinning en instandhouding in kapillêre UF membraan-stelsels tydens kruisvloeï en doodloop bedryf, te ondersoek. Verskeie meganiese en hidrouliese metodes word gebruik in membraan stelsels om die koeklaag op die membraan se oppervlak te verwyder en die gestadigde-toestand vloed te verbeter. Van hierdie metodes word permeaat-terugwas die meeste gebruik, maar het sy nadele insluitend verlies van produk en produksietyd. In 'n loodsstudie vir die ultrafiltrasie van oppervlakwaters wat hoë beladings NOM, turbiditeit en katione bevat, is die waarneming gemaak dat kruisvloeï terugwas met vloeï-destabilisering (voerrigting-verandering) die genormaliseerde vloed met 10.7 ± 3.4 % kon verbeter, vergeleke met 'n 3.2 ± 1.6 % verbetering sonder voerrigting-verandering. Vir 'n tweede terugwas was die verbetering 7.0 ± 2.0 % vergeleke met 4.3 ± 2.5 % sonder voerrigting-verandering. Die hipotese was voorgestel dat die vloeï-destabilisering die geoiënteerde koeklaag van die oppervlak gelig het, en die kruisvloeï terugwas die geligde koeklaag uit die lumen kon vee. Indien hierdie vloeï-destabilisering bewerk kan word deur 'n eenvoudige maar effektiewe manier, en indien dit gekombineer kan word met terugvloeï van produk vir kort tydperke, sal hierdie "lig-en-vee" benadering die ideale metode wees om die membrane se vloed te verbeter en leeftyd te verleng. So 'n vloeï-destabiliseringsmetode, nou genoem "terugdruk-pulsering", is ontwikkel. Die metode behels die sirkulering van voer-water vir 2 s in 'n hersirkulasielus om momentum op te bou, gevolg deur die toemaak van 'n snel-aksie klep stroom-op van die modules. Die water in die konsentraat-lus se momentum dra dit vorentoe tot in 'n lug-ge vulde voer-akkumulator, terwyl konsentraat en terug-vloeï permeaat (wat ook tot 'n mate die koeklaag lig) ook na die atmosfeer gewend word vir 15 s deur die hersirkulasiepomp. As die klep weer oopgaan, ontspan die lug in die akkumulator, en forseer die water daarin onder druk deur die membraan-lumens. Die druk-puls en vloeï-perturbasies lig, skuif en breek die koeklaag op. Tydens 3 agtereenvolgende "lig-en-vee" aksies word die koeklaag effektief opgebreek en uit die lumen gevee. Eksperimentele uitslae vir ononderbroke doodloop bedryf op uitermate aangevulde membrane van 'n ultrafiltrasie loodsaanleg toegerus met terugdruk-pulsering, het getoon dat die vloed met 18.4 % verbeter kon word en die dP met 8.2 % verminder kon word in slegs 7.2 h. Die metode breek die koeklaag effektief op, en geen langtermyn vloed-afname is waargeneem vir meer as 555 h sedert die vorige chemiese was-prosedure nie.

Acknowledgements

Ed Jacobs

for his dedication to the advancement of membrane technology in South Africa, his assistance during this project as well as in the preparation of this document, and for always having a sympathetic ear for students in need of assistance.

Steven Bradshaw

for his willingness to act as supervisor, his patience and valuable advice throughout the project as well as in the preparation of this document.

The Stellenbosch Municipality

for allowing the Paradyskloof pilot project to continue on-site from 1998 till the present.

Spier Home Farms, Stellenbosch

for allowing the Mon Villa pilot project to continue on-site until decommissioning in 1999.

The Water Research Commission

for their major sponsorship of the project.

Technical personnel

at the Institute for Polymer Science and the Department of Chemical Engineering, University of Stellenbosch, for their willingness to provide assistance promptly.

My family and friends

for their continued moral support through trying times.

Ingrid

for her love and support, and her faith in me.

Table of Contents

Chapter 1 : INTRODUCTION	1-1
1.1 MEMBRANE FILTRATION OPERATIONS	1-1
<i>1.1.1 Definitions and Characteristics</i>	<i>1-1</i>
<i>1.1.2 Process Equipment for Membrane Operations</i>	<i>1-3</i>
1.2 UF LIMITATIONS AND FLUX ENHANCEMENT	1-4
1.3 AIMS OF THE THESIS	1-5
1.4 APPROACH OF THE THESIS	1-5
1.5 STRUCTURE OF THE THESIS	1-7
Chapter 2 : ULTRAFILTRATION PROCESSES	2-1
2.1 MEMBRANE PROCESS DEVELOPMENT	2-1
2.2 FILTER CLASSIFICATION	2-2
<i>2.2.1 Filter Type</i>	<i>2-2</i>
<i>2.2.2 Membrane Morphology</i>	<i>2-2</i>
2.2.2.1 Microporous Membranes	2-2
2.2.2.2 Asymmetric Membranes	2-3
<i>2.2.3 Hydrophilicity of the Membrane Surface</i>	<i>2-4</i>
2.3 MEMBRANE MANUFACTURE	2-5
<i>2.3.1 Material Selection</i>	<i>2-5</i>
<i>2.3.2 Membrane Formation by Phase Inversion</i>	<i>2-6</i>
<i>2.3.3 Membrane Geometries</i>	<i>2-6</i>
2.3.3.1 Capillary Membranes	2-6
2.3.3.2 Fabric-supported Tubular Membranes	2-7
2.3.3.3 Fabric-supported Flat-sheet Membranes	2-8
2.3.3.4 Unsupported Flat-sheet Membranes	2-8

2.4 MODULE DESIGN CONSIDERATIONS	2-8
2.4.1 Design Objectives	2-8
2.4.2 Definition of Module Parameters	2-9
2.4.3 Capillary Membrane Modules	2-11
2.4.4 Other Types of Modules	2-11
2.4.5 Summary of Module Types	2-12
2.5 UF MEMBRANE PERFORMANCE CHARACTERIZATION	2-13
2.5.1 Pore Size Distribution and Retentivity	2-13
2.5.1.1 The Bubble Point Technique	2-13
2.5.1.2 Direct Microscopic Observation	2-14
2.5.1.3 The Challenge (Solute Passage) Test	2-14
2.5.2 Effect of Operating Mode on Energy Consumption	2-15
2.5.2.1 Dead-end mode	2-15
2.5.2.2 Cross-flow mode	2-16
2.5.2.3 Theoretical Power Consumption in Steady UF	2-16
2.5.3 Boundary Layer Development and Flow Destabilization	2-18
2.5.3.1 Hydrodynamic Boundary layer	2-18
2.5.3.2 Mass transport boundary layer	2-20
2.5.3.3 Flow Destabilization	2-23
2.5.4 Limiting Flux	2-24
2.5.5 Temperature Dependency of Fluid Properties	2-26
2.5.5.1 Effect on Viscosity	2-26
2.5.5.2 Effect on Density	2-29
2.6 CONCLUSIONS	2-30
Chapter 3 : UF OF AQUEOUS SOLUTIONS	3-1
3.1 GUIDELINES FOR POTABLE WATER QUALITY	3-1
3.1.1 Microbial Quality and Indicator Organisms	3-1
3.1.2 Aesthetic Quality of Water	3-2
3.1.2.1 Turbidity	3-2
3.1.2.2 Colour	3-3
3.1.2.3 Taste and Odour	3-3

3.1.3 Water Quality Classification Systems	3-4
3.1.4 Natural Organic Material	3-6
3.1.4.1 Characterization and Structure	3-6
3.1.4.2 Effects of NOM on Potable Water Quality and UF	3-7
3.2 FOULING OF UF MEMBRANES	3-7
3.2.1 Concentration Polarization and Fouling Effects	3-8
3.2.2 Fouling Mechanisms	3-8
3.2.2.1 Adsorption	3-8
3.2.2.2 Aggregation	3-8
3.2.2.3 Pore Blocking	3-9
3.3 FLUX ENHANCEMENT STRATEGIES	3-9
3.3.1 Selection Criteria	3-9
3.3.2 Periodic Backflushing (Reverse Filtration)	3-10
3.3.2.1 Principle	3-10
3.3.2.2 Recent Work in the Field	3-10
3.3.2.3 Effectiveness of Different Backwash Media and Methods	3-11
3.3.3 Pulsatile Flow (Flow Destabilization)	3-11
3.3.3.1 Principle	3-11
3.3.3.2 Recent Work and Proposed Mechanisms	3-12
3.3.3.3 Viability of Existing Pulse Generators	3-13
3.3.4 Gas Sparging of the Feed	3-14
3.3.4.1 Recent Work in the Field	3-14
3.3.4.2 Effectiveness and Viability Considerations	3-15
3.3.5 Chemical Cleaning	3-16
3.4 CONCLUSIONS	3-17
Chapter 4 : CASE STUDY 1 - MON VILLA	4-1
4.1 INTRODUCTION	4-1
4.2 AIMS OF THE INVESTIGATION	4-2
4.3 SYSTEM DESCRIPTION	4-2
4.3.1 Membranes	4-2

4.3.2 Modules and Manifolding	4-4
4.3.3 Process Layout and Description	4-6
4.4 DATA COLLECTION AND ANALYSIS	4-8
4.5 EXPERIMENTAL	4-8
4.5.1 Automatic Operation and Backflush Procedure	4-8
4.5.2 Manual Operation and Backflush Procedure	4-10
4.5.3 Chemical Cleaning	4-12
4.6 RESULTS AND DISCUSSION	4-13
4.6.1 Process Flux Performance	4-13
4.6.2 Turbidity Reduction	4-14
4.6.3 Chemical Cleaning	4-15
4.6.4 System Operation in General	4-16
4.6.5 Backflush Operation with Feed Flow Reversal	4-16
4.6.5.1 Operating Range	4-16
4.6.5.2 Results of Fouling and Cake Layer Growth	4-17
4.6.5.3 Strategy for Assessing Backflushing Effectiveness	4-18
4.6.5.4 Visualisation of Backflush Effectiveness	4-21
4.6.5.5 Analysis of Variance	4-22
4.7 CONCLUSIONS	4-24
Chapter 5 : REVERSE-PRESSURE PULSE GENERATOR	5-1
5.1 INTRODUCTION	5-1
5.2 PRINCIPLE AND DESCRIPTION	5-1
5.2.1 Backflushing	5-1
5.2.2 Reverse-Pressure Pulsing without Simultaneous Venting	5-3
5.2.2.1 Two Pumps and Two Accumulators	5-3
5.2.2.2 One Pump and Two Accumulators	5-4
5.2.3 Reverse-Pressure Pulsing with Simultaneous Venting	5-6
5.2.3.1 Two Pumps, Two Accumulators and a Venting Line	5-6
5.2.3.2 One Pump, Two Accumulators and a Venting Line	5-7

5.3 CONCLUSIONS	5-9
Chapter 6 : CASE STUDY 2 - PARADYSKLOOF	6-1
6.1 INTRODUCTION	6-1
6.2 AIMS OF THE INVESTIGATION	6-2
6.3 SYSTEM DESCRIPTION	6-2
<i>6.3.1 Membranes and Modules</i>	<i>6-2</i>
<i>6.3.2 Process Layout and Description</i>	<i>6-3</i>
6.4 DATA ACQUISITION AND PROCESS CONTROL	6-7
<i>6.4.1 Hardware</i>	<i>6-7</i>
<i>6.4.2 Software</i>	<i>6-7</i>
6.5 EXPERIMENTAL	6-8
<i>6.5.1 General Procedures</i>	<i>6-8</i>
<i>6.5.2 R/P Without Simultaneous Venting of Product</i>	<i>6-10</i>
6.5.2.1 Experiments 1 to 4	6-10
6.5.2.2 Experiments 5 to 9	6-10
6.5.2.3 Experiments 10 and 11	6-11
6.5.2.4 Experiment 12	6-12
<i>6.5.3 R/P With Simultaneous Venting of Product</i>	<i>6-12</i>
6.5.3.1 Experiments 13 to 14	6-12
<i>6.5.4 Comparison of B/F and R/P: Consecutive Experiments 15 to 16</i>	<i>6-13</i>
<i>6.5.5 Monitoring of Separation Efficiency</i>	<i>6-15</i>
6.6 RESULTS AND DISCUSSION	6-15
<i>6.6.1 Maximization of Negative R/P Peak dP and Flux</i>	<i>6-15</i>
6.6.1.1 R/P without Simultaneous Venting of Product	6-15
6.6.1.2 R/P With Simultaneous Venting (Discharge) of Product	6-21
<i>6.6.2 Monitoring of Separation Efficiency</i>	<i>6-23</i>
<i>6.6.3 Comparison of B/F and R/P: Consecutive Experiments 15 to 16</i>	<i>6-24</i>
6.6.3.1 Experiment 15A: Operation with B/F Only	6-24
6.6.3.2 Experiments 15B and 15C: Operation with R/P Only	6-26
6.6.3.3 Experiment 15D: Illustration of "Lift-and-Sweep" with a Fouled Membrane	6-30

6.6.3.4 Long-term Flux and <i>dP</i> Responses of the System: Experiment 16	6-30
6.7 CONCLUSIONS	6-33
Chapter 7 : CONCLUSIONS	7-1
7.1 SIGNIFICANCE OF MON VILLA B/F INVESTIGATION	7-1
7.2 SIGNIFICANCE OF PARADYSKLOOF R/P INVESTIGATION	7-3
7.3 SUGGESTIONS FOR FUTURE RESEARCH	7-6
REFERENCES	R-1
Appendix A : Indicator organisms	A-1
A.1 HETEROTROPHIC BACTERIA	A-1
A.2 TOTAL COLIFORM BACTERIA	A-1
A.3 FAECAL COLIFORM BACTERIA	A-2
A.4 COLIPHAGES	A-2
A.5 ENTERIC VIRUSES	A-2
A.6 PROTOZOAN PARASITES	A-2
Appendix B : Head vs. Capacity Pump Curves	B-1
Appendix C : Additional Results From Case Study 1	C-1
C.1 DESIGN CONSIDERATIONS	C-1
C.2 TEMPERATURE CORRECTION	C-2
C.3 MICROBIAL INDICATORS	C-2
C.4 COLOUR REDUCTION	C-3
C.5 IRON AND NOM REDUCTION	C-4
C.6 ANALYSIS OF VARIANCE TABLES FOR B/F EXPERIMENTS	C-6
Appendix D : Additional Results from Case Study 2	D-1
D.1 MARKER OUTPUTS AND DURATIONS FOR EXPERIMENTS 1 TO 14	D-1
D.2 ADDITIONAL <i>dP</i> AND FLUX RESPONSES	D-4

List of Tables

Table 1:	Characteristics of pressure-driven membrane processes	1-2
Table 2:	Comparison of different module types according to the design objectives listed in section 2.4.1	2-12
Table 3:	Relative sizes of selected microorganisms	3-2
Table 4:	Hierarchical classification of potable water quality	3-5
Table 5:	Variables and hydraulic module parameters for the experimental modules used in Case Study 1.	4-5
Table 6:	Sequence of actions for a Strategy A backflush (Filter up, FFR, B/F A1 down, FFR, B/F A2 up, Filter up)	4-11
Table 7:	Sequence of actions for a Strategy B backflush (Filter up, B/F B1 up, FFR, B/F B2 down, FFR, Filter up)	4-11
Table 8:	Backflush result Set A (Filter up, FFR, B/F A1 down, FFR, B/F A2 up, Filter up)	4-20
Table 9:	Backflush result Set B (Filter up, B/F B1 up, FFR, B/F B2 down, FFR, Filter up)	4-21
Table 10:	Summary of results from ANOVA	4-23
Table 11:	Summary of differences between conventional backflushing and the proposed reverse-pressure pulsing method	5-9
Table 12:	Variables and hydraulic module parameters for the experimental modules used in Case Study 2	6-3
Table 13:	List of pumps, valves, measurement devices and miscellaneous equipment of the Paradyskloof plant	6-6
Table 14:	General summary of experimental planning and execution	6-9
Table 15:	Markers and description of R/P sequence actions for Experiments 1 to 4	6-10
Table 16:	Markers and description of R/P sequence actions for Experiments 5 to 9	6-11
Table 17:	Markers and description of R/P sequence actions for Experiments 10 and 11	6-11
Table 18:	Markers and description of R/P sequence actions for Experiment 12	6-12
Table 19:	Markers and description of R/P sequence actions for Experiments 13 to 16	6-13
Table 20:	Filtration time per R/P cycle, R/P peak dP , peak flux and water temperature for experiments 1 to 12	6-16

LIST OF TABLES

Table 21: Filtration time per R/P cycle, R/P peak dP , peak flux and water temperature for experiments 13 and 14	6-22
Table 22: Weekly turbidity reduction at the Paradyskloof plant	6-24
Table 23: Grab samples of microbial indicators	C-3
Table 24: Summary of statistics for individual and combined experiments	C-6
Table 25: ANOVA Table for Experiments A1 and B1	C-6
Table 26: ANOVA Table for Experiments A1 and B2	C-7
Table 27: ANOVA Table for Experiments A1 and A2	C-7
Table 28: ANOVA Table for Experiments B1 and B2	C-7
Table 29: ANOVA Table for Experiments A2 and B1	C-8
Table 30: ANOVA Table for Experiments A2 and B2	C-8
Table 31: ANOVA Table for combined Experiments (A1+A2) and (B1+B2)	C-8
Table 32: Outputs activated by markers (M) and duration (Δt) of R/P events for Experiments 1 to 4	D-1
Table 33: Outputs activated by markers (M) and duration (Δt) of R/P events for Experiments 5 to 9	D-2
Table 34: Outputs activated by markers (M) and duration (Δt) of R/P events for Experiments 10 to 11	D-2
Table 35: Outputs activated by markers (M) and duration (Δt) of R/P events for Experiment 12	D-3
Table 36: Outputs activated by markers (M) and duration (Δt) of R/P events for Experiments 13 to 16	D-3

List of Figures

Figure 1:	Flow diagram of a typical pressure-driven membrane filtration operation.	1-3
Figure 2:	Schematic representation of different membrane morphologies.	2-3
Figure 3:	Schematic representation of contact angle measurement of a liquid droplet on a solid surface.	2-4
Figure 4:	Capillary membrane spinning line setup.	2-7
Figure 5:	Schematic representation of the prototype capillary membrane modules used in this investigation (not drawn to scale).	2-9
Figure 6:	Schematic representation of the cake layer build-up in (a) dead-end (DE) and (b) cross-flow (XF) operating modes.	2-16
Figure 7:	Schematic diagram of energy requirements for a typical membrane operation.	2-18
Figure 8:	Velocity and boundary layer development at the inlet to a porous tube.	2-19
Figure 9:	Pressure-flux relationships denoting the pressure-controlled and mass transfer controlled regions.	2-25
Figure 10:	Effect of temperature on pure-water viscosity as calculated by eqs. (2.35), (2.36) and (2.38) in the range of 5 to 40 °C.	2-27
Figure 11:	Percentage viscosity bias of equations (2.35), (2.36) and (2.38) in the prediction of the viscosity of pure water as a function of temperature.	2-28
Figure 12:	Effect of temperature on pure-water density as calculated by eq. (2.41) in the range of 5 to 40 °C.	2-29
Figure 13:	Cross-section of an externally unskinned polysulphone membrane (IPS membrane code #763) used in Case Study 1.	4-3
Figure 14:	Outer surface of an externally unskinned polysulphone membrane (IPS membrane code #763) used in Case Study 1.	4-4
Figure 15:	Inlet velocity versus inlet Reynolds number for a 1.2 mm ID membrane.	4-5
Figure 16:	Flow diagram of the Mon Villa pilot plant.	4-7
Figure 17:	Corrected specific flux performance at Mon Villa.	4-14
Figure 18:	Turbidity reduction at Mon Villa.	4-15
Figure 19:	Corrected specific flux for fouled and cleaned membranes as a function of CIP number.	4-15

Figure 20: Corrected flux, dP and temperature over the latter part of the Mon Villa investigation as a function of operating time (C133 to C139).	4-17
Figure 21: Normalised headloss and cross-flow velocity over the latter part of the Mon Villa investigation as a function of operating time (C133 to C139).	4-18
Figure 22: Normalised headloss as a function of cycle operating time for selected filtration cycles C135, C137 and C139.	4-18
Figure 23: Effect of feed flow reversal on flux recovery with backflush.	4-22
Figure 24: Flowsheet of a membrane unit with feed, recycle and backflush pumps, a permeate accumulator and suitable valve arrangement for conventional backflush operation.	5-2
Figure 25: Flowsheet of a membrane unit with two pumps, two accumulators and valve arrangement for reverse-pressure pulsing without simultaneous venting.	5-3
Figure 26: Flowsheet of an alternative membrane unit with one pump, two accumulators and suitable valve arrangement for reverse-pressure pulsing without simultaneous venting.	5-5
Figure 27: Flowsheet of a membrane unit with two pumps, two accumulators, a venting line and valve arrangement for reverse-pressure pulsing with simultaneous venting.	5-7
Figure 28: Flowsheet of an alternative membrane unit with one pump, two accumulators, a venting line and suitable valve arrangement for reverse-pressure pulsing with simultaneous venting.	5-8
Figure 29: Piping and instrumentation diagram of the Paradyskloof plant.	6-5
Figure 30: R/P flux and dP response for experiment 1.	6-17
Figure 31: R/P flux and dP response for experiment 9.	6-18
Figure 32: R/P flux and dP response for experiment 10.	6-19
Figure 33: R/P flux and dP response for experiment 12.	6-20
Figure 34: R/P flux and dP response for experiment 13.	6-23
Figure 35: Product flux and temperature responses of experiment 15A for 18 h of operation with B/F only.	6-25
Figure 36: dP response of experiment 15A for 18 h of operation with B/F only.	6-25
Figure 37: Product flux and temperature responses of experiment 15B for 7 h of operation after switching from B/F to R/P only.	6-26
Figure 38: dP response of experiment 15B for 7 h of operation after switching from B/F to R/P only.	6-27

Figure 39: Magnified view of flux response of experiment 20B for the first 2 h of operation after switching from B/F to R/P only.	6-28
Figure 40: Product flux and temperature responses of experiment 15C for 15 h of uninterrupted DE operation with R/P only after experiment 15B.	6-29
Figure 41: dP response of experiment 15C for 15 h of uninterrupted DE operation with R/P only after experiment 15B.	6-29
Figure 42: Flux response illustrating the "lift-and-sweep" concept of flow destabilization with the reverse-pressure pulse method on a fouled membrane.	6-30
Figure 43: Long-term flux and temperature responses for experiment 16A.	6-31
Figure 44: Long-term dP response for experiment 16A.	6-31
Figure 45: Long-term flux and temperature responses for experiment 16B.	6-32
Figure 46: Long-term dP response for experiment 16B.	6-32
Figure 47: Characteristic curves of total head vs. capacity for the centrifugal pumps used during the course of this investigation.	B-1
Figure 48: Daily production at Mon Villa.	C-1
Figure 49: Operating temperature and viscosity at Mon Villa.	C-2
Figure 50: Apparent colour reduction at Mon Villa.	C-3
Figure 51: Iron reduction at Mon Villa.	C-4
Figure 52: Calibration curve for the Theewaterskloof NOM.	C-5
Figure 53: NOM reduction at Mon Villa.	C-6
Figure 54: R/P flux and dP response for experiment 2.	D-4
Figure 55: R/P flux and dP response for experiment 3.	D-4
Figure 56: R/P flux and dP response for experiment 5.	D-5
Figure 57: R/P flux and dP response for experiment 8.	D-5

List of Abbreviations

B/F	Backflush
BSA	Bovine serum albumin
CP	Concentration polarization
CSIR	Council for Scientific and Industrial Research
DE	Dead-end
df	Degrees of freedom
DECF	Dead-end constant flux mode
DECP	Dead-end constant pressure mode
EDTA	Ethylene diamine tetracetic acid
FFR	Feed flow reversal
FA	Fulvic acid
HA	Humic acid
H ₀	Null hypothesis
ID	Internal diameter of membrane
IPS	Institute for Polymer Science
MF	Microfiltration
MM	Molecular mass
MS	Mean square
MMCO	Molecular mass cut-off
N/C	Normally closed (fails open)
N/O	Normally open (fails closed)
NF	Nanofiltration
NOM	Natural organic material
NPSH	Net positive suction head

LIST OF ABBREVIATIONS

OD	Outer diameter of membrane
PEG	Polyethylene glycol
PES	Polyethersulphone
PLC	Programmable logic controller
PSf	Polysulphone
PWF	Pure-water flux
R	Reset marker (off)
RO	Reverse osmosis
R/P	Reverse-pressure pulse
S	Set marker (on)
SABS	South African Bureau of Standards
SEM	Scanning electron microscope
SS	Sum of squares
TEM	Transmission electron microscope
UF	Ultrafiltration
US	University of Stellenbosch
WRC	Water Research Commission
XF	Cross-flow
XFCF	Cross-flow constant flux
XFCP	Cross-flow constant pressure

List of Symbols

General Symbols

A	Solute component in fluid stream	(-)
A	Liquid/solid contact angle, eq. (2.8)	(°)
A_F	Frontal flow area of module, eq. (2.7)	(m ²)
A_m	Module membrane area, eq. (2.6)	(m ²)
B	Solvent component in fluid stream	(-)
B	Constant; eq. (2.16)	(-)
B_μ	Bias error; eq. (2.39)	(%)
C	Concentrate flow rate	(m ³ /h)
C_A	Concentration of solute component A, eq. (2.20)	(g/L)
$C_{A,b}$	Concentration of solute component A in the bulk stream, eq. (2.21)	(g/L)
$C_{A,p}$	Concentration of solute component A in the permeate	(g/L)
$C_{A,s}$	Concentration of solute component A at the membrane surface	(g/L)
C_{NOM}	Concentration of natural organic material	(mg/L)
d_i	Internal diameter of membrane, eq. (2.2)	(m)
d_o	External diameter of membrane, eq. (2.1)	(m)
d_o	Hydraulic diameter, eq. (2.18)	(m)
d_p	Pore diameter; eq. (2.8)	(m)
dP	Effective trans-membrane pressure, eq. (2.29)	(Pa)
D_i	Module housing external diameter	(m)
D_{AB}	Diffusion coefficient, eq. (2.20)	(m ² /s)
E_P	Specific pressure power consumption, eq. (2.10)	(kWh/m ³)
E_Q	Specific recirculation power consumption, eq. (2.10)	(kWh/m ³)
E_T	Specific thermal power consumption, eq. (2.10)	(kWh/m ³)

F	Feed flow rate, eq. (1.2)	(m ³ /h)
F_{calc}	Calculated F-statistic in ANOVA	(-)
$F_{\text{crit},0.05}$	Critical F-statistic at the 0.05 significance level in ANOVA	(-)
G	Gibbs free energy; eq. (1.1)	(J)
J_{lim}	Limiting flux	(m/s)
J_v	Process permeate flux; eq. (2.31)	(m/s)
J_S	Specific process flux	(LMH/kPa)
J_{S20}	Specific process flux corrected to 20 °C	(LMH/kPa)
$(J_{S20})_n$	Specific process flux corrected to 20 °C (current data point)	(LMH/kPa)
$(J_{S20})_{n-1}$	Specific process flux corrected to 20 °C (previous data point)	(LMH/kPa)
$(J_{S20})_0$	Specific process flux corrected to 20 °C (start of run after CIP)	(LMH/kPa)
J_w	Pure-water permeate flux; eq. (2.29)	(m/s)
k	Mass transfer coefficient	(m/s)
L_F	Length of membranes available for filtration, eq. (2.3)	(m)
L_T	Total length of module	(m)
N	Number of moles of all components in system; eq. (1.1)	(mole)
N_i	Number of moles of component i in system; eq. (1.1)	(mole)
N_m	Number of membrane fibres in a module; eq. (2.1)	(-)
P	Permeate flow rate, eq. (1.2)	(m ³ /h)
P	Pressure	(Pa)
P-value	Probability of a type-1 error in ANOVA, i.e. rejecting H_0	(%)
P_B	Bubble pressure; eq. (2.8)	(Pa)
P_F	Feed pump operating pressure, eq. (2.11)	(kPa)
P_i	Inlet manifold pressure, eq. (2.13a)	(Pa)
P_o	Outlet manifold pressure, eq. (2.13a)	(Pa)
P_p	Permeate back-pressure, eq. (2.30)	(Pa)
Q	Recirculation flow rate, eq. (2.12)	(m ³ /h)
R	Water recovery, eq. (1.2)	(%)

R_a	Adsorption resistance, eq. (2.32)	(m^{-1})
R_c	Reversible cake or gel layer resistance, eq. (2.32)	(m^{-1})
R_{cp}	Concentration polarization resistance, eq. (2.32)	(m^{-1})
R_m	Membrane resistance, eq. (2.29)	(m^{-1})
R_{tot}	Total resistance, eq. (2.32)	(m^{-1})
Re_D	Reynolds number, eq. (2.18)	(-)
Sc	Schmidt number, eq. (2.25)	(-)
Sh	Sherwood number, eq. (2.24)	(-)
T	Temperature, eq. (1.1)	($^{\circ}C$)
T_C	Relative temperature; eq. (2.34)	($^{\circ}C$)
T_K	Absolute temperature; eq. (2.33)	(K)
U	Velocity; eq. (2.15)	(m/s)
U_b	Bulk velocity; eq. (2.15)	(m/s)
U_i	Inlet manifold velocity; eq. (2.13b)	(m/s)
U_m	Mean velocity; eq. (2.19)	(m/s)
U_o	Outlet manifold velocity; eq. (2.13b)	(m/s)
VF_H	Feed-side hold-up volume of module, eq. (2.3)	(L)
VM_H	Hold-up volume of wetted membranes in module, eq. (2.5)	(L)
VP_H	Permeate side hold-up volume of module, eq. (2.4)	(L)
W_M	Mechanical work, eq. (2.13b)	(J/kg)
$x_{fd,h}$	Hydrodynamic entry length for fully developed flow; eq. (2.16)	(m)
Z	Temperature dependent parameter, eq. (2.37)	(-)
Z_i	Inlet pressure tapping point elevation, eq. (2.13b)	(m)
Z_o	Outlet pressure tapping point elevation, eq. (2.13b)	(m)

Greek Symbols

α	Kinetic energy coefficient, eq. (2.13b)	(-)
α	Level of significance in ANOVA	(-)
δ_c	Mass transport boundary layer thickness; eq. (2.21)	(m)
δ_h	Hydrodynamic boundary layer thickness; eq. (2.14)	(m)
ε	Porosity; eq. (2.9)	(-)
Δe_f	Frictional energy dissipation, eq. (2.13b)	(J/kg)
ΔP_f	Headloss in module, eq. (2.13a)	(kPa)
$\Delta t_{M(i)}$	Duration of events for marker i , eq. (7.1)	(s)
Δx	Channel length (membrane skin thickness) ; eq. (2.9)	(m)
θ	Liquid/solid surface contact angle	($^\circ$)
ρ	Fluid density; eq. (2.18)	(kg/m ³)
ρ_w	Water density; eq. (2.41)	(kg/m ³)
η_F	feed pump efficiency, eq. (2.12)	(-)
η_Q	recirculation pump efficiency, eq. (2.12)	(-)
τ_s	Shear stress	(N/m ²)
γ	Solvent/air interfacial surface tension; eq. (2.8)	(-)
μ	Chemical potential; eq. (1.1)	(J)
μ	Dynamic fluid viscosity; eq. (2.18)	(kg/m.s)
μ_b	Bulk dynamic fluid viscosity; eq. (2.24)	(kg/m.s)
μ_{calc}	Calculated dynamic fluid viscosity; eq. (2.39)	(kg/m.s)
μ_{true}	True dynamic fluid viscosity; eq. (2.39)	(kg/m.s)
ν	Kinematic fluid viscosity; eq. (2.26)	(m ² /s)
ψ	Packing density, eq. (2.1)	(%)
ϕ	Membrane area per unit volume, eq. (2.2)	(m ² /m ³)

Chapter 1: INTRODUCTION

1.1 MEMBRANE FILTRATION OPERATIONS

1.1.1 Definitions and Characteristics

A membrane may be defined as a permeable or semi-permeable phase forming a barrier, often of a polymeric material, between two fluids which restricts the movement of one or more components of one or more fluids across the barrier [Howell *et al.*, 1993; Scott and Hughes, 1996]. While the term filtration conventionally refers to the separation of solid, immiscible particles from liquid or gaseous streams, the application of membrane filtration includes the separation of dissolved solutes from liquid streams and the separation of gas mixtures [Cheryan, 1986; 1998].

Analogously to heat transfer, which is the result of a temperature difference between two solid, liquid or gas bodies, the driving force for mass transport across the membrane surface is the difference in chemical potential on either side of the membrane [Rautenbach and Albrecht, 1989]. Defined in terms of Gibbs free energy, the chemical potential is a measure of the change in the Gibbs function for a system of j components at a pressure P (Pa) and absolute temperature T (K), when a specified amount of component i (moles) is added to, or removed from, the system:

$$\mu(T, P, N) = \left(\frac{\partial G}{\partial N_i} \right)_{T, P, N_i} \quad (1.1)$$

Thus it is possible to separate components from fluid streams by utilising pressure or concentration differences on opposite sides of the membrane. Conventional water filters (e.g. slow sand, rapid sand and dual-media) utilise only the static pressure difference between the water level above the filter and the discharge level. In addition, all feed solution exits a conventional filter as permeate (dead-end). Pressure-driven membrane filtration operations can be distinguished from conventional filtration by the application of hydraulic (pumping) pressure on the upstream side of the membrane to speed up the filtration rate.

Trans-membrane pressures (dP) can range from a few Pa to several MPa, depending upon the membrane operation involved. During cross-flow (XF) membrane filtration the feed stream is pumped across the membrane surface, resulting in a permeate stream that contains the solvent and other permeating components, and a concentrate stream that contains retained solutes and other non-permeating components. Table 1 lists general characteristics such as the typical operating pressures, general retention capabilities and water recovery of the ideal pressure-driven membrane separation processes [Cheryan, 1986; Cheryan, 1998]. The water recovery is defined by eq. (1.2).

Table 1: Characteristics of pressure-driven membrane processes

Separation Process	dP (bar)	Permeate	Concentrate (including water)	Water Recovery (%)
Reverse Osmosis (RO)	10 to 100	Water	Solutes	45 to 80
Nanofiltration (NF)	5 to 15	Water & mono-valent ions	Divalent ions	75 to 90
Ultrafiltration (UF)	1 to 5	Water & small molecules	Large molecules	90 to 98
Microfiltration (MF)	<3	Water & small suspended solutes	Large suspended particles	90 to 98

Adapted from: Cheryan [1986; 1998]

By definition, *reverse osmosis* (RO) retains all components other than the solvent e.g. water (low molecular mass organic and ionic range) and can be classified as a de-watering technique [Cheryan, 1986; Cheryan, 1998]. *Ultrafiltration* (UF) retains macromolecules and colloidal particles larger than about 1 to 50 nm (macromolecular range). UF is considered a method for simultaneous purifying, concentrating and fractionating of macromolecular or fine colloidal suspensions. *Microfiltration* (MF) retains suspended particles in the micron range between 0.1 and 5 μm , and can be considered a method for separating suspended particles from liquid streams. For separation of particles larger than 5 μm , conventional cake filtration methods should be used [Cheryan, 1986; Cheryan, 1998].

1.1.2 Process Equipment for Membrane Operations

Figure 1 shows the requirements and main process equipment of a typical pressure-driven membrane filtration operation. This includes a feed source such as a tank, stream, dam etc, other capital items such a feed pump to supply sufficient driving pressure, as well as valves to regulate feed and permeate pressures and flow rates, and thus the water recovery. Water recovery is expressed as a percentage by the following relationship:

$$R = \frac{P}{F} \times 100 \quad (1.2)$$

where R (%) is the water recovery while P (m^3/h) and F (m^3/h) are the permeate and feed flow rates respectively. Thus when the water recovery is 100 %, all feed water exits the module as permeate.

Membranes are housed in modules, which are connected to the rest of the flow system by means of feed inlet and concentrate outlet manifolds. A recycle pump may also be installed to maintain a minimum cross-flow velocity across the membrane surface in cross-flow mode as illustrated in Figure 1.

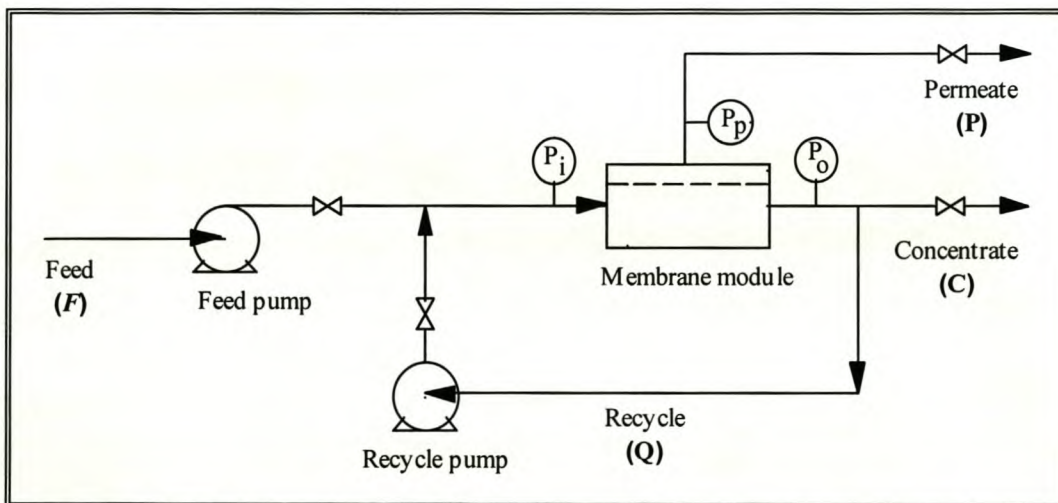


Figure 1: Flow diagram of a typical pressure-driven membrane filtration operation.

1.2 UF LIMITATIONS AND FLUX ENHANCEMENT

During membrane filtration the components that are retained by the membrane (macromolecules, particles, microorganisms etc.) accumulate at the wall, offering an additional resistance to permeation. This reversible phenomenon is called *concentration polarization* (CP) and is often the rate-limiting factor in membrane filtration separations.

The accumulated material may undergo physico-chemical interactions with itself and other components e.g. calcium and phospholipids (aggregation) and/or the membrane material (adsorption and gel formation) on the surface and/or in the pores [Howell and Nyström, 1993]. These mechanisms are complex and interdependent to such an extent that it becomes difficult to distinguish between competing phenomena, and collectively such flux reduction mechanisms are known as *fouling*.

Fouling is manifested as a decline in flux with time of operation, when all operating parameters such as pressure, flow rate, temperature and feed concentration are kept constant. The most obvious consequence of fouling is an increase in the operating cost caused by the lower average flux for a process cycle. The membranes may also require chemical cleaning more frequently, depending on the nature and extent of fouling. This will result in a reduction of the membrane operating life and more frequent membrane replacement.

Various mechanical and/or chemical flux enhancement strategies have been proposed in the literature and evaluated experimentally, either on laboratory or bench scale units for various membrane configurations and applications. Because of the variability of concentration and type of foulants in these investigations, it is not possible to extrapolate results to other types of feed streams.

Available mechanical and/or hydraulic flux enhancement strategies include [Belfort, 1984; Mulder, 1991] permeate backflushing, pulsating feed and/or permeate flow, Taylor vortices in stationary and rotary module systems, turbulence promoters such as unsteady jets, and gas sparging of the feed. Each of these strategies has certain advantages and disadvantages that will determine their suitability to reduce or prevent a particular type of fouling in a particular process or application. However, by gaining an understanding of the fouling mechanisms in a certain application, it may be possible to introduce general guidelines to prevent or reduce reversible and irreversible fouling.

1.3 AIMS OF THE THESIS

The aim of the thesis is to investigate the use of flow destabilization methods, combined with permeate backflushing (B/F) or on their own, on flux recovery and maintenance in capillary UF membrane systems under cross-flow (XF) and dead-end (DE) operating conditions. Flow destabilization is defined as the rapid interruption of flow into the module on the upstream side of the membrane, i.e. by either reversing the feed flow direction or halting the flow completely. In other words, the term flow destabilization refers to a sudden change in the momentum of the feed water.

The UF systems investigated are used for the production of potable water from surface waters containing high loads of natural organic material (NOM), as well as metals such as iron, aluminium, calcium etc. Cations of these metals are known to form stable metal-organic complexes by cross-linking with the NOM present in the water. When these complexes are formed in the fouling layer on the hydrophobic membrane surface over extended periods of membrane filtration, it is believed that a more dense fouling layer is formed, that is more resistant to break-up and removal by normal backflushing methods.

1.4 APPROACH OF THE THESIS

The investigation will be divided into two pilot plant case studies using capillary membrane UF on feed waters from the Theewaterskloof/Helderberg irrigation scheme in Stellenbosch, South Africa.

From a number of flux enhancement strategies tested at Mon Villa over a 27 000 h period with cross-flow filtration, B/F with flow destabilization in the form of feed flow reversal (FFR) looked the most promising, and these results will be highlighted in Case Study 1. Permeate B/F conducted at 24 to 48 h intervals was used to assess the effectiveness of flow destabilization by FFR prior to a B/F on the resultant flux recovery from before to after the B/F. Evaluation of B/F with FFR was conducted using externally unskinned capillary membranes (IPS code #763) over a period of 2620 h. The membrane resistance of IPS code #763 membranes is in the order of $2.0 \times 10^{12} \text{ m}^{-1}$. The flux recovery was expressed as the change in corrected (to 20 °C) specific process flux $J_{S,20}$ (LMH/kPa) from before (data point $n-1$) to after (data point n) the backflush. Normalisation of the flux recovery data was done by dividing this measured change ($(J_{S,20})_n - (J_{S,20})_{n-1}$) by the corrected specific flux at the start of the run $(J_{S,20})_0$ and expressing the result as a percentage in eq. (5.1).

Two strategies were adopted. Strategy A consisted of a B/F with FFR (relative to the direction of cross-flow filtration) followed immediately by a B/F without FFR, while Strategy B consisted of a B/F without FFR followed immediately by a B/F with FFR. In each case the results from the first (A #1 and B#1) and second (A #2 and B#2) backflashes were analysed individually, and then the two results were combined.

In Case Study 2 a new approach for flux enhancement using flow destabilization and reverse flow, now known as reverse-pressure pulsing (R/P), was investigated during dead-end filtration on the same surface water as in Case Study 1, but drawn from a different point. The reason dead-end filtration was used was to reduce the (electrical) operating cost of the filtration unit. Experimental evaluation was conducted at the Paradyskloof water purification works in Stellenbosch, South Africa. The approach of R/P was developed as a result of work done during the course of Case Study 1, and a South African patent [WRC, 1999] was recently granted in the name of the Water Research Commission of South Africa under the title "Reverse-pressure pulse generator". A control sequence was established whereby a number of design variables were changed in order to maximize the design objectives, namely the negative peak dP and peak flux attained with R/P. In Case Study 2 double-skinned membranes with a sponge-like substructure (IPS membrane code #798) were used, with membrane resistance in the order of $1.0 \times 10^{13} \text{ m}^{-1}$. The reason these two design objectives were initially chosen was to attain the maximum reverse flow in the short time interval used for reverse-pressure pulsing. However, the result of this way of operation was only to effect another backflush. Consequently a new design objective was chosen, i.e. the rapid destabilization of flow into the module (by closure of the inflow valve) combined with discharge of product from the outflow (concentrate) side of the module. This conservation of momentum on the outflow side of the module resulted in a hydraulic shock on the membrane surface, which was able to break up the fouling layer. In an R/P sequence three consecutive periods of cross-flow recycle (to build up momentum) and flow destabilization (to shock and create reverse flow from the permeate to concentrate side of the membrane) were used to create a controlled water hammer effect. Thus during the flow destabilization period the fouling layer was broken up and lifted, while in the subsequent recycle period debris was flushed from the lumen in a sweeping action.

The effect of this established R/P sequence on process parameters such as flux and dP was lastly investigated by evaluation of the method on fouled membranes over an extended period of dead-end filtration operation. The results indicated that the R/P sequence was an effective strategy for flux maintenance in UF without the need for backflushing.

1.5 STRUCTURE OF THE THESIS

Chapter 2 presents an overview of membrane morphology, surface characteristics and production protocols, and the effect of membrane geometry on module design. Dead-end and cross-flow operating modes are discussed in terms of energy consumption. A general description of boundary layer development, concentration polarization and flow destabilization as well as a qualitative description of limiting flux behaviour illustrates the concepts of membrane resistance and fouling resistances during membrane filtration. The temperature-dependent variation in viscosity and density and their effect on flux calculation is also demonstrated for pure water.

In Chapter 3 the aesthetic and microbial guidelines for potable water quality are discussed. The causes and consequences of fouling are presented, and available flux enhancement strategies are compared on the basis of a number of viability considerations. It is shown that for capillary membrane systems in potable water supply, the physico-chemical interaction between the membrane and the feed solution is one of the primary factors causing fouling and flux decline.

Chapter 4 presents the flux enhancement results of B/F with flow destabilization from Case Study 1 on turbid feed water containing high levels of NOM. Two B/F strategies with flow destabilization were investigated namely B/F with and without feed flow reversal during the first B/F, followed by a B/F in the opposite direction as the first. The results from this chapter led to the conceptual development of flux enhancement by using the reverse-pressure pulsing principle.

Chapter 5 presents a description of backflushing, which is compared with the conceptual operating principle and description of the reverse-pressure pulsing method. Four different cases are presented, including R/P with and without simultaneous venting of product in the presence and absence of a recycle pump.

In Chapter 6 the results from Case Study 2 into the implementation of the R/P principle are presented. A PLC control sequence was established to maximize the effect of R/P in terms of the peak dP and flux attained. Flux decline over extended periods was used to compare the effectiveness of B/F and the final "lift-and-sweep" R/P sequence established. Product quality was also monitored to determine the effect of R/P on separation capability and possible damage to the membranes.

In Chapter 7 the main conclusions of this investigation are discussed, along with suggestions for future research.

Chapter 2: ULTRAFILTRATION PROCESSES

2.1 MEMBRANE PROCESS DEVELOPMENT

Compared with more traditional process industries, membrane separations are a relatively recent development. Large-scale use of synthetic membranes did not become feasible until the mid 1960s when scientists and engineers started investigating the use of RO as an energy-saving process to desalinate seawater [Howell *et al.*, 1993].

After Sourirajan and Loeb produced the first asymmetric RO membranes from cellulose acetate [Loeb and Sourirajan, 1960; Loeb and Sourirajan, 1962], major research programs were initiated by some of the industrially developed nations to develop high-performance membranes and modules. The newer generation thin-film RO membranes were characterized by a 0.1 to 0.2 μm thick perm-selective layer with a porous support layer underneath. These RO membranes could consequently be operated at much lower pressures than previously achieved while fluxes improved dramatically. Thermal annealing of asymmetric cellulose acetate membranes also resulted in improving salt retention to greater than 99 % by shrinking the effective pore size [Cheryan, 1986; 1998].

Shortly after the RO membrane breakthrough, Michaels succeeded in producing an asymmetric poly-ionic UF membrane, which started a wave of progress in the UF field [Howell *et al.*, 1993]. However, UF was developed commercially only during the 1970s, and since then it has found applications in many of the more traditional process industries. According to Cheryan [1986;1998] and Bemberis and Neely [1986] UF processes include applications in the electro-coat paint, dairy, textile, pulp and paper, and tanning and leather industries. UF has recently also been applied successfully in the biotechnology, medical and waste-water treatment fields [Cheryan, 1986; 1998]. Since the 1980s potable water treatment with UF membranes has also been introduced and commercialised to the extent where UF membrane plants are supplying communities with potable and domestic water in the United Kingdom, Europe, Japan, Australia and the United States of America.

2.2 FILTER CLASSIFICATION

2.2.1 Filter Type

Although filters in general are manufactured from a range of materials, they are classified in two groups, namely depth and screen filters.

A depth filter consists of randomly oriented *fibres* or beads bonded together in a *matrix* to form tortuous flow channels. Insoluble or colloidal particulate material is removed from the feed in the depths of the filter material by *entrapment or adsorption* [Cheryan, 1986; 1998]. An example of a depth filter is a conventional sand filter.

A screen filter removes material from the feed stream on the filter surface, and thus *operates as a sieve* with accurately controlled pore sizes. Membrane filters fall into the latter category of screen filters, which offer certain advantages over depth filters [Cheryan, 1986; 1998]:

- ◆ there is little danger of retained material migration into the membrane sub-surface;
- ◆ “grow-through” of micro-organisms is usually not a problem;
- ◆ because of narrowly controlled pore sizes, screen filters have a quantitative or absolute rating; and
- ◆ much higher recovery of the retained material is possible with screen filters.

2.2.2 Membrane Morphology

Membrane filters can further be classified according to their *ultrastructure*, namely either *microporous* or *asymmetric* (integrally skinned) membranes [Cheryan, 1986; 1998]. In Figure 2 the two membrane filter morphologies are illustrated schematically.

2.2.2.1 Microporous Membranes

Microporous membranes have a *uniform morphology* i.e. the porosity is uniform throughout the membrane (isotropic), and the membrane retains all components above the membrane pore size rating. If enough pores are blocked by retained material, the filter may become irreversibly plugged and will need replacement.

2.2.2.2 Asymmetric Membranes

Asymmetric (anisotropic) membranes are characterized by a thin *skin section*, usually 0.1 to 0.2 μm thick, on the membrane surface. The skin determines the membrane *separation capability*, thus no macromolecules or retained particles above the nominal cut-off will enter the main filter body. Asymmetric membranes may also be *single-skinned* or *double-skinned*, depending on the fabrication protocol. The sub-structure may either have a *spongy* or *finger-like* nature, as illustrated schematically in Figure 2. Since this layer of the membrane may be up to 100-300 μm thick, its structure should provide the *mechanical strength* needed to withstand the operating pressure in an application such as water filtration, whether it be RO, UF or MF.

Although asymmetric membranes subsequently do not get plugged as easily as microporous membranes, they are still susceptible to fouling and experience reversible and irreversible flux loss [Cheryan, 1986; 1998]. Another advantage of asymmetric membranes is the lower hydraulic resistance associated with the thin skin layer or layers, which will be discussed in section 2.5.4.

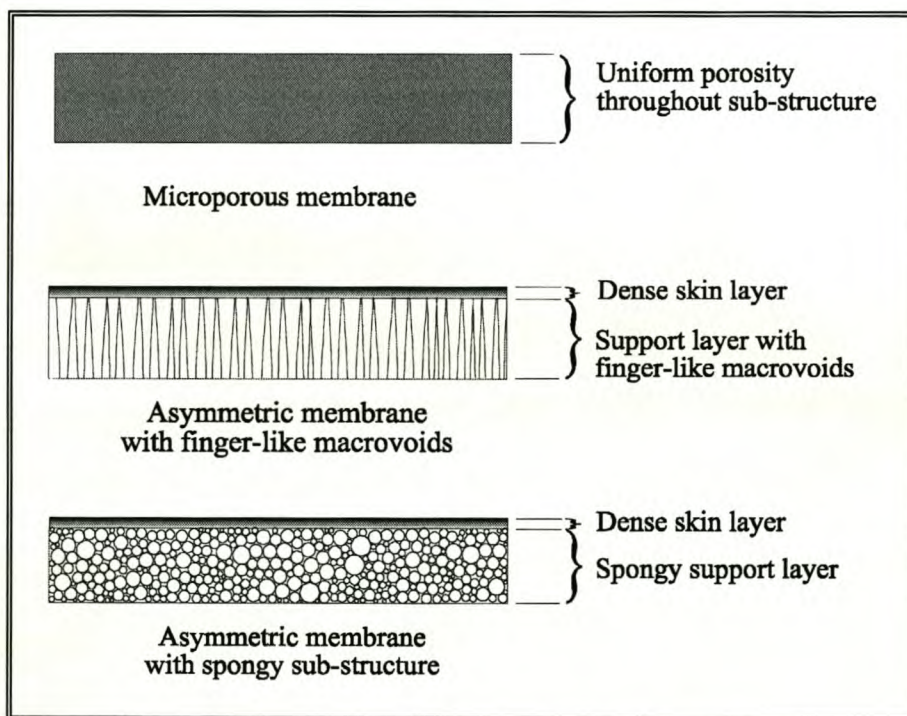


Figure 2: Schematic representation of different membrane morphologies.

2.2.3 Hydrophilicity of the Membrane Surface

Hydrophilic surfaces have an affinity for water, i.e. are easily wetted, while for hydrophobic surfaces the converse is true.

Quantitatively, the hydrophilicity of a material is described in terms of the contact angle θ ($^{\circ}$) between a sessile droplet (of pure water in this case) and the solid (non-porous) surface of the material in question. Methods for determining contact angles include the sessile drop, the captive bubble and the Wilhelmy method [Howell and Nyström, 1993].

Mulder [1993] illustrates three different cases. A highly hydrophilic surface, depicted in Figure 3 (a), will be wetted completely by the droplet with a contact angle of zero ($\theta = 0^{\circ}$). In Figure 3 (b) the surface is less hydrophilic, the droplet spreads less over the surface and the contact angle θ lies between 0° and 90° . The more hydrophilic the surface, the smaller is the contact angle. In Figure 3 (c) the surface is not wetted by the droplet, the contact angle is greater than 90° and the material is referred to as hydrophobic.

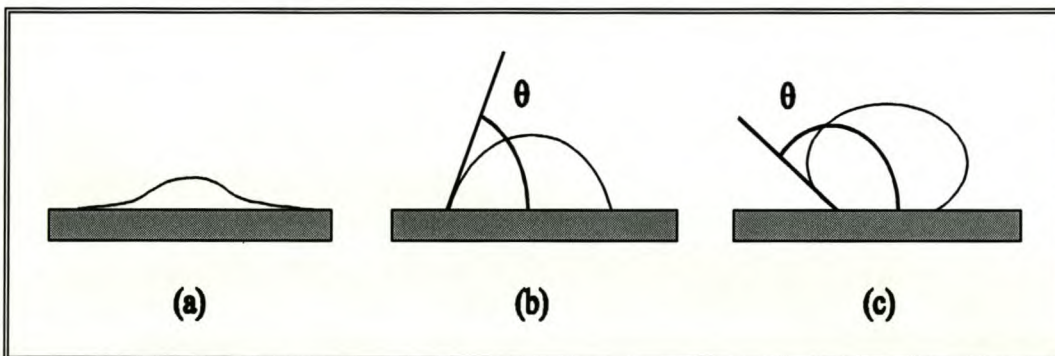


Figure 3: Schematic representation of contact angle measurement of a liquid droplet on a solid surface.

Contact angle values may be useful in determining the relative hydrophilicity of different membranes. However, the accurate measurement and reproducibility of contact angles are influenced by a number of factors such as surface porosity, roughness and heterogeneity, as well as surface alteration and/or contamination [Mulder, 1993; Rosa and de Pinho, 1997].

2.3 MEMBRANE MANUFACTURE

2.3.1 Material Selection

According to Merry [1996] a number of criteria that must be met when selecting a material destined for commercial membrane or other use. These selection criteria include:

- ◆ availability of the polymer or other materials to be used;
- ◆ chemical stability in a range of operating conditions and environments;
- ◆ processability; i.e. the polymers must be able to form a stable homogeneous solution in a suitable solvent, or must be able to withstand stretching; and
- ◆ certain markets may require that the material be approved for food or water contact.

Traditionally, hydrophilic materials are not recommended for UF membranes that require mechanical strength and thermal stability, because water molecules act as *plasticizers* [Lacy and Loeb, 1972, Toyomoto and Higuchi, 1992]. Consequently, UF membranes are generally prepared from amorphous (glassy) polymers with a high glass transition temperature. Lloyd [1985] has listed over 90 different polymers and blends studied in membrane manufacture, although the number will certainly be much higher today. However, very few polymeric materials have been used as successfully in commercial UF applications as polysulphone (PSf), polyethersulphone (PES) and cellulose derivatives. The advantages and disadvantages of PSf and PES will be discussed below.

Polysulphone is a synthetic polymer generally used for UF membrane fabrication, by virtue of its characteristics that increase the robustness of the membranes and offer greater flexibility in operation [Cheryan, 1986; 1998]. The advantages of PSf and especially PES as membrane materials include [Cheryan, 1986; 1998]:

- ◆ temperature limits of up to 75 °C;
- ◆ wide pH tolerance of 1 to 13, which is an advantage when one considers the conditions at which detergent cleaning is done (pH 10 to 12);
- ◆ good resistance to chlorine for short-term sanitation (200 ppm) and storage (50 ppm);
- ◆ easy to fabricate in a variety of membrane configurations; and
- ◆ a wide range of commercial membranes are available in pore sizes ranging from 1 to 20 nm, or molecular mass cut-offs (MMCO) of 1000 to 500 000 Da.

The disadvantages of PSf and PES as membrane materials include the following [Cheryan, 1986; 1998]:

- ◆ polysulphone is a hydrophobic material, thus if the membranes are allowed to dry out completely, the finely-porous structure in the skin section may collapse under surface tension effects, causing permanent flux loss [Jacobs *et al.*, 1993];
- ◆ generally low pressure limits of flat sheet (7 bar) and PSf capillary (1,7 bar) membranes, although more recent thin-film composite membranes are made on top of a PSf substrate with RO operating pressures of 40 bar; and
- ◆ smallest pore MMCO sizes are 500 to 1000 Da while the largest are 100 kDa.

2.3.2 Membrane Formation by Phase Inversion

Polymeric are manufactured from a viscous, homogenous casting solution, which is made up by dissolving prescribed quantities of polymer beads and swelling agents, or non-solvents in a suitable organic solvent. The procedure and activities for preparation of the casting solution are listed elsewhere [Jacobs *et al.*, 1993].

Broadly speaking, all polymeric membranes are formed by way of a *phase inversion* process [Cheryan, 1998; Jacobs *et al.*, 1993]. According to Kesting [1971], phase inversion results in a “solvent-cast structure, which owes its porosity to immobilisation of the polymer gel prior to complete solvent evaporation or depletion”.

2.3.3 Membrane Geometries

Polymeric membranes may either be formed on a *porous support fabric* (fabric-supported tubular membranes and fabric-supported flat-sheet membranes) or as an *unsupported membrane* (capillary and hollow fiber membranes and unsupported flat-sheet membranes) [Cheryan, 1986; 1998]. Therefore the specific fabrication procedures employed may differ considerably, depending on to the desired geometry or configuration.

2.3.3.1 Capillary Membranes

Capillary or hollow fibre membranes (0.5 to 2.5 mm OD) are formed continuously by *extruding or spinning* the casting solution through an annular tube-within-tube *spinnerette* into a solvent/non-solvent casting bath or *coagulation tank*. A *lumen coagulant* is metered continuously into the lumen to keep the nascent membrane from collapsing, and is instrumental

in the formation of the internal skin structure of the membrane. Jacobs *et al.* [1997] illustrates the setup for a capillary membrane spinning line in Figure 4. After the membrane is formed, the residual solvents and swelling agents are leached from the membrane by passing the membrane over a *series of rollers* in the tank, and winding the membrane on a *rotary take-up roller or drum*. Choice of the core and coagulation bath fluids makes it possible to form the skin on the inside, outside or on both sides of the membrane, as outlined by Jacobs *et al.* [1997].

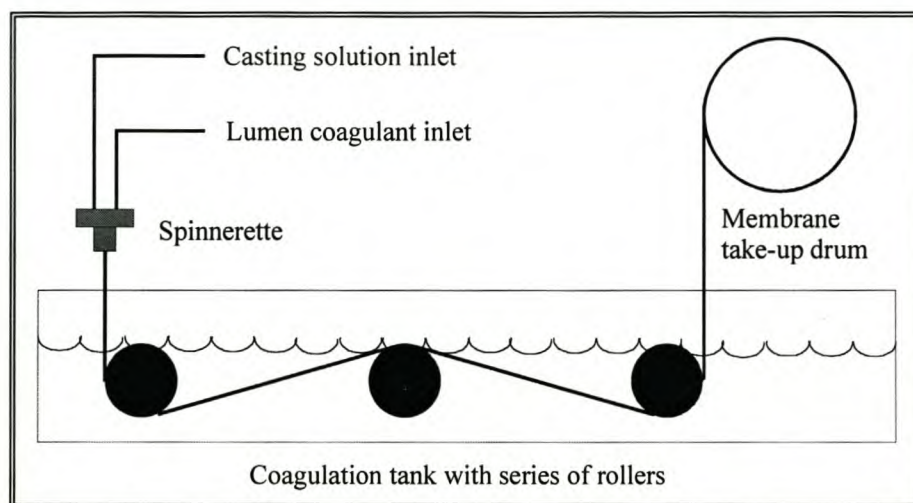


Figure 4: Capillary membrane spinning line setup.

Post-treatment strategies differ according to the membrane material (natural or synthetic polymer) and the type of membrane. Polysulphone membranes *cannot* be annealed by *thermal treatment* in a water bath. Generally, synthetic membranes are post-treated with substances that act as *plasticizers*. After the membrane has been formed, it is rinsed for 24 hours in a water bath. During this post-treatment step, the residual solvent and swelling agents in the membrane structure are replaced with water molecules. PSf membranes are then conditioned in a 1:1 *aqueous glycerine solution*, before being dried in a *high-humidity chamber* at ambient temperature for 7 days [Jacobs and Leukes, 1996].

2.3.3.2 Fabric-supported Tubular Membranes

Tubular membranes (12 to 25 mm OD) are formed similarly to fabric-supported flat-sheet membranes, with the only difference being that, before deposition of the casting solution, the support fabric is shaped into a *tube*. The membrane is usually formed on the inside of the support tube in a continuous process, although externally skinned membranes are common in industry [Cheryan, 1986; 1998].

2.3.3.3 Fabric-supported Flat-sheet Membranes

These membranes may be cast continuously by depositing a layer of casting solution of pre-determined thickness (usually 0.2 to 0.5 mm) on a *flexible porous woven or non-woven support fabric*. The support fabric is then passed into a *solvent/non-solvent coagulation bath* to initiate phase inversion, while final solvent leaching occurs in a *rinsing bath*.

2.3.3.4 Unsupported Flat-sheet Membranes

Membranes of this type are cast in a batch process directly on a smooth surface such as a glass plate or on a moving stainless steel belt. *Precipitation* occurs when the glass plate is dipped in a water (non-solvent) bath that is kept at a controlled temperature. The membrane may then be removed from the glass plate, and left in the water bath to complete the leaching process.

2.4 MODULE DESIGN CONSIDERATIONS

Membrane geometry determines largely the type of filtration module that will house the membranes, as well as possible methods to enhance the flux. A module consists of the *membranes, pressure support structures, feed inlet and concentrate outlet ports, and permeate draw-off points* [Aptel and Buckley, 1996].

Four major types of modules are commercially available: *plate-and-frame, spiral-wrap, tubular and capillary membrane modules*. A comparison of the design and operational characteristics of each type of module will be discussed later in this section.

2.4.1 Design Objectives

According to Aptel and Buckley [1996], the design of a module should aim to achieve the objectives stated below.

- ◆ At membrane level, a sufficient circulation of the fluid to be treated should be insured, in order to limit concentration polarization and particle deposits.
- ◆ The module should have a high packing density, ψ (%), with a maximum membrane area per unit volume, ϕ (m^2/m^3).
- ◆ No leakage should occur between the feed and permeate compartments.
- ◆ Membranes and modules should be easy to clean and disinfect (hydraulic and chemical cleaning).

- ◆ Modules should be easy to install or remove from the filtration assembly.
- ◆ Modules should have a low hold-up volume.
- ◆ Pressure drops should be low to limit energy consumption.

2.4.2 Definition of Module Parameters

The packing density of a lumen flow capillary membrane module, represented schematically in Figure 5, ψ (%), is defined as the ratio of the frontal area calculated from the external membrane diameter, divided by the total internal cross-sectional area of the module, expressed as a percentage. For the modules of the tubular and capillary types the packing density can be expressed as:

$$\psi(\%) = \frac{N_m \times \frac{\pi d_o^2}{4}}{\frac{\pi D_i^2}{4}} \times 100 = \frac{100 N_m d_o^2}{D_i^2} \tag{2.1}$$

Void space = 100- ψ

where N_m is the number of membranes in the module, d_o (m) is the external diameter of the membranes, and D_i (m) is the internal diameter of the module housing.

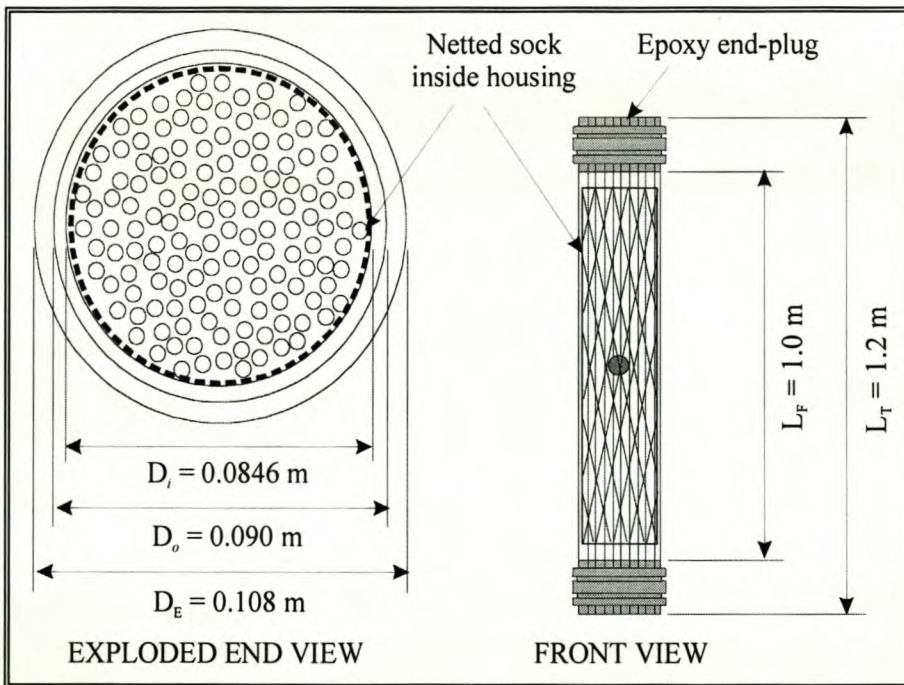


Figure 5: Schematic representation of the prototype capillary membrane modules used in this investigation (not drawn to scale).

The void space (%) in the end-plug, as expressed in eq. (2.1), is the space available for penetration of the end-plug material to form a hydraulic seal between the feed and permeate sides of the membranes. The *specific membrane area*, or membrane area per unit volume ϕ (m^2/m^3), is *the membrane area available for filtration*, divided by the *internal module volume*. For lumen flow membranes the membrane area is calculated from the internal diameter, thus ϕ can be expressed as:

$$\phi = \frac{N_m \pi d_i L_F}{\frac{\pi}{4} D_i^2 L_F} = \frac{4 N_m d_i}{D_i^2} \quad (2.2)$$

where L_F (m) is the membrane length available for filtration.

The feed side hold-up volume VF_H (L) of a module is the volume on the *upstream side* of the module, in other words, in a capillary or tubular module this is expressed as:

$$VF_H = 1000 \times N_m \left(\frac{\pi}{4} \right) d_i^2 L_F = 250 \times N_m \times \pi \times d_i^2 L_F \quad (2.3)$$

while the permeate side hold-up volume VP_H (L) is the volume on the *down-stream side* of the membranes in the module:

$$VP_H = 1000 \times \left[\left(\frac{\pi}{4} \right) D_i^2 L_F - N_m \left(\frac{\pi}{4} \right) d_o^2 L_F \right] = 250 \times \pi \times L_F (D_i^2 - N_m d_o^2) \quad (2.4)$$

The volume taken up by (wetted) membranes, VM_H (L) in the module is:

$$VM_H = 1000 \times \left[N_m \frac{\pi}{4} d_o^2 L_F - N_m \frac{\pi}{4} d_i^2 L_F \right] = 250 \times N_m \times \pi \times L_F (d_o^2 - d_i^2) \quad (2.5)$$

The *total membrane area* available for filtration in a tubular or capillary module, A_m (m^2) can be calculated from the following expression:

$$A_m = N_m \times \pi \times d_i \times L_F \quad (2.6)$$

and the *frontal flow area* of the module, A_F (m^2) has the form:

$$A_F = N_m \left(\frac{\pi}{4} \right) d_i^2 \quad (2.7)$$

The module parameters as expressed by eqs. (2.1) to (2.7) were calculated in Table 5 for the capillary modules used in this investigation.

2.4.3 Capillary Membrane Modules

Capillary membranes are bundled together and potted in cartridges or modules similar to tube-in-shell heat exchangers. These modules may have the feed stream flowing on the inside or outside of the membrane, depending on the type of membrane (internally- or externally-skinned) and the application involved [Bemberis and Neely, 1986; Koros, 1995]. The characteristics of capillary membrane modules are listed below.

- ◆ Because of the small inner and outer membrane diameters, capillaries offer a large surface area per unit volume and low permeate hold-up volume [Koros, 1995] which results in a very compact module design.
- ◆ High cross-flow velocities and shear rates can be attained at moderate volumetric flow rates, which are usually in the laminar region for capillary UF membranes.
- ◆ Defective membranes in modules can be easily identified and isolated, with the result that the productive life of a module is increased. This was demonstrated during the first phase of this study in 1995 [Jacobs *et al.*, 1995].
- ◆ The cylindrical lumen geometry of tubular and capillary membranes has well defined flow-paths in the lumen feed mode, which simplifies modelling of the filtration process.
- ◆ Backflushing is possible by reversing the flow direction of permeate through the membrane wall. This has the effect of disturbing and removing the deposited cake layer to a certain extent.

2.4.4 Other Types of Modules

The modules constructed from other membrane types include the following:

- ◆ *tube-in-shell* modules used for *tubular* membranes [Cheryan, 1986; 1998; Aptel and Buckley, 1996]; and
 - ◆ *plate-and-frame* and *spiral-wrap* modules used for *flat-sheet* membranes [Cheryan, 1986; 1998; Rautenbach and Albrecht, 1989; Aptel and Buckley, 1996].
-

2.4.5 Summary of Module Types

Although the design of different module types may be radically different, a comparison of different designs is possible according to the design objectives listed in section 2.4.1. In Table 2 adapted from Aptel and Buckley [1996], the four main types of commercial modules are compared. It can be seen from Table 2 that, excluding hollow fiber modules (not listed because the hollow fiber membranes would be impractical in surface water UF due to lumen plugging), capillary membrane modules offer the highest *packing densities* attainable, and thus the most *compact* module design. Although *in situ cleaning* of capillary modules may be a problem, the *backflush* (or *backwash*) capability is a clear advantage over the other designs. With regard to replacement cost, spiral-wrap and capillary modules are both very cost-effective, while tubular units indicate the highest cost.

Table 2: Comparison of different module types according to the design objectives listed in section 2.4.1

Design Criteria	Plate-and-Frame	Spiral-Wrap	Tubular	Capillary
Packing density	+	++	-	+++
Ease of cleaning <i>in situ</i>	+	-	++	-
by backwash	-	-	-	+++
Module cost	+	+++	-	+++
Pressure drop	-	++	+++	++
Hold-up volume	+	+	-	++
Pretreatment required	+	-	+++	++

Adapted from Aptel and Buckley [1996]. Key: +++ Clear advantage, - Clear disadvantage.

Low to moderate *pressure drops* in capillary modules (operation under laminar conditions with low shear rates) is a definite advantage while plate-and-frame modules exhibit the highest pressure drops. Naturally, this pressure drop is related to the magnitude of the circulation velocity. Capillary modules also exhibit the lowest hold-up volume because of small membrane diameters and high packing densities.

A possible disadvantage of capillary membrane operation under laminar conditions is that suspended solids, present in the feed water, may accumulate on the tube-sheet. This may cause

bridging and eventually clogging of the capillary membrane lumens, especially at high water recovery rates and high suspended solid concentrations, as indicated by Jacobs *et al.* [1997]. Bridging of a membrane lumen will result in a decreased linear cross-flow velocity and eventually a cessation of cross-flow for the affected membrane. In such a scenario the affected membrane will effectively be operating as a dead-end filter, with progressive plugging of the lumen [Jacobs *et al.*, 1997].

2.5 UF MEMBRANE PERFORMANCE CHARACTERIZATION

Porous membranes may be characterized according to their *structure-related* parameters such as pore size distribution, thickness of the selective skin layer and surface porosity; and *process-related parameters*, such as flux and retentivity.

2.5.1 Pore Size Distribution and Retentivity

Because of the manufacturing process of polymeric UF membranes, a *distribution of pore sizes* is usually observed, as opposed to only one pore diameter. Thus the solute retention (or retentivity) of UF membranes depend on the size distribution of species in the feed stream, the pore size distribution on the surface of the membrane, and the probability that species that may pass through pores of a given size may never encounter such pores. Several methods have been used to determine pore diameters. These are listed below.

2.5.1.1 The Bubble Point Technique

The bubble point technique is based on Cantor's equation [Cheryan, 1986; 1998]:

$$P_B = \frac{4\gamma \cos A}{d_p} \quad (2.8)$$

where P_B is the bubble pressure, γ is the solvent/air interphase surface tension, A is the liquid/solid contact angle and d_p is the pore diameter. The method described in detail in [ASTM, 1976], has been developed for flat-sheet membranes.

Since eq. (2.8) indicates only the size of the largest pores, this method is of limited use for characterizing UF membranes. It is, however, a good tool for membrane quality control. A modified bubble point technique may also be used to evaluate membrane modules for broken fibers, as described in section 6.5.4.

2.5.1.2 Direct Microscopic Observation

Electron microscopy and near field microscopy are the only direct methods of determining pore statistics, especially in studying the surface structure of MF membranes. The pore sizes of MF membranes (0.1 to 10 μm) are well within the 5 to 10 nm resolution range of scanning electron microscopes (SEM). For UF membranes with pore sizes in the 1 to 30 nm range, transmission electron microscopy (TEM) with a resolution range 0.3 to 0.4 nm is usually used [Cheryan, 1986; 1998]. The Hagen-Poiseuille equation in adapted form is sometimes used to estimate the solvent flux in terms of the membrane characteristics:

$$J_v = \frac{\varepsilon \times d_p^2 \times dP}{32 \times \Delta x \times \mu} \quad (2.9)$$

where J_v is the permeate flux (m/s), ε is the surface porosity of the membrane, d_p is the average channel (pore) diameter (m), dP is the trans-membrane pressure (Pa), Δx is the channel length or membrane skin thickness (m), and μ is the dynamic viscosity of the permeating fluid (kg/m.s).

Eq. (2.9) was derived assuming that:

- ◆ all pores are right-circular cylinders;
- ◆ flow through the pores be laminar ($\text{Re}_D < 2\,000$);
- ◆ constant density;
- ◆ steady state conditions exist;
- ◆ Newtonian fluid; and
- ◆ end-effects are negligible.

However, discrepancies between experimental and calculated flux occur, and become more pronounced with decreasing pore size. With increasing pore size, the experimental flux increases, while calculated flux decreases. The assumption that all pores are right-circular cylinders of equal pore diameters, is not justified in the light of asymmetric membrane pore characteristics, and therefore eq. (2.9) should be used with extreme caution.

2.5.1.3 The Challenge (Solute Passage) Test

The challenge test is one of the few *practical methods* whereby the separation capability of membranes may be determined. It involves the measurement of the *permeability* of selected solutes (of different molecular mass) under *controlled conditions* [Cheryan, 1986; 1998]. The

solutes should be *soluble* in water and should *not interact or adsorb* onto the membrane. The membrane is then rated nominally in terms of the molecular mass cut-off (MMCO) at which the solute retention reaches an *arbitrarily selected point*, usually 90 %. Solutes commonly used, include Dextran T10 (10 000 Da), polyethylene glycols (PEGs) (MM 500 to 35 000 Da), large proteins such as immunoglobulins (MM greater than 900 000 Da) etc. [Cheryan, 1986; 1998]. For tight UF membranes the pore size is usually below 5 nm, which in terms of PEG MMCO translates to less than 40 kDa [Anselme and Jacobs, 1996]. No standard challenge test solutes or test conditions presently exist, although Cheryan [1986;1998] has proposed a number of test conditions that need to be standardised during such tests:

- ◆ trans-membrane pressure, 100 kPa;
- ◆ temperature, 25 °C;
- ◆ maximum stirring or agitation intensity, or cross-flow velocity;
- ◆ solute concentration, 0,1 % m/v;
- ◆ permeate-to-feed ratio, less than 10 %;
- ◆ whether solutes will be tested individually or mixed; and
- ◆ membranes should be new and washed to remove any glycerine, and a reproducible pure-water flux (PWF) should be measured before and after the challenge test.

2.5.2 Effect of Operating Mode on Energy Consumption

2.5.2.1 Dead-end mode

In dead-end (DE) operation, illustrated in Figure 6 (a), all the feed water passes out of the module on the permeate side, resulting in a *rapid accumulation of retained particles* and macromolecules on the filter surface. This could lead to a *rapid decline in flux or increase in differential pressure* across the membrane, depending on whether the system is operated in dead-end constant pressure (DECP) or dead-end constant flux (DECF) mode. Dead-end filtration is a *very energy efficient* operating mode since it relies only on the feed pump for water delivery and pressure. As an alternative, the static feed pressure can be generated by elevating the feed tank to a sufficient height above the feed manifold inlet (about 10 kPa/m elevation), while the trans-membrane pressure can be regulated by a back-pressure valve on the permeate outlet line.

Although energy consumption for the DECP filtration cycle can be as low as 0.15 to 0.3 kWh/m³, it is used mainly for feed streams with low fouling potential. With high fouling potential feed

streams rapid flux decline and possible blockage of membranes could occur. DECF filtration is less energy efficient than DECP, because an extra pump is needed to remove the permeate at a required constant rate. However, the energy consumption for the DE operations is still substantially lower than both the XF operating modes.

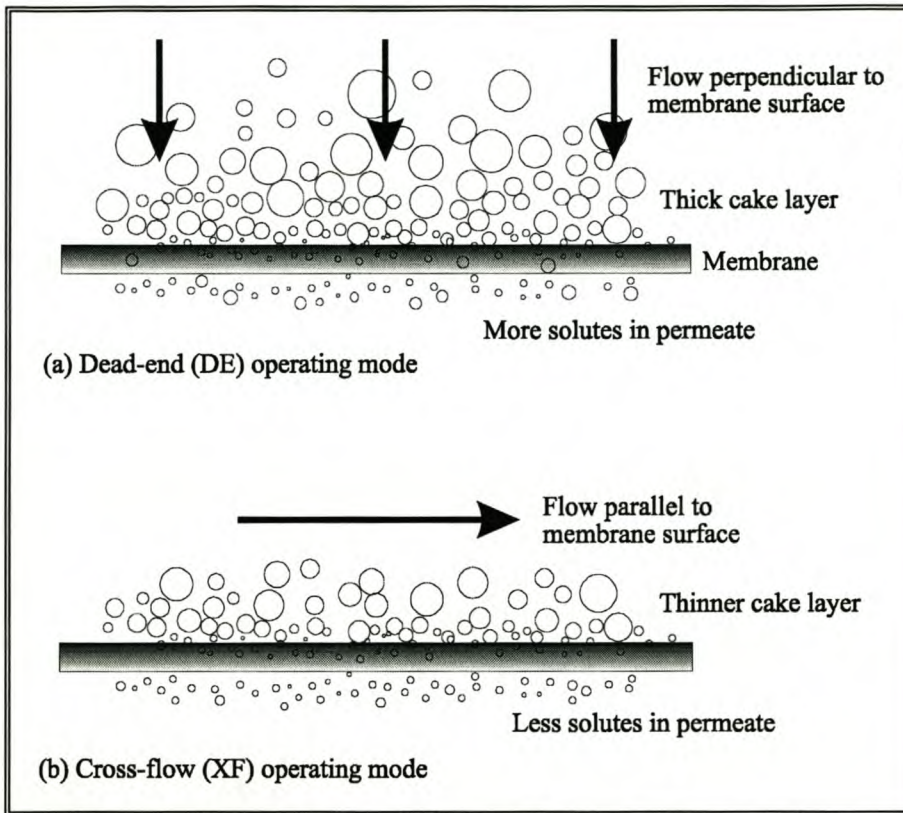


Figure 6: Schematic representation of the cake layer build-up in (a) dead-end (DE) and (b) cross-flow (XF) operating modes.

2.5.2.2 Cross-flow mode

In cross-flow operation, illustrated Figure 6 (b), the feed solution flows *parallel or axially* to the filter surface, resulting in high shear rates on the surface. Part of the feed passes out of the module as concentrate, which may be recycled to the feed side or pumped to waste. Again, the process may be operated in cross-flow constant pressure (XFCP) or cross-flow constant flux (XFCF) mode.

2.5.2.3 Theoretical Power Consumption in Steady UF

Power consumption is the total of several input terms, as shown schematically for a typical *feed-and-bleed* system. The *total specific power consumption* (E_{tot}), for a typical feed-and-bleed filtration system shown schematically in Figure 7, is the sum of the power terms required to

operate the system at the desired trans-membrane pressure (E_P), the desired cross-flow velocity (E_Q) and the desired feed temperature (E_T):

$$E_{tot} = E_P + E_Q + E_T \quad (2.10)$$

where E_P is the specific pressure power consumption, E_Q is the specific recirculation power consumption and E_T is the thermal power consumption.

UF processes in potable water applications may be operated *without heat exchange*, thus the thermal energy term will be neglected in this discussion. The E_P and E_Q terms are both calculated in the same way, as both represent pumping energy in kWh/m³ of permeate produced [Cheryan, 1986; 1998]:

$$E_P = \frac{P_F \times F}{3600 \times J_v \times A_m \times \eta_F} \quad (2.11)$$

$$E_Q = \frac{\Delta P_f \times Q}{3600 \times J_v \times A_m \times \eta_Q} \quad (2.12)$$

$$\Delta P_f = P_i - P_o \quad (2.13a)$$

where P_F is the feed pump pressure (kPa), F is the fresh feed flow rate (L/h), Q is the recirculation flow rate (L/h), J_v is the process flux (L/m².h), A_m is the membrane area (m²), η_F is the feed pump efficiency expressed as a fraction, η_Q is the recirculation pump efficiency expressed as a fraction and ΔP_f is the headloss from inlet P_i to outlet P_o (kPa) of a module in a horizontal configuration. When the module is configured vertically, an appropriate expression may be derived from the energy equation for steady flow to account for vertical height difference:

$$\frac{P_i}{\rho} + \alpha_i \frac{U_i^2}{2} + Z_i g = \frac{P_o}{\rho} + \alpha_o \frac{U_o^2}{2} + Z_o g + W_M + \Delta e_f \quad (\text{J/kg}) \quad (2.13b)$$

where P_i and P_o are the pressures in the inlet and outlet manifolds, U_i and U_o are the inlet and outlet manifold velocities (m/s), and Z_i and Z_o are the vertical elevations of the pressure tapping points at inlet and outlet manifolds respectively. The term g is the acceleration due to gravity (9.81 m/s²) and ρ is the density of pure water for the applicable temperature.

The term W_M is equal to zero (no mechanical work input between inlet and outlet), and the kinetic energy coefficient, α , has a value of 2 for laminar flow and 1.02 to 1.10 for turbulent

flow in the manifold adjacent to the module face. In most XF UF applications $Q \gg F$ and P_F is relatively low, meaning that $E_P \ll E_Q$ [Cheryan, 1986; 1998].

The expression may be rewritten as:

$$\Delta P_f = (P_i - P_o) + \frac{\rho}{2}(\alpha_i U_i^2 - \alpha_o U_o^2) + \rho g(Z_i - Z_o) \text{ (Pa)} \quad (2.13c)$$

At the flows and pressures in the present investigation, the velocity terms are negligibly small and the equation reduces to:

$$\Delta P_f = (P_i - P_o) + \rho g(Z_i - Z_o) \text{ (Pa)} \quad (2.13d)$$

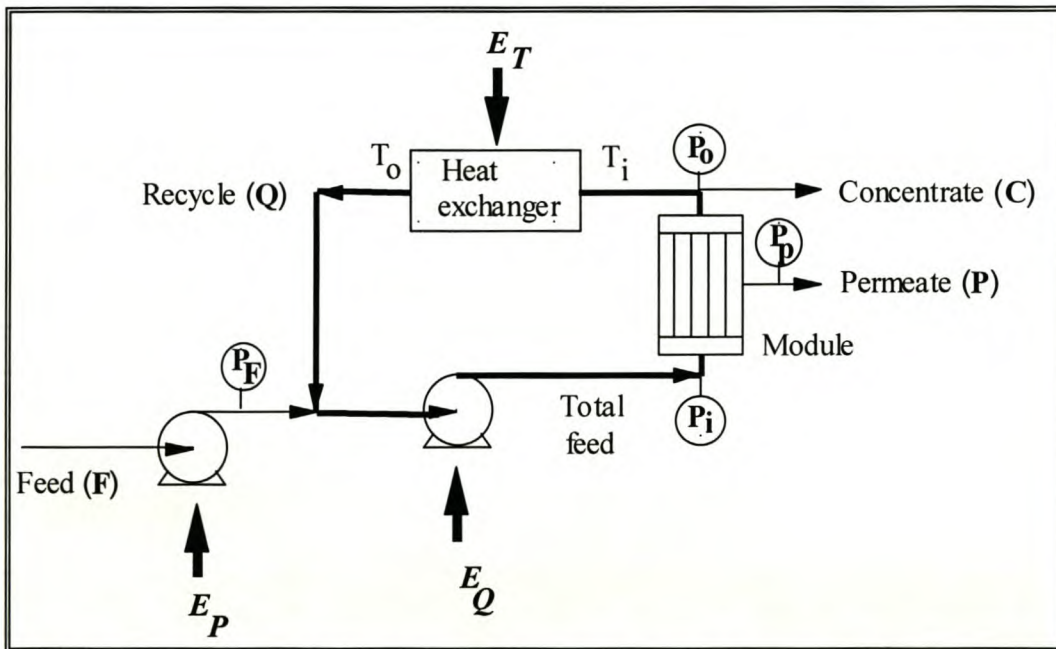


Figure 7: Schematic diagram of energy requirements for a typical membrane operation.
 [Cheryan, 1986; 1998]

2.5.3 Boundary Layer Development and Flow Destabilization

In order to understand the basics of the UF process better, it will be useful to review the fundamental aspects of viscous fluid flow past solid surfaces.

2.5.3.1 Hydrodynamic Boundary layer

A *boundary layer* develops whenever a fluid flows past a porous or non-porous surface. In the case of a lumen-fed membrane of tubular or capillary geometry, the fluid (feed water) enters the fibre inlet at an assumed constant bulk velocity (U_b). Figure 8, adapted from Incropera and De

Witt [1985] is a schematic representation of the development of the hydrodynamic and mass transport boundary layers at the inlet to a porous tube of inside diameter D .

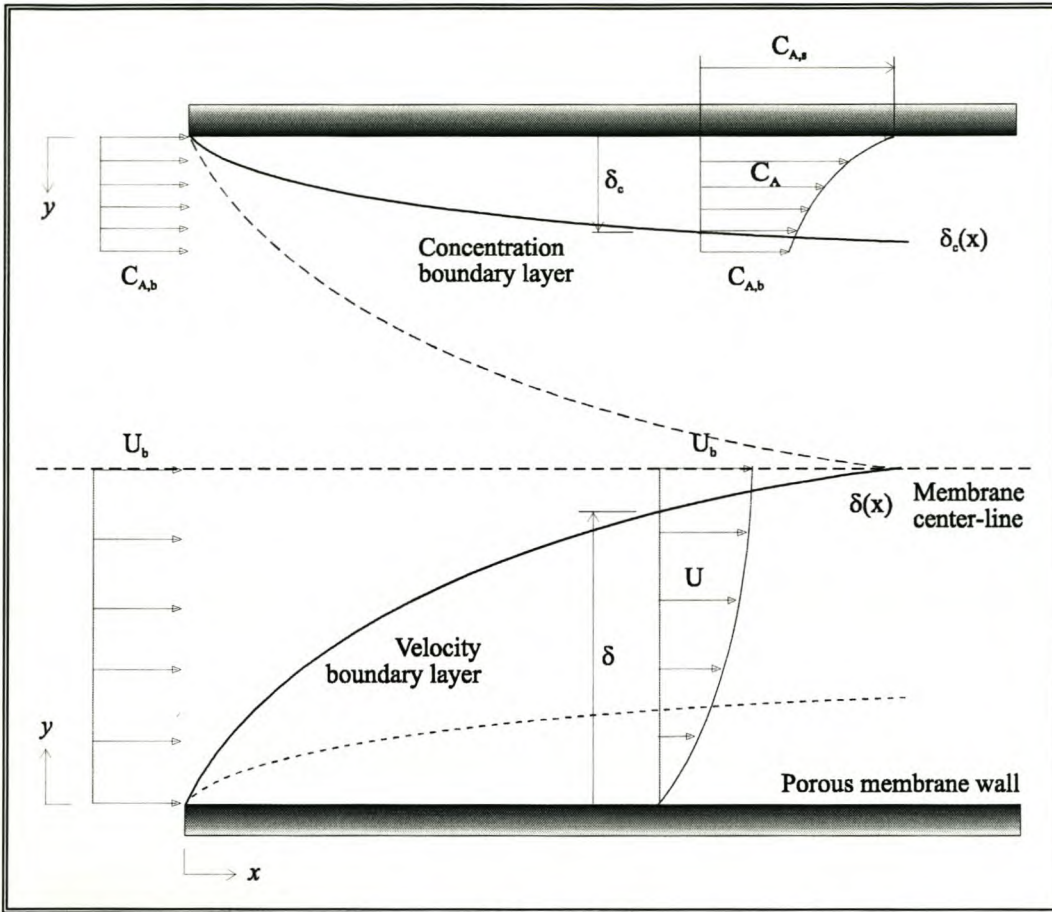


Figure 8: Velocity and boundary layer development at the inlet to a porous tube.
 [Incropera and De Witt, 1985]

The axial velocity of fluid particles in contact with the solid surface is assumed zero (no-slip condition). As a result of shear stresses (τ_s) acting in planes parallel to the fluid velocity, these particles retard the motion of particles in adjacent fluid layers; until at a distance:

$$y = \delta_h \tag{2.14}$$

from the surface, the effect becomes negligible. The quantity δ_h is termed the *hydrodynamic boundary layer thickness*, and is defined as the value of y for which:

$$U = 0.99 \times U_b \tag{2.15}$$

From the leading edge (tube inlet) δ_h increases with increasing distance until, at an axial distance $x_{fd,h}$ from the tube inlet, it merges with the boundary layer from the opposite inner surface. From this point forward in the tube, the flow is termed *fully developed*. The hydrodynamic entry length

$x_{fd,h}$ required for fully developed laminar and turbulent flow respectively, is [Cheryan, 1986; Incropera and De Witt, 1985]:

$$\left(\frac{x_{fd,h}}{d_h} \right)_{lam} \approx B Re_D \quad (2.16)$$

$$10 \leq \left(\frac{x_{fd,h}}{d_h} \right)_{turb} \leq 60 \quad (2.17)$$

where the Reynolds number is defined as :

$$Re_D = \frac{\rho U_m d_h}{\mu} \quad (2.18)$$

for the different flow regimes:

$Re_D < 2\,000$; laminar

$Re_D \approx 2\,300$; transition to turbulent regime begins

$Re_D \geq 4\,000$; fully developed turbulent flow

where B is a constant between 0.029 and 0.05, d_h is the hydraulic diameter (equal to inner diameter D in the case of a cylinder), ρ is the density, μ is the dynamic viscosity of the fluid and U_m is the mean or average velocity in the flow field. For laminar flow, the following relationship applies:

$$U_b = \frac{U_m}{0.5} \quad (2.19)$$

2.5.3.2 Mass transport boundary layer

Similarly to the velocity boundary layer, a *mass transport (concentration) boundary layer* develops if the concentration of some component A at the surface $C_{A,s}$ differs from the free stream or bulk concentration $C_{A,b}$. This is the case when solvent (component B) is removed at the surface, as in membrane filtration. Solvent and solutes are transported to the surface as a result of convective flow. As component B is removed at the surface, the concentration of component A increases above that of the bulk, creating a concentration gradient for diffusive back flow into the bulk stream from the surface of the membrane.

Steady state is reached, usually after a few seconds [Howell and Velicangil, 1982], when the convective flow of component A through the boundary layer to the surface equals the convective flow of component A through the membrane, plus the diffusive flow of component A away from the surface into the bulk [Howell *et al.*, 1993]:

$$JC_A + D_{AB} \left(\frac{dC}{dy} \right) = JC_{A,p} \quad (2.20)$$

where D_{AB} is the diffusivity of the solute A in solvent B (m^2/s), and $C_{A,p}$ is the solute concentration in the permeate (g/L). Assuming D_{AB} independent of solute concentration, eq. (2.20) can be integrated between the boundary conditions:

$$C = C_{A,s} \text{ at } y = 0 \text{ (surface condition); and}$$

$$C = C_{A,b} \text{ at } y = \delta_c \text{ (bulk condition)}$$

This yields the equation:

$$J = \left(\frac{D_{AB}}{\delta_c} \right) \ln \left(\frac{C_{A,s} - C_{A,p}}{C_{A,b} - C_{A,p}} \right) \quad (2.21)$$

where the quantity (D_{AB}/δ_c) is the mass transfer coefficient k (m/s), and according to Rautenbach and Albrecht [1989], it should be interpreted as the mass transfer coefficient at zero flux. This phenomenon, whereby a dynamic layer of retained components accumulates on the membrane surface, is known as *concentration polarization* (CP).

As illustrated schematically in Figure 8, the mass transport boundary layer is usually much thinner than the momentum boundary layer [Howell *et al.*, 1993]:

$$\delta_c \ll \delta_h \quad (2.22)$$

Analogously to the hydrodynamic boundary layer thickness, the mass transport boundary layer thickness δ_c is defined as the value of y for which [Incropera and de Witt, 1985]:

$$\frac{C_{A,s} - C_A}{C_{A,s} - C_{A,b}} = 0.99 \quad (2.23)$$

This means that although the solute concentration in the boundary layer approaches the bulk concentration, it is never reached. It is, however, reasonable to assume that in the fluid region adjacent to the membrane, there is [Howell *et al.*, 1993]:

- ◆ a bulk region of uniform concentration $C_{A,b}$; and
- ◆ a film on the membrane surface across which the solute concentration changes from the bulk concentration $C_{A,b}$ to the membrane surface concentration $C_{A,s}$.

This is known as the *film model*, and was used implicitly in the derivation of eqs. (2.13) to (2.16). For a tubular system, the mass transfer correlation for forced convection can be used to estimate the mass transfer coefficient (k), as follows [Incropera and de Witt, 1985]:

$$\frac{kD}{D_{AB}} \equiv Sh = E Re^a Sc^b \left(\frac{L}{D}\right)^f \left(\frac{\mu_s}{\mu_b}\right)^g \quad (2.24)$$

$$Sc \equiv \frac{\nu}{D_{AB}} \quad (2.25)$$

$$\nu = \frac{\mu}{\rho} \quad (2.26)$$

where E , a , b , f and g are constants for a particular flow regime and prescribed geometry. The *Sherwood* number (Sh) is a dimensionless concentration gradient at the membrane surface, i.e. it provides a measure of the convection mass transfer occurring at the membrane surface. The *Schmidt* number (Sc), also dimensionless, is a ratio of the momentum and mass diffusivities, in other words it provides a measure of the relative effectiveness of momentum and mass transport by diffusion in the hydrodynamic and concentration boundary layers. The term ν (m^2/s) is the kinematic viscosity of the fluid in the mass transport boundary layer.

Under laminar flow conditions ($Re_D < 2\,000$) the aspect ratio (L/D) is significant, but for turbulent conditions Sh is independent of (L/D), thus $f = 0$. The viscosity ratio may be significant in the case of ultrafiltration if the viscosity is concentration dependent, in which case the constant $g \neq 0$. For laminar and turbulent flow respectively, the following semi-empirical relationships have been used [Incropera and de Witt, 1985]:

$$\frac{kD}{D_{AB}} \equiv Sh = 1.62 Re^{0.33} Sc^{0.33} \left(\frac{D}{L}\right)^{0.33} \left(\frac{\mu_s}{\mu_b}\right)^g, \text{ laminar} \quad (2.27)$$

$$\frac{kD}{D_{AB}} \equiv Sh = 0.04 Re^{0.75} Sc^{0.33} \left(\frac{\mu_s}{\mu_b}\right)^g, \text{ turbulent} \quad (2.28)$$

From eqs. (2.20) to (2.26) it is evident that the mass transfer coefficient is a function a number of parameters. These are:

- ◆ feed flow velocity (U_m);
- ◆ diffusion coefficient of the solute (D_{AB});
- ◆ viscosity of the bulk feed solution (μ_b) and at the surface (μ_s);
- ◆ density of the bulk feed solution (ρ); and
- ◆ module shape and dimensions.

It should be noted that on the size scale of macromolecules and particles, the diffusivity (D_{AB}), as used in eq. (2.20) onwards, would be so close to zero as to be insignificant. However, the fluid motion (suction from the permeate side of the membrane) would carry particles to the surface, while cross-flow fluid motion would cause the particles to “diffuse” away from the surface. In this way a steady state mass transport boundary layer thickness would still be established in the case of cross-flow filtration, while there would be no upper limit on the boundary layer thickness for dead-end filtration.

2.5.3.3 Flow Destabilization

The two most important parameters affecting the mass transfer coefficient in cross-flow filtration are the *feed flow velocity* and the *diffusion coefficient*. It should be noted that CP is the result of solvent removal under a pressure gradient. However, the film model assumes cross-flow in only one direction through the porous tube. If the *pressure gradient* is increased or decreased, or the *hydrodynamics* of the flow field adjusted by increasing or decreasing the cross-flow *velocity* or *direction*, the concentration boundary layer will reach a new steady state thickness. The same applies for filtration in dead-end mode, where all feed water entering the module exit as permeate, and all foulants entering the module in the feed stream accumulate on the membrane surface as a cake or adsorbed layer.

The film model also does not take into account the shape and physico-chemical properties of the solutes present in the feed stream. Although CP may be reversible by any of the above procedures, the fact that solute particles are in close proximity with one another and the membrane surface material for extended periods of time will increase the probability of secondary interactions between particles and the surface. Solutes will also align themselves in the direction of the flow field and if these solutes are elongated particles or other suspended solids, it will result in a "directional" fouling layer parallel to the surface and in the direction of flow. When water is circulated through the lumen in cross-flow, with or without removal of permeate, a momentum is associated with the travelling body of water. When a valve between

the recycle pump and the feed (inlet) side of the module is closed rapidly (1 s or less), there is a sudden loss of momentum of the water between the pump and the valve. However, on the concentrate (outlet) side the momentum on the body of water exiting the module is conserved, i.e. the concentrate will retain its momentum while the recycle pump is running and concentrate is drawn out of the module. If the flow of water from the permeate to feed side of the membrane is unobstructed, the concentrate exiting the module will be replaced by permeate.

However, in the fractions of a second after closure of the inflow valve, a shock wave is created on the concentrate side of the membrane until reverse flow is established. During this period the fouling layer, which offers less resistance to be moved inward than the membrane itself, will be dislodged from the surface because of the shock wave. Consequently the integrity of the fouling layer will be partially or completely disrupted or destroyed, and the debris can be flushed out of the lumen.

2.5.4 Limiting Flux

When pure solvent passes through a membrane wall, the only *resistance* to solvent flow is the resistance of the membrane itself R_m (m^{-1}). According to the *resistance model* of flux, this pure-water flux (PWF) can be expressed as:

$$J_w = \frac{dP}{\mu R_m} \quad (2.29)$$

where J_w is the pure-water flux (m/s), dP the effective trans-membrane pressure (Pa) and μ is the fluid viscosity (kg/m.s). The effective dP is calculated from the relationship:

$$dP = \frac{(P_i + P_o)}{2} - P_p \quad (2.30)$$

where P_i and P_o refer to the module *feed* and *concentrate* pressures, and P_p the down-stream *permeate* back-pressure respectively.

In the presence of *solutes in the feed stream*, additional resistances contribute to a larger total resistance R_{tot} (m^{-1}) observed on the membrane surface. Under the same applied pressure, the expected process flux J_v would be lower than the PWF, expressed by the resistance in series model as [Mulder, 1991]:

$$J_v = \frac{dP}{\mu R_{tot}} \quad (2.31)$$

$$R_{tot} = R_m + R_{cp} + R_c + R_a \tag{2.32}$$

where R_m (m^{-1}) is the membrane resistance, R_{cp} (m^{-1}) and R_c (m^{-1}) are the reversible concentration polarization and cake (or gel) layer resistances and R_a (m^{-1}) is the irreversible adsorption resistance. The combined effects of concentration polarization, cake layer formation and adsorption thus increase the total resistance and consequently decrease the flux. However, operation under high trans-membrane pressure may cause compaction of the membrane, thus increasing the membrane resistance and lowering flux.

As the applied dP is increased, the process flux will increase proportionally (pressure-controlled region) until a point is reached where the flux becomes independent of applied pressure. This signifies the start of the mass transfer controlled region. Operation at high shear rates, or low bulk concentration of solutes, will result in an increase in the limiting flux, J_{lim} as can be seen in Figure 9 [Howell *et al.*, 1993].

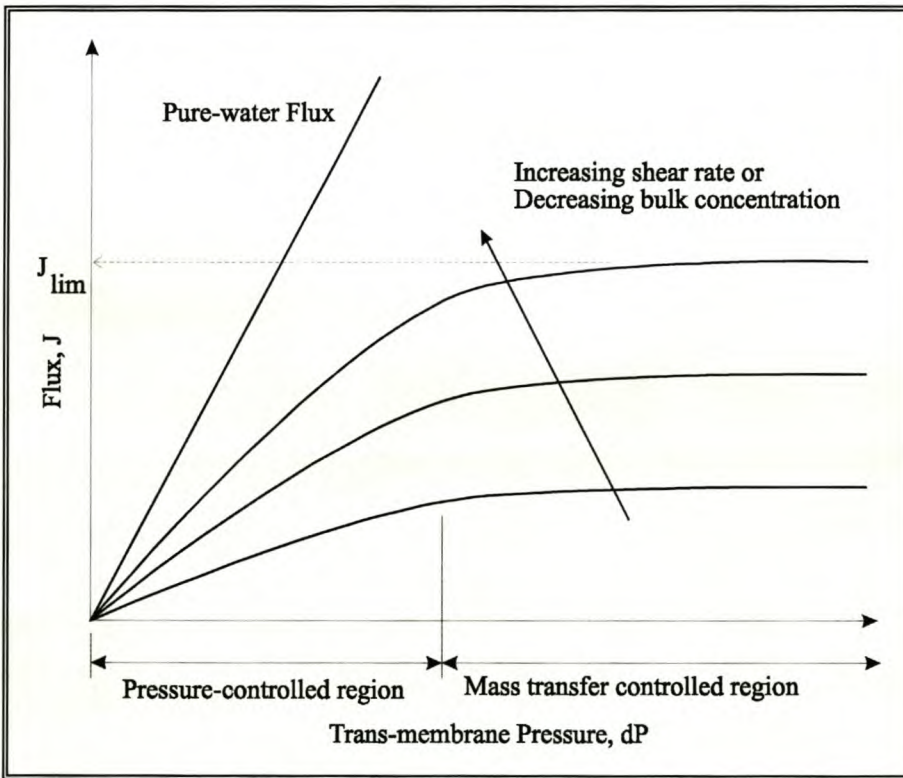


Figure 9: Pressure-flux relationships denoting the pressure-controlled and mass transfer controlled regions.

Although operation in the mass transfer controlled region will produce a higher flux than in the pressure-controlled region, compaction of the fouling layer may occur, resulting in additional difficulties in fouling layer removal. Previous researchers have recommended that membrane

processes be operated at *the minimum pressure* in the *mass transfer controlled region* [Cheryan, 1986; 1998], in other words, at the transition from the pressure-controlled region to the mass transfer controlled region. Intermittent flow destabilization could also reduce these resistances and consequently increase the average process flux over extended periods of operation.

2.5.5 Temperature Dependency of Fluid Properties

2.5.5.1 Effect on Viscosity

The viscosity of aqueous solutions is a function of the *temperature* and *pressure* as well as the *solids concentration* [Miller, 1989; Reid *et al.*, 1977]. Qualitatively, an increase in process fluid temperature will reduce the viscosity while an increase in operating pressure will increase the viscosity, but to a much lesser extent. The dependency of viscosity on pressure is more pronounced for petroleum products and liquids with more complex molecular structures than for pure water. According to Miller [1989] the viscosity of water at 34.5 MPa is 1.14 times the viscosity measured at standard atmospheric pressure. Thus, in the present work, liquid viscosity will be adjusted only for temperature. The relationship between temperature and liquid viscosity has been described by Reid *et al.* [1977] for pure water as:

$$\log_{10}(\mu \times 10^{-3}) = \left(\frac{230.298}{T_K - 146.797} \right) - 1.5688 \quad (2.33)$$

where μ is the dynamic viscosity of water (kg/m.s) and T_K is the absolute water temperature (K). Conversion between absolute (T_K) and relative (T_C) temperature takes the following form [Himmelblau, 1982]:

$$T_K = T_C + 273.15 \quad (2.34)$$

Rearranging eqs. (2.33) and (2.34), the viscosity of pure water can be calculated as:

$$\mu = \frac{a \log \left(\frac{230.298}{T_C + 126.353} \right) - 1.5688}{1000} \quad (2.35)$$

Another correlation is given by White [1994]:

$$\mu(T) = \mu_0 \times \exp(7.003 \times Z^2 - 5.306 \times Z - 1.704) \quad (2.36)$$

where $\mu_0 = 1.788 \times 10^{-3}$ kg/m.s and Z is a temperature dependent parameter as defined by the following equation:

$$Z = \frac{273}{(273 + T_C)} \tag{2.37}$$

Another relationship commonly used for water temperatures between 5 and 40 °C is the following [Crozes *et al.*, 1997; Glucina *et al.*, 1998]:

$$\mu(T_C) = \mu_{20} \times \exp [-0.0239 \times (T_C - 20)] \tag{2.38}$$

where μ_{20} is the water viscosity at 20 °C, and according to Geankoplis [1993], μ_{20} has a value of 1.005×10^{-3} kg/m.s. Figure 10 shows the agreement between pure-water viscosity values reported in the literature [Geankoplis, 1993] and values calculated from eqs. (2.35), (2.36) and (2.38) for the temperature range between 5 and 40 °C, which is within the temperature range of potable water UF applications.

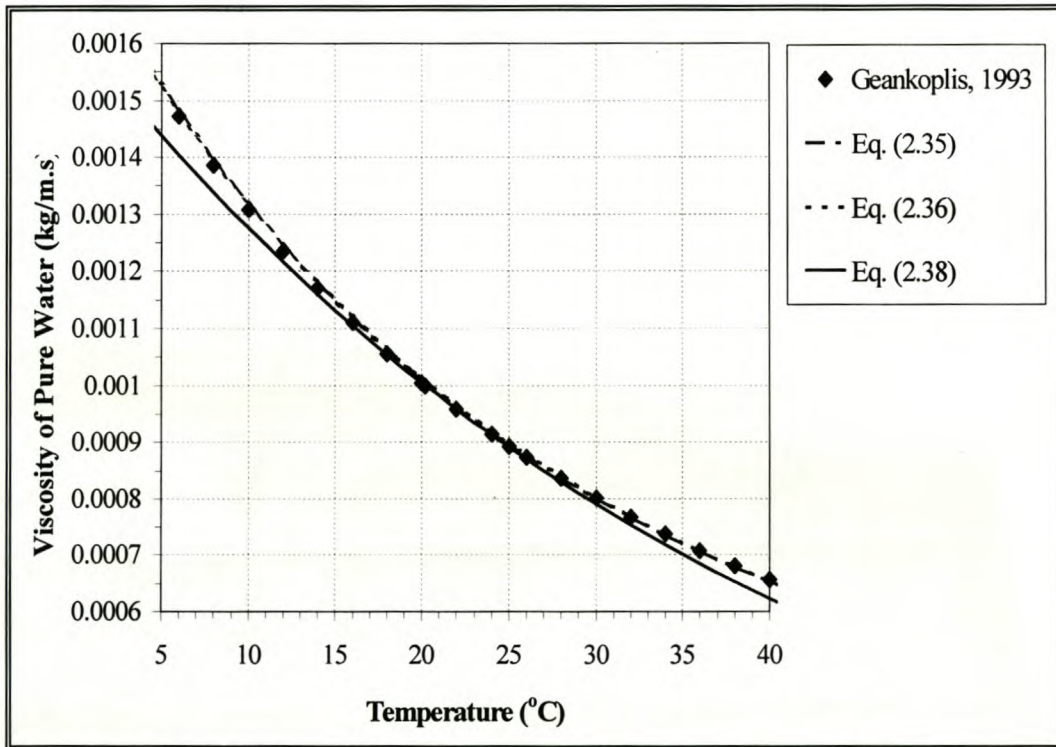


Figure 10: Effect of temperature on pure-water viscosity as calculated by eqs. (2.35), (2.36) and (2.38) in the range of 5 to 40 °C.

The viscosity bias errors B_μ (%), shown in Figure 11, were calculated as:

$$B_\mu = \left(\frac{\mu_{calc} - \mu_{true}}{\mu_{true}} \right) \times 100 \tag{2.39}$$

where μ_{calc} is the calculated viscosity value and μ_{true} is the viscosity from Geankoplis [1993].

Comparing the three equations, Figure 11 indicates that over the range of 15 to 25 °C eq. (2.38) gives the most accurate prediction of the viscosity; with bias values ranging between -0.7 and -0.2 %. Eqs. (2.35) and (2.36) give viscosity bias values of +0.9 to +0.6 and +0.8 to +0.6 % respectively. Eq. (2.38) will thus be used to calculate water viscosity in Case Study 1, as the day time water temperatures ranged between 15 and 25 °C at Mon Villa. For Case Study 2 the water temperatures at Paradyskloof ranged between 8 and 17 °C. Thus it was decided to use eq. (2.36) for the calculation of water viscosity in Case Study 2. Flux values will be corrected to a flux value J_{20} at a reference temperature of 20 °C with the following relationship:

$$J_{20} = J_T \times \frac{\mu_T}{\mu_{20}} \tag{2.40}$$

where J_T is the measured flux at the water temperature, while μ_{20} and μ_T are the water viscosity values at 20 °C and the water temperature respectively.

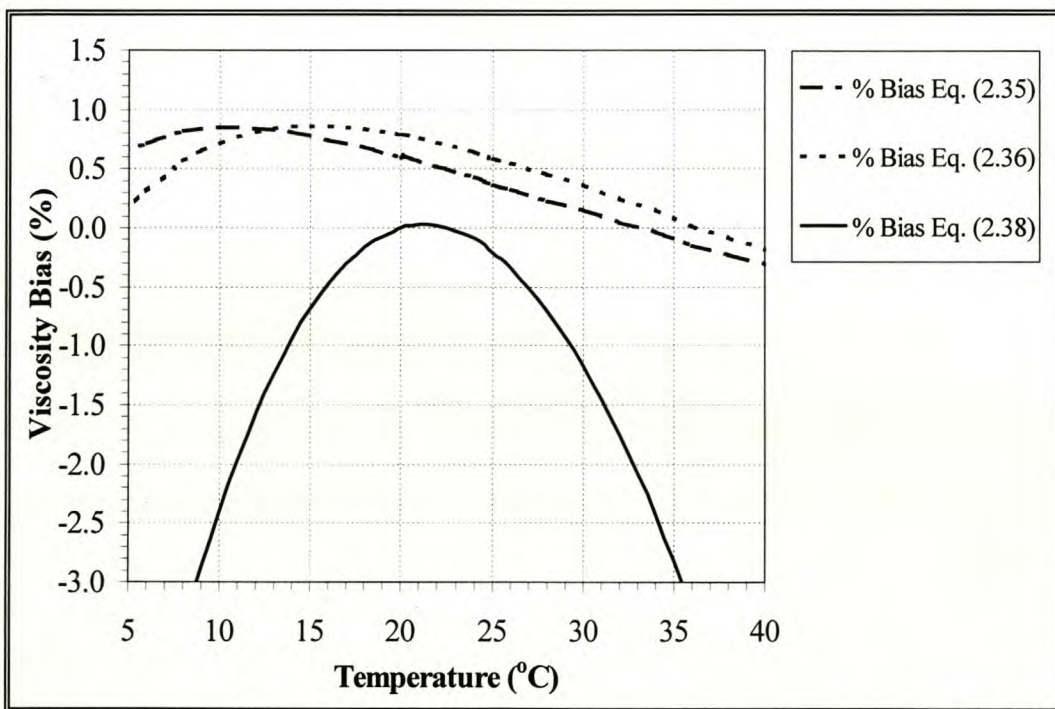


Figure 11: Percentage viscosity bias of equations (2.35), (2.36) and (2.38) in the prediction of the viscosity of pure water as a function of temperature.

From eq. (2.31) it follows that filtration at a high temperature should produce a higher flux than at a low temperature. Temperature may also have an effect on the interactions between the membrane and particles in the feed water, and this may influence the cake or gel layer resistance [Delgrange *et al.*, 1998]. Although some authors [Bacchin *et al.*, 1995; 1996] have tried to predict interaction effects for clay model suspensions, no reliable mathematical models or model

foulants exist to describe the complex behaviour of the mixture of organic and inorganic matter present in surface waters.

2.5.5.2 Effect on Density

Generally, liquid density *decreases* with increasing temperature, and to a lesser extent, density *increases* with increasing pressure. Slightly different values are cited in the literature for the density of water at both 60 and 68 °F (15.6 and 20 °C) [Miller, 1989]. A standard used in this work to calculate liquid densities is the PTB [1971] equation, which is plotted in Figure 12:

$$\begin{aligned} \rho_w = & 9.998395639 \times 10^2 + 6.798299989 \times 10^{-2} T_C \\ & - 9.106025564 \times 10^{-3} T_C^2 + 1.005272999 \times 10^{-4} T_C^3 \\ & - 1.126713526 \times 10^{-6} T_C^4 + 6.591795606 \times 10^{-9} T_C^5 \end{aligned} \tag{2.41}$$

where ρ_w (kg/m³) is the water density at standard atmospheric pressure of 101.325 kPa, and T_C is the fluid temperature in °C.

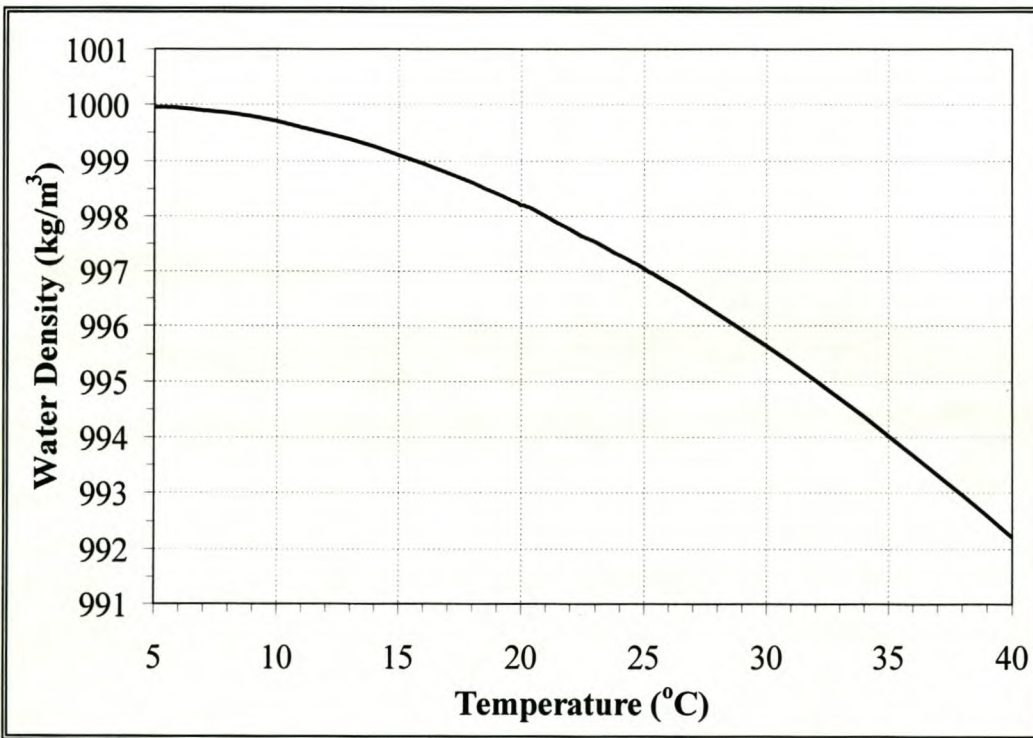


Figure 12: Effect of temperature on pure-water density as calculated by eq. (2.41) in the range of 5 to 40 °C.

2.6 CONCLUSIONS

In this chapter it was shown to what extent membrane morphology and surface characteristics influence membrane filter performance. Existing membrane production protocols were also presented to indicate to what extent membrane geometry determines module design. Different module designs were then compared according to a number of design objectives.

The theory necessary to describe UF membrane performance in terms of pore size distribution and retentivity demonstrated that the bubble point technique and direct microscopic observation method may prove useful as quality control measures during membrane production, but that these methods have little use in predicting actual process flux. One of the few practical methods to predict process flux is the so-called challenge test. The different operating modes, being dead-end and cross-flow operation, were also discussed in terms of energy consumption.

A general description of boundary layer development and concentration polarization was presented to illustrate the dynamic behaviour of solutes in the feed stream, and flow destabilization was cited as a possible method to interrupt the development of these boundary layers or to destroy the formed mass transfer boundary layer. A qualitative description of limiting flux behaviour illustrated the concepts of membrane resistance and fouling resistances during membrane filtration. It was concluded that operating near the minimum pressure in the mass transfer controlled region is recommended, in order to maximize the process flux, and hence minimize the specific energy consumption.

Finally the temperature-dependent variation in viscosity and density was demonstrated for pure water. These values were used to normalise flux values to a standard temperature of 20 °C in subsequent calculations. No correction was made for possible pressure- and concentration-dependent variation in either viscosity or density.

Chapter 3: UF OF AQUEOUS SOLUTIONS

3.1 GUIDELINES FOR POTABLE WATER QUALITY

The *nature* and *concentration* of organic and inorganic material found in raw water sources are affected by both *geographical location* and *seasonal fluctuations*. Characterization of these foulants is thus of utmost importance in developing a comprehensive strategy to combat membrane fouling when ultrafiltering aqueous solutions for portable water production.

3.1.1 Microbial Quality and Indicator Organisms

The primary health risks associated with potable water are of biological origin [Anselme and Jacobs, 1996]. A variety of pathogens such as bacteria, viruses, worms and protozoa may transmit water-borne diseases such as gastroenteritis, giardiasis, hepatitis, typhoid fever, cholera, salmonellosis, and dysentery as well as eye, ear and nose infections. Other microorganisms present in surface waters include fungi, algae, rotifers and crustaceans. Infections may be contracted by [DWAF, 1996] drinking of contaminated water, recreational exposure to contaminated water, inhaling contaminated aerosols, or the consumption of raw food such as irrigated vegetables or raw shellfish that have been exposed to polluted water supplies.

For *technical* and *economic* reasons it would be impractical to test potable water supplies for all pathogens that may be present. Since most water-borne diseases are caused by pathogens typically transmitted by the faecal-oral route, *indicator organisms* are generally used for the routine monitoring of the potential presence of such pathogens. These indicator organisms include heterotrophic bacteria, coliform and faecal coliform bacteria, coliphages, enteric viruses and protozoan parasites [DWAF, 1996], which are discussed briefly in Appendix A. More information concerning indicator organisms and testing methods is available in Genthe and Kfir [1995], and Genthe and du Preez [1995].

Table 3 lists the relative sizes of some microorganisms discussed in this section and in Appendix A. As the pores in UF membranes are in the range of 1 to 50 nm, bacteria as well as some viruses and other pathogenic organisms will be removed from waters containing them.

Table 3: Relative sizes of selected microorganisms

Microorganism	Size (µm)	Microorganism	Size (µm)
Bacteria	0.15-4.0	Protozoan Parasites	
Spherical	0.5-4.0	<i>Giardia lamblia</i>	5-15 x 10-20
Rod-shaped	0.3-1.5 x 1-10	Ovoid cyst of <i>Giardia</i>	6 x 10
<i>E. Coli</i>	0.5 x 2.0	<i>Entamoeba histolytica</i>	15 x 25
Spiral	< 50 in length	Cyst of <i>Entamoeba</i>	10 x 15
Enteric Viruses	0.01-0.3	Proteins (10 ⁴ -10 ⁶ kDa)	0.002-0.1
Adenoviruses	0.07-0.9	Enzymes	0.002-0.005
Enteroviruses	0.02-0.3	Antibiotics, Polypeptides	0.0006-0.0012
<i>Polio virus</i>	0.01		
Reoviruses	0.06-0.08		

[Doetsch and Cook, 1973; Knight, 1975; Brock and Brock, 1978; Gelman and Williams, 1983; Tchobanoglous and Schroeder, 1985; Tate and Arnold, 1990].

3.1.2 Aesthetic Quality of Water

A number of naturally occurring constituents in water supplies impart certain physical or aesthetic qualities to the water, although these qualities may or may not contribute to the suitability of water supplies for domestic use. These aesthetic qualities *are physical appearance* of the water (colour and turbidity), as well as the *odour* and *taste* [APHA, 1992; DWAF, 1996]:

3.1.2.1 Turbidity

Turbidity is a measure of the *light-scattering ability of water*, which is indicative of the *suspended matter* concentration in the water. Suspended matter usually is a mixture of inorganic matter such as clay and soil particles, and organic matter. Turbidity is measured in Nephelometric Turbidity Units (NTU).

Without any external disturbances in water (such as forced convection), the settleable material fraction will tend to settle to the bottom gradually, while smaller particles and colloidal substances will be kept in suspension by Brownian motion and mutual electrical repulsion between particles. The addition of a flocculant effectively neutralises these electrical charges, with the result that the particles start to cohere and settle out of solution.

The possible occurrence of microorganisms is also associated with turbidity; therefore low turbidity minimizes the potential for the transmission of infectious diseases. A maximum turbidity of 1.0 NTU is recommended at the point of chlorination for the effective disinfection of potable waters. The reason for this is that microbial growth usually occurs on the surface of particulate matter and inside loose, naturally occurring flocs. Viruses and bacteria are also readily adsorbed by river silt. During conventional treatment of potable water sources, microorganisms may become entrapped in the flocs formed during the coagulation stage. When breakthrough of flocs occur during the sand filtration stage of conventional water treatment, these entrapped microorganisms will be shielded from the oxidizing effects of chlorine.

3.1.2.2 Colour

Colour in natural water supplies is caused by natural sources of coloured natural organic matter (NOM) such as humic acids (HA) and fulvic acids (FA), as well as metals such as iron and manganese. Industrial effluents and discharges from the pulp and paper, and textile industries may also be the cause of colour in water supplies. The *true colour* of a water sample is measured after the turbidity has been removed by filtering the sample through a 45 µm filter, while *apparent colour* includes the colour and appearance of suspended matter.

Colour is measured by a visual comparison method in Pt-Co colour units or Hazen (°H), or by spectrophotometric methods. With the latter method, colour characteristics are reported as the dominant wavelength in nm, the hue, the percentage luminance or the percentage purity. Although no direct health effects result from the presence of colour in water (except from toxic colourants), some colourants such as iron (reddish-brown stains) and manganese (dark-brown-to-black stains) compounds may stain clothes and household appliances.

3.1.2.3 Taste and Odour

Odour and taste depend on the contact of a *stimulating substance with the appropriate human cell receptor*. Potable water supplies should not have any discernible taste or odour. Taste and odour may result from the presence of biological organisms such as algae, or from pollution by industry, domestic seepage or agriculture. The presence of dissolved gases such as hydrogen sulphide (H₂S), or chlorinated products of phenolic compounds may also be the cause of increased tastes or odours. Organic materials causing tastes and odours may be removed by adsorption on activated carbon.

3.1.3 Water Quality Classification Systems

Historically, international water quality guidelines have been developed with the emphasis on *cut-off values* applicable to various *pollutants* in water supplies [WHO, 1984; WHO, 1993].

In South Africa a second value, called the *maximum allowable limit*, has been introduced and used on occasion [SABS, 1984]. A third value, the *crisis limit* (that indicates water sources unsuitable for human consumption without suitable treatment), was proposed by Kempster and Smith [1985]. In such instances the implication would be that urgent measures be undertaken to rectify the quality of such water sources.

In South Africa a *tiered approach* has been adopted recently whereby water supplies are classified in four classes according to the suitability for drinking-water use [DWAF, 1996; Kempster *et al.*, 1997]. In Table 4 the tiered approach is illustrated for 20 representative indicator organisms (described in Appendix A), inorganic constituents and a number of aesthetic qualities (discussed in section 3.1.2):

- ◆ **Class 0:** This is the ideal water quality, i.e. water that is suitable for lifetime use, with no adverse health effects on the user. No further treatment is necessary.
 - ◆ **Class 1:** This water is safe for lifetime use, but does not meet the ideal water quality standard, which means that there may be rare instances where (usually mild) adverse health effects may occur. Aesthetic effects may also be apparent. Home treatment should be sufficient to shift the quality of such waters to Class 0.
 - ◆ **Class 2:** Adverse health effects are unusual for short-term use of this water in limited quantities, but may become common especially with prolonged use over many years, or with lifetime use. Water of this class may be used for short-term periods or in emergencies, but treatment is required to render the water fit for continued use.
 - ◆ **Class 3:** This water contains pollutants in the concentration range where serious health effects might be anticipated, especially in infants or elderly people with short-term use. Water in this class is not suitable for potable use without adequate (conventional or advanced) treatment to shift the water quality to a lower class.
-

Table 4: Hierarchical classification of potable water quality

Constituent (mg/L unless stated otherwise)	Class 0	Class 1	Class 2	Class 3	Thee-waters-kloof
Total dissolved solids	0-450	450-1000	1000-2450	>2450	93
Electrical conductivity (mS/m)	0-70	70-150	150-370	>370	
Heterotrophic plate count (Colonies/1 mL)	0-100	100-1000	>1000	>1000	188* and 34500**
Total coliforms (Colonies/100 mL)	0-5	5-100	>100	>100	96*
Faecal coliforms (Colonies/100 mL)	0	0-1	1-10	>10	10*
Turbidity (NTU)	0-1	1-5	5-10	>10	5-20
Apparent colour (Pt-Co units)	15	>15	>15	>15	25-70 [#]
pH (pH Units)	6.0-9.0	5-6 or 9.0-9.5	4-5 or 9.5-10	< 4 or >10	5.5
Nitrate & Nitrite (as N)	0-6	6-10	10-20	>20	
Fluoride	0-1.0	1.0-1.5	1.5-3.5	>3.5	
Sulphate	0-200	200-400	400-600	>600	
Magnesium	0-30	30-70	70-100	>100	
Sodium	0-100	100-200	200-400	>400	
Chloride	0-100	100-200	200-600	>600	
Total iron (Fe ²⁺ + Fe ³⁺)	0-0.1	0.1-0.2	0.2-2.0	>2.0	0.2-0.6 [#]
Manganese	0-0.05	0.05-0.1	0.1-1.0	>1.0	
Zinc	0-3.0	3.0-5.0	5.0-10.0	>10.0	
Arsenic	0-0.010	0.010-0.050	0.050-0.2	>0.2	
Cadmium	0-0.005	0.005-0.010	0.010-0.020	>0.020	
Ammonia (as N)	0-1	1-2	2-10	>10	

Adapted from [DWAF, 1996; Kempster *et al.*, 1997].

* Raw water sample analysed by CSIR, Stellenbosch, 27 September 1995.

** Feed tank sample analysed by CSIR, Stellenbosch, 27 September 1995.

Samples analysed on-site, 27 July 1998 to 3 February 1998.

The last column in Table 4 lists typical concentrations of a number of constituents in raw water and feed tank grab samples from the Theewaterskloof/Helderberg irrigation scheme. Chemical and microbiological analyses of water samples were performed by the Division of Water, Environment and Forestry Technology, CSIR in Stellenbosch. Turbidity and apparent colour analyses were regularly done on-site at Spier Home Farms during the investigation period of February 1995 to May 1999 for Case Study 1 described in Chapter 4.

It can be seen from Table 4 that the raw water heterotrophic plate count and total coliform levels fall within the recommended limit for Class 1 water supplies, but due to concentrate recycle to the feed tank the feed tank plate count had risen within a week to a level far exceeding that of Class 3 waters. However, the faecal coliforms and iron levels in the Theewaterskloof/Helderberg raw irrigation water are above the recommended limit for Class 0 and Class 1 water sources. In other words, this water is safe for short-term or emergency use but treatment is necessary in order to render the water fit for continued use.

3.1.4 Natural Organic Material

3.1.4.1 Characterization and Structure

About 80 % of the dissolved organic carbon in surface waters consists of a variety of molecules loosely termed NOM [Higgo *et al.*, 1993; Jucker and Clark, 1994; Leenheer, 1994] which can be distinguished in two groups, namely HA and FA. The remaining 20 % are made up of identifiable compounds that include carbohydrates, carboxylic acids, amino acids and hydrocarbons. Being found in soils, NOM is often present in surface waters in low concentrations, which may vary seasonally.

NOM has no precisely defined structure but is known to contain *polyphenolic* molecules with a MMCO of 5 000 to 500 000 Da that cause the yellow-black colour in Cape Brown Water (CBW), as discussed in section 3.1.2.2. Generally HA structure has been shown to vary with salt content, pH, and concentration. At low concentrations with little salt present, it has a *linear* structure at pH values ranging from 6.5-9.5. At high concentrations in the presence of salts, it forms a *spherocolloidal* structure.

The size difference of a HA molecule at different ionic strengths and pH values also has an effect on its diffusion properties. At high ionic strength it has a higher diffusivity because of its coiled structure. The same phenomenon is observed at low pH and low ionic strength.

3.1.4.2 Effects of NOM on Potable Water Quality and UF

Apart from the aesthetic undesirability of NOM in potable water, the polyphenolic molecules are known to form *complexes* with *heavy metals* (Al^{3+} , Fe^{3+} , Ca^{2+} and other cations) and *pesticides* [Rashid, 1970; Stefanova *et al.*, 1993; Higgo *et al.*, 1993; Leenheer, 1994; Jucker and Clark, 1994; Nyström *et al.*, 1996]. It has also been observed by these researchers that this cross-link bonding of metals with NOM forms a stable, more dense structure than NOM in the absence of cations, which may be more difficult to remove from the membrane surface by hydraulic and mechanical methods.

NOM is also considered the *precursor* of organic halogenated compounds formed by disinfection of drinking water with chlorine [Agui *et al.*, 1992]. In addition, disinfection by ozonation may lead to the release of heavy metals or pesticides formerly bound in humate complexes. Therefore it is essential to reduce NOM from water intended for domestic and/or potable use [Leenheer, 1994].

Medium MMCO UF has been proven effective for NOM reduction in potable water [Jucker and Clark, 1994; Maartens *et al.*, 1998]. According to Trägård [1989] the most suitable membrane for NOM removal from aqueous solutions would be hydrophilic and homogeneously permeable. However, hydrophobic membranes manufactured from glassy polymers are generally used for UF processes. These membranes are mechanically and chemically robust, but because of their surface characteristics, much more susceptible to NOM foulant adsorption [Toyomoto and Higuchi, 1992].

3.2 FOULING OF UF MEMBRANES

Some disagreement exists in fouling terminology to distinguish exactly between flux decline, fouling and concentration polarization.

Fouling may be defined as any process that results in *loss of performance* of a membrane due to the deposition of suspended or dissolved (colloidal) substances on its surface, at its pore openings or within its pores [Koros *et al.*, 1996]. This loss of performance may occur over a *time period* of a few seconds or minutes through to several days [Howell and Nyström, 1993], and is possibly the most important reason for the slow acceptance of UF in various areas of the chemical and biological processing industry [Belfort, 1984; Wetterau *et al.*, 1996].

The consequences of fouling may be experimentally observed as reduced flux when operating in CP mode or increased dP when operating in CF mode. Irrespective of the mode of operation, the net result of the loss of productivity with time is an increase of the unit processing cost of treated water. Possibly the only advantageous effect of fouling is a possible increase in rejection for some solutes [Howell and Nyström, 1993].

3.2.1 Concentration Polarization and Fouling Effects

The development of the hydrodynamic and mass transport boundary layers where the removal of solvent (and smaller molecules) occurs under a pressure gradient in a porous tube has been discussed briefly in section 2.5.3. Because concentration polarization is by definition a reversible process that occurs in solution, it is not considered as a membrane fouling mechanism *per se*, but rather as a flux reduction phenomenon inherent to all membrane filtration processes, that may either precede fouling or occur simultaneously with fouling. The partial irreversibility of fouling implies that a change in the hydrodynamic flow conditions (increased cross-flow velocity or increased trans-membrane pressure) is not sufficient to restore the flux to its original value. Usually a chemical wash, referred to as cleaning-in-place (CIP), is needed for restoration of the original membrane flux.

3.2.2 Fouling Mechanisms

3.2.2.1 Adsorption

Adsorption refers to *physico-chemical interactions* occurring between solutes, which may be of inorganic or organic origin, and the membrane material, because of a number of interfacial forces acting between them. These forces can be electrostatic, van der Waals, solvation or steric forces [Howell and Nyström, 1993].

Adsorption of hydrophobic organic foulants such as NOM, proteins and lipids occurs even when the membrane has been brought into (static) contact with the feed solution in the absence of a trans-membrane pressure driving force [Maartens *et al.*, 1996]. It has also been observed in previous studies [Fane and Fell, 1987; Kim *et al.*, 1989] that increased hydrophilicity of the membrane results in decreased adsorption of NOM and less irreversible fouling.

3.2.2.2 Aggregation

Aggregation refers to a variety of interactions between retained solute molecules or particulates present in the feed stream (and especially in the mass transport boundary layer). These

interactions include *gelation*, *polymerization*, *flocculation*, *adhesion*, and *coagulation* [Howell and Nyström, 1993]. The result of this mechanism is the growth and consolidation of the fouling or cake layer, which increases the total resistance as described by eqs. (2.31) and (2.32).

3.2.2.3 Pore Blocking

The influence of adsorbed macromolecules in the vicinity of membrane pores is that the macromolecules can *obstruct* the passage of solvent and membrane-permeable solutes. The size and shape of the macromolecule in relation to the size and spatial distribution of membrane pores is believed to result in a number of pore blocking permutations [Howell and Nyström, 1993].

Three models have been proposed which include:

- ◆ complete pore blocking, whereby the pore entrance is sealed;
- ◆ pore bridging, which is partial obstruction of the pore entrance; and
- ◆ internal pore blinding, whereby material not retained at the pore entrance is adsorbed or trapped on the pore wall or the membrane support material.

Pore blocking occurs mainly at high pressures and feed concentrations and is usually irreversible. When pore blocking occurs the membrane modules may have to be replaced. Selection of the correct membrane for a specific application is thus very important for the successful long-term operation of a membrane plant.

3.3 FLUX ENHANCEMENT STRATEGIES

3.3.1 Selection Criteria

A number of investigations have been documented concerning chemical and/or mechanical methods to destabilize the growth of the mass transfer boundary layer during membrane process operation. Each of these flux enhancement strategies has certain advantages and disadvantages that will determine their suitability to reduce or prevent a particular type of fouling.

Factors to be considered before implementing any flux enhancement strategy, include:

- ◆ degree of flux enhancement attainable;
- ◆ capital and additional operating cost (energy consumption, chemical cost etc.) of implementing a certain strategy;

- ◆ robustness of the membrane to withstand mechanical or chemical stresses over an extended period;
- ◆ technical viability to scale from laboratory to industrial size; and
- ◆ ease of automation and operation.

The various mechanical and hydraulic flux enhancement strategies will be discussed in the following sections with the preceding selection criteria in mind. Chemical cleaning will also be discussed as a chemical method to remove irreversible fouling.

3.3.2 Periodic Backflushing (Reverse Filtration)

3.3.2.1 Principle

Of the various hydraulic or mechanical flux enhancement strategies already studied in the laboratory, periodic backflushing or reverse filtration is the *only method* that has been used extensively on full-scale *capillary-type* membrane plants. The principle of backflushing is simple. Fouling denotes the accumulation (and possible compaction) of retained material at the membrane surface while the solvent (water) passes through the pores. Thus it should be possible to remove this accumulated fouling layer partially or completely by *reversing the pressure differential (dP)* across the membrane, thus forcing solvent in the reverse direction through the membrane. The deposited fouling layer is expected to become re-suspended and swept away by the tangential or cross-flow [Redkar and Davis, 1995].

3.3.2.2 Recent Work in the Field

Various authors have used different terms to describe similar reverse filtration practices. Matsumoto *et al.* [1987; 1988] and Xu *et al.* [1995] referred to *backwashing*, while Rodgers and Sparks [1991;1992;1993] and Rodger and Miller [1993] used the term *backpulsing*. Johnson and Wenten [1994] referred to *back-shocking*, while the term *periodic reverse filtration* was coined by Redkar and Davis [1995]. *Flushing* generally refers to rinsing of the system with filtered water while *backflushing* refers to the same, but from the shell side of the modules.

Different forward filtration and backflush or backpulse times resulted in the different terms. Authors generally refer to *backflushing* when the filtration time is in the order of a couple of minutes to several hours while backwash times may vary between a few seconds and several minutes, depending on the membranes used. The term *backpulsing* is usually used when the feed and/or permeate is pressure- and/or flow-pulsed with a frequency in the order of 0.5 to 20 Hz.

The use of pressurised air as a backflush medium has been investigated in UF, generally with poor results. Matsumo *et al.* [1988] showed that *backflushing with permeate* is more effective than *back-pulsing with air*. The reason can be found in the combination of the small membrane pore sizes (less than 50 nm) and the high bubble-pressure (greater than 300 kPa) of UF membranes, compared to the much larger pore sizes (less than 0.1 μm) of MF membranes. Hillis *et al.* [1998] also reported that *gas-based backflush* is restricted to out-to-in membrane systems with hydrophobic membranes, such as the in-situ cleaning process developed by USF Memcor for MF applications.

3.3.2.3 Effectiveness of Different Backwash Media and Methods

A number of factors have to be accounted for and taken into consideration when designing and evaluating a backflushing system.

- ◆ Backflushing reduces the net production time and volume of product water. Although potable water is a relatively low-value product (R 0.30 to R1.50 /m³), this cost has to be taken into account when calculating the net product cost.
- ◆ Backflush water containing foulants first need to be purged or bled from the recirculation loop before filtration commences, since re-deposition can occur, thus negating the flux enhancing effect of the backflush.
- ◆ Backflushing is effective in the reduction of concentration polarization and removal of accumulated cake and/or gel layers, but ineffective in the removal of adsorbed material from the membrane surface and pores, for which a chemical clean is needed.
- ◆ In XF operation deposition of the cake layer is a local phenomenon, i.e. it occurs mainly near the inlet side of the module where the local trans-membrane pressure is the highest. Thus it may be advantageous if modules are backflushed in cross-flow mode from both axial directions. This will serve the dual purpose of destabilizing the formed cake layer and removing the cake layer at both ends of the module.

3.3.3 Pulsatile Flow (Flow Destabilization)

3.3.3.1 Principle

In UF systems where flux is limited by the formation of a gel-type fouling layer, pressure pulsing may be useful to reduce the formation of such a layer. During trans-membrane pressure pulsing the trans-membrane pressure across the membrane is oscillated between positive and negative at various frequencies and durations [Rogers and Miller, 1993; Redkar *et al.*, 1996].

3.3.3.2 Recent Work and Proposed Mechanisms

Several authors have investigated the use of pressure pulsing in tubular UF, MF and inorganic membrane systems. Single proteins, protein mixtures and yeast cell suspensions have been used as effective test media for which pulsed UF could significantly improve steady-state fluxes [Matsumoto *et al.*, 1987,1988; Johnson and Wenten, 1994].

Matsumoto *et al.* [1987] could maintain a constant permeate flux much higher than the pseudo-steady-state flux during cross-flow UF of yeast suspensions. Rodgers and Sparks [1991] reported increased solute transmission by two orders of magnitude for tubular cross-flow UF of a binary protein mixture. They concluded that trans-membrane pressure pulsing altered the CP layer by *translation of body forces* through the membrane, and small but significant *membrane motion*. The net result would be improved solvent and solute flux [Rodgers and Sparks, 1992]. Rodgers and Sparks [1993] also determined that changes in the feed concentration caused the most significant flux improvement due to backpulsing.

Nikolov *et al.* [1993] investigated the effect of both feed and permeate pressure pulsing on the flux, in a tubular UF system that was used to ultrafilter a 10 % dextran solution at different cross-flow velocities. They reported that simultaneous pulsing on both sides of the membrane was more effective in 'destroying' the gel layer and improving flux than for permeate pulsing only. During simultaneous pulsing the minimum of the pulsating pressure in the feed coincided with the maximum pulsating pressure in the permeate. They also concluded that for gel-forming systems the use of pulsing in the feed actually decreases the concentration polarization, and causes instability in the gel layer. Because of the periodic densification and rarefaction of the gel layer, back transport of solute from the gel layer to the bulk stream would be enhanced. Pulsation of the permeate would also cause the membrane to vibrate and cause an instability in the gel layer. It was also observed that an increase in the amplitude of pulsation resulted in a higher increase in flux, due to the almost incomplete gel layer formation.

The key difference between backflushing and backpulsing (or feed pulsing) is the shorter intervals between backpulses, which may be of the same order as the characteristic growth time of the fouling layer. This means that the fouling layer may be removed or disrupted before flux decline can occur [Redkar *et al.*, 1996]. For a given application there should be an optimum combination of backpulsing frequency and duration that will maximize the permeate flux. A *too short backpulse* duration may not provide enough time to allow for the cake to lift and be swept away, while a *too long pulse* leads to unnecessary loss of permeate. On the other hand, a *too short interval between pulses* may not allow enough time for permeate collection compared

to that lost by backpulsing, while a too long interval between pulses leads to unnecessary fouling and flux decline.

3.3.3.3 Viability of Existing Pulse Generators

From the preceding sections it is evident that pulsatile flow can improve the pseudo-steady-state flux of UF and MF operations in a variety of applications. It should also be noted that although a variety of pulse generators have been used to induce unsteady flow, most of these were intended for laboratory sized equipment. Pulse generators quoted in the literature include:

- ◆ a rotating distributor disc system, judiciously perforated and placed in front of the entrance plane of a tubular membrane bundle containing 5 Carbosep ceramic tubes, patented by TechSep [Grangeon *et al.*, 1991] for industrial size modules and investigated by Spiazzi *et al.* [1993];
- ◆ collapsible tube pulse generators were used by Bertram *et al.* [1993] and Hadzismajlovic and Bertram [1998] during turbulent flow conditions on ceramic membranes;
- ◆ volumetric pumps and pistons have been used extensively by Gupta *et al.* [1992, 1993] and Jaffrin *et al.* [1994] to induce pulsatile flow in ceramic MF membranes on both laboratory and pilot scale equipment. An improvement of up to 200 % in flux was reported by Finnigan and Howell [1989] with the use of pump-induced pulsatile flow on baffled tubular membranes; and
- ◆ valve arrangements at the feed, concentrate and permeate sides of membrane modules have also been used, as reported by Stairmand and Bellhouse [1985] and Milisic and Bersillon [1986]. The pulsation frequency will be limited by the type and response time of the actuated valves that are used.

The technique of pulsatile flow has not been extensively studied on capillary membranes, most probably due to the lower operating pressures (1 to 2 bar) compared with the operating pressure (8 bar) and pressure pulsations possible with the more robust ceramic membranes. Methods such as the rotating disc would also not be technically feasible with capillary membranes due to the irregular distribution of up to 1200 fibres in a 5 m² module. The manifolding would also have to be re-designed to accommodate such a setup. A new type of pulse generator has recently been investigated for which a South African patent has been granted in the name of the WRC of South Africa [WRC, 1999]. Termed the "Reverse-pressure pulse generator", the conceptual operating principle of the patent will be described in a following section (Chapter 5).

3.3.4 Gas Sparging of the Feed

Gas sparging refers to the introduction of bubbles or slugs of compressed air into the feed stream during the filtration cycle, which generates a two-phase flow on the feed side of the membrane.

3.3.4.1 Recent Work in the Field

This approach was first studied experimentally by Cui and Wright [1994;1996] using 5.0 mm ID tubular membranes and dextrans and bovine serum albumin (BSA) as test media. They examined the effect of gas sparging on permeate flux and membrane retention over a range of parameters including trans-membrane pressure, cross-flow velocity, gas sparging rate, feed concentration and membrane orientation. Both centrifugal and peristaltic pumps were used to investigate the effect of pumping conditions on flux enhancement. It was found that a very low flow rate of gas bubbles in the feed stream can significantly enhance flux while changing the apparent retention ratio of the membrane. Also, the degree of flux enhancement was significantly greater with centrifugal pumps (steady flow) than with peristaltic pumps (pulsatile flow). Cui and Wright [1996] found the most pronounced flux increase for continuous gas sparging in vertical downward XF operation, followed by vertical upward gas sparged XF and then horizontal flow. The flux enhancement was also more significant under conditions of severe concentration polarization, i.e. low cross-flow velocity, high feed concentration and high trans-membrane pressure.

At low liquid and gas flow rates in the *downward flow configuration*, an unstable or *non-current* flow pattern is to be expected, owing to the counter-acting buoyancy force and downward liquid flow. Bubble frequency will be low while large slugs are drawn into the 5.0 mm ID membranes. Consequently, the residence time of gas bubbles in the module is longer, with lower gas requirements and a higher degree of flux enhancement expected for individual bubbles. As the gas flow rate is increased, more bubbles are being drawn down into the tube inlets, creating a bubble or slug flow pattern while the degree of flux enhancement increases to a maximum value, after which it decreases with increasing gas flow rate.

Barella *et al.* [1996] also investigated gas sparged flux enhancement in 0.2 mm ID hollow fibre membranes with a MMCO of 30 000 Da with dextrans (83 000 Da) as test media. Another set of experiments were conducted by Barella *et al.* [1996] with 200 000 Da MMCO membranes and human serum albumin of 66 000 Da. The maximum degree of flux enhancement was significantly less in hollow fibres (*ca* 63 %) than in tubular membranes (*ca* 250 %), and was

explained by the inherently high shearing rates present in hollow fibre membranes at comparable conditions (about two orders of magnitude).

Cabassud *et al.* [1997] investigated gas sparged flux enhancement of clay suspensions on 0.93 mm ID, 1.2 m length, cellulose acetate membranes. With the aid of a theoretical approach it was demonstrated that the high shear stresses generated by slug flow in the hollow fibre lumens enhanced flux by limiting particle deposition.

In an investigation by Mercier *et al.* [1997] of gas sparged flux enhancement with bentonite suspensions on a single 15 mm ID, 0.75 m length, axisymmetric zirconia-coated alumina tubular membrane, it was concluded that the energy consumption could be reduced from 30 kWh/m³ permeate to 10 kWh/m³. For smaller diameter membranes (toward capillary and hollow fibre sizes) the specific energy consumption would naturally be much less than in tubular membranes of 15 mm ID. Their study also concluded that a steady gas injection rate was more effective than an intermittent gas injection process at similar experimental conditions.

Laborie *et al.* [1998] attained flux enhancements of up to 110 % in an investigation on continuous air sparging inside hollow fibre membranes to reduce particle deposits in drinking water applications. Bentonite suspensions of 1.0 µm mean d_p used to model natural waters, were filtered through a 7.2 m² membrane area module (membrane ID = 0.93 mm). At a liquid flow rate of 0.5 m/s and increasing gas flow rates, the calculated energy consumption decreased from 0.35 kWh/m³ (at no gas flow) to a minimum of *ca* 0.25 kWh/m³ (gas flow rate of *ca* 0.2 m/s). The investigators also concluded that the flow pattern observed in capillaries (or hollow fibres) of *ca* 1.0 mm ID under gas/liquid two-phase flow conditions is a succession of liquid and gas slugs, which are cylindrically shaped and surrounded by a thin liquid film. The net result is that a point near the membrane wall is submitted to alternate liquid and gas slug shear stresses.

3.3.4.2 Effectiveness and Viability Considerations

From the preceding studies it is evident that *downward cross-flow gas sparging* is effective in reducing particle deposits on tubular, capillary and hollow fibre membranes. It may be used successfully in potable water applications where the flux decline is mainly governed by particle deposits, as indicated by Laborie *et al.* [1998].

Ancillary equipment that would typically need to be provided, would include:

- ◆ compressors or gas bottles for gas supply;
- ◆ gas flow rate measurement device as well as flow meters for liquid flow rate;

- ◆ a sight glass to set the gas flow rate, as described by Cui *et al.* [1996], Cabassud *et al.* [1997] and Mercier *et al.* [1997]; and
- ◆ a specially designed gas-liquid separator chamber to prevent gas bubbles from entering the recycle pump and causing pump damage, as described elsewhere [SAPMA, 1996].

3.3.5 Chemical Cleaning

Detergent cleaning is still the most effective way of restoring the initial flux of a membrane, but the literature does not specify which cleaning agents to use. This is because the type of membrane and the feed stream to be treated will have some specific interactions, such as *complexation* and *adsorption* of retained solutes onto the membrane surface etc. Thus the cleaning regime used will differ from application to application, and must be determined experimentally. A number of factors that need to be considered:

- ◆ chemicals concentration, since this will also have an economic impact on system operation; and
- ◆ cleaning time, i.e. the time that the CIP solution is in contact with the fouled membranes.

Cleaning solutions usually contain one or more of the following components [Mulder, 1991;1993]:

- ◆ detergent (alkaline, non-ionic, etc.), such as sodium lauryl sulphate (SLS);
- ◆ complexing agent (chelatatant), such as ethylene diamine tetracetic acid (EDTA) or sodium hexametaphosphate [Cheryan, 1986; 1998];
- ◆ sufficient amount of acid (strong such as H_3PO_4 , or weak such as citric acid) or alkali (NaOH) to correct the pH to an optimum level for the cleaning solution. For the polysulphone capillary membranes used in this study and on the type of water it was found that a high pH produced the best results, typically pH 10-12;
- ◆ disinfectants, such as H_2O_2 or NaOCl. Hypochlorites are known as membrane-swelling agents [Cheryan, 1986; 1998], and as such may be effective for flushing out lodged material from within the membrane pores; and
- ◆ Enzymes.

Membrane manufacturers usually develop their own procedures for performing a chemical clean.

3.4 CONCLUSIONS

The aesthetic and microbial quality guidelines for potable water were discussed in this chapter along with consideration of water quality classification systems in South Africa. Special mention was given to the effects of natural organic matter on potable water quality and UF flux. The causes and consequences of fouling were presented in general, and it was shown that for capillary membrane systems, the physico-chemical interaction between membrane and feed solution is one of the primary factors causing fouling and flux decline. Available mechanical and or hydraulic flux enhancement strategies including reverse filtration, pulsatile flow and gas sparging of the feed were discussed on the merit of a number of selection criteria. Chemical cleaning was also discussed as a method to remove irreversible fouling.

It was demonstrated that periodic backflushing with permeate has been used successfully to improve UF process fluxes. The liquid flow from shell to lumen effectively re-suspends the fouling or cake layer, which can be washed from the surface by cross-flow operation. The major drawbacks of this method are the product loss and increased down-time, and the installation of an additional backflush pump or other means to reverse product flow. This method was chosen as the most viable option to restore process fluxes in potable water applications where the main fouling mechanism was a combination of particulate and gel-type fouling.

Different pulse generators have been used for flow destabilization to hinder the formation of the fouling layer during UF. However, it has been used mainly on robust ceramic tubular membranes that can tolerate high operating pressures (greater than 8 bar) and pressure pulsations that would destroy the more fragile structure of capillary PSf membranes. A new backpulsing method that evolved from this study will be discussed in Chapter 5.

Gas sparging has also been effective in reduction of the fouling layer thickness in cross-flow UF. The flux enhancement attainable with downward gas sparging has been ascribed to the shear stresses acting between the membrane wall and alternate liquid and gas slugs. Major drawbacks of gas sparging are the installation of a gas production unit such as a compressor, as well as a gas-liquid gas separator if the concentrate is to be recycled to the modules in cross-flow mode.

The final flux enhancement method discussed in this chapter was chemical cleaning, which will always be needed to remove adsorbed fouling layers such as NOM. Effective CIP procedures were developed and are discussed in the pilot plant investigation referred to in Chapter 4.

Chapter 4: CASE STUDY 1 - MON VILLA**4.1 INTRODUCTION**

The Helderberg Irrigation Scheme supplies irrigation water to about a thousand farms in the Stellenbosch and greater Boland areas of South Africa. Irrigation water is often also provided to farm workers and their families for potable and other domestic use. However, this water is not fit for direct human consumption without adequate treatment, because of unacceptable high levels of turbidity caused by suspended solids, slight yellow to brown colour caused by natural organic matter (NOM), iron and aluminium as well as faecal and other coliform bacteria. The water is also chemically aggressive due to low levels of carbonate alkalinity.

In November 1994, the Institute for Polymer Science, Stellenbosch (IPS), installed a 3 m² bench-scale ultrafiltration unit at the then Mon Villa Seminar Centre of the University of Stellenbosch, situated on a farm 15 km outside the town of Stellenbosch. After initial experimentation, the Water Research Commission of South Africa (WRC) was approached to fund a 15 m² pilot plant study at the site. The initial results, which were presented as a final year undergraduate project report [Botes, 1995] and was awarded the first annual "Jac van der Merwe Prize for Innovation" by the Faculty of Engineering at the University of Stellenbosch, encouraged further interest of the WRC who provided funds for continuation and extension of the work. Although the farm has since been sold to Spier Estate Farms, long-term field-testing of locally developed UF membrane technology has continued on-site until May 1999 when the plant was decommissioned.

Results from this long term pilot plant investigation run by the author have since been presented in various oral paper and poster presentations by Botes [May 1998, July 1998, August 1998], Botes *et al.* [September 1996, October 1997, September 1999], De Villiers *et al.* [November 1996], Jacobs *et al.* [September 1995, February 1996, May 1996, August 1996, November 1996, May 1998, November 1998, June 1999] and Pryor *et al.* [September 1998]. Results also featured in a number of written publications by Jacobs and Botes [1995], Jacobs *et al.* [1997], Botes *et al.* [1998] and Pryor *et al.* [1998].

The work done in this 27 000 h pilot plant investigation resulted in substantial engineering know-how, the results of which have since been incorporated into various pilot plant studies, including the reverse-pressure pulsing flow destabilization method discussed in Chapter 6.

4.2 AIMS OF THE INVESTIGATION

The aims of the Mon Villa pilot project investigation were to:

- ◆ *continue evaluation* of the IPS low-cost modular membrane system in an application to upgrade sub-standard surface waters from the Helderberg Irrigation Scheme to potable standard without the addition of chemicals prior to filtration;
- ◆ determine the *long-term effects* of raw water on permeate flux and separation capability of the IPS code #763 UF membranes used; by monitoring the *product quality* regularly to determine its compliance with SABS 241 (1984, 1999) guidelines for potable water;
- ◆ develop effective *operating protocols* to maintain the system operating flux; and
- ◆ establish effective *chemical cleaning* regimes to restore the flux.

From a range of UF plant operating and flux enhancement protocols tested over 4½ years at Mon Villa and reported in publications, backflushing combined with flow destabilization showed specific promise. In this chapter the focus will be on flow destabilization ideas and the backflush results, which in turn led to the reverse-pressure pulsing development. With regard to backflushing with flow destabilization, two strategies were adopted. Strategy A consisted of a backflush with FFR (relative to the direction of cross-flow filtration) followed immediately by a backflush without FFR, while Strategy B consisted of a backflush without FFR followed immediately by a backflush with FFR.

4.3 SYSTEM DESCRIPTION

4.3.1 Membranes

The IPS recently developed a range of low-cost externally unskinned polysulphone (PSf) and polyethersulfone (PES) capillary membranes [Jacobs *et al.*, 1993; WRC, 1996b; Jacobs and Leukes, 1996]. Research work conducted with similar membranes (IPS membrane code #748 which were tighter than the "skinless" code #763 membranes) included seawater prefiltration before RO on the Atlantic coast of South Africa [Strohwalld and Jacobs, 1992]; and polishing of

secondary treated sewage water in Uitenhage [Jacobs and Barnard, January 1997], both with very promising results. Figure 13 shows an electron micrograph of the cross-section of an externally unskinned PSf membrane, designated IPS membrane code #763.

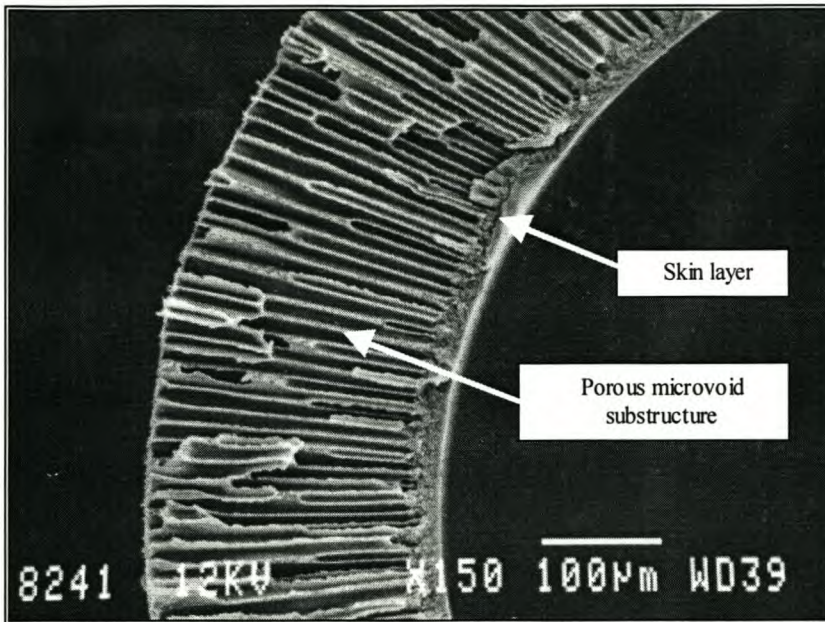


Figure 13: Cross-section of an externally unskinned polysulphone membrane (IPS membrane code #763) used in Case Study 1.

The (lumen-side) skin layer is typically 1 to 5 μm thick, while the porous microvoid substructure (250 to 300 μm) extends the full width of the membrane (Figure 14). The ultrastructure of these membranes results in a self-supporting structure able to withstand pressurization from the in- or the outside. Typical internal membrane diameters are 1.2 mm, external diameters 1.8 mm and the instantaneous burst-pressure of the membranes has been experimentally determined to be in excess of 1.2 MPa.

These membranes display superior pure-water fluxes (PWF) at low operating pressures (dP below 1.0 bar) due to the absence of any skin layer on the external surface (an additional resistance to solvent flow). The absence of an external skin layer can be observed in Figure 14. Performance-evaluation studies of these membranes indicated a medium molecular-mass cut-off (MMCO) of about 50 kDa. The resistance of the IPS code #763 membranes is in the order of $2 \times 10^{12} \text{ m}^{-1}$, calculated from eq. (2.29).

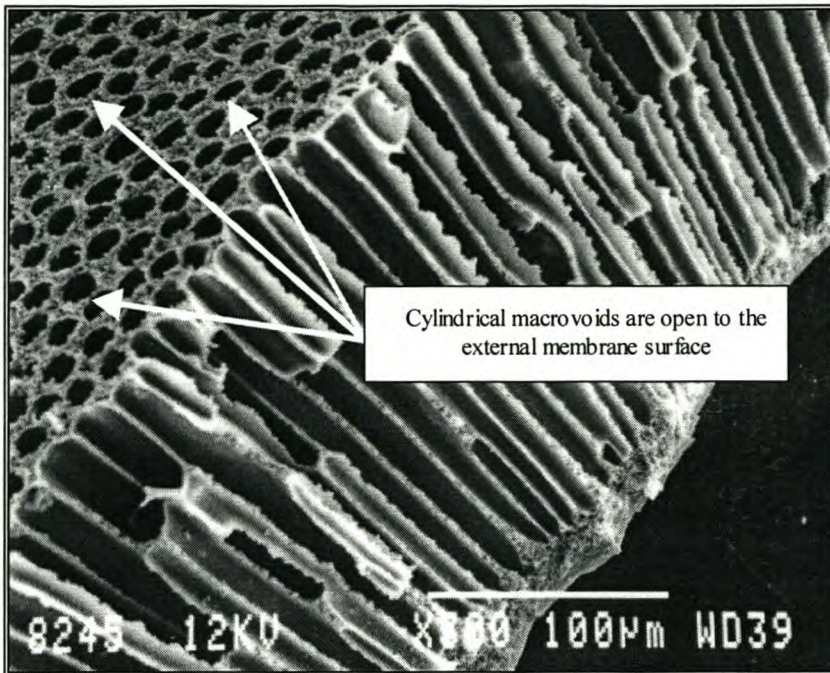


Figure 14: Outer surface of an externally unskinned polysulphone membrane (IPS membrane code #763) used in Case Study 1.

4.3.2 Modules and Manifolding

The membranes are housed in the familiar lumen-fed shell-and-tube arrangement. The modules were aligned vertically with feed and concentrate manifolds at the top and bottom and a central single permeate outlet. As can be seen from Figure 15, for pure water at 15, 20 and 25 °C respectively, the flow in a membrane of 1.2 mm inside diameter will theoretically be laminar if U_m is below 1.9, 1.7 and 1.5 m/s respectively. The transition from laminar to turbulent flow only begins at U_m of 2.2, 1.9 and 1.7 m/s respectively. For fully developed turbulent flows, the lumen inlet velocities should be 3.8, 3.4 and 3.0 m/s respectively for the three chosen temperatures.

In a 90 mm OD class 6 uPVC pipe the wall thickness is 2.7 mm. Thus D_I is 84.6 mm, while the internal diameter of the membranes (d_i) is 1.33 mm and external diameter (d_o) is 1.85 mm. The membrane bundle is contained in a netted nylon sock to keep it together before embedding the ends in epoxy end-plugs, as illustrated earlier in Figure 5 in section 2.4.3. The volume taken up by the netted sock in the module shell was considered negligible in subsequent calculations. In the present investigation, the hydraulic module parameters in Table 5 were calculated for the modules used at Mon Villa (Mod 1).

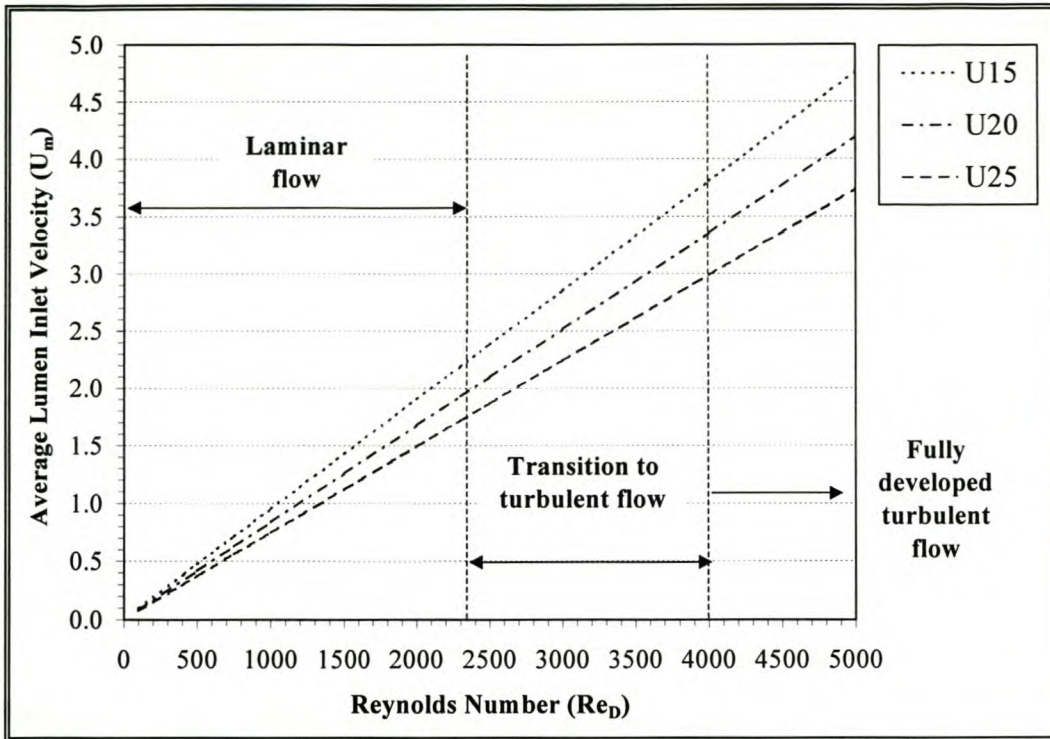


Figure 15: Inlet velocity versus inlet Reynolds number for a 1.2 mm ID membrane.

Table 5: Variables and hydraulic module parameters for the experimental modules used in Case Study 1.

Description of Variable	Variable	SI Units	Mod 1
Number of membranes in module	N_m		1200
Membrane internal diameter	d_I	m	0.00133
Membrane external diameter	d_o	m	0.00185
Module housing internal diameter	D_I	m	0.0846
Module external diameter	D_o	m	0.090
Membrane filtration length	L_F	m	1.0
Membrane total length	L_T	m	1.2
Description of Calculated Parameters	Parameter	SI Units	Mod 1
Packing density	ψ	%	57.4
Membrane area per unit volume	ϕ	m^2/m^3	892.0
Feed-side hold-up volume	VF_H	Liter	1.667
Permeate-side hold-up volume	VP_H	Liter	2.396
Wetted membrane hold-up volume	VM_H	Liter	1.558
Total internal hold-up volume	VH_T	Liter	5.621
Module membrane area	A_m	m^2	5.014
Module frontal flow-area	A_F	m^2	0.001667

The prototype modules for housing the capillary membranes were designed according to the criteria listed in section 2.4.1. A *hydraulic seal* in the form of a 10 cm thick tube-sheet at each face end of the module was created between the feed and permeate sections [WRC, 1996a]. A urethane-modified epoxy was used for embedding the membranes in a horizontal rotational embedder [Jacobs *et al*, 1993]. After the epoxy had been cured, the membrane ends were sliced open and the module finished to its completed dimensions. A small *permeate-side hold-up volume* (2.4 L) was created by maximizing the *packing density* (57.4 %), while the void space (42.6 %) was sufficient to allow penetration of the epoxy between the membranes in the end-plug and to remove trapped gas bubbles. The *feed-side hold-up volume* of a prototype module was 1.667 L. In the prototype manifold design three such modules were arranged in parallel by solvent-welding PVC stubs with galvanised steel backing rings onto the T-pieces, and bolting the individual units together [WRC, 1993].

4.3.3 Process Layout and Description

Figure 16 shows the flow diagram of the Mon Villa pilot plant. Feed water was drawn from the high-pressure irrigation line into a 4.5 m³ feed tank with the inflow being controlled by a hydraulic valve. A centrifugal pump P1 was used to transfer the feed water from the tank, through a 200 µm metal mesh vortex strainer (VS1) and a conventional sand filter (SF1) to remove particulate matter that may plug the membrane inlets, to the feed manifold. For the pump curves, see Figure 47 in Appendix B.

The sand filter was installed during January 1996 (at 6 400 h) in order to decrease the physical load on the membranes but was found to become blocked within 1-2 days of continuous operation, and had to be backflushed manually. A recycle pump (P2) was operated in parallel with the feed pump to maintain a minimum linear cross-flow velocity through the membranes, thereby inducing shear stresses to limit the build-up of a polarized gel layer on the membrane surface. The recycle line was also fitted with a 150 µm metal mesh vortex strainer (VS2) to limit re-deposition of material loosened from the membrane surface after each backflush cycle.

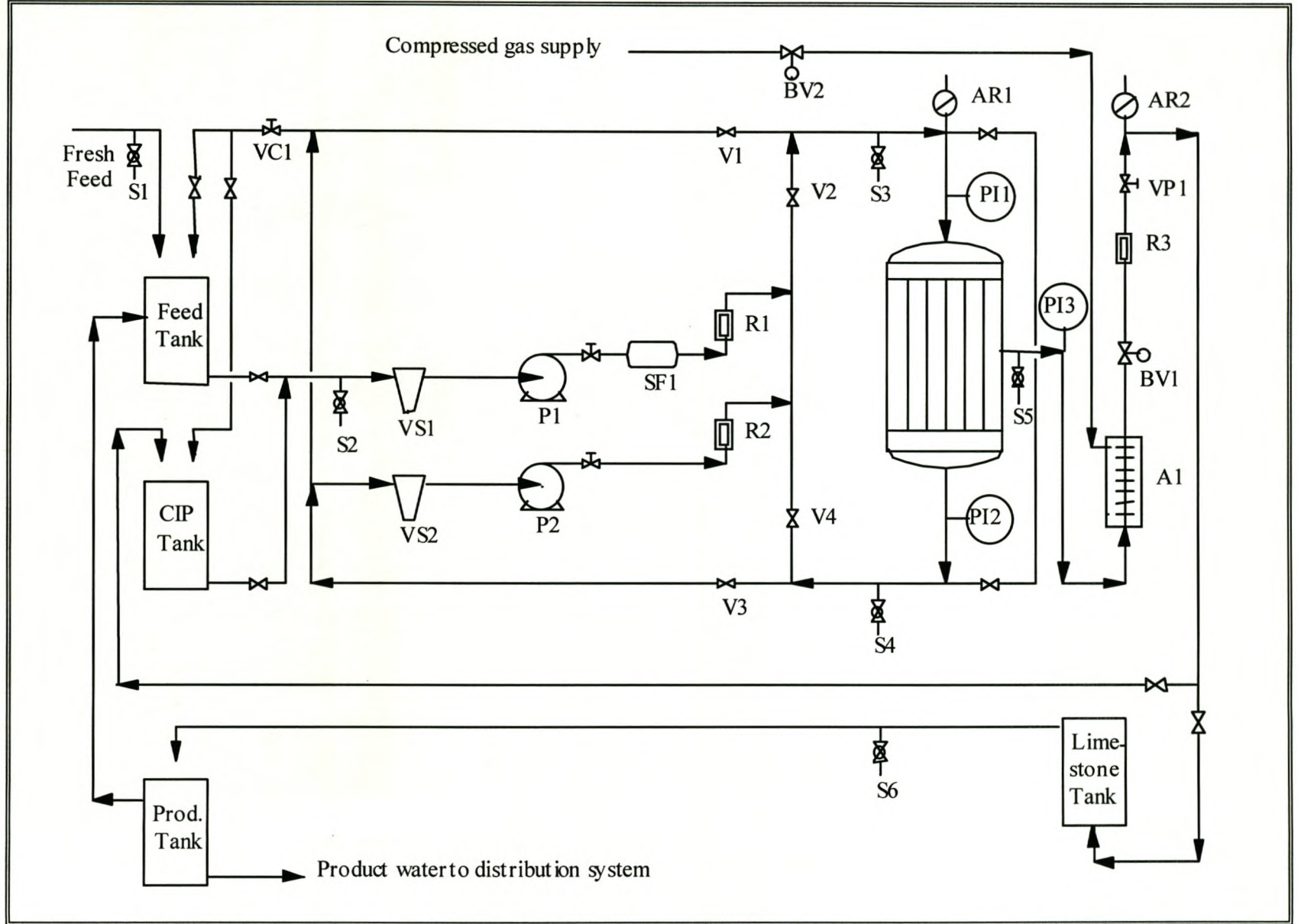


Figure 16: Flow diagram of the Mon Villa pilot plant.

4.4 DATA COLLECTION AND ANALYSIS

Data were collected manually on-site on a daily basis, as no computerized data-logging system was available at the start of the investigation. Although the unit operated continuously day and night, data were only collected during daytime. Thus no data are available for nighttime operation.

Collected data included the current date, time of day (h:m), total run time (h), total net water production (m³), operating temperature (°C) and the inlet, outlet and permeate side pressures (kPa). The pressure gauges were calibrated once a year. Although *variable area flow meters* had been installed to get a quick indication of plant liquid flows, the concentrate and permeate flow rates were measured with the stopwatch and container method (10 L). As the volume of this container (bottle) had been accurately determined and the neck of the bottle was 50 mm, the error that would result from flow measurements was considered negligible. The in-line recirculation pump flow rate (L/h) was measured with a variable area flow meter (2 500 to 25 000 L/h) that had been installed in September 1997.

The turbidities of the raw water, feed tank content and total feed to the modules, concentrate and individual and combined permeate were also measured by taking the average of 3 readings on-site. Grab samples were also collected on occasion for inorganic and microbial analysis at the CSIR in Stellenbosch and NOM characterisation at the Department of Biochemistry, University of Stellenbosch. A log was also kept of all plant construction changes, modes of operation, maintenance to the unit or ancillary equipment etc. All collected data was fed daily into a Microsoft[®] Excel 97 spreadsheet for further calculations.

4.5 EXPERIMENTAL

4.5.1 Automatic Operation and Backflush Procedure

A prototype permeate backflush system was developed to enable the permeate flow direction to be reversed. In order to accomplish this, a motor-operated ball valve (BV1) was installed downstream of the permeate accumulator A1 (Figure 16). This valve was closed automatically at the start of the pre-set backflush cycle to stop filtration. The procedure for automatic backflush operation was active when the plant was operated in automatic mode.

The sequencing of events for automatic mode operation is listed below.

- ◆ Start feed pump (P1): Pressurization of the system for a filtration cycle. The recycle pump (P2) starts when a pre-set low-pressure switch is activated. This usually took less than 5 s.
- ◆ Start P2: Backflush only works if P2 is running.
- ◆ Delay (T1): T1 is the duration of filtration cycle. This time delay could be pre-set up a maximum of 6 h.
- ◆ Close backflush valve (BV1): Valve BV1 (N/O) closes in 2.5 s. This allowed a gradual decline of permeate flow without the possibility of damage to the membranes.
- ◆ Delay (T2): T2 is the duration of backflush and must be more than 2.5 s. The backflush flow rate was controlled by the supply pressure of the compressed gas (N₂).
- ◆ Open BV2: Valve BV2 (N/C) opens almost instantaneously.
- ◆ Delay (T3): T3 is the actual backflush time.
- ◆ Close BV2: Valve BV2 closes almost instantaneously.
- ◆ Open BV1: Filtration cycle resumes.
- ◆ Go to Step 3 (Delay(T1)).

After the motor-operated ball valve BV1 was closed, compressed gas was injected into the accumulator through a solenoid valve (BV2), which increased the permeate pressure to between 40 and 120 kPa above the feed pressure to force a predetermined volume of permeate in the reverse direction through the membranes. The backflush volume could be varied between 0.5 and 5.0 L/module.

Regulating the gas regulator pressure and backflush time controlled the backflush volume. Opening and closing of valves BV1 and BV2 respectively were controlled by pre-set variable-cycle timers when operating the system in automatic mode, but only BV2 could be switched on and off in manual mode as well. Two air-release valves (AR1, AR2) were used to vent air from the feed manifold during start-up, and from the permeate line after backflushing respectively. When filtration resumed after step 8 (Close BV1), the system pressure decreased slowly as the compressed air was purged from A1 through AR2.

4.5.2 Manual Operation and Backflush Procedure

The investigation regarding the use of flow destabilization before a backflush was performed over a total operating time of 2620 hours during filtration cycles C133 to C139. At the end of each of these filtration cycles, a CIP was implemented to clean the membranes, followed by a 30 minute chlorine wash to remove and prevent bacterial growth.

For filtration cycles C133 to C139 the plant was operated in manual mode. The hard-wiring of the plant allowed certain actions to take place and excluded others, which are listed below.

- ◆ The feed and recycle pumps could be switched on individually with switches on the control panel, but the pumps could not be stopped individually, except when the emergency stop button was pressed to cut power to all electrical devices.
- ◆ Another switch on the control panel could switch BV2 on and off in manual mode when the feed and recycle pumps were running, but not when only the feed pump was running.
- ◆ Because BV1 could not close in manual mode, a manual type diaphragm valve VP1 was installed downstream from the permeate variable area flow meter R3. This valve would be used to stop permeate flow at the start of a manual backflush.
- ◆ Another manual type diaphragm valve VC1 was situated in the concentrate line. This valve was opened completely during implementation of cross-flow backflushing to vent upstream system pressure during the backflush sequence.

In manual filtration mode the feed and recycle pumps would be started sequentially, and the filtration dP set by adjusting VC1 and VP1 to the dP and water recovery. All filtration runs were conducted in up-flow mode, i.e. with flow reversal valves V1 and V4 open, and V2 and V3 closed. Then the system would be left to filter until the next backflush was performed. All manual backflushes were performed at 120 kPa dP with 15 L of permeate (3 times the lumen-side hold-up volume).

The sequencing of actions for Strategy A and B manual backflush operations are listed in Table 6 and Table 7 respectively. Care was taken with every visit to the plant to reset the dP to 80 kPa if it had drifted slightly since the last visit..

Table 6: Sequence of actions for a Strategy A backflush (Filter up, FFR, B/F A1 down, FFR, B/F A2 up, Filter up)

Event No.	Action	Description
1	Arrive at system	Measure permeate flow, take samples
2	Open V2 and V3, Close V1 and V4	FFR 1 (change to down-flow)
3	Close VP1	Permeate flow stops
4	Open VC1 completely	Vent system pressure
5	Open BV2	Perform B/F A#1 with 15 L, vent air
6	Close BV2	Flush membranes
7	Close V2 and V3, Open V1 and V4	FFR 2 (change to up-flow)
8	Reset VC1 & open VP1 to set dP	Measure permeate flow, take samples
9	Close VP1	Permeate flow stops
10	Open VC1 completely	Vent system pressure
11	Open BV2	Perform B/F A#2 with 15 L, vent air
12	Close BV2	Flush membranes
14	Reset VC1 & open VP1 to set dP	Measure permeate flow, take samples
15	Leave system to filter	Accumulate cake layer till next B/F

Table 7: Sequence of actions for a Strategy B backflush (Filter up, B/F B1 up, FFR, B/F B2 down, FFR, Filter up)

Event No.	Action	Description
1	Arrive at system	Measure permeate flow, take samples
2	Close VP1	Permeate flow stops
3	Open VC1 completely	Vent system pressure
4	Open BV2	Perform B/F B#1 with 15 L, vent air
5	Close BV2	Flush membranes
6	Open V2 and V3, Close V1 and V4	FFR 1 (change to down-flow)
7	Reset VC1 & open VP1 to set dP	Measure permeate flow, take samples
8	Close VP1	Permeate flow stops
9	Open VC1 completely	Vent system pressure
10	Open BV2	Perform B/F B#2 with 15 L, vent air
11	Close BV2	Flush membranes
12	Close V2 and V3, Open V1 and V4	FFR 1 (change to up-flow)
14	Reset VC1 & open VP1 to set dP	Measure permeate flow, take samples
15	Leave system to filter	Accumulate cake layer till next B/F

4.5.3 Chemical Cleaning

The chemicals used during CIP included *detergents* such as [Anselme and Jacobs, 1996]:

- ◆ 1 to 2.5 g/L sodium lauryl sulphate (SLS), which also acts as a biocide;
- ◆ 1 g/L commercial household enzymatic Bio-Tex[®], which has previously been used effectively at a SASOL membrane plant to clean tubular polysulphone membranes; and
- ◆ 0.1 vol. % commercial Triton X100[®], which has also been used previously as a cleaning agent and precoat chemical.

Other chemicals included:

- ◆ 0.15 to 3.0 g/L EDTA, which is known as a strong complexing agent;
- ◆ 0.25 to 1.0 g/L ammonium hydroxide (NH₄OH), which has been shown to remove some organic foulants from polysulphone membranes at the Biochemistry Department of the University of Stellenbosch; and
- ◆ sodium hydroxide (NaOH) to adjust the pH of the cleaning solution to between 10 and 12 when necessary.

The procedure for the cleaning-in-place (CIP) cycle consisted of the steps listed below.

- ◆ Drain the system completely before CIP;
 - ◆ Dissolve the chemicals in the CIP tank, and circulate the solution through the system for 2 to 5 min to ensure complete mixing;
 - ◆ Static soak for 10 to 30 min in order to swell/dissolve foulants on the membrane surface;
 - ◆ Circulate the solution through the system at very low permeate flow rate (typically 50 L/h per module) while backflushing with permeate every 2 to 10 min;
 - ◆ Change feed direction (up/down) in order to ensure complete backflushing and cleaning of the entire module length;
 - ◆ Monitor the feed tank for changes in colour to ascertain the CIP effectiveness;
 - ◆ Rinse the system with water from the feed tank to remove all traces of the cleaning solution and measure the process flux; and
 - ◆ Repeat the CIP if the restoration of flux was not satisfactory.
-

4.6 RESULTS AND DISCUSSION

4.6.1 Process Flux Performance

Initially the system was operated in constant pressure mode at dP between 30 and 40 kPa (30 to 40 % water recovery because of pumping limitations) to test the integrity of the experimental PSf membranes, while the concentrate was recycled back to the feed tank in an external concentration loop. This continually increased the load on the membranes during a cycle, until a CIP was carried out and the content of the feed tank was drained to waste.

After 3 000 h of operation, constant flow valves were installed downstream from AR2 and operation was changed to constant flux mode. However, this proved an ineffective method to control the flux. For the constant flow valves to operate properly, the minimum permeate back-pressure upstream of the valves had to be more than 80 kPa, while the actual upstream pressure was only 20 to 50 kPa. The system was also operated during this time at 60 to 120 kPa dP , which caused compaction of the fouling layer on the membrane surface, and decreased the specific flux even further. The specific flux corrected to 20 °C with eqs. (2.38) and (2.40), is shown in Figure 17 for the entire 27 000 h investigation period.

It was also found that an extremely high NOM concentration (greater than 50 mg/L) in the feed caused precipitation of a gel layer on the membranes, which restricted the lumen cross-flow path, which increased feed-side pressure as well as the module headloss, with subsequent decrease of the flux.

After 18 000 h of operation, more efficient pumps were installed. System operation was changed again to constant pressure mode and continued to the end of the investigation. The permeate recovery per pass increased to between 85 and 95 %, the concentrate was pumped to waste and the specific flux was recovered to about 15 % below the initial specific flux.

During the latter period the system was operated at a differential pressure of *ca* 80 to 90 kPa, which limited the possibility of fouling layer compaction and increased the operating time between CIPs. The effect of flow destabilization on flux recovery with backflushing was also investigated during this latter period.

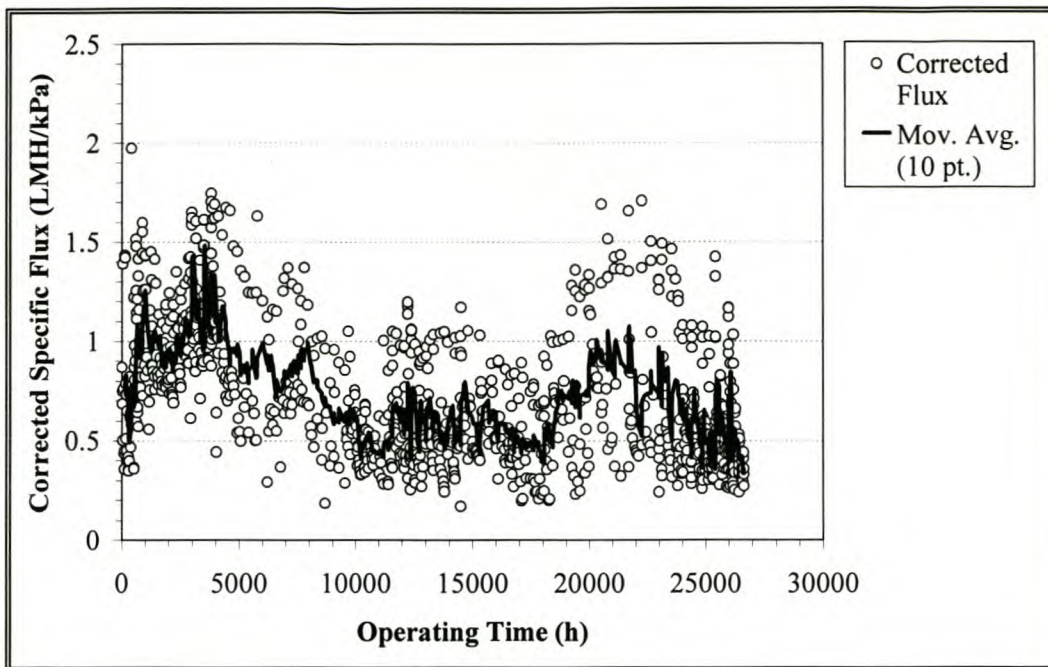


Figure 17: Corrected specific flux performance at Mon Villa.

4.6.2 Turbidity Reduction

During the investigation period, turbidity was used to monitor the membrane separation efficiency. An HACH 2100P portable turbidimeter was acquired for this purpose, and water samples taken daily at sampling points S1 to S6 (Figure 16) were analysed on-site. Figure 18 shows the reduction in turbidity effected by membrane filtration over the investigation period of 27 000 h. The total feed refers to the combined feed and recycle streams before entering into the modules, while the individual and combined permeate turbidities were measured daily before post-treatment. The permeate turbidity values, plotted in Figure 18, were for the combined permeate from the three prototype modules. Although some spikes are observed in the permeate turbidity values, these were probably caused by imperfections in membranes that resulted in ruptures during severe fouling conditions and high operating pressures. A simple *location and plugging* method was eventually developed to identify and isolate such compromised membranes on-site [Botes, 1995]. This resulted in a total decrease of 6.4 % in the available membrane area over the entire investigation period, which was accounted for in flux calculations.

Nevertheless, individual permeate turbidities of between 0.08 and 0.15 NTU were recorded regularly (on the modules without defective membranes), irrespective of the total feed turbidity which at times increased to above 110 NTU. It can be concluded that there was no correlation between the feed and permeate turbidities, and the reduction in turbidity was greater than 95 %.

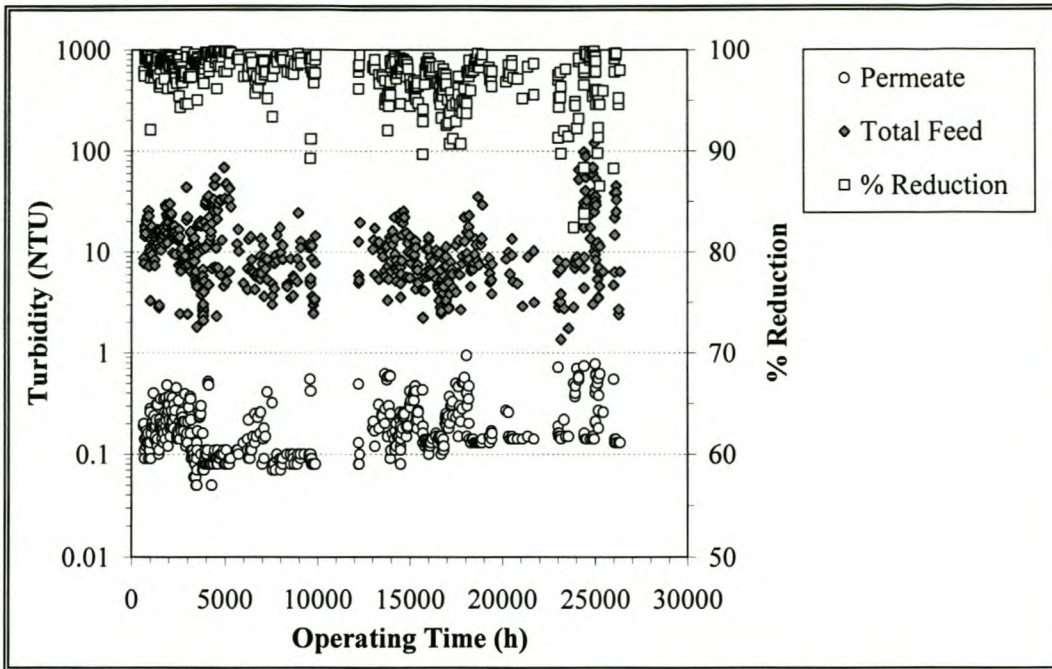


Figure 18: Turbidity reduction at Mon Villa.

4.6.3 Chemical Cleaning

The results of chemical cleaning on membrane flux are illustrated in Figure 19. Fouled and cleaned membrane fluxes, corrected to 20 °C, are plotted as a function of CIP number. The flux could be restored to *ca* 1.0 to 1.5 LMH/kPa throughout the entire investigation period.

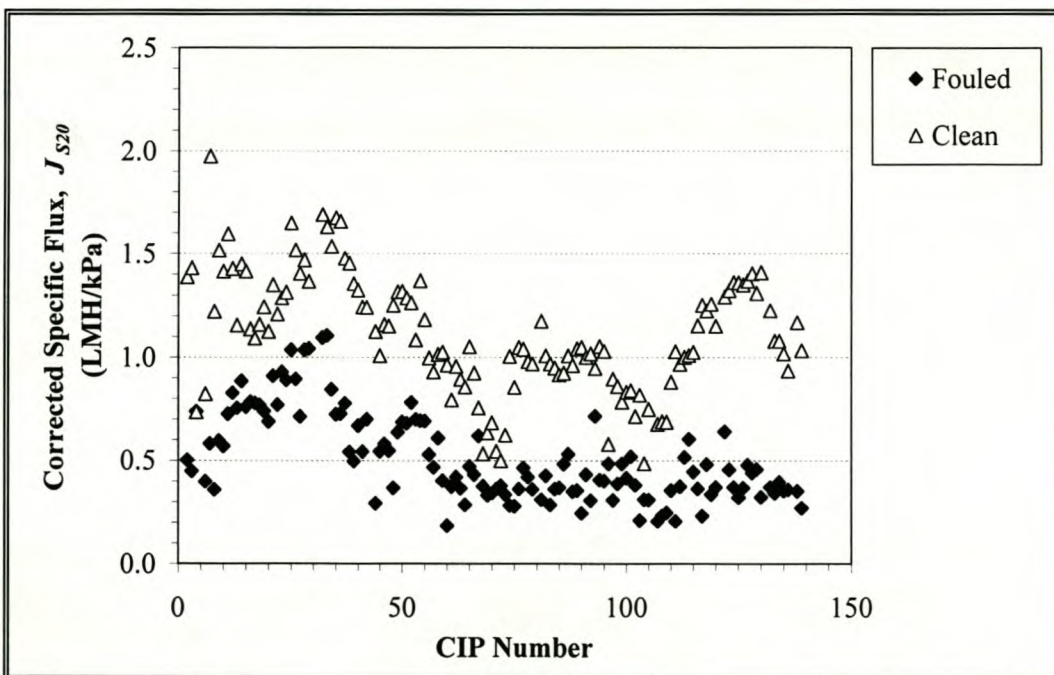


Figure 19: Corrected specific flux for fouled and cleaned membranes as a function of CIP number.

4.6.4 System Operation in General

The system was initially not equipped with a feed flow reversal system, and the feed water was fed to the modules at the top while the concentrate exited at the bottom. This necessitated that the system be backflushed with downward cross-flow as well. Different combinations of backflush trans-membrane pressures, volumes and times were tested to find starting values for backflush characterisation or optimization. However, this proved very difficult as the quality of the feed water changed continuously and rapidly at times. Details can be found in [Jacobs *et al.*, 1997] and [Botes *et al.*, 1998].

The reason for this was partly seasonal, as more organic and inorganic material was present in the feed water during the rainy winter season. Another factor that contributed to sudden changes in water quality was the fact that an irrigation pipeline supplied the raw water inlet to the feed tank. The operating pressure in the pipeline varied between 3 and 10 bar. Any opening or closure of hydraulic irrigation valves on the farm (including the inlet valve to the feed tank) dislodged large amounts of fouling material from the inside of the pipeline, which ended up in the feed tank.

Filtration runs C133 to C139 were selected to test the effectiveness of backflush operation with feed flow reversal because during this (late spring to late summer) time the raw feed water quality remained fairly constant. Destabilization runs were performed that showed considerable promise. The results of these destabilization runs are discussed in the next section.

4.6.5 Backflush Operation with Feed Flow Reversal

4.6.5.1 Operating Range

The process flux, corrected to 20 °C using eqs. (2.38) and (2.40) respectively (LMH), dP (kPa) and operating temperature (°C) of filtration cycles C133 to C139 are plotted as a function of cumulative operating time (h) in Figure 20.

The operating temperature during this time ranged between 15 and 25 °C. During C133 to C139 the system was operated at *ca* 80 to 90 kPa dP , as can be seen from Figure 20.

The water recovery was 85 to 95 %. The concentrate that was not recycled to the feed manifold was returned to the feed tank, which resulted in a slow accumulation of organic material in the system over the duration of a filtration cycle. After each backflush the manifolds were flushed with water from the feed tank to remove debris and to limit accumulation in the feed tank.

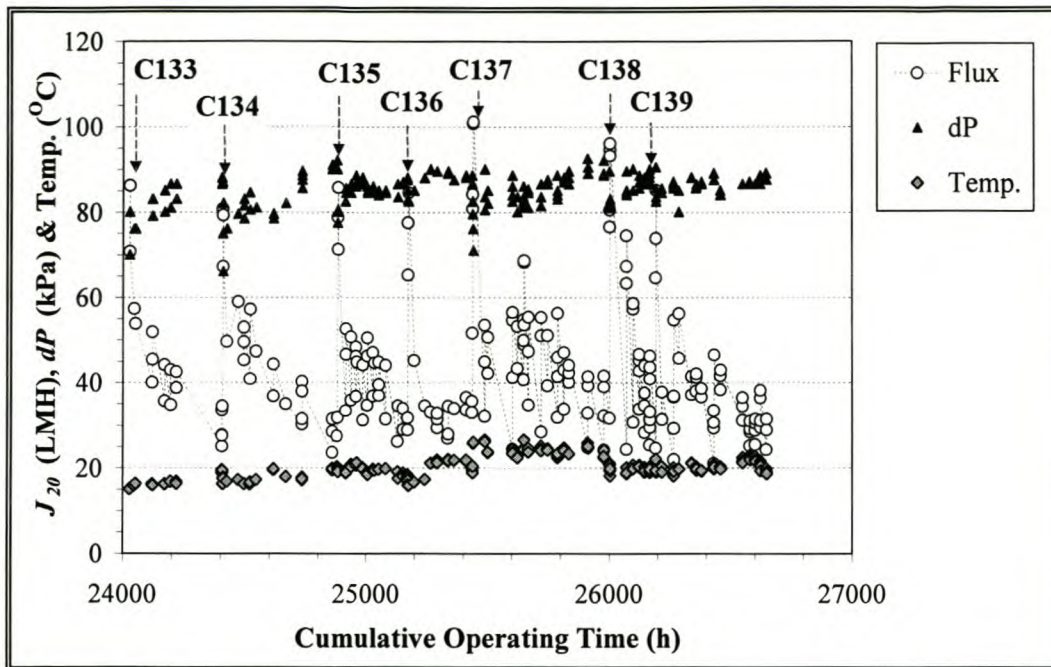


Figure 20: Corrected flux, dP and temperature over the latter part of the Mon Villa investigation as a function of operating time (C133 to C139).

4.6.5.2 Results of Fouling and Cake Layer Growth

It was observed at the plant that, as fouling occurred during the course of a run, not only did the flux decrease with time but the headloss, dP_f (kPa), would also increase (because of smaller cross-section for flow through the membrane lumen). This had the secondary result that the centrifugal type recycle pump would discharge at a lower flow rate as a filtration cycle continued. When a backflush was performed, the headloss would decrease slightly (0.5 to 3.0 kPa).

The normalised headloss (calculated from eq. (2.13c) and linear cross-flow velocity, U_m (m/s), are illustrated graphically as a function of cumulative operating time (h) in Figure 21. In Figure 22 the normalised headloss is plotted for selected cycles C135, C137 and C139 to illustrate the headloss reduction with an effective backflush when the recycle pump flow rate was adjusted to the same value as before the backflush. In cases where the headloss increases after the backflush, the recycle pump flow rate was not adjusted, resulted in a higher cross-flow velocity after the backflush than before, and consequently a greater headloss.

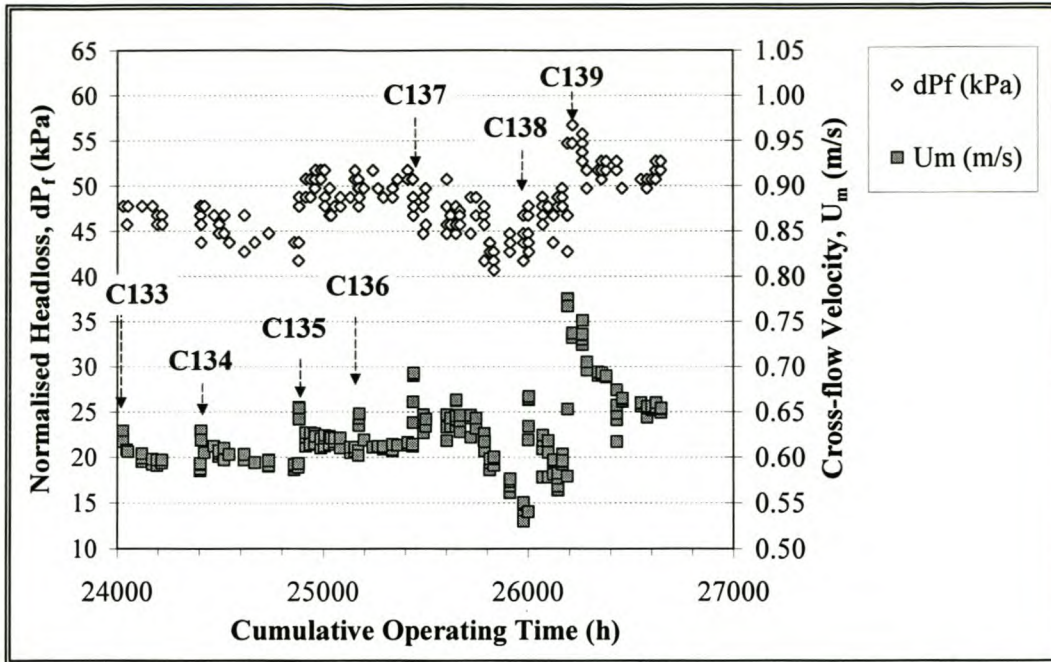


Figure 21: Normalised headloss and cross-flow velocity over the latter part of the Mon Villa investigation as a function of operating time (C133 to C139).

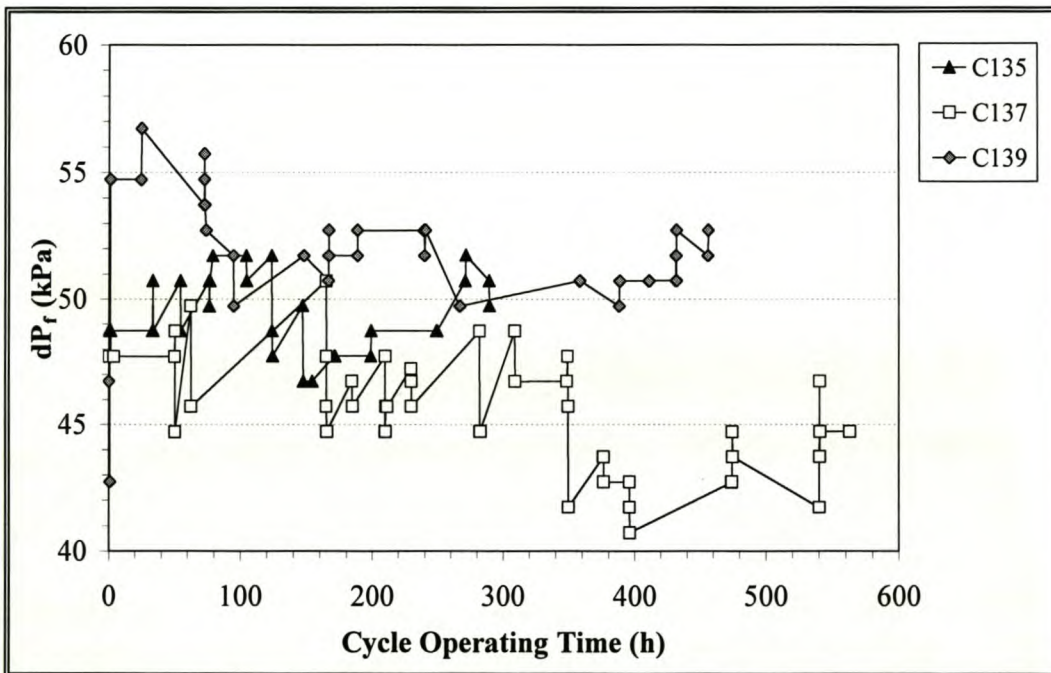


Figure 22: Normalised headloss as a function of cycle operating time for selected filtration cycles C135, C137 and C139.

4.6.5.3 Strategy for Assessing Backflushing Effectiveness

It was generally found over the entire Mon Villa investigation period that backflushing at a backflush dP below the filtration dP and backflush volumes below the feed side hold-up volume was not very effective in removing the cake layer and improving the flux.

An indirect manner of evaluating the effectiveness of a backflush was by monitoring the concentrate turbidity before and after the backflush. If a backflush succeeded in breaking up the accumulated cake layer, the concentrate turbidity would increase rapidly during and immediately after the backflush. If not, the concentrate turbidity after the backflush would be more or less the same as before.

Therefore it was decided to conduct subsequent backflushes during C133 to C139 at a standard backflush dP of 120 kPa, as this pressure had previously produced satisfactory results, had not damaged the membranes, and was 1.5 times the dP during filtration (80 kPa). The membranes were thus backflushed manually every 24 to 48 h at 120 kPa backflush dP with 15 L of permeate.

Before and after each of the manual backflushes, the permeate flux and trans-membrane pressure were measured, the specific process flux J_S (LMH/kPa) was calculated and corrected to a specific flux value $J_{S,20}$ at a standard temperature of 20 °C with the relative viscosity relationship given in eq. (2.38).

The change in corrected specific flux from the previous data point ($n-1$) to the current data point (n) was then calculated and expressed as a percentage of the corrected specific flux at the start of the run ($J_{S,20})_0$ (directly after a CIP) according to the following relationship:

$$\% \text{ Flux Change} = \frac{(J_{S,20})_n - (J_{S,20})_{n-1}}{(J_{S,20})_0} \times 100 \quad (5.1)$$

Although the effect of irreversible fouling (adsorption and pore blocking) could not be separated from reversible fouling effects (cake growth and removal), this normalisation at least allowed comparison of effectiveness of a backflush with and without feed flow reversal for different runs when the initial flux was not the same for different runs. All cross-flow filtration runs for C133 to C139 were done in upward flow mode at a (cross-flow velocity of 0.5 to 0.75 m/s); i.e. the feed water entered the module at the bottom manifold and concentrate exited at the top manifold. To assess the effect of linear feed flow reversal (as a means to destabilize the accumulated cake layer) prior to a backflush two strategies were adopted.

The *first strategy* (referred to as "Strategy A") was to do a first backflush in the downward direction (i.e. after feed flow reversal prior to backflushing); followed by reversing the feed flow direction again to upward flow and doing a second backflush (i.e. without feed flow direction change relative to upflow filtration). The *second strategy* (referred to as "Strategy B") was to conduct a backflush first in the upward direction (i.e. without feed flow reversal prior to

backflushing); followed by reversing the feed flow direction to downward flow and doing a second backflush (i.e. with feed flow direction opposite to filtration). Refer to Table 8 and Table 9 for two sets of backflush results from Strategy A and B respectively.

In Table 8 backflush result Set A represents 13 different backflush runs performed accordingly to Strategy A. Under these conditions the average change in process flux immediately after the first backflush was 10.7 ± 3.4 %, while the average change was 4.3 ± 2.5 % for the second backflush. For the two backflushes combined, the percentage change was 15.0 ± 5.5 %.

Table 8: Backflush result Set A (Filter up, FFR, B/F A1 down, FFR, B/F A2 up, Filter up)

t (h)	A1 (% Change)	A2 (% Change)	A1 + A2 (% Change)
451	5.8	3.3	9.1
33.5	15.9	8.8	24.7
123.9	16.4	5.3	21.7
50.5	14.0	5.8	19.8
165	14.3	5.6	19.9
210	8.0	1.3	9.3
229	10.8	8.6	19.4
282	12.4	4.7	17.1
349	9.0	4.6	13.6
376	7.8	3.1	10.9
474	6.1	1.2	7.3
122	9.4	3.3	12.7
239	9.1	0.8	9.9
Average	10.7	4.3	15.0
Standard Deviation	3.4	2.5	5.5
Variance	12.9	6.5	32.2

In Table 9 backflush result Set B represents 8 different backflush runs from Strategy B. Under these conditions the average change in process flux (from before to after the backflush) for the first backflush was 3.2 ± 1.6 %, while the average change in process flux was 7.0 ± 2.0 % for the second backflush. For the two backflushes combined, the percentage change was 10.2 ± 3.4 %.

Table 9: Backflush result Set B (Filter up, B/F B1 up, FFR, B/F B2 down, FFR, Filter up)

t (h)	B1 (% Change)	B2 (% Change)	B1 + B2 (% Change)
92	6.4	10.8	17.2
376	2.5	4.5	7.0
87	4.0	7.8	11.8
327	1.9	4.2	6.1
171	2.8	7.8	10.6
120	2.3	6.4	8.7
164	1.0	7.0	8.0
69	4.4	7.8	12.2
Average	3.2	7.0	10.2
Standard Deviation	1.6	2.0	3.4
Variance	2.9	4.4	12.8

4.6.5.4 Visualisation of Backflush Effectiveness

All flow destabilization backflush results (% Change) from Sets A and B are given in Figure 23 as a function of operating time into a filtration run when the backflush was performed.

As already mentioned, the effects of reversible and irreversible fouling could not be separated in this investigation. However, it is known that NOM forms cross-linking bonds with metal ions such as calcium, aluminium and iron. Because UF on this type of water containing high NOM concentrations also removes calcium (~ 5 %) and iron (97 to 99 %), it may be assumed that these ions will cross-link in the fouling layer and thus form a more stable fouling layer as filtration time increases into a run. As a result it could be expected that the cake layer will become more resistant to break-up and removal by backflushing alone with increasing filtration time.

Thus for the visualisation of the flow destabilization backflushing results from the present constant pressure cross-flow UF investigation it was decided to fit the four individual sets of data in Figure 23 to linear curves, with the aim of identifying general trends, if any. Although this is not a true representation of the effect of operating time on cake layer densification, the slope of the line (positive or negative) may confirm or oppose the assumption.

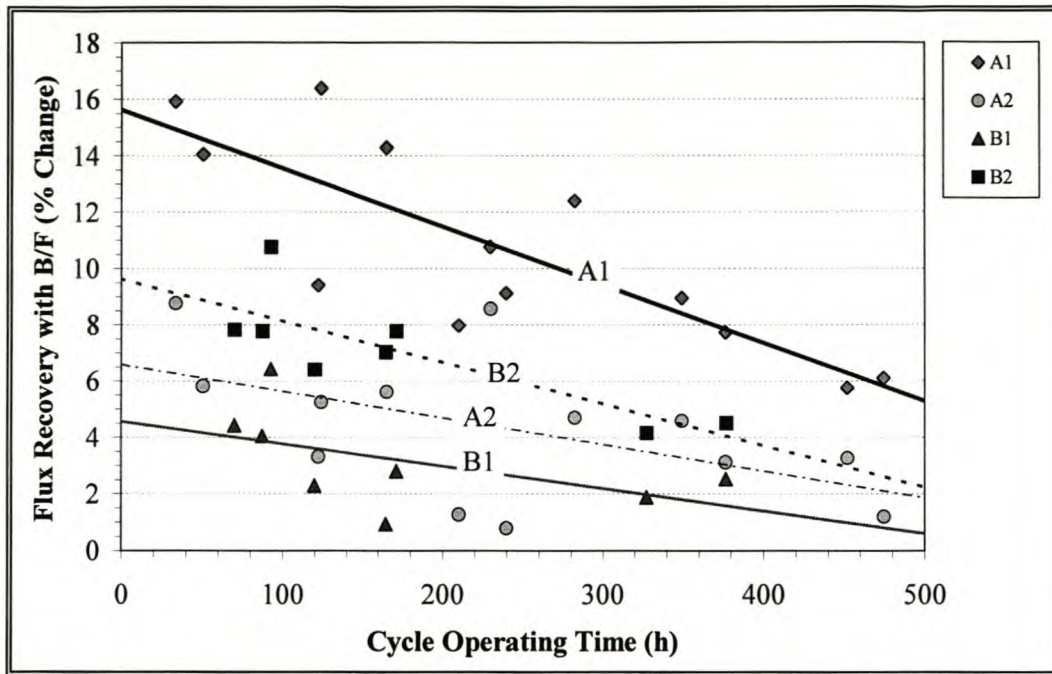


Figure 23: Effect of feed flow reversal on flux recovery with backflush.

From the negative slopes of the four linear curves fitted to the data in Figure 23 it appears that there is a general decreasing trend in the backflush effectiveness with increasing cycle operating time for all four data sets, which confirms the assumption of cake layer densification or irreversible adsorption with increasing operating time into the run.

When the feed flow direction was changed before the first backflush, the concentrate turbidity increased to between 600 and 800 NTU in the first 1 to 3 minutes directly after the backflush; compared to concentrate turbidity of between 200 and 500 NTU without feed flow reversal before the first backflush. After the backflush(es) the system was forward-flushed in cross-flow mode. From these results it appears that changing the feed flow direction directly before the backflush is more effective than backflushing without feed flow reversal.

4.6.5.5 Analysis of Variance

A single factor analysis of variance (ANOVA) was performed to test the *null hypothesis* (H_0) that the averages for the four individual sets of data (A1, A2, B1, B2) were equal (drawn from populations with the same average) and that there was no difference between the percentage normalised change in flux obtained from the four different experiments. The level of significance (α) at which the critical values for the F statistic was to be evaluated, was chosen as 0.05, or 5 %.

If the calculated F-statistic (F_{calc}) was greater than the critical F-statistic at the 0.05 level ($F_{crit,0.05}$), H_0 could be rejected and it could be concluded that there was a significant difference

between the normalised percentage change in flux obtained for two different experiments e.g. A1 and A2. However, if the calculated F-statistic (F_{calc}) was smaller than the critical F-statistic at the 0.05 level ($F_{\text{crit},0.05}$), H_0 was true and it could be concluded that there was *not* a significant difference between the normalised percentage change in flux obtained for two different experiments.

In this way each data set from Strategy A was compared with each data set from Strategy B, and the combined flux recovery from both sets of data (A1+A2 and B1+B2) were also compared. The P-value indicated the percentage probability of a *type-1 error*, i.e. rejecting a true H_0 . The summary of averages, statistics from each data set is listed in Table 24 (Appendix C), while the ANOVA tables for comparison of experiments are listed in Table 25 to Table 31 (Appendix C). The results from the ANOVA are summarised in Table 10.

Table 10: Summary of results from ANOVA

Experiments	Is H_0 True or Rejected at 5 % level?	Conclusion at 5 % level	P-value (%)
A1 & B1	Rejected	Significant difference	0.0025
A1 & B2	Rejected	Significant difference	1.7
A1 & A2	Rejected	Significant difference	0.0025
B1 & B2	Rejected	Significant difference	0.1
A2 & B1	True	No significant difference	26.5
A2 & B2	Rejected	Significant difference	2.1
(A1+A2) & (B1+B2)	Rejected	Significant difference	4.5

From Table 10 the conclusion can be drawn that in comparison of all the experiments except for A2 and B1 there was a significant difference between the average percentage change in flux obtained from backflushing with flow destabilization. In the case of A2 and B1 however, there was a 26.5 % probability of rejecting H_0 .

Between experiments A1 and B1 the difference arose from the FFR before A1 as opposed to no FFR before B1. Between experiments A1 and B2 the difference arose from the fact that B1 had already removed some of the cake layer prior to B2, while A1 had FFR and a fouled membrane to clean. Between A1 and A2 the difference arose from the fact that A1 had already removed a large fraction of the cake layer, which left less for A2 to remove. Between B1 and B2 the difference could be ascribed to the FFR prior to B2, while between A2 and B2 the difference

arose from the fact that A2 was preceded by an effective A1 while B2 was preceded by an ineffective B1. When combining the two backflushes, the difference between (A1+A2) and (B1+B2) was that the Strategy A backflushes had been subjected to 2 feed flow reversals, while the Strategy B backflushes had only been subjected to 1 feed flow reversal.

It appears that one cross-flow backflush alone at 120 kPa dP may not necessarily remove all of the accumulated cake layer from the surface of the membrane, whether this backflush is implemented with or without feed flow reversal prior to the backflush. However, the conclusion can be drawn that flow destabilization (i.e. reversing the flow direction for the cross-flow backflush) does make a significant difference at the 0.05 level in breaking up the cake layer and improving the flux.

4.7 CONCLUSIONS

The Mon Villa pilot plant was operated semi-continuously for 27 000 h in cross-flow mode; and subjected to an alkaline CIP treatment containing SLS and EDTA at a pH of between 10 and 12 every 1 to 3 weeks to restore the flux chemically. In this investigation the cross-flow operation was supposed to give longer operating runs because of the shear that is higher. Excellent reductions in turbidity (above 95 %), colour (92 to 97 %), iron (97 to 99 %), NOM (60 to 85 %) and microbial content were recorded, depending on the feed-water quality. Additional results are discussed in Appendix C.

In manual backflush experiments conducted over a 2680 h period near the latter part of the investigation, two strategies were adopted to investigate the effect of feed flow reversal on backflush effectiveness. Strategy A consisted of a backflush, first with feed flow reversal, followed by a second backflush without feed flow reversal, while Strategy B consisted of a backflush first without feed flow reversal (flow destabilization) followed by a second backflush with feed flow reversal. Backflushes from both strategies were performed at random for various intervals ranging from 24 to 48 h for a maximum filtration cycle time of 500 h before a CIP was implemented.

The observation was made that feed flow reversal before the first backflush (Strategy A) increases the effectiveness of the backflush, when expressed as a normalised percentage change (from before to after the backflush), by almost a factor of 3 over a backflush without feed flow reversal (Strategy B). If a second backflush is performed (directly following the first one, in the opposite direction than the first), the Strategy B second backflush (now in the opposite cross-

flow direction as filtration) is still more effective than the second Strategy A backflush (now in the same direction as filtration). A single factor analysis of variance confirmed this result.

The backflush system that was developed to increase the process flux highlighted some factors that have an effect on the backflush effectiveness. These include:

- ◆ the *backflush dP* ($>$ filtration *dP*), which in this investigation was set at 120 kPa when the filtration *dP* for constant pressure operation was *ca* 80 to 90 kPa;
- ◆ the *backflush volume*, which in this investigation was set at 5 L/module (equal to the total internal hold-up volume of the module);
- ◆ the *operating time* into a run when a backflush is performed, which in this study was carried out at intervals of between 24 and 48 h for a total filtration cycle of up to 500 h, before a CIP was implemented;
- ◆ whether or not the *feed flow direction is reversed* before a backflush; and
- ◆ whether this backflush is followed by a *second backflush* in the *opposite axial direction* as the first backflush.

From these results the hypothesis was proposed that intermittent flow destabilization with reverse axial flow might hinder the formation, growth and densification of the cake layer in UF of surface waters containing high NOM and cations that can complex with the NOM. This flow destabilization method would preferably have to be implemented using existing equipment such as pumps and valves normally found on a UF plant. Also, to reduce the specific power consumption of the operation, it was decided to incorporate this proposed flow destabilization method in dead-end filtration mode, and only to use cross-flow intermittently to flush the membrane modules.

Chapter 5: REVERSE-PRESSURE PULSE GENERATOR

5.1 INTRODUCTION

This invention came about because of work done in Case Study 1 relating to the effect of feed flow reversal combined with backflushing on flux restoration and cake layer removal. During the course of the Case Study 1 (Mon Villa) investigation, it was argued that in the overall design of UF plants operating with axial-flow capillary membrane, linear feed flow reversal systems would most probably be incorporated.

Thus it would be possible to reverse the axial feed flow direction of feed water intermittently (flow destabilization), either during a backflush or during cross-flow filtration operations in an attempt to reduce fouling and/or concentration polarization. A possible method would be by utilising *four rapid-response controlled valves* and a suitable pipe layout up- and downstream from the membrane modules. The idea of opening and closing the upstream valves intermittently to destabilize the feed flow evolved from this, and so the "Reverse-pressure pulse generator" concept, presented in this chapter, was born. In the next chapter, the conceptual idea will be implemented on a full scale pilot plant containing six 90 mm modules.

5.2 PRINCIPLE AND DESCRIPTION

In Figure 24 a flowsheet is shown of a membrane unit equipped with a conventional backflush system comprising a backflush (mono) pump, permeate accumulator and suitable valve arrangement. In Figure 25 to Figure 28 the layout has been slightly altered to accommodate the conceptual operating principle of the reverse-pressure pulsing system [WRC, 1999].

5.2.1 Backflushing

During the XF membrane filtration cycle, feed water is pumped axially through the membrane module to produce a permeate and concentrate stream, while a recycle pump may return a portion of the concentrate water to the module via a recycle line. In the case of DE filtration, all water entering the module will exit as permeate, while no recycle pump will be used.

In Figure 24 the feed and recycle pumps may be throttled by valves V1 and V2 respectively. During DECP or XFCP filtration a manual type diaphragm valve V4 regulates the permeate back-pressure (and thus filtration rate) while V6 is a concentrate back-pressure valve (which is closed during DE operation). During DECF or XFCF filtration V4 is closed, V5 and V8 are open and the filtration rate is controlled by regulation of the rotation speed of the product/backflush pump. The direction of rotation of the product pump is reversed for backflushing to act as a backflush pump. Conventional permeate backflushing may be accomplished with a backflush pump and permeate accumulator (A1) which is open to the atmosphere via a non-return valve V9 (passing air in and out, but no water out), as illustrated in Figure 24. The negative dP for effective backflushing is obtained by increasing the permeate pressure (P_p) sufficiently above the system pressure ($(P_i+P_o)/2$).

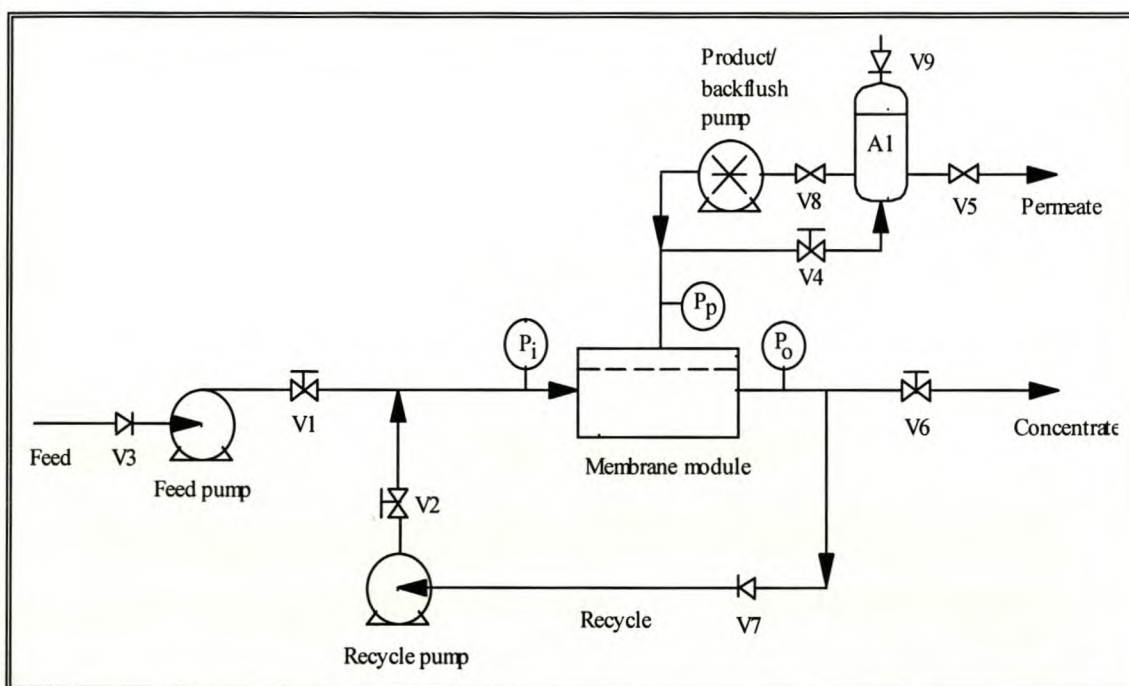


Figure 24: Flowsheet of a membrane unit with feed, recycle and backflush pumps, a permeate accumulator and suitable valve arrangement for conventional backflush operation.

During the backflush operation V4 is throttled or closed and V5 is closed while V8 is opened to pump permeate back through the membranes. During the backflush operation the feed pump is also switched off (to reduce feed side pressure) while the non-return valve V3 prevents back-flow through the feed pump. Backflush water exits the system through V6 while the recycle pump may be switched on for a XF backflush or off for a DE backflush.

5.2.2 Reverse-Pressure Pulsing without Simultaneous Venting

For conventional backflushing reverse flow is generated by forcing water from the permeate to feed side at a controlled rate by increasing the permeate side pressure sufficiently above the feed side pressure. The main difference between conventional backflushing and reverse-pressure pulsing lies in the fact that to accomplish the latter the feed side system pressure has to be reduced sufficiently below the permeate back-pressure in a very short time (less than 1 s). This may be effected in a number of ways, as will be discussed in the following sections.

5.2.2.1 Two Pumps and Two Accumulators

The flowsheet in Figure 25 illustrates an example in accordance with SA Patent 99/4620 [WRC, 1999]. In this example, valves V1 to V7 and V9 have the same reference numerals and are of the same type as in Figure 24.

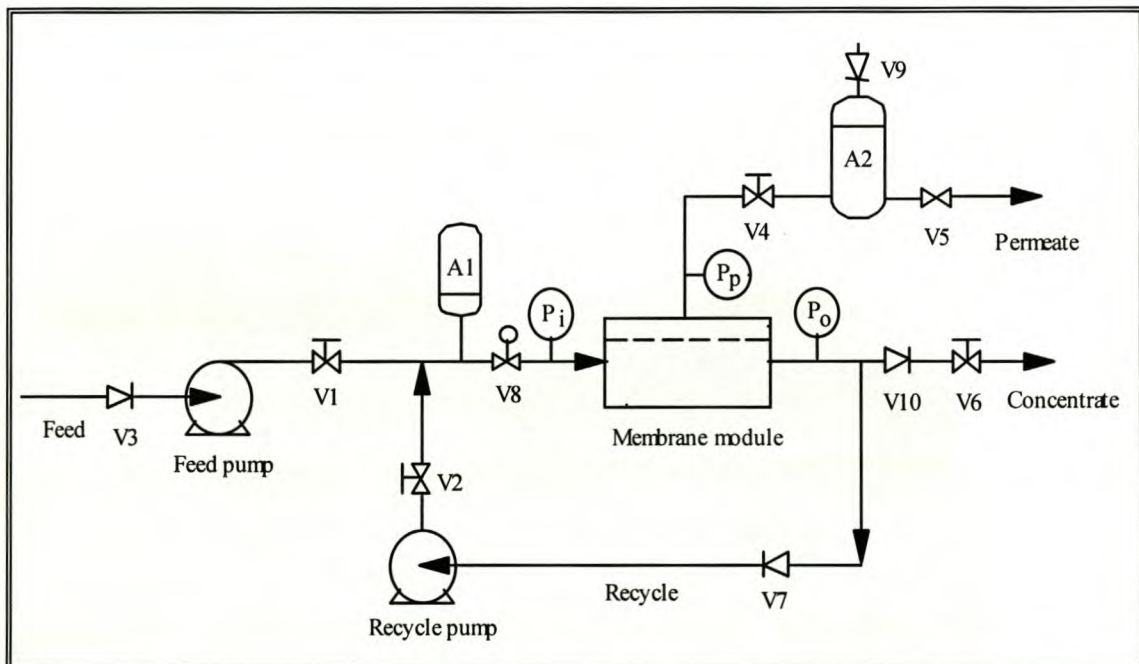


Figure 25: Flowsheet of a membrane unit with two pumps, two accumulators and valve arrangement for reverse-pressure pulsing without simultaneous venting.

A non-return valve (or actuated valve) V10 has been added downstream from the recycle/concentrate separation point to prevent back-flow of concentrate into the system. This valve V10 may be either upstream or downstream from the back-pressure valve V6. A pneumatically actuated butterfly valve V8 has also been added upstream of the membrane module entry port, but downstream from a gas-filled accumulator A1. The function of V8 is to

close off the entry line into the module rapidly, while liquid taken up by A1 results in compression of the gas in the accumulator. With this setup, filtration may commence in DE (recycle pump off and V6 closed) or XF (recycle pump on and V6 set to control back-pressure) mode.

In order to initiate the reverse-pressure pulse cycle, the recycle pump is switched on to set recirculation motion (transfer momentum to the feed water) and the feed pump is switched off. After a short delay to vent system pressure, V8 is closed to shut off inflow of feed water into the module. Thus V3 prevents back-flow of water through the feed pump while the non-return valve V10 (or closed actuated valve V10) prevents back flow of concentrate. The only source of inflow water through the suction side of the recycle pump at this stage is through the membranes from the permeate accumulator A2. In this way a rapid negative dP pulse may be applied to the membranes for backpulsing purposes.

Since the recycle pump is of the centrifugal type, the peak negative dP pulse can only be maintained for a couple of seconds before slippage starts to occur in the recycle pump. The result is a steadily decreasing negative dP across the membranes with accompanying decreasing flow of permeate from the downstream to upstream side of the membrane until the upstream system pressure ($(P_i+P_o)/2$) and downstream pressures (P_p) are equal.

This back-flow of permeate through the membranes may dislodge accumulated material on the membrane surface to become re-suspended in the recycle loop. Before resuming DE filtration, the recycle pump is switched off, the feed pump is switched on, V8 opens and actuated valve V10 is kept open for a short time duration to rinse re-suspended material from the system. Thereafter V10 is closed and DE filtration is resumed. In the case of XF filtration resumption, the feed pump is switched on; the recycle pump is kept running, and actuated valves V8 and V10 are opened.

5.2.2.2 One Pump and Two Accumulators

The flowsheet in Figure 26 illustrates an example in accordance with a second embodiment of SA Patent 99/4620 [WRC, 1999]. In this example the valves V1, V4 to V6, V7 and V9 have the same reference numerals and are of the same type as in Figure 24.

As in Figure 25 a non-return valve V10 (in the case of XF mode) or actuated valve V10 (in the case of DE mode) has been added downstream from the recycle/concentrate separation point to prevent back-flow of concentrate into the system. This valve V10 may again be either upstream or downstream from the back-pressure valve V6. Also as in Figure 25 a pneumatically actuated

butterfly valve V8 has been added upstream of the membrane module entry port, but downstream from the gas-filled accumulator A1. The function of V8 is again to close off the entry line into the module rapidly while liquid taken up by A1 results in compression of the gas in the accumulator.

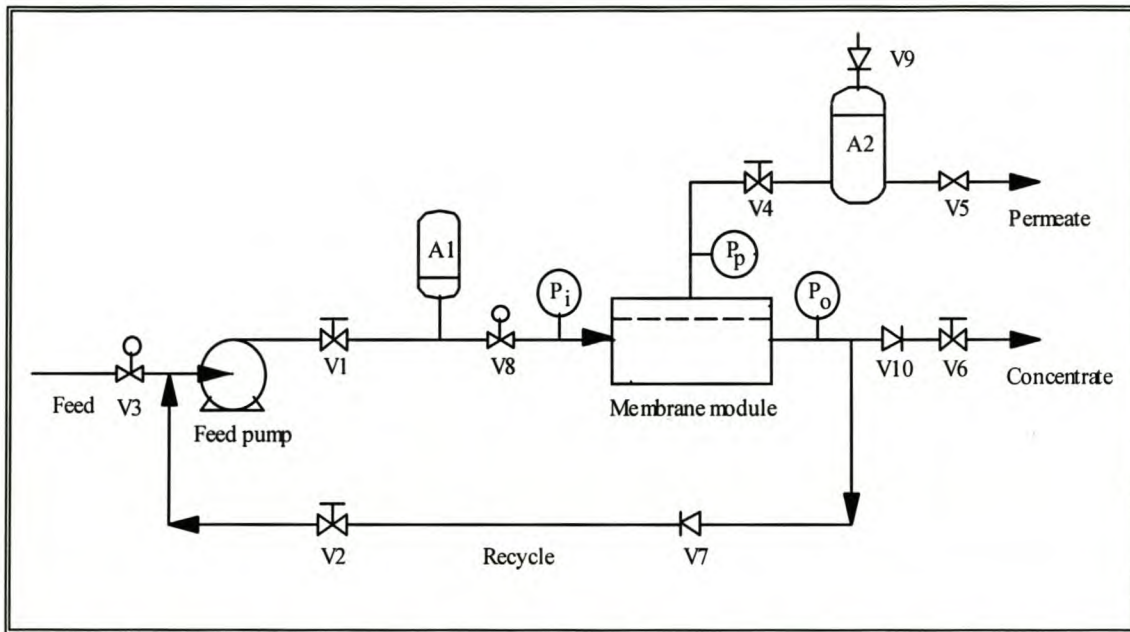


Figure 26: Flowsheet of an alternative membrane unit with one pump, two accumulators and suitable valve arrangement for reverse-pressure pulsing without simultaneous venting.

An actuated valve V3 in Figure 26 has replaced the non-return valve V3 upstream of the feed pump (in Figure 24 and Figure 25) while the recycle pump from Figure 24 and Figure 25 has been removed. In this case the manual type diaphragm valve V2 would serve as a recycle line shut-off valve during DE filtration mode (with actuated valve V10 closed); or XF mode (V2 partially or completely open and V6 set to control back-pressure). The return point of the recycle line enters the feed line at a point between V3 and the feed pump.

In order to initiate the reverse-pressure pulse cycle, the feed pump is switched off for a short delay to vent system pressure, followed by closure of V3 and start-up of the feed pump to set the recirculation motion (transfer of momentum) at reduced system pressure. However, stopping and starting of pumps causes power consumption peaks. It would therefore be cheaper to open a vent valve to reduce the pressure in the system. Thereafter V8 is closed to shut off inflow of feed water into the module. The closed V3 prevents inflow of water through the feed pump while the non-return valve V10 (or closed actuated valve V10) prevents back flow of concentrate. The only source of inflow water to the suction side of the feed pump at this stage is through the

membranes from the permeate accumulator A2. In this way the membranes experience a rapid negative dP pulse.

Since the feed pump is of the centrifugal type that cannot pump above a certain head, the peak negative dP pulse can only be maintained for a couple of seconds before slippage starts to occur in the pump. The result is a steadily decreasing negative dP across the membranes with accompanying decreasing reverse flow of permeate.

To resume DE filtration, V3 and V8 are opened and actuated valve V10 is kept open for a short time duration to rinse re-suspended material from the system. Thereafter actuated valve V10 is closed and DE filtration is resumed. In the case of XF filtration resumption, V3 and V8 are opened while the feed pump is kept running.

5.2.3 Reverse-Pressure Pulsing with Simultaneous Venting

A further reverse-pressure pulsing method to the procedures described in the previous section is discussed below.

5.2.3.1 Two Pumps, Two Accumulators and a Venting Line

In this instance a process layout similar to the one described in section 5.2.2.1 is used, as illustrated in Figure 27. However, the current layout differs from Figure 25 in that a venting line containing an actuated valve V11 and a manual back-pressure valve V12 has been added between the feed pump throttle valve (V1) and the accumulator A1. The venting line may be up- or downstream from, or at the feed/recycle mixing point.

The filtration cycle is still the same as described in section 5.2.2.1, but during the backpulse cycle V11 opens concurrently with the switching on of the recycle pump and closure of V8. This allows the volume of water that is drawn back through the membranes via the recycle pump to be (partially compressing the air in A1 and partially) vented from the system immediately. In other words, an additional rinse cycle may not be necessary, and the negative dP across the membranes can be maintained for a longer period because the momentum of water between the membrane and the suction side of the recycle pump is conserved.

In large systems the inclusion of the accumulator A1 would buffer the momentum loss of feed water for the fraction of a second that V11 takes to open. Without A1 the sudden loss of momentum of water upstream from V8 might cause uncontrolled water hammer, which would be

undesirable. The throttling valve V2 serves as an additional protection mechanism as it is set so that the recycle pump operates on its pressure curve to prevent cavitation.

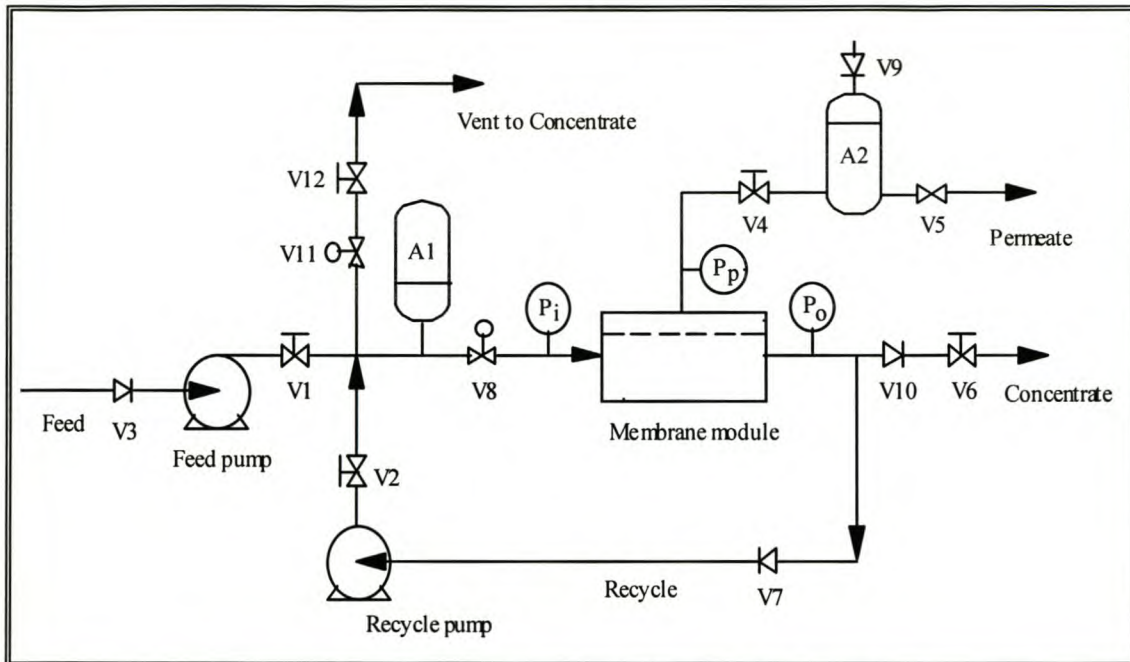


Figure 27: Flowsheet of a membrane unit with two pumps, two accumulators, a venting line and valve arrangement for reverse-pressure pulsing with simultaneous venting.

To resume DE filtration, the recycle pump is switched off, the feed pump is switched on and V8 opens while actuated valve V10 stays closed. In the case of XF filtration resumption, the feed pump is switched on; the recycle pump is kept running, and actuated valves V8 and V10 are opened. All reference to XF filtration in this chapter is only by way of example since all experiments in the next chapter were conducted in DE operating mode, with the assumption that DE filtration was the worst-case scenario and if R/P works for DE filtration it will work for XF filtration as well.

5.2.3.2 One Pump, Two Accumulators and a Venting Line

In this instance a process layout similar to the one described in section 5.2.2.2 is used, as illustrated in Figure 28. However, this layout differs from Figure 26 in that a venting line containing an actuated valve V11 and a manual back-pressure valve V12 has been added between the feed pump throttle valve (V1) and the accumulator A1. The function of the accumulator is the same as in the previous example.

The filtration cycle is still the same as described in section 5.2.2.2, but a controlled valve V13 has been added to bypass the pressure restriction valve V2 during XF filtration (while V6 is shut during DE and XF operation). During the backpulse cycle V11 and V13 open concurrently with the closure of V8 and V3. This allows the volume of water that is drawn back through the membranes via the feed pump to be vented from the system immediately while compression of the air in A1 takes place simultaneously. In other words, an additional rinse cycle is not necessary, and the negative dP across the membranes can be maintained longer because the momentum of water between the membrane and the suction side of the feed pump (now used for recycling) is conserved. The back-pressure valve V12 now serves as a protection mechanism for preventing cavitation in the feed pump.

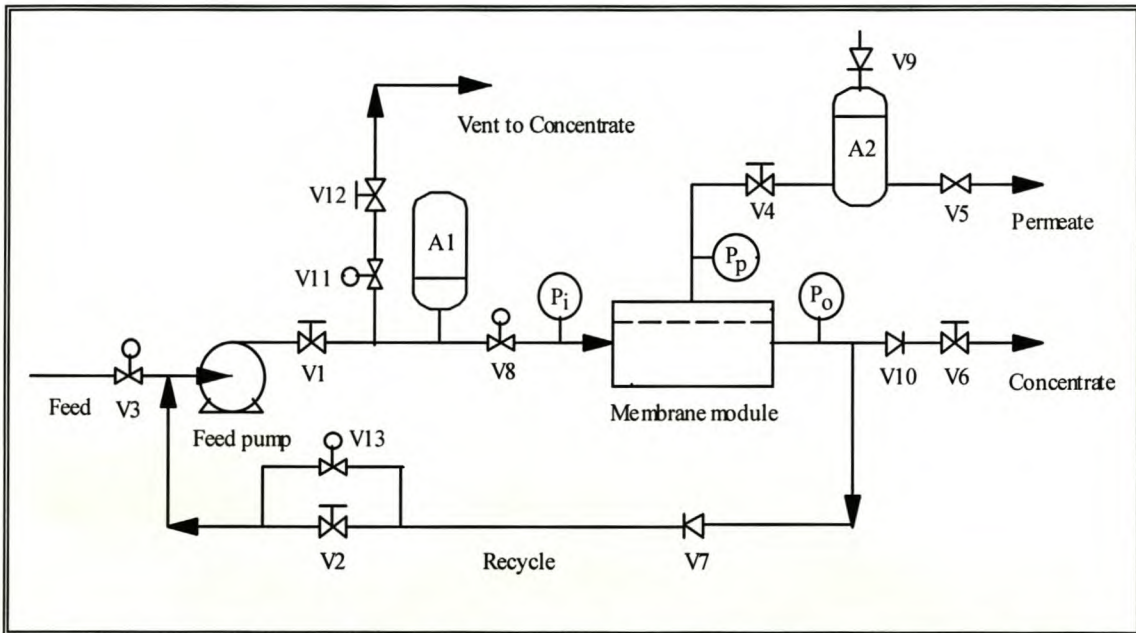


Figure 28: Flowsheet of an alternative membrane unit with one pump, two accumulators, a venting line and suitable valve arrangement for reverse-pressure pulsing with simultaneous venting.

To resume either DE or XF filtration, V3 and V8 are opened simultaneously with closure of V11 while the feed pump is kept running. The advantage of this setup is that only one pump is needed for filtration and recycle (momentum build-up), while down-time is reduced by the simultaneous backpulsing and venting actions.

5.3 CONCLUSIONS

In Chapter 5 the layout and operation of a conventional backflush system was discussed, followed by four different examples of the conceptual principle and operation of the "Reverse-pressure pulse generator" in both DE and XF modes of filtration.

In general terms the differences between conventional backflushing and the proposed reverse-pressure pulsing method may be summarised in Table 11.

Table 11: Summary of differences between conventional backflushing and the proposed reverse-pressure pulsing method

Parameter	Backflushing	Reverse-pressure pulsing
Generation of negative dP	Increase permeate pressure sufficiently above feed pressure	Decrease feed pressure sufficiently below permeate pressure
$d(dP)/dt$ (negative)	Small	Likely to be very large
Flush volume (product loss)	Large	Likely to be small
Filtration time between cycles	Long	Shorter than for B/F
Overall product water recovery	Fair	Larger than for B/F

The four examples proposed in this chapter included reverse-pressure pulsing with:

- ◆ two pumps and two accumulators *without* simultaneous venting of backflushed water;
- ◆ one pump and two accumulators *without* simultaneous venting of backflushed water;
- ◆ two pumps and two accumulators *with* simultaneous venting of backflushed water; and
- ◆ one pump and two accumulators *with* simultaneous venting of backflushed water.

In each example where two pumps are used, the possible advantages of the specific method of DE operation was evaluated at the Paradyskloof Water Treatment Works in Stellenbosch. The results will be discussed in the next chapter.

Chapter 6: CASE STUDY 2 - PARADYSKLOOF

6.1 INTRODUCTION

The conceptual idea of the "reverse-pressure pulse generator" was first tested on a laboratory scale unit containing one 90 mm module, where it was shown that a negative dP could be attained following closure of the valve upstream of the module in cross-flow. However, testing of the method was hampered by the fact that a *model foulant* was not available that displayed fouling characteristics similar to those found in natural surface waters. Thus it was decided to evaluate UF operation with flow destabilization on a demonstration membrane filtration system which had to comply with certain requirements.

The requirements for the evaluation facility are listed below.

- ◆ *Actual surface water* from the Theewaterskloof impoundment would be used as feed.
 - ◆ The filtration system had to have a computerised *software-driven control strategy and data logging ability*, as this would simplify and accelerate evaluation of the effect of changes in the control strategy.
 - ◆ In Case Study 1 it was found that the operating cost associated with cross-flow filtration (when both feed and recycle pumps operate continuously) was too high for the cost-effective delivery of a potentially low-value potable product. Thus in Case Study 2 filtration would commence in DE mode in order to reduce the (electrical) operating cost of the unit.
 - ◆ Rapid response pressure transducers and flow sensors were needed to log *dynamic response* of system pressures and flows before, during and after reverse-pressure pulsing. This requirement was set because of the anticipated short time-scale of dP and flux changes during the reverse-pressure pulse.
-

6.2 AIMS OF THE INVESTIGATION

The plant is situated at the Paradyskloof water works of the Stellenbosch Municipality and the aims of the Paradyskloof investigation were to:

- ◆ test the *principle* and *operation* of DE UF with intermittent flow destabilization on a full-scale plant in a potable water application;
- ◆ establish a control sequence which would *maximize* the R/P peak dP and (reverse) flux achieved with the membranes and modules used;
- ◆ evaluate operation of the different *embodiments* of the reverse-pressure pulsing concept as described in Chapter 5 with regard to *sustaining* the R/P peak dP and reverse flux achieved;
- ◆ evaluate the effectiveness of flow destabilization to maintain system flux over extended periods of operation; and
- ◆ monitor the *feed and product quality* to establish the effect of reverse-pressure pulsing on the membranes used.

6.3 SYSTEM DESCRIPTION

6.3.1 Membranes and Modules

The filtration unit is equipped with capillary membranes housed inside axial flow modules as described in sections 4.3.2. These IPS code #798 membranes are hydrophobic double-skinned polysulphone capillaries with a sponge-like substructure, as opposed to the porous microvoid substructure of the IPS code #763 membranes shown in Figure 13 and Figure 14. Although the outer skin layer will reduce the pure-water flux somewhat (when compared with the flux of the IPS code #763 membranes), the sponge-like substructure and the outer skin contributes to higher mechanical strength that can withstand more intense shocks during filtration, backflushing and reverse-pressure pulsing.

The variables and hydraulic module parameters for these modules can be found in Table 12. Six such modules were used, namely 2 modules containing 1200 fibres of IPS code #798 membranes (referred to as Mod 2) each and 4 modules containing 1228 fibres of IPS code #798 membranes

(referred to as Mod 3) each. Thus the total membrane area available for filtration was 29.77 m² with a total frontal flow-area of 0.0083 m².

Table 12: Variables and hydraulic module parameters for the experimental modules used in Case Study 2

Description of Variable	Variable	SI Units	Mod 2 (x2)	Mod 3 (x4)	
Number of membranes in module	N_m		1200	1228	
Membrane internal diameter	d_i	m	0.0012	0.0012	
Membrane external diameter	d_o	m	0.0018	0.0018	
Module housing internal diameter	D_i	m	0.086	0.086	
Module external diameter	D_o	m	0.090	0.090	
Membrane filtration length	L_F	m	1.08	1.08	
Membrane total length	L_T	m	1.2	1.2	
Description of Parameters	Parameter	SI Units	Mod 2 (x2)	Mod 3 (x4)	Plant Totals
Packing density	ψ	%	52.6	53.8	
Membrane area per unit volume	ϕ	m ² /m ³	778.8	797.0	
Feed-side hold-up volume	VF_H	Liter	1.466	1.500	8.93
Permeate side hold-up volume	VP_H	Liter	2.976	2.899	17.55
Wetted membrane hold-up volume	VM_H	Liter	1.832	1.875	11.16
Total internal hold-up volume	VH_T	Liter	6.274	6.274	37.64
Module membrane area	A_m	m ²	4.886	5.000	29.77
Module frontal flow-area	A_F	m ²	0.00136	0.00139	0.0083

6.3.2 Process Layout and Description

Figure 29 shows the piping and instrumentation diagram of the UF testing facility at the Paradyskloof water purification works in Stellenbosch, South Africa. This testing facility will henceforth be referred to as the "Paradyskloof plant".

An equipment list of pumps, valves, measurement devices and miscellaneous equipment for the Paradyskloof plant is shown in Table 13. For information on the calibration of measurement devices, see Human [1998].

A centrifugal feed pump supplies feed water at the required pressure to the vertically installed membrane modules. Centrifugal pumps were used because of their relatively low operating cost and maintenance-free operation. Four centrifugal recycle pumps may be switched and throttled individually to regulate the cross-flow velocity across the membrane surface. Four recycle pumps were initially installed when the plant was built in 1996 to accommodate up to 12 modules in cross-flow operation. All centrifugal pumps are fitted with spring-loaded non-return valves to prevent feed water from bypassing the modules. A variable speed mono pump may be used to operate the process in constant flux mode by regulating the frequency of the inverter. The pump motor is cooled by an industrial fan to prevent overheating. The mono pump may be bypassed to operate the process in constant pressure mode with ProdV open. This option was followed in all experiments to operate the system in DE constant pressure mode during this part of the investigation. Four pneumatic actuated 90 mm butterfly valves (UpflowV1, UpflowV2, DownflowV1 and DownflowV2 with individual switching capability) are employed to control the flow direction of the feed water. In default DE and XF filtration modes feed water flows upward into and/or through the modules; i.e. UpflowV1 and UpflowV2 are open while DownflowV1 and DownflowV2 are closed. When the reverse-pressure pulse is initiated, UpflowV1 closes to shut off the flow of feed water into the modules while UpflowV2 stays open to draw permeate back through the membranes with the recycle pump(s).

A feed-side accumulator, A1 (15 L with external sight glass), was installed in the feed line as shown in Figure 29, while two permeate accumulators were employed on the product side of the modules. Accumulator A2 (200 L) was situated on the roof of the cargo container while permeate accumulator A3 (15 L with external sight glass) was installed between the product flow transducer and permeate shut-off valve ProdV. The outlet pipe of A3 was constructed in such a way that it ran down to the bottom of the accumulator while the inlet pipe from the product flow transducer was situated above the outlet pipe. By closing ProdV during the R/P sequence the volume of air in the accumulator could thus be pressurized to increase the product pressure.

A low pressure switch (PSLP) in the feed line downstream from the feed pump switched off the system when the feed water supply was interrupted during filtration mode. This was to safeguard the centrifugal pump motors from damage when running dry. A high pressure switch (PSHP) also switched off the system in the event of outlet valve failure during backflush operation. This was to prevent over-pressurization and damage to the membranes and system during backflush or R/P. A differential pressure switch (PSDP) monitored the pressure difference between feed and permeate, and switched off the system when this differential pressure exceeded 2.5 bar. This also safeguarded the membrane modules against over-pressurization and damage.

Figure 29: Piping and instrumentation diagram of the Paradyskloof plant.

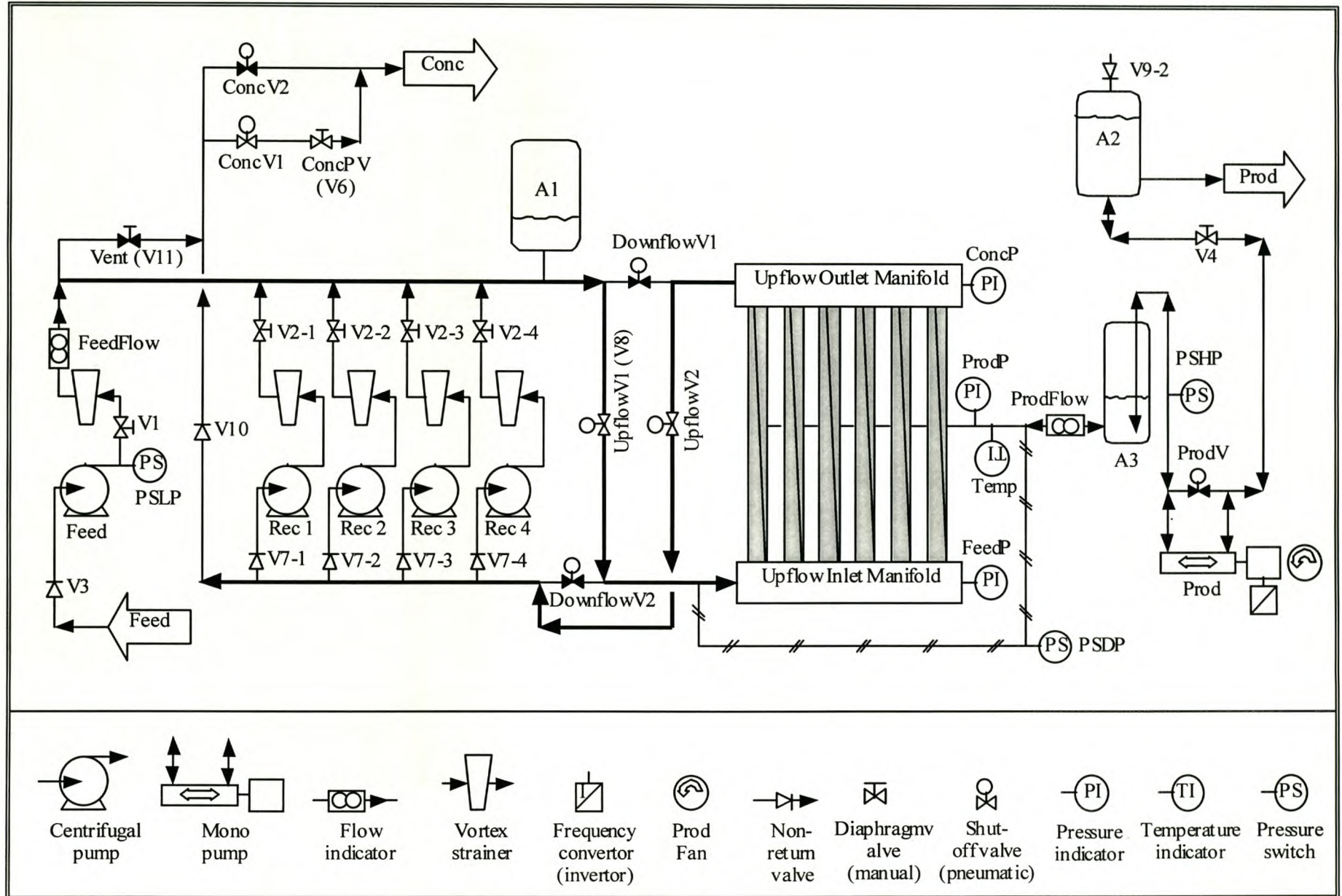


Table 13: List of pumps, valves, measurement devices and miscellaneous equipment of the Paradyskloof plant

Abbreviation	Full Name	Type/Specifications	Setting
Feed	Feed pump	Centrifugal	
Rec 1 to Rec 4	Recycle pumps 1 to 4	Centrifugal	
Prod	Product pump	Mono	
UpflowV1 (V8) & UpflowV2	Upflow valves 1 & 2	90 mm Butterfly	N/O - pneumatic
DownflowV1 & DownflowV2	Downflow valves 1 & 2	90 mm Butterfly	N/C - pneumatic
ProdV	Product valve	32 mm Ball	N/C - pneumatic
ConcV1	Concentration valve 1	32 mm Ball	N/O - pneumatic
ConcV2	Concentration valve 2	32 mm Ball	N/C - pneumatic
ConcPV (V6)	Concentration back-pressure valve	32 mm Diaphragm pressure control	0-4 bar
V1	Feed pump throttle valve	32 mm Diaphragm	Manual
V2-1 to V2-4	Recycle pumps throttle valves	50 mm Diaphragm	Manual
V3	Feed non-return valve	32 mm Non-return	Spring-loaded
V4	Permeate back-pressure valve	32 mm Ball	Manual
V7-1 to V7-4	Recycle non-return valve	50 mm Non-return	Spring-loaded
Vent (V11)	Reverse-pulse vent valve during simultaneous venting experiments	32 mm Ball: Open (with venting) Closed (without)	Manual (V11 in Figure 27 and Figure 28)
V9-2	Air vent valve	32 mm Non-return	Spring-loaded
FeedP	Feed pressure transducer	Wika Instr.	4-20 mA signal
ConcP	Concentrate pressure transducer	Wika Instr.	4-20 mA signal
ProdP	Permeate pressure transducer	Wika Instr.	4-20 mA signal
FeedFlow	Feed flow transducer	Danfoss	4-20 mA signal
ProdFlow	Permeate flow transducer	Danfoss	4-20 mA signal
Temp	Temperature transducer	Wika Instr.	4-20 mA signal
PSHP	High pressure switch	Wika Instr.	4-20 mA signal
PSLP	Low pressure switch	Wika Instr.	4-20 mA signal
PSDP	Differential pressure switch	Wika Instr.	4-20 mA signal
Power	Power transducer		4-20 mA signal

N/O - Normally open (fails open); N/C - Normally closed (fails closed)

6.4 DATA ACQUISITION AND PROCESS CONTROL

6.4.1 Hardware

The data acquisition and control system for this plant was initially developed as part of a WRC project (K5/965) aimed at automation of a UF plant [Human, 1998]. Therefore only a brief description will be given here.

The control system consists of a number of components (Table 13), which will be listed below.

- ◆ A *programmable logic controller* (PLC) from the vendor Moeller Electric (Pty) Ltd is used. Program execution is cyclic instead of continuous execution as used in analogue controllers.
- ◆ *Measurement devices* include magnetic flow meters, a thermocouple, a power transducer and pressure transducers.
- ◆ *Pneumatic valve actuators* are used to change feed flow direction and shut off flow into the modules at the start of the reverse-pressure pulse sequence; while solenoid valves are used to open/close pneumatic lines.
- ◆ *Pump switchgear* includes contactors for pumps and a frequency inverter to control the mono pump forward and reverse delivery rates.
- ◆ The *control panel* consists of user input buttons and status display lights.
- ◆ A *personal computer* is used to receive, display and store data from the PLC. Data are stored in text files.

6.4.2 Software

The initial PLC control program has since been adapted to accommodate the needs of the reverse-pressure pulsing investigation. Frequent changes were made to allow evaluation of the different embodiments of the invention. The feed, concentrate and permeate pressures as well as the feed and permeate flow rates are recorded at regular intervals according to user input specifications, along with the total power consumption of the system and the permeate temperature. Eq. (2.36) was used to calculate water viscosity in Case Study 2. The data logging time intervals may vary from 1 second upward to 300 s.

6.5 EXPERIMENTAL

6.5.1 General Procedures

In all experiments the PLC control sequence was adapted to accommodate experimental protocol. The graphic user interface program window on the PC shows real time data. The data logging time intervals could be set for the experiment, and information on the experiment user, experiment number and comments concerning the experiment were logged together with the recorded data.

The experiment was started while simultaneously initiating the data-logging program via the data-logging interface from the PC keyboard. From this point on the user had to wait for the experiment to run its duration while data were logged to the PC text file. When the experiment was completed, the data text file was automatically closed by the control program. Data could then be downloaded onto a data disk for analysis in a Microsoft[®] Excel 97 spreadsheet.

It has become the standard that potable water filtration plants operate in DE mode. It was decided to conduct all experiments in this investigation also in DE constant pressure filtration mode. In DE mode only the feed pump operates to pressurize the membrane system, and the instantaneous permeate recovery would be 100 % as all feed water would exit the system as permeate. No product pump would be needed in DECP mode as the recycle pump in combination with UpflowV1 would be used to effect the R/P.

All filtration and reverse-pressure pulsing sequences occurred in *up-flow* mode, i.e. with feed water flowing in the same direction as for filtration. This was not an oversight, since the concentration blow-down valve ConcV2 remained open for 2 to 5 s to allow the feed pump to rinse dislodged foulants from within the system. However, in the case of experiments 14 to 16, backflush volume flow was used to rinse foulants dislodged during earlier R/P cycles from the system. *Up-flow* mode was chosen for R/P, since the hypothesis was made that if flow destabilization with reverse flow were even partially effective in up-flow mode, then it would be even more effective in down-flow mode. In automatic DE mode filtration and backflush sequences are executed consecutively by adjusting the respective timers in the PLC program before compiling, e.g. filtration may continue for 18 000 s (5 h) followed by 300 s (5 min) of backflushing, followed by filtration again etc. The R/P sequence is looped within the filtration sequence alone, i.e. the R/P sequence cannot be invoked from within the B/F sequence.

A general summary of the experimental planning and execution is listed in Table 14. However, this table should be read in conjunction with Table 15 to Table 19 in this chapter, and Table 32 to Table 36 in Appendix D. In experiments 1 to 12 the aim was to maximize the R/P dP , since in this way the maximum amount of water could be returned through the membrane in reverse flux. These turned out to be just another method of backflushing, which is known not to be very effective in removal of the cake layer. In experiments 13 and 14 the aim was to destabilize the flow, i.e. to create a rapid dP pulse across the membrane, superimposed on a rapid deceleration of the lumen-flow velocity. The effectiveness of the R/P method (used in experiments 13 and 14) was evaluated in experiments 15 to 16.

Table 14: General summary of experimental planning and execution

Exp	Product venting	Initial system press. vent	Recycle first	Press. Prod. accum. before R/P	Pumps running during flush	Result or effect on R/P
1 to 4	No	No	Yes	No	Feed	Low peak dP & flux.
5 to 9	No	Yes	No	No	Feed	Increase peak dP & flux.
10 to 11	No	Yes	No	Yes	No	High initial peak dP & flux, fast decline.
12	No	Yes	No	Yes	Both	High initial peak dP & flux, fast decline, then stabilization.
13 to 14	Yes	Yes	Yes	Yes	No flush	Sustain peak dP & flux, repeated lift & sweep by destabilizing the flow across the membrane.
15A						No R/P, only B/F & fouled membranes.
15B-15C	Yes	Yes	Yes	Yes	No flush	Sustain peak dP & flux, repeated lift & sweep to remove fouling layer after 15A.
15D	Yes	Yes	Yes	Yes	No flush	Illustrate "lift-and-sweep" on fouled membrane.
16	Yes	Yes	Yes	Yes	No flush	Sustain peak dP & flux, repeated lift & sweep, continued long-term evaluation.

6.5.2 R/P Without Simultaneous Venting of Product

Initial trials were conducted with a small volume (2 L) accumulator A1 to evaluate changes to the sequencing of control events. The feed pressure transducer was also moved from upstream of A1 to its present position on the feed manifold, as shown in Figure 29. Results from these early trials will not be presented. For the purposes of reverse-pressure pulsing (R/P) a number of timer and marker statements were included in the control program. A timer was invoked and the next marker was set (S). When this marker was high, certain outputs were activated, i.e. pumps, valves etc. were set (S) or reset (R) to their default state. When the timer had run its duration, the next timer would start its count and the next marker would be set. This made it possible to sequence events and change the duration of events online during experimentation.

6.5.2.1 Experiments 1 to 4

Before the start of experiment 1 the system was subjected to a CIP and feed water flush. The markers with description of events for experiments 1 to 4 are listed in Table 15. The timer routines of marker outputs and events are listed in Table 32 in Appendix D.

Table 15: Markers and description of R/P sequence actions for Experiments 1 to 4

R/P Marker No.	Event Description
1	Set recirculating motion
2	Vent upstream system pressure
3	Accumulate product
4	Dispense accumulated product
5	Flush system with feed pump
6	Resume filtration sequence

6.5.2.2 Experiments 5 to 9

The control program was changed in experiments 5 to 9 to vent the upstream system pressure (by opening ConcV2) before flow destabilization occurred. In experiment 7 a manual vent valve was installed in the top manifold to vent air (drawn in at the O-rings where modules slot into the manifolds) from the system. Before experiment 9 the product accumulator A3 was installed in the product line downstream of the product flow transducer while PLC routines were kept the same as for experiments 5 to 8. The markers with description of events for experiments 5 to 9 are

listed in Table 16. The durations of marker outputs and events for these experiments are listed in Table 33 in Appendix D.

6.5.2.3 Experiments 10 and 11

The PLC routine was changed for experiments 10 and 11 to allow for pressurization of the product accumulator A3 during marker 1 cycle. At the start of experiment 10 the accumulator was emptied to the 4 L mark, i.e. containing 11 L of air at atmospheric pressure. By accumulating product during marker 4 cycle with ProdV closed, the last portion of positive pressure in A3 could be utilised. During the dispensing cycle (marker 6) neither feed nor recycle pump was running. The markers with description of events for experiments 10 and 11 are listed in Table 17. Durations of marker outputs and events and are listed in Table 34 in Appendix D.

Table 16: Markers and description of R/P sequence actions for Experiments 5 to 9

R/P Marker No.	Event Description
1	Vent upstream system pressure
2	Set recirculating motion
3	Accumulate product
4	Dispense accumulated product
5	Flush system
6	Resume filtration sequence

Table 17: Markers and description of R/P sequence actions for Experiments 10 and 11

R/P Marker No.	Event Description
1	Initiate R/P routine & start pressurizing product A3
2	Vent upstream system pressure
3	Start recirculating motion
4	Accumulate product, ProdV still closed
5	Accumulate product, ProdV open
6	Dispense accumulated product (no pumps running)
7	Flush system
8	Resume filtration sequence

6.5.2.4 Experiment 12

The PLC routine was changed for experiment 12 to allow for pressurization of the product accumulator A3 during marker 1 cycle. During marker 6 cycle both pumps were running to dispense the accumulated volume via ConcV2. The markers with description of events for experiment 12 are listed in Table 18. Durations of marker outputs and events and are listed in Table 35 in Appendix D.

Table 18: Markers and description of R/P sequence actions for Experiment 12

R/P Marker No.	Event Description
1	Initiate R/P routine & start pressurizing product A3
2	Vent upstream system pressure
3	Start recirculating motion
4	Accumulate product, ProdV still closed
5	Accumulate product, ProdV open
6	Dispense accumulated product (feed and recycle pumps running)
7	Flush system
8	Resume filtration sequence

6.5.3 R/P With Simultaneous Venting of Product

6.5.3.1 Experiments 13 to 14

The previous experiments were aimed at maximizing the reverse flux. This did not provide satisfactory results. Consequently it was decided to look at destabilizing the flow. When the feed accumulator is small, maximization of the reverse flux becomes less important. What is more important is the back-pulse achieved. Also, when the accumulator in the system is small, the largest accumulator one can find to accumulate the reverse flux water is to vent it to the atmosphere.

All previous experiments had utilised A2 to accumulate product during the R/P cycle, no venting line was available between the discharge side of the recycle pumps and valves ConcV1, and ConcV2. A ball-type manual venting valve, V11, and non-return valve V10, were thus installed to fulfil this purpose. The purpose of V10 was to prevent discharged water from being drawn back through the recycle pumps. However, the system could not be flushed with clean feed water

from the feed pump due to the piping arrangement. Here one relies on the backflush pump to rinse debris from the system. When in DE filter mode, both ConcV1 and ConcV2 were closed, this eliminated bypassing of feed water via V11, which was open during experiments 13 and 14.

The markers with description of events for experiments 13 to 14 are listed in Table 19. Durations of marker outputs and events are listed in Table 36 in Appendix D. The same R/P timer durations were subsequently used for experiments 15B to 16. In an R/P cycle the consecutive recycle and product venting cycles were repeated 3 times. During experiment 13 filtration and R/P were in up-flow mode. In experiments 14 and 15B to 16 filtration and R/P were done in up-flow mode, with the R/P cycle looped in a 12 000 s filter cycle followed by a 120 s upward B/F cycle.

Table 19: Markers and description of R/P sequence actions for Experiments 13 to 16

R/P Marker No.	Event Description
1	Initiate R/P routine, start recirculating motion, stop feed pump & pressurize product accumulator
2	Vent product to atmosphere via ConcV1 with ProdV open
3	Continue recirculating motion & pressurize product accumulator
4	Vent product to atmosphere via ConcV1 with ProdV open
5	Continue recirculating motion & pressurize product accumulator
6	Vent product to atmosphere via ConcV1 with ProdV open
7	Continue recirculating motion & pressurize product accumulator
8	Resume filtration sequence

The fact that dislodged material could not be flushed from the system was not thought to be a problem. The recycle line has a 150 μm vortex strainer and much of the debris collected in this strainer. The system thus goes into a normal B/F sequence not to dislodge cake layer from the membrane surface but to remove accumulated material from the pipes and manifolds. By maintaining all linear flow in one direction, the possibility of dislodged material to be swept up by the incoming feed and re-deposited on the membranes is thus circumvented.

6.5.4 Comparison of B/F and R/P: Consecutive Experiments 15 to 16

Experiment 15 was performed to compare the effects of R/P and B/F using the timer sequence settings from experiment 14. In experiment 15A the control program was adapted so that marker 1 was never activated, i.e. the Paradyskloof plant system was operated in DE mode with upward B/F only. The rate of the product pump was reduced in order to B/F at the same B/F flux as

would be used for R/P in the consecutive experiment 15B. The feed pressure during DE filtration was arbitrarily set at 150 kPa. Thus for experiment 15A a B/F flux of 22.5 LMH would be used, while the interval and duration would be 12 000 s (3.33 h) and 120 s (2 min) respectively. The experiment was run for 18 h while data were logged every 5 s to track the flux, dP and product temperature response of the system.

At the end of experiment 15A the control program was changed to exclude B/F, while only the R/P sequence was activated. During the time it took (10 min) to change and re-load the control program into the PLC the UF unit was never switched off. The reason for this was that stopping and starting of the plant could be excluded as a reason for any improvement in flux or decrease in dP , since switching off of the plant would constitute a flow destabilization action in its own right. It was however found that an air pocket had accumulated in the top manifold. It was assumed that the air had been present in the manifold for the duration of experiment 15A, as only filter and B/F operations had occurred during experiment 15A. This air had to be vented before experiment 15B, and a dP reduction of 13 kPa as a result of air venting was observed between the end of experiment 15A and the start of experiment 15B. This was subtracted from the measured dP for each data point in subsequent calculations for experiment 15A.

Air finding its way into the system is a problem. One must realise that the modules are fitted into the branch arms of uPVC T-pieces and that a water tight seal is provided by two O-rings. The manifold pressure continuously swings between operating pressure (150 kPa) and vacuum (-40 kPa). This will inevitably cause O-ring movement and air seepage resulting in trapped air pockets in the top sections of the manifolds.

If the R/P sequence in experiment 15B would be able to improve the flux and reduce the dP it would be a certain indication that the R/P was effective in removing the fouling layer. Experiment 15B was run for 7 h while flux, dP and temperature were logged every 5 s to track the dynamic response of the system. Experiment 15C was then conducted without switching the plant off for an additional 15 h during which time data were logged every 20 s to track the long-term flux, dP and temperature response of the system.

To illustrate the concept of the "lift-and-sweep" hypothesis, the plant was run for experiment 15D in DE filter mode for 0.5 h to foul the membranes before data logging and initiating an R/P sequence of 3 sequential pulses. Once a baseline was established, the plant was operated in experiment 16 for a duration of 120 h at an R/P frequency of 600 s and a duration of 53 s with 3 sequential pulses per R/P event.

6.5.5 Monitoring of Separation Efficiency

Turbidity was used to monitor the separation efficiency of the membranes during the investigation. Samples were collected weekly (for experiments 1 to 14) from the feed manifold, as well as permeate from the individual membrane modules and the combined permeate downstream from the modules and analysed on-site on a portable HACH 2100P turbidimeter. In this way each module could be monitored for possible membrane damage. During experiment 15 the feed water quality worsened dramatically and turbidity was measured for each sub-experiment.

A module air-pressure retaining test (a modified bubble method) was also carried out before and after a set of R/P experiments on each module. The shell side was pressurized to 150 kPa with air to displace the permeate in the module. Once the pressure stabilized, a sign that all the water was forced back through the membrane, the shell was re-pressurized to 150 kPa and the air supply line closed off. The pressure was then monitored for the next 5 minutes.

If the shell side pressure dropped by more than *ca* 10 kPa during the 5 min duration, it would be a sign that some membrane fibers were damaged during previous experiments since the last pressure-holding test.

6.6 RESULTS AND DISCUSSION

6.6.1 Maximization of Negative R/P Peak dP and Flux

Each of the developments was aimed at increasing the negative dP peak pressure and the reverse flux that could be achieved with reverse-pressure pulsing.

6.6.1.1 R/P without Simultaneous Venting of Product

Table 20 lists the filtration time per R/P cycle, the peak dP achieved, as well as the measured and corrected (to 20 °C) peak R/P fluxes along with the product temperature at the time of R/P for experiments 4 to 17. The last two columns list the average dP (kPa) during filtration just prior to reverse-pressure pulsing, and cross-flow velocity, U_m , used for recirculation of water at the start of the R/P sequence.

The filtration time per R/P cycle (a measure of the fraction of operating time spent filtering) was calculated with the following relationship:

$$Filtration\ Time\ (\%) = 100 \times \frac{\left(\sum_{1}^{n-1} \Delta T_{M(i)} \right)}{\Delta T_{M(n)}} \quad (7.1)$$

where $\Delta t_{M(i)}$ denotes the duration of marker i for markers 1 to n .

Table 20: Filtration time per R/P cycle, R/P peak dP , peak flux and water temperature for experiments 1 to 12

Exp. No.	Filtration time per R/P cycle (%)	dP Peak (kPa)	Measured R/P Peak Flux (LMH)	Corrected R/P Peak Flux (LMH)	Product Water Temp. (°C)	Ave. DE Filtration dP (kPa)	U_m (m/s)
1	88.0	-49.5	-20.01	-26.18	10.1	103	0.1446
2	87.2	-43.6	-12.90	-15.50	13.3	155	0.1687
3	87.7	-44.9	-16.11	-20.54	11.0	145	0.1687
4	84.5	-44.9	-13.37	-16.64	10.1	120	0.1687
5	84.5	-45.3	-14.05	-17.77	11.5	165	0.1687
6	91.6	-45.5	-12.33	-15.92	10.5	218	0.1687
7	91.6	-44.9	-16.72	-21.56	10.6	120	0.1687
8	91.6	-44.6	-19.31	-22.18	14.9	135	0.1687
9	91.6	-63.3	-15.55	-19.36	11.9	120	0.1687
10	98.8	-96.2	-21.34	-25.24	13.8	120	0.1687
11	92.5	-94.5	-21.24	-26.78	11.4	140	0.1687
12	91.6	-84.2	-19.28	-22.52	14.2	125	0.1687

The maximum negative dP peak for experiments 1 to 4 was -49.5 kPa, attained in experiment 1, with a measured peak flux of -20.01 LMH. In Figure 30 the R/P dP and flux responses are plotted to illustrate the effect of R/P on these system variables. The plotted flux is the flux value corrected to 20 °C with eqs. (2.36) and (2.40). The accumulator A1 started leaking during the course of experiment 1, while the recycle pump (Rec 1) developed a leak on its suction side. This had the effect that air was being drawn into the system and reduced the effective suction power of the recycle pump. Note the sudden dip in the R/P dP at the start of the accumulation stage, which had the effect that the initial reverse flux decreased and then started increasing again. In further experiments Rec 3 was used for recycling.

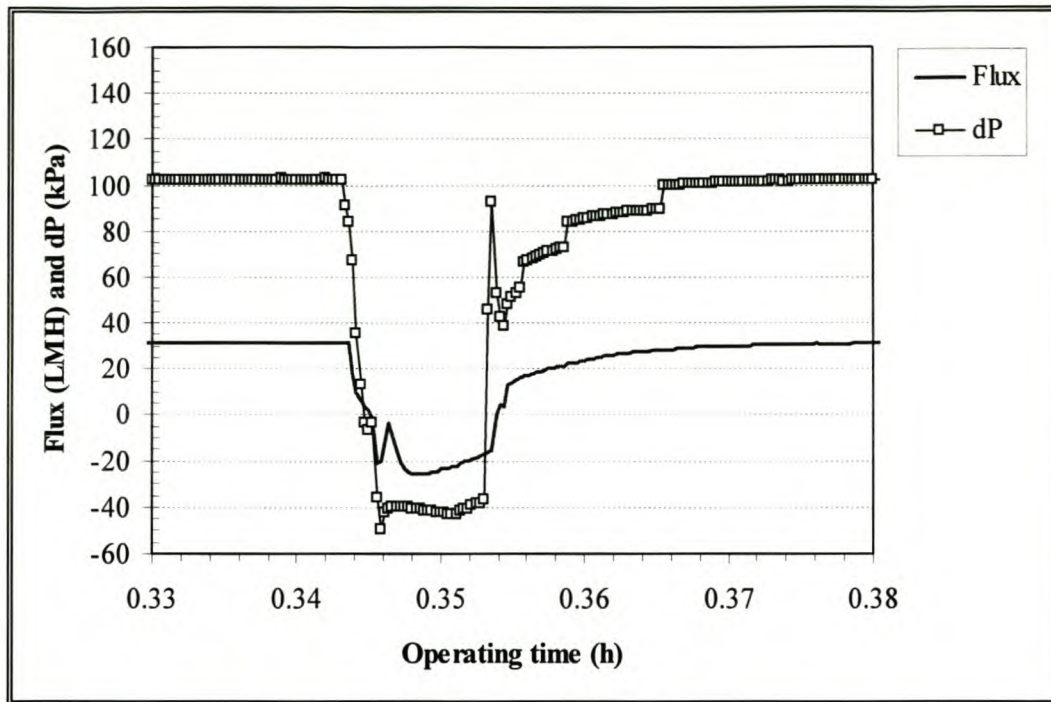


Figure 30: R/P flux and dP response for experiment 1.

The R/P flux and dP responses for experiments 2 and 3 are shown for reference in Figure 54 and Figure 55 (Appendix D) respectively. Note the sudden dP dip in experiment 3 near the end of the accumulation stage. For experiment 1 the average filtration dP was 103 kPa compared to 155 and 145 kPa for experiments 2 and 3 respectively.

In experiments 5 to 8 the upstream system pressure was vented (by opening ConcV2) before the recycle pump started. This was done to discharge water from the feed-side accumulator, so that space could be made for the water drawn through the membrane in reverse flux. The product valve was also shut at the start of marker duration M1, which caused a rapid increase in product pressure from *ca* 27 to 98 kPa. When UpflowV1 was shut to accumulate product, ProdV opened after a short delay (to make use of static head and for reverse flow of product from A2) and ConcV2 shut again for the duration of the product accumulation stage. The R/P flux and dP responses for experiments 5 and 8 are shown in Figure 56 and Figure 57 in Appendix D.

During experiments 5 to 8 the upstream system pressure was observed to drift down during filtration cycles due to air being drawn into the system through leaking fittings. The dP peak value could not be increased above -45.7 kPa (at a peak flux of -12.33 LMH), although the peak flux increased to -19.31 LMH in experiment 8. The filtration time per R/P cycle for experiments 6 to 9 also increased to 91.6 %.

Experiment 9 was conducted with accumulator A3 installed in the product line and filled to the 4 L mark on the sight glass (total volume 15 L), while the control sequence and timing of events was kept the same as for experiments 6 to 8. This time the R/P peak dP increased to -63.3 kPa and the peak R/P flux was -15.55 LMH. The corrected flux and dP response for experiment 9 is plotted in Figure 31 for which the filtration dP was 120 kPa.

When experiment 9 is compared with earlier experiments without the additional product accumulator, the product pressure only increased from 27 to 38 kPa when the product valve was closed at the start of marker M1 duration, due to compression of the air in accumulator A3. When ProdV opened again with closure of UpflowV1 and ConcV2, the expansion of the volume of compressed air aided the reverse flux of product through the membranes initially, but as this pressure decreased because of the high initial reverse flux, the reverse flux decreased more rapidly toward the end of the accumulation stage.

This result was in stark contrast to the sustained reverse flux that was observed during earlier experiments when the product accumulator was not used.

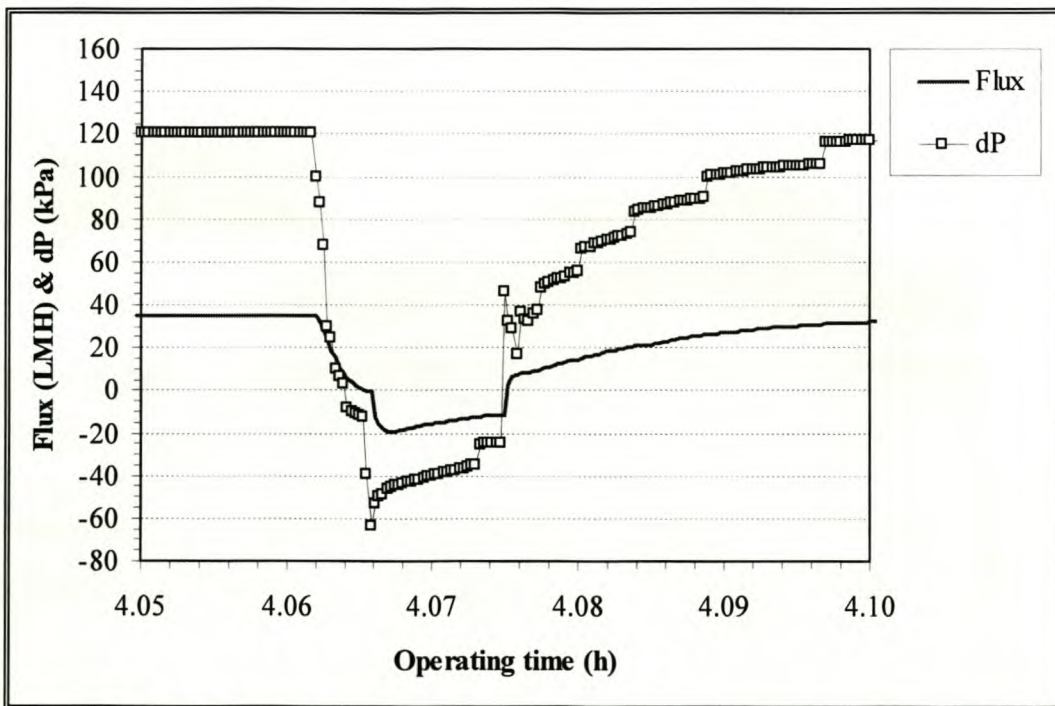


Figure 31: R/P flux and dP response for experiment 9.

For experiments 10 and 11 the product accumulator A3 was pressurized for 8 s prior to venting of the upstream system pressure and recycling motion. The R/P corrected flux and dP responses for experiment 10 are shown in Figure 32.

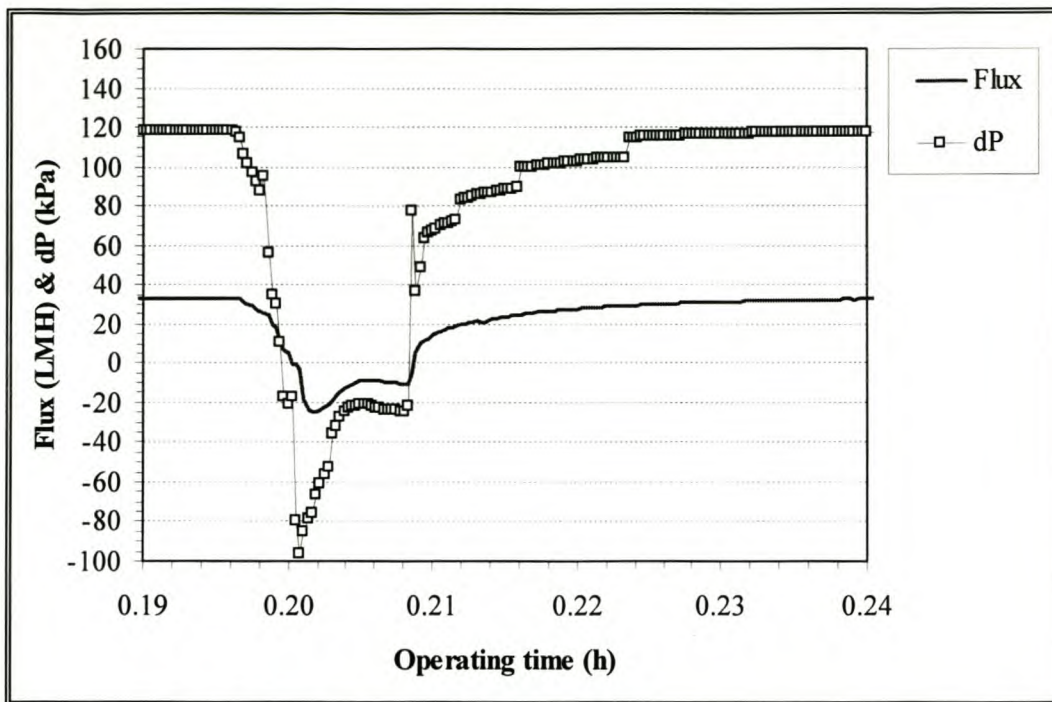


Figure 32 R/P flux and *dP* response for experiment 10.

For experiments 10 and 11 the R/P peak *dP* increased to -96.2 and -94.5 kPa respectively while R/P peak fluxes of -21.34 and -21.24 LMH were measured at 13.8 and 11.4 °C respectively. During filtration the *dP* was 120 and 140 kPa for experiments 10 and 11 respectively. This result indicates that the compression of product prior to R/P is important in maximizing the peak R/P *dP* and flux. When marker 4 was activated to accumulate product with ProdV still closed, the accumulated pressure in A3 was vented rapidly by forcing product through the membranes. It would appear that before ProdV was opened 10 s later, the R/P flux decreased as a result of product suction against vacuum, and then increased again as a result of added static pressure obtained from product accumulator A2 on the roof of the plant. The latter resulted in a sustained R/P flux and *dP* for the next 20 s until the accumulated volume was dispensed with no pumps running by opening of ConcV2.

For experiment 12 the durations of events at the start of R/P changed from the previous two experiments, but the sequencing stayed the same. For experiment 12 the upstream system pressure was vented for 8 s (instead of 5 s for experiments 10 and 11), and the recirculating motion started only 1 s instead of 2 s prior to closure of UpflowV1. The product was then accumulated for 6 s instead of 10 s (experiments 10 and 11) with ProdV closed, and for 29 s with ProdV open, instead of 20 s previously. During the dispensing cycle both pumps were running

for the duration of marker 6 (1 s instead of 2 s in experiments 10 and 11 when no pumps were running).

During the course of these experiments A3 started leaking air at the top and water at the bottom. Thus when A3 was pressurized, air was released, resulting in less effective compression. When the product accumulation from A3 started with ProdV closed, air leakage would continue. This resulted in a lower negative dP peak and flux. Another consequence would be that the volume of water in A3 would not remain constant, but slowly increase for consecutive reverse-pressure pulsing sequences. Thus for the next R/P sequence there would be a smaller volume of air in A3 to be compressed, resulting in a further decrease in R/P peak dP and initial reverse flux for the next cycle.

Another difficulty encountered was that during the accumulation cycle air would be drawn into the system at the O-rings where the modules slotted into the feed and concentrate manifolds. The consequence of these difficulties during experimentation was that the peak dP decreased and could not be sustained for long, and sometimes the R/P dP would dip suddenly. Thus in experiment 12 the R/P peak dP and flux was only -84.2 kPa and -19 28 LMH respectively at a temperature of 14.2 °C. The R/P corrected flux and dP responses for experiment 12 are shown in Figure 33. Note the sudden reduction in R/P dP towards the end of the accumulation cycle with ProdV open, when air leakage occurred from A3.

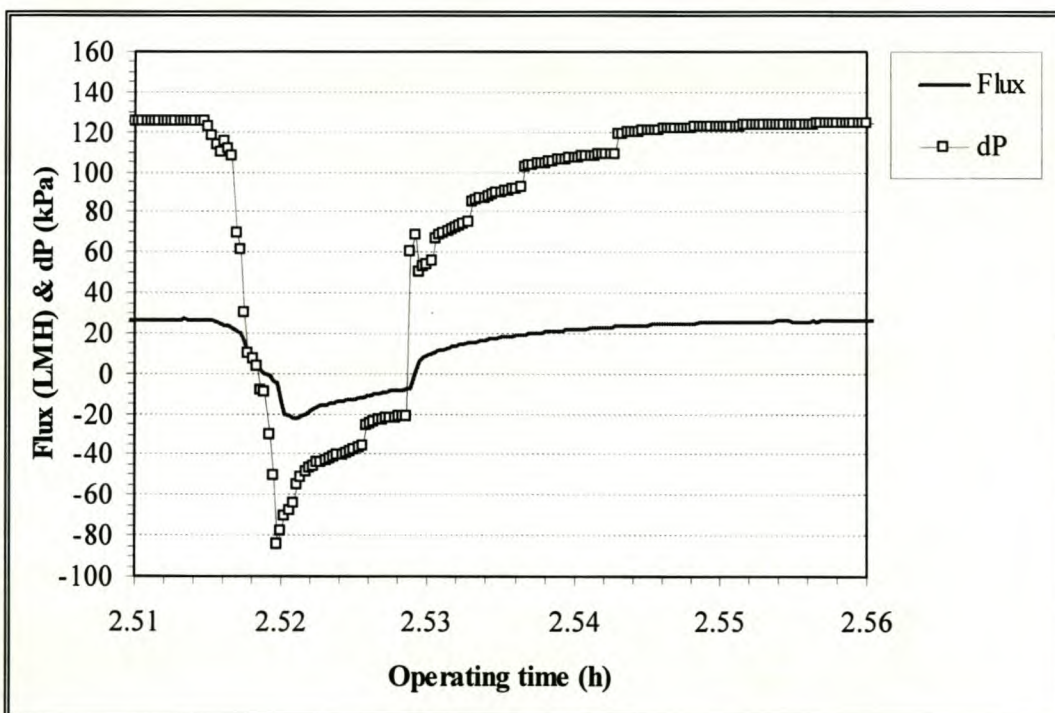


Figure 33: R/P flux and dP response for experiment 12.

6.6.1.2 R/P With Simultaneous Venting (Discharge) of Product

From the previous experiments it was observed that the initial R/P peak and flux could be increased considerably by a combination of upstream system pressure venting (or a low dP during filtration, which is counter-productive) and pressurization of air in a product accumulator A3 before the actual R/P action. However, this peak dP and flux could not be sustained for long. The reason is to be found in the relative size of the feed accumulator A1 and the action of compression of water against air in the accumulator. The centrifugal type recycle pump has a net positive suction head (NPSH) of 20 kPa and a maximum head of 200 kPa at zero flow. When the UpflowV1 valve closes, the forward momentum of the water carries it into the accumulator and a pressure is reached that is greater than the maximum head of the recycle pump. At this point slippage starts to occur in the pump, and the effective R/P dP is reduced. This reduction could theoretically continue until a steady state was reached with equalization of pressures on both sides of the membrane. Thus the effective dP would reach zero and the reverse flux would cease. Also, there was no apparent correlation between experiments where the R/P dP and flux were maximized.

A possible way to sustain the R/P peak dP and flux would consequently be to discharge the water that is drawn in reverse flow through the membranes to the atmosphere (the biggest accumulator available). This could be done by opening a vent valve downstream from the recycle pump but still upstream of the UpflowV1 valve. In this way the R/P flux might be effectively *sustained* for the duration of the R/P cycle, especially now that the system pressure is somewhat lower than operating pressure. Another point considered was that, once the cake layer was being broken up and foulants were dislodged from the membrane surface during R/P with discharge, the membrane lumen would be filled with a mass of floating cake layer debris. To remove the debris, it would be preferable to alternate recycle and R/P with discharge actions in the same R/P cycle. Effectively it would result in alternating *lifting* of the cake layer during the reverse flow sequence, and *sweeping* of the removed debris during the next recycle period. Consequently this "*sustained-lift-and sweep*" hypothesis was put to the test in the experiments 13 and 14.

Table 21 lists the filtration time per R/P cycle, the peak dP achieved, as well as the measured and corrected (to 20 °C) peak R/P fluxes along with the product temperature at the time of R/P for experiments 13 and 14. The last two columns list the average dP during filtration, and cross-flow velocity, U_m , used for recirculation of water at the start of the R/P sequence. The filtration time per R/P cycle was again calculated with eq. (7.1).

Table 21: Filtration time per R/P cycle, R/P peak dP , peak flux and water temperature for experiments 13 and 14

Exp. No.	Filtration time per R/P cycle (%)	dP Peak (kPa)	Measured R/P Peak Flux (LMH)	Corrected R/P Peak Flux (LMH)	Product Water Temp. (°C)	Ave. DE Filtration dP (kPa)	U_m (m/s)
13	91.9	-47.1	-16.51	-18.13	16.6	170	0.3374
14	91.9	-44.2	-14.94	-16.26	16.9	180	0.3374

For simultaneous venting of product experiments, the (manual type) venting valve V11 was open (see Figure 29), while only 2 s durations were used to start the recycle motion, stop the feed pump and pressurize the product accumulator. This was followed by closure of UpflowV1, opening of ConcV1 and ProdV, for a 15 s controlled discharge of product drawn through the membranes by recycle pump Rec3. In a R/P cycle, 3 such recirculating and discharge cycles were conducted. Although a longer duration could have been used to vent upstream system pressure, the aim in these two experiments was not to maximize the R/P dP and flux, but to test the hypothesis concerning the sustainment of the R/P dP and reverse flow achieved while sweeping the surface intermittently.

Consequently the peak dP and flux was only -47.1 kPa and -16.51 LMH respectively for experiment 13 at 16.6 °C, and -44.2 kPa and -14.94 LMH respectively for experiment 14 at 16.9 °C. The dP during filtration, being 170 and 180 kPa respectively, largely contributed to this low R/P dP . The short duration of fluid circulation and system pressure venting initially, combined with the lower dP during filtration for experiment 13, resulted in the lower R/P dP and flux achieved.

The R/P dP and corrected flux responses for experiment 13 are shown in Figure 34. Note that the peak R/P dP and flux could be sustained for the full duration of the three discharge periods. In this case an unfouled membrane was used. Because the R/P dP could be sustained during the discharge period, the reverse flux could be established rapidly and sustained as well. If there was a dense fouling layer on the membrane surface, the hypothesis was proposed that this rapid establishment and subsequent sustainment of reverse flux might be able to lift and break up the fouling layer. In the case of such an event, a larger reverse flux would be observed with each of the subsequent "lift" durations. This hypothesis would be tested in experiment 15D.

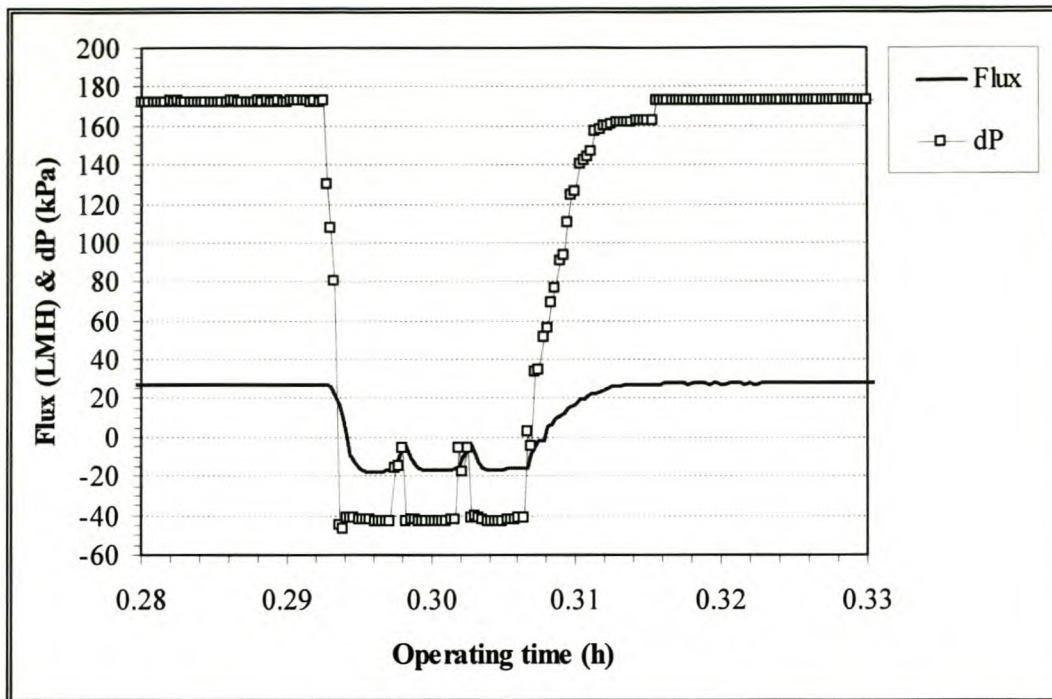


Figure 34: R/P flux and dP response for experiment 13.

6.6.2 Monitoring of Separation Efficiency

Table 22 shows the weekly turbidity reduction results obtained at the Paradyskloof plant over the investigation period of 6 weeks. Because no online turbidity meter was available, it was not possible to monitor the feed turbidity continuously throughout each individual experiment. However, since this was not an optimization investigation and because of practical implications, it was considered unnecessary to monitor turbidity continuously. Although the turbidity that was measured each week gave an indication of general feed water quality, major changes in turbidity could have been missed in between measurements. Since the plant operated on inlet water from the Helderberg irrigation scheme to the Paradyskloof water purification works, operational changes upstream from the UF unit might have affected water quality.

However, it appears from the individual turbidities of individual modules (0.10 to 0.14 NTU) that no membranes were damaged during operation of the plant with reverse-pressure pulsing. Both the Mod 2 and Mod 3 modules produced clear permeate streams, even though the Mod 2 modules had been in operation since 1997 when the plant was situated at Suurbraak and the Hangklip Water Works. For the combined permeate stream a turbidity of 0.11 to 0.12 NTU was measured throughout the investigation period, while the feed turbidity ranged between 5.32 and 13.20 NTU. This translates to a reduction of 97.81 to 99.09 % in turbidity over the investigation period of 6 weeks.

Table 22: Weekly turbidity reduction at the Paradyskloof plant

Turbidity (NTU)	Week 1	Week 2	Week 3	Week 4	Week 5	Week 6
P2-1	0.13	0.13	0.14	0.13	0.12	0.13
P2-2	0.11	0.13	0.11	0.11	0.11	0.11
P3-1	0.11	0.12	0.11	0.11	0.11	0.11
P3-2	0.14	0.13	0.11	0.12	0.12	0.10
P3-3	0.10	0.11	0.12	0.11	0.11	0.11
P3-4	0.13	0.12	0.11	0.12	0.12	0.12
Permeate Average.	0.12	0.12	0.12	0.12	0.12	0.11
Feed	13.20	7.05	5.32	8.75	11.8	9.6
Reduction (%)	99.09	98.25	97.81	98.67	99.03	98.82

The pressure retaining tests also revealed no damage to fibers before or after the R/P tests were conducted. This indicated that the IPS code #798 membranes used in the investigation were mechanically strong enough to withstand the sudden dP changes and trans-membrane flow reversal involved in reverse-pressure pulsing and backflushing.

6.6.3 Comparison of B/F and R/P: Consecutive Experiments 15 to 16

6.6.3.1 Experiment 15A: Operation with B/F Only

The measured product flux and temperature responses of experiment 15A, when only B/F was used to halt the flux decline and dP increase, are plotted in Figure 35. The dP response (13 kPa due to the air pocket subtracted in the dP results) is plotted in Figure 36. Note that for both the graphs the negative flux and dP responses attained during B/F are not plotted. The 6 backflushes were partially effective in improving the flux for a period of 30 minutes, after which a linear decline would occur again.

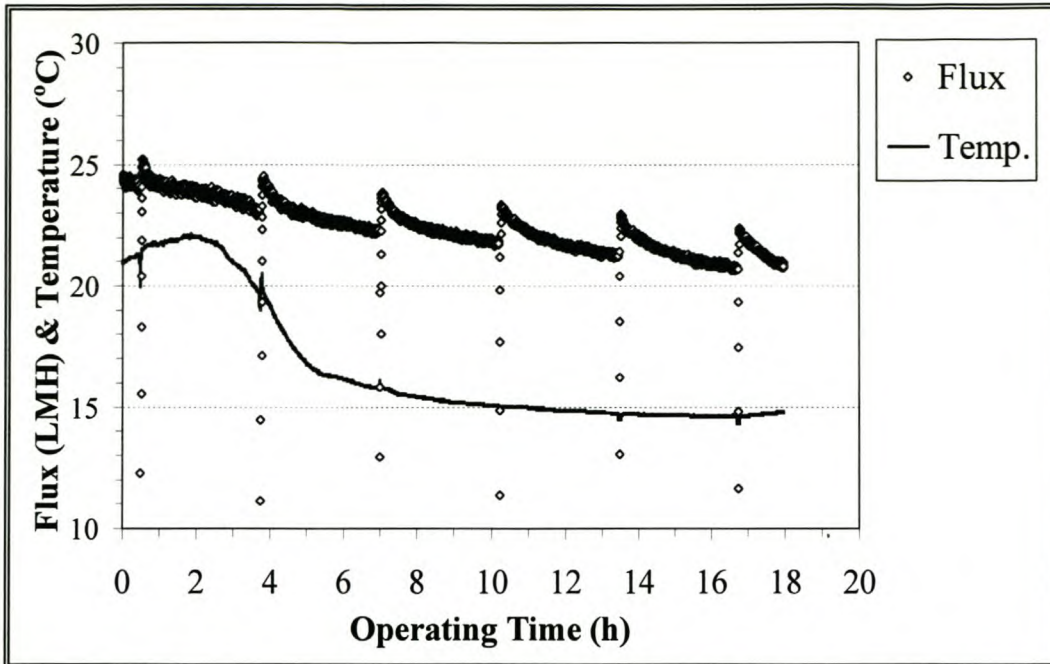


Figure 35: Product flux and temperature responses of experiment 15A for 18 h of operation with B/F only.

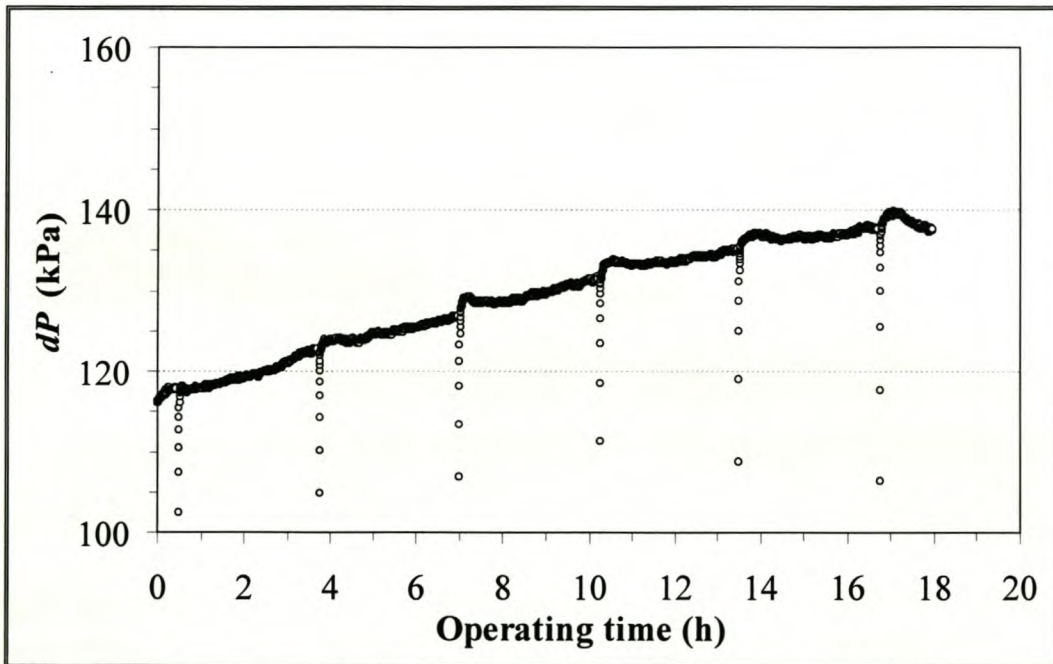


Figure 36: dP response of experiment 15A for 18 h of operation with B/F only.

In experiment 15A the flux declined from 24.38 LMH to 20.81 LMH (14.64% reduction) over the 17.96 h duration of the experiment, while the dP increased from 116.5 to 137.6 kPa (17.60 % increase). The average local flux improvement from before to after backflushes was 1.39 LMH. The temperature at the start of the experiment was 21.1 °C and declined to 14.8 °C at the end with a local maximum of 22.1 °C at 2.05 h. From this maximum a sharp decline was observed, followed by less steep decline starting at 5 h. If the flux decrease and dP increase were caused by

increased viscosity, these trends would have been much more pronounced in the measured responses. At the end of experiment 15A the feed turbidity was measured as 94 NTU. Backflushing at these conditions is not effective in maintaining the flux and limiting dP increase. However, at the end of experiment 15A the membranes were severely fouled and the R/P was put to the ultimate test.

6.6.3.2 Experiments 15B and 15C: Operation with R/P Only

The measured product flux and temperature responses of experiment 15B, when only R/P was used in an attempt to improve the flux and reduce the dP after experiment 15A, are plotted in Figure 37. The dP response is plotted in Figure 38.

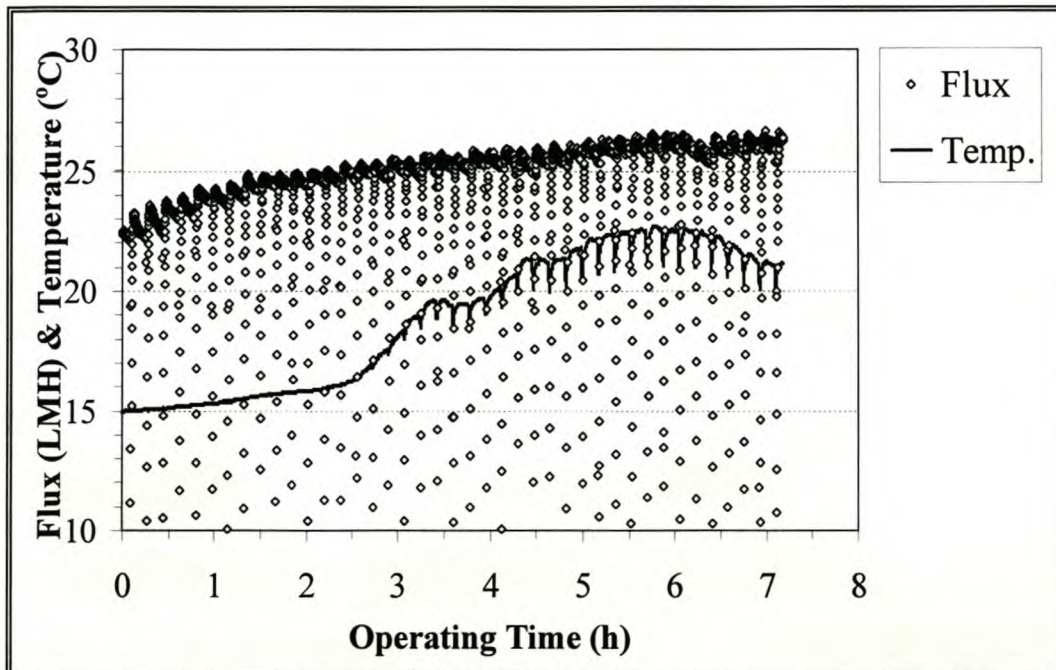


Figure 37: Product flux and temperature responses of experiment 15B for 7 h of operation after switching from B/F to R/P only.

From the start of the data logging interval (when a reverse-pressure pulse sequence had already been performed), the flux improved from 22.28 to 26.38 LMH (18.40 % improvement from the start of experiment 15B), while the dP decreased from 137.1 to 125.9 kPa (8.17 % from start of experiment 15B) over the 7.24 h duration of the experiment. The temperature at the start of the experiment was 14.9 °C and increased to 21.1 °C at the end. A linear increase of 0.4 °C/h was followed by a change in slope at 2.5 h, two local maxima at 3.34 and 4.45 h respectively and a global maximum of 22.6 °C at 5.84 h.

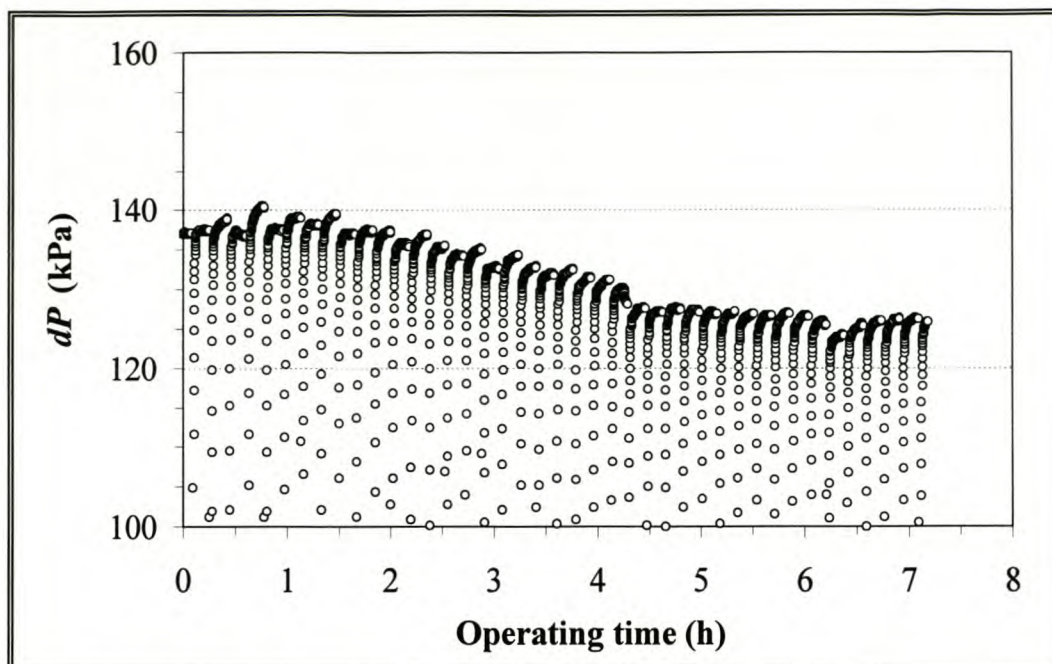


Figure 38: dP response of experiment 15B for 7 h of operation after switching from B/F to R/P only.

Again, the flux increase and dP decrease over the duration of the experiment do not show these trends, which suggests that the observed trends were the result of cake layer removal rather than viscosity changes. The feed water turbidity at the end of experiment 15B was 90 NTU, which indicates that the membranes would have been subjected to the same harsh fouling conditions as in experiment 15A.

Since the NOM loads expected in water of this low quality would be very high, it would be expected that the R/P method would not be able to remove adsorbed foulants and restore the flux and dP to values before experiment 15A. Nevertheless, over the duration of experiment 15B, the flux could still be enhanced by 8.20 % above the flux at the start of experiment 15A. After experiment 15B the net dP increase of 17.60 % observed after experiment 15A could be reduced to 8.07 % above the dP at the start of experiment 15A, which could largely be attributed to adsorption.

The effectiveness of the R/P in breaking up and removing the fouling layer left behind during experiment 15A is illustrated in a magnified view of the flux response during the first 2 h of experiment 15B in Figure 39. As the flux improved after every consecutive R/P cycle, the local rate of flux decline between R/P cycles decreased for consecutive cycles, which indicated permanent removal of foulants with little re-deposition. Less cake debris was left behind in the lumen to be re-compressed into a dense fouling layer in the next DE filtration cycle. This removed cake was observed as a thick, dark brown sludge that was left behind in the vortex

screen of the recycle pump. The evidence suggests that the R/P is indeed effective in gradually removing the fouling layer in the membrane lumens with the alternating *lift-and-sweep* actions for each R/P.

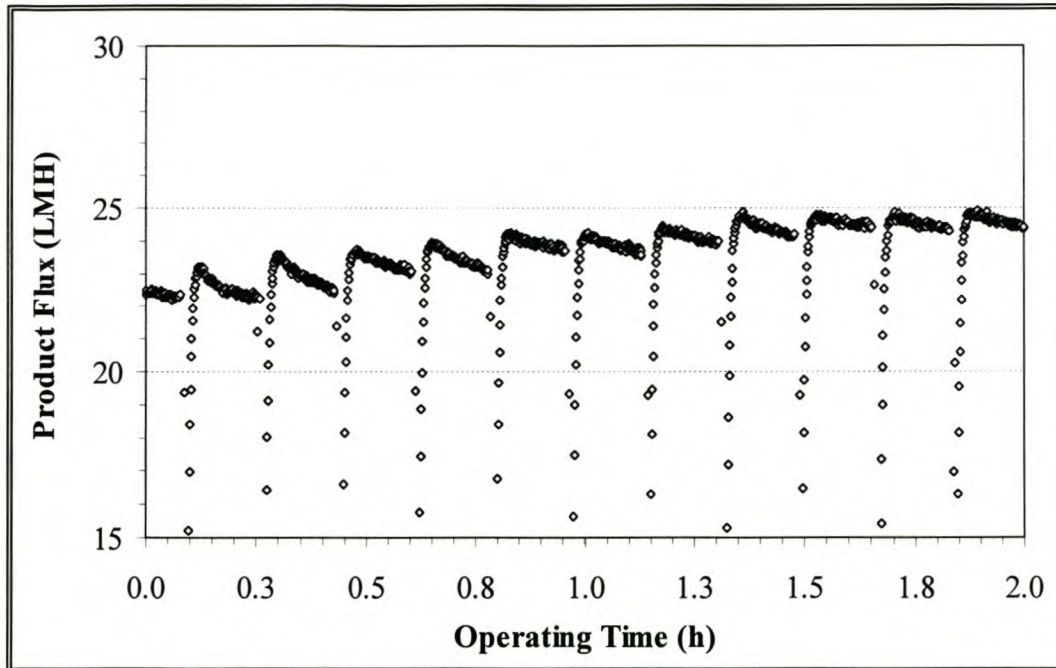


Figure 39: Magnified view of flux response of experiment 20B for the first 2 h of operation after switching from B/F to R/P only.

For experiment 15C the plant filtered again in DE mode with only R/P with simultaneous discharge to lift the cake and sweep the debris intermittently. This experiment ran for 15.22 h through the night until the next morning, when the feed turbidity was measured as 75 NTU.

The flux and temperature responses are shown in Figure 40 while the dP response is plotted in Figure 41. No major re-occurrence of flux decline had occurred, with the flux increasing from 26.01 LMH at the start to 26.59 LMH at the end of the experiment. A maximum flux of 26.87 LMH was observed at 12.9 h. The dP , however, increased from 125.1 to 127.2 kPa with a maximum of 129.6 kPa occurring at 11.72 h. The product temperature decreased from 19.9 to 16.9 °C while a minimum of 15.9 °C occurred at 10.88 h.

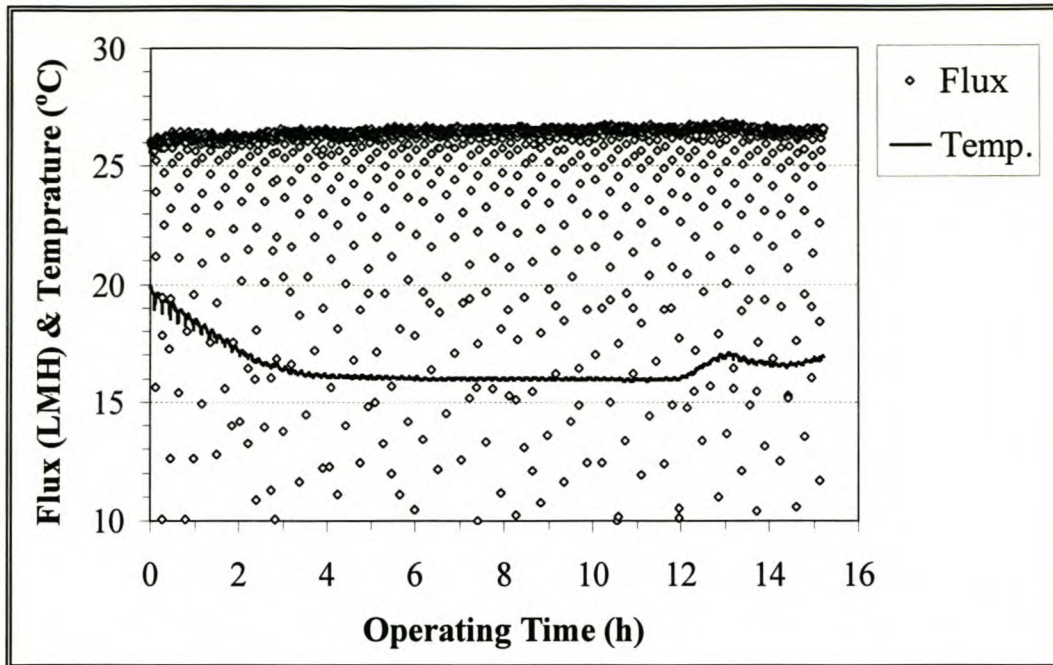


Figure 40: Product flux and temperature responses of experiment 15C for 15 h of uninterrupted DE operation with R/P only after experiment 15B.

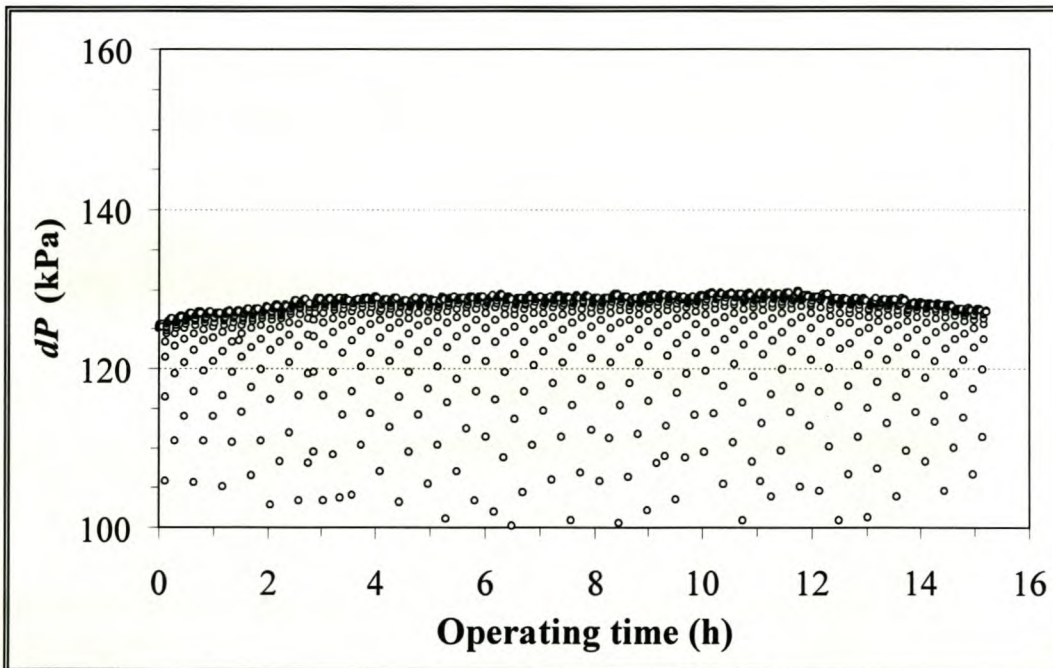


Figure 41: dP response of experiment 15C for 15 h of uninterrupted DE operation with R/P only after experiment 15B.

Thus, at the end of experiment 15C, the flux was still 9.06 % above the flux at the start of experiment 15A, while the dP after 22.46 h of operation with R/P was still only 9.18 % above the dP at the start of experiment 15A.

6.6.3.3 Experiment 15D: Illustration of "Lift-and-Sweep" with a Fouled Membrane

The flux response of experiment 15D is shown in Figure 42; data logged at 1 s intervals. When the R/P sequence is initiated, the recycle pump, pumping just on its efficiency curve against a half-cocked valve, must draw product water through the membrane and in the process break up the fouling layer.

In the first discharge or "lifting" period, the fouling layer is assumed to be quite dense, and the resulting first reverse flux peak in this case is only -15.2 LMH. After the first sweeping action during which time the excess debris has been swept from the surface and is on its way to end up on the recycle pump strainer screen, the second reverse flux peak increases to -19.0 LMH, while the third peak increases further to a maximum of -19.6 LMH.

This result indicates that the choice of more than one "lifting" or reverse flow periods alternated by "sweeping" actions in experiments 13 and 14 was justified.

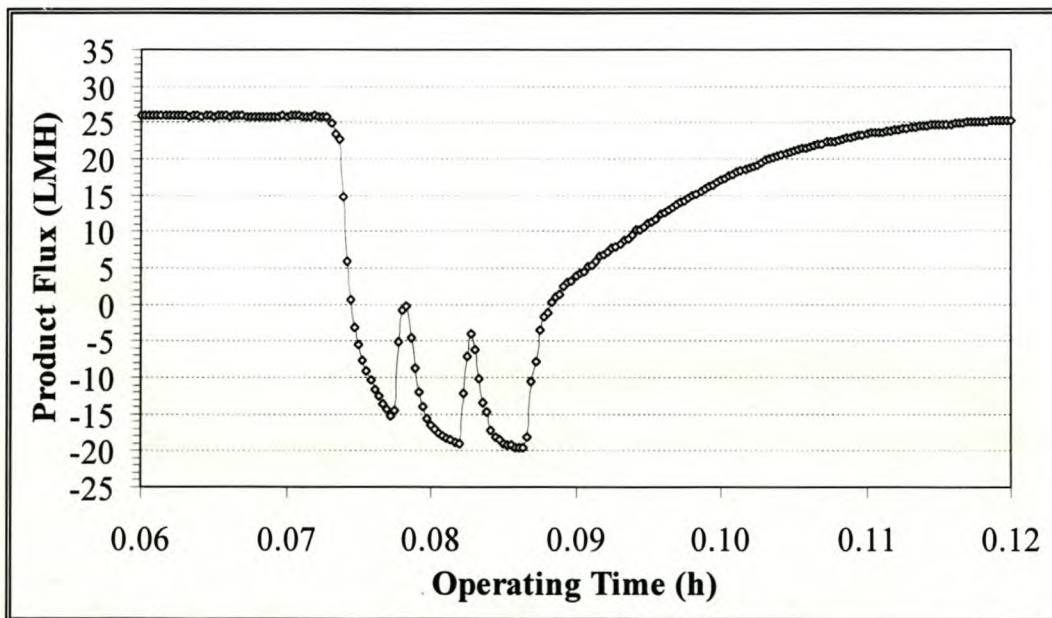


Figure 42: Flux response illustrating the "lift-and-sweep" concept of flow destabilization with the reverse-pressure pulse method on a fouled membrane.

6.6.3.4 Long-term Flux and dP Responses of the System: Experiment 16

To show that the flux improvement for experiment 15 was not just a short-term effect, the plant has since been running with the same R/P cycle as in experiment 15 but with an upward B/F of 140 s duration every 4 h. The purpose of the B/F is not to improve the flux anymore, but to flush accumulated debris from the pipes and manifolds. The flux and temperature responses for

experiments 16A and 16B are plotted in Figure 43 and Figure 45 while the dP responses are plotted in Figure 44 and Figure 46 respectively.

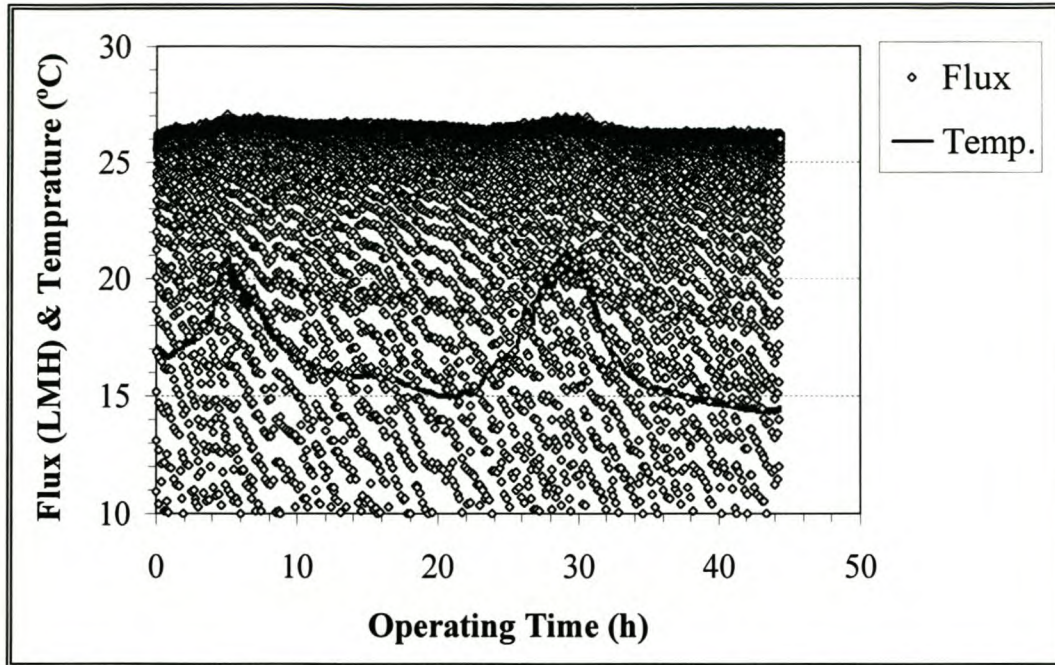


Figure 43: Long-term flux and temperature responses for experiment 16A.

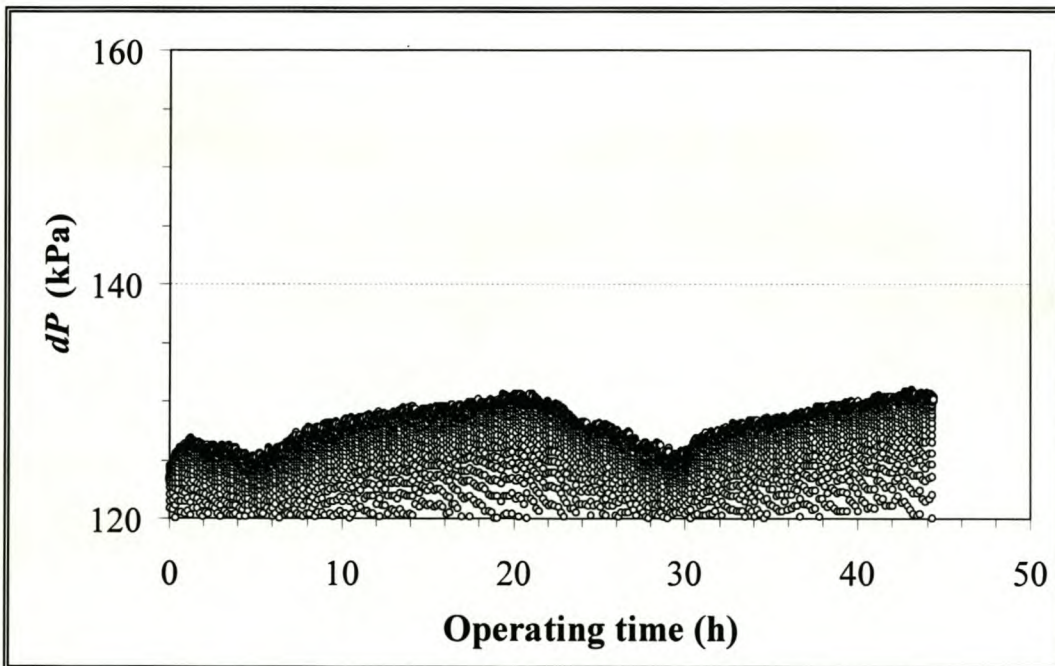


Figure 44: Long-term dP response for experiment 16A.

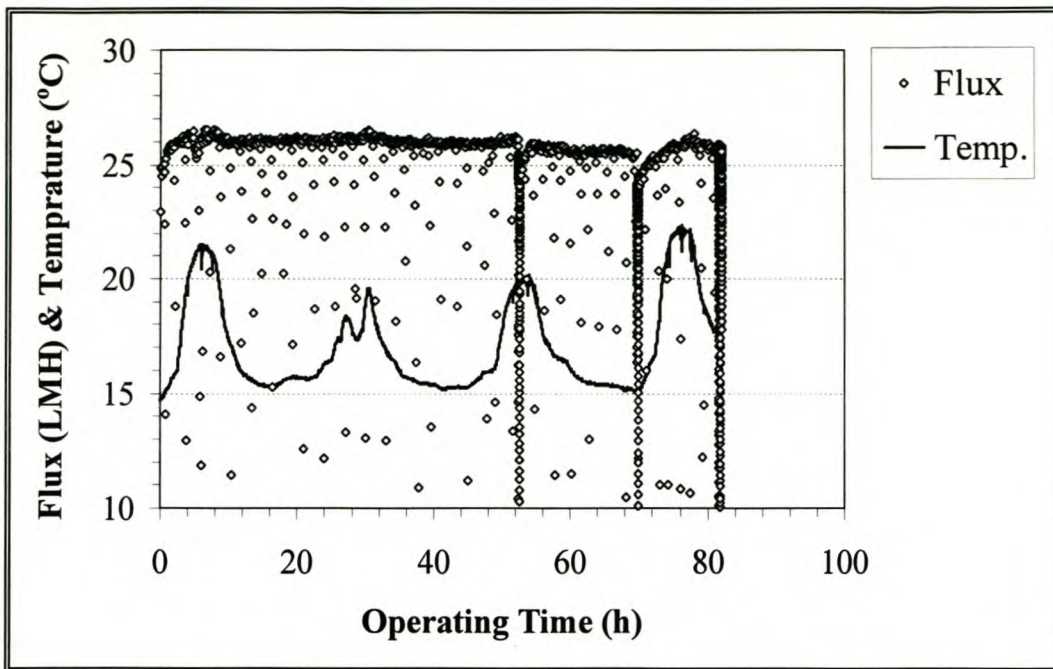


Figure 45: Long-term flux and temperature responses for experiment 16B.

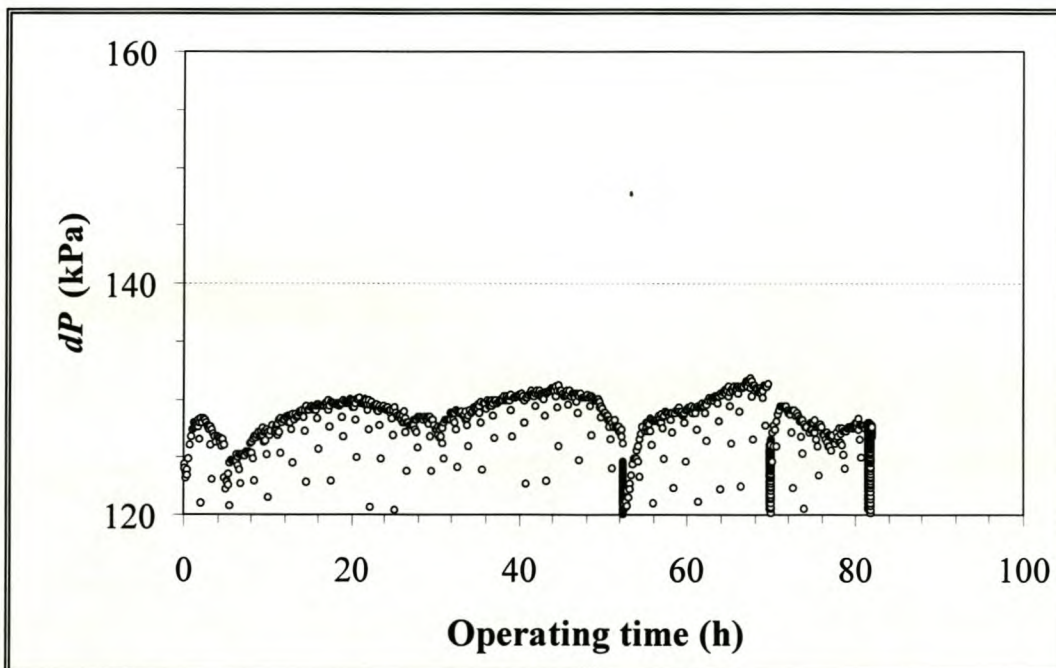


Figure 46: Long-term dP response for experiment 16B.

Although there are small flux fluctuations between of 25 and 27 LMH and dP fluctuations between 120 and 130 kPa, it appears from the plotted system responses that no significant flux decline or dP increase has occurred over the 45.77 h and 82.08 h operating periods for experiments 16A and 16B respectively. Since the start of experiment 15B the plant was operated for over 158 h without a CIP, with no signs of long-term fouling. Since the last CIP (start of experiment 7), the plant has been operated for over 555 h with no long-term flux decline.

6.7 CONCLUSIONS

A method was developed to operate a UF capillary membrane plant in DE filtration mode whereby flow destabilization, combined with reverse flow initiation, could be used effectively to remove the accumulated cake layer from the membrane surface intermittently. The proposed method included filtration with a feed accumulator downstream from a recycle pump, but upstream from the membrane modules. Between the feed accumulator and the modules would be a pneumatic actuated rapid-shut butterfly valve.

The principle of the proposed method was that the feed water would be set in motion at the start of the reverse-flow period by switching on the recycle pump to destabilize the formed cake layer. The direction of cross-flow sweep could either be in the same or opposite direction as feed water flow during filtration. For the purposes of this work it was proposed that if the method worked for sweep in the same direction as feed flow during filtration, it would definitely work for sweeping in the opposite direction.

During DE filtration the rapid-shut valve would be open, and when the feed water had circulated for a very short period of time, the valve would be closed, and the momentum of the water in the recycle loop would carry it into the accumulator. As there would be no other source of water to replace the water carried forward through the pump, but from the membranes, a rapid reverse-pressure pulse could be created across the membrane surface. The magnitude of this reverse-pressure pulse would then, according to the conceptual idea, be sufficient to establish reverse flux through the membrane in order to break up the cake layer.

Various strategies were investigated in order to increase and sustain the peak R/P dP , since this would increase the total volume of water drawn through the membrane as reverse flux. These included initial system pressure venting, initial recycle and pressurizing a product accumulator prior to closure of the inflow valve. The problem was that the reverse-pressure peak dP was either too low or the flow could not be sustained. Because of the relative size of the feed accumulator and the maximum head that the recycle pump could deliver at zero flow (after closure of the inflow valve), the air in the feed accumulator would be compressed rapidly. The reverse-flow would cease after a few seconds because the pressure in the accumulator would exceed the maximum head of the pump. The inclusion of a second (permeate) accumulator in the product line downstream from the membrane modules, that could be pressurized prior to closure of the feed valve, did increase the initial dP peak, but venting of the pressure by an initial high

reverse flux resulted in a rapid decrease in the reverse flux while the problem still persisted of compression of air in the feed accumulator.

Since previous experiments had succeeded only in creating another backflush, which is known not to break up the fouling layer effectively, it was decided to investigate flow destabilization rather than maximizing the reverse flux. It was hypothesised that the R/P dP may be sustained by discharging the accumulated water from the product side of the membrane simultaneously with the reverse-pressure pulse event. This might create a large and fast enough pulse to break up the fouling layer. However, as the cake layer was broken up in the lumen, debris might become entrapped in the lumen, and would just re-compress into a dense cake layer during the next filtration period. The "lift-and-sweep" principle was proposed, whereby reverse-flow and sweeping of the lumen would be conducted sequentially. There was decided on three such pulses of 15 s duration each to be alternated by sweeping actions of 2 s each. Initial evaluation of the method on "clean" surface water ascertained that the reverse flux and dP could be sustained. The method did not damage the membranes, as attested by turbidity and pressure retaining tests.

The effectiveness of the "lift-and-sweep" R/P method under development was evaluated by first fouling the membranes with surface water containing high NOM and particle loads from the Helderberg Irrigation scheme, Stellenbosch. For experiment 15A the system was operated in DE filtration mode while conducting backflushing at a backflush flux equivalent to the initial filtration flux for a duration of 120 s, and at 3.33 h intervals. During the 17.96 h duration of experiment 15A the flux of the membranes decreased by 14.64 % while the dP increased by 17.6 %. Without switching the plant off (which would be flow destabilization *per se*) DE filtration was continued for 7.24 h in experiment 15B, with R/P consisting of 3 alternating 2 s recycle and 15 s pulse durations for every 10 min of filtration. It was possible to restore the flux to 8.20 % above the flux at the start of experiment 15A, and reduce the net dP increase from 17.6 % to 8.07 %. Again without switching off, DE filtration for experiment 15C commenced for an additional 15.22 h, after which time a net flux increase of 9.06 % and dP increase of 9.18 % above the values at the start of experiment 15A were observed. Experiment 15D was conducted, during which the membranes were fouled for 30 min of DE filtration and then subjected to the same R/P as in experiments 15B and 15C. Flux response data indicated that the reverse-flux increased after each of the sweeping actions of feed water recycle. Thus it was concluded that the 3 alternating lift and sweep actions proposed were more effective in removing the cake layer than one long reverse flux period.

To ascertain whether the flux improvement and dP reduction obtained during experiments 15B and 15C was only a short-term effect, the plant was (again without switching off) operated in experiment 16A and 16B for another 127.85 h using the same R/P method. The only change was that a B/F in the same axial flow direction as filtration and R/P was incorporated, not to remove the cake layer, but to flush debris left in the system pipes and manifolds from preceding R/P sequences. This B/F was performed every 4 h for a 140 s duration. Although small fluctuations were observed in the flux and dP during experiments 16A and 16B, no significant fouling was observed during this time. In total the plant had been operated for over 158 h since the start of experiment 15B using the developed R/P method and the backflush rinsing method (without CIP) with no apparent long-term fouling. The R/P method proved itself to be a very powerful tool for maintaining flux and limiting dP increase without the use of chemicals or the need for a CIP.

In conclusion it could be said that the plant was, in effect, being operated in constant flux mode, since the R/P was able to restore the flux and decrease the dP every 10 min by removal of the cake layer. The percentage filtration time per cycle, which for the R/P was 91.9 %, could be said to be a measure of the product recovery. Therefore, in the design of future plants using the R/P method, the required membrane area could be more accurately calculated. By over-designing the membrane area by *ca* 9 to 10 % (to make up for lost filtration time during R/P) the design capacity of such a plant could be easily met.

Part of the reason why the R/P technique is effective in breaking up the fouling layer, is the rapid acceleration and deceleration that occurs when the feed flow across the membrane is halted and started by the rapid closing and opening actions of the pneumatic operated butterfly valve (that controls the operation). The pressure pulse that occurs when the valve is opened at the end of the discharge period, and flow perturbations that occur as the water from the accumulator is forced under pressure through the membrane lumens, lift and shift the fouling layer, and in the process break it up.

Since the type of double-skinned membrane (IPS code #798 with resistance of $1 \times 10^{13} \text{ m}^{-1}$, calculated from flux and dP data using eq. (2.29)) used in Case Study 2 is more dense than the membranes used in Case Study 1 (IPS code #763 with resistance of $2 \times 10^{12} \text{ m}^{-1}$), it may be concluded that the new flow destabilization method that was developed in this investigation will work equally well, if not better, with less dense membranes such as the #763 type, or higher permeability microfiltration membranes.

Chapter 7: CONCLUSIONS

7.1 SIGNIFICANCE OF MON VILLA B/F INVESTIGATION

The Mon Villa pilot plant was successfully operated by the author for 27 000 h on the same set of IPS membrane modules in cross-flow mode using irrigation water containing high loads of turbidity, metals, NOM and bacteria as feed. The investigation provided a vast body of engineering experience toward the operation of such UF plants without the use of chemicals. The membranes, which were initially developed for a biotechnology application and were never intended for potable water supply, performed excellently under harsh conditions. Depending on the feed water quality, reductions above 95 % were recorded for turbidity, 92 to 97 % for colour, 97 to 99 % for iron and 60 to 85 % for NOM. The microbial content of the permeate was also reduced to acceptable levels.

Near the latter part of a long-term capillary UF investigation, two strategies were adopted to investigate the effect of feed flow reversal prior to a backflush on backflush effectiveness. These manual backflush experiments were conducted over a 2680 h period. The Strategy A B/F sequence consisted of an A1 backflush with feed flow reversal (flow destabilization) followed by an A2 backflush without feed flow reversal. The Strategy B B/F sequence consisted of a B1 backflush without feed flow reversal followed by a B2 backflush with feed flow reversal. During all these experiments the system was operated continuously in constant pressure cross-flow mode without backflush for up to 48 h at a dP of 80 to 90 kPa before a manual backflush was implemented. As a B/F dP of 120 kPa had proven during the course of the long-term investigation not to damage the high-flux membranes (and had increased the intervals between CIP treatments), all manual backflushes were conducted at this pressure. The backflush effectiveness was expressed in terms of a percentage of the initial flux (i.e. at the start of the run, just after a CIP) that could be recovered with the backflush.

The observation was made that feed flow reversal before the first backflush (A1) increases the percentage change in flux by almost a factor of 3 over a backflush without feed flow reversal (B1). If a second backflush is performed (directly following the first one, in the opposite

direction than the first), the Strategy B second backflush (now in the opposite cross-flow direction as filtration) is still more effective than the Strategy A second backflush. This result was confirmed by a single factor analysis of variance at a 0.05 significance level, in which all individual experiments (A1, B1, A2 and B2) were compared on the merit of the percentage normalised change in flux from before to after the backflush. When combined, the (A1+A2) result was also found to be more effective than the (B1+B2) result at the 0.05 significance level.

It was also hypothesised that during constant pressure filtration of surface waters containing high levels of NOM and metal ions (as was the case with the Theewaterskloof water), the flux improvement with backflushing might decrease with increasing time into the run because of densification of the fouling layer. This densification may occur as a result of cross-link bonding between NOM and metal ions present in the feed water. Plotting of the individual backflush effectiveness results against a time scale (of when the B/F was performed into the run) added confirmation to the hypothesis.

The backflush system that was developed during the course of the Mon Villa pilot plant investigation highlighted some factors that have an effect on the effectiveness of a backflush. These include:

- ◆ the *backflush dP* which must be greater than the filtration *dP*, and in this investigation had been set at 120 kPa when the constant pressure filtration *dP* was *ca* 80 to 90 kPa;
- ◆ the *backflush volume*, which should be at least equal to the total internal hold-up volume of the module (5 L/module in this case);
- ◆ the *operating time into a run* when a backflush is performed, which in this study was carried out with intervals of between 24 and 48 h for a total filtration cycle of up to 500 h between consecutive CIPs;
- ◆ whether or not the *feed flow direction is reversed* before a backflush; and
- ◆ whether the first backflush is followed by a *second backflush* in the *opposite direction*.

The hypothesis was then proposed that intermittent flow destabilization might prevent the formation, growth and densification of the cake layer in surface waters containing high NOM and cation loads. This proposed flow destabilization method would preferably utilise existing equipment such as pumps and valves normally found on a UF plant. Also, since DE filtration has become the standard on filtration plants used for potable water production (to reduce power consumption), it was decided to operate this proposed flow destabilization method in dead-end mode, and only to use cross-flow intermittently to flush the membrane modules.

7.2 SIGNIFICANCE OF PARADYSKLOOF R/P INVESTIGATION

From the flow destabilization backflush results of the Mon Villa pilot plant investigation a conceptual idea was formulated whereby flow reversal valves up- and downstream from the membrane modules could be used to effect a rapid reversal in the dP .

In this way a method of operating a UF capillary membrane plant in DE mode was developed whereby flow destabilization, combined with reverse flow initiation, could be used to remove the accumulated cake layer from the membrane surface intermittently. The proposed method included filtration with a feed accumulator downstream from a recycle pump, but upstream from the membrane modules. Between the feed accumulator and the modules would be a rapid-shut valve. Pneumatically actuated valves were chosen for the experiments, since for this type of valve the closure time is less than one second, compared with the longer closure time of electrically motor-operated ball valves.

The principle of the proposed method was that the feed water would be set in motion at the start of the reverse-flow period by switching on the recycle pump to destabilize the formed cake layer in a sweeping motion. The direction of cross-flow sweep could either be in the same or opposite direction as feed water flow during filtration. Also, the water in the recycle loop would gain momentum, which would be crucial in effecting the reverse-pressure pulse. For the purposes of the thesis the worst-case scenario was chosen, since the assumption was made if the method worked for sweep in the same direction as feed flow during filtration, it would definitely work for sweeping in the opposite direction. During DE filtration the rapid-closure valve would be open. When the feed water had circulated for a very short period of time (*ca* 2 s), the valve upstream from the module would be closed, and the momentum of the water in the recycle loop would carry it into the accumulator. As there would be no other source of water to replace the water carried forward through the pump but from the membranes, a rapid reverse-pressure pulse could be achieved on the membrane surface.

Various alternatives of increasing and sustaining the magnitude of the peak R/P dP and flux were investigated, including initial system pressure venting, initial recycle and a product accumulator that could be pressurized. The problem was that the reverse-flow peak dP was either too low or the flow could not be sustained, even when the system pressure was vented before the R/P event. The air in the relatively small feed accumulator (8 L) would be compressed rapidly, and the reverse-flow would cease after a few seconds because a condition would be encountered where the pressure in the accumulator was higher than the maximum head of the recycle pump at zero

flow. The inclusion of a second accumulator in the product line downstream from the membrane modules, that could be pressurised prior to closure of the feed valve, did increase the initial dP peak, but venting of the pressure by an initial high reverse flux resulted in a rapid decrease in the reverse flow.

Then it was hypothesised that a possible way to overcome the problem of compression of the air in the feed accumulator would be to discharge the accumulated water to the atmosphere. However, as the cake layer was broken up in the lumen, debris might become entrapped in the lumen, and would just re-compress into a dense cake layer during the next filtration period. The "lift-and-sweep" principle was proposed, whereby reverse flow and sweeping of the lumen would be conducted alternately. Three pulses were chosen, which would be alternated by three sweeping actions. Initial evaluation of the 3-pulse method on "clean" surface water indicated that the dP and flux could be sustained. Turbidity and pressure retaining tests also indicated that the method did not damage the membranes.

The "lift-and-sweep" R/P method under development was finally evaluated by first fouling the membranes with surface water containing high NOM and particle loads. For experiment 15A the system was operated in DE filtration mode while performing backflushing at a backflush flux equivalent to the initial filtration flux for a duration of 120 s, and at 3.33 h intervals. During the 17.96 h duration of experiment 15A the flux of the membranes decreased by 14.64 % while the dP increased by 17.6 %. The effects of temperature on viscosity were ruled out to account for the flux decrease and dP increase.

Without switching the plant off (which in principle would be flow destabilization) DE filtration was continued for 7.24 h in experiment 15B, with R/P consisting of 3 alternating 2 s recycle and 15 s pulse durations for every 10 min of filtration. During experiment 15B no backflushing was done. Using the R/P only, it was possible to restore the flux to 8.20 % above the flux at the start of experiment 15A, and reduce the net dP increase from 17.6 % to 8.07 %. Here again the effects of temperature alone could not account for the flux restoration and dP decrease. Again without switching off, DE filtration for experiment 15C continued for an additional 15.22 h, after which time a net flux increase of 9.06 % and dP increase of 9.18 % above the values at the start of experiment 20 A were observed.

To test the validity of the "lift-and-sweep" hypothesis, experiment 15D was conducted, during which the membranes were fouled for 30 min of DE filtration and then subjected to the same R/P as before. Flux response data indicated that the reverse-flux increased after each of the sweeping actions of feed water recycle. Thus it was concluded that the 3 alternating lift and sweep actions

proposed were more effective in removing the cake layer effectively than would be one long reverse flux period. After experiment 15D the plant was operated for another 127.85 h in experiment 16, using R/P to remove the cake layer at 10 min intervals and conventional backflushing at 4 h intervals to flush removed cake from the pipes and manifolds. During this time small fluctuations were observed, but no apparent long-term fouling and flux decline or dP increase occurred. It was concluded that the developed R/P method is effective in removing the cake layer intermittently, thus preventing long-term growth and densification of the cake layer.

Part of the reason why the R/P technique is effective in breaking up the fouling layer, is the rapid acceleration and deceleration that occurs when the feed flow across the membrane is halted and started by the rapid closing and opening actions of the pneumatic operated butterfly valve (that controls the operation). The pressure pulse that occurs when the valve is opened at the end of the discharge period, and flow perturbations that occur as the water from the accumulator is forced under pressure through the membrane lumens, lift and shift the fouling layer, and in the process break it up.

A South African patent [WRC, 1999] has already been granted for this method of operating a filtration assembly under the name "Reverse-pressure pulse generator".

7.3 SUGGESTIONS FOR FUTURE RESEARCH

Since the type of double-skinned membrane (IPS code #798 with resistance of $1 \times 10^{13} \text{ m}^{-1}$) used in this Case Study 2 is more dense than the membranes used in Case Study 1 (IPS code #763 with resistance of $2 \times 10^{12} \text{ m}^{-1}$), it may be concluded that this flow destabilization method that was developed will work equally well if not better with less dense membranes such as the #763 type, or higher permeability microfiltration membranes.

The aim of this investigation was concerned only with developing the "reverse-pressure pulsing" method into a workable tool and not aimed at optimization of the method. Further research that needs to be done concerning operation of the R/P generator, may include the following:

- ◆ increasing the initial recycle duration and to vent system pressure;
- ◆ reversing the initial recycle flow direction to sweep the cake layer against its orientation;
- ◆ reversing the flow direction with every following sweeping action;
- ◆ including a flushing sequence at the end of the R/P sequence to clear the manifolds of debris that did not reach the recycle pump strainer;
- ◆ increasing the duration between R/P sequences to decrease the filter down-time; and
- ◆ evaluating the effectiveness of the method on different types of waters, and other process streams and capillary membrane systems.

REFERENCES

(Presenting Author* for Poster and Oral Presentations)

Agui, W., Tamura, S., Abe, M. and Ogino, S., (1992), "Removal of dissolved humic substances from water with a reverse osmosis membrane", *The Science of the Total Environment*, **117/118**, 543-550.

Anselme, C. and Jacobs, E. P., (1996), "Ultrafiltration", Chapter 10 in: *Water treatment membrane processes*, Mallevalle, J., Odendaal, P. E. and Wiesner, M. R. (Eds.), McGraw-Hill, Inc., New York.

Applequist, D., Depuy, C. H. and Rinehart, K. L., (1982), *Introduction to organic chemistry*, 3rd Edition, John Wiley & Sons Inc., New York.

Aptel, P. and Buckley, C. A., (1996), "Categories of membrane operations", in: *Water treatment membrane processes*, Mallevalle, J., Odendaal, P. E. and Wiesner, M. R. (Eds.), McGraw-Hill, Inc., New York.

American Public Health Association, (APHA, 1992), *Standard methods for the examination of water and wastewater*, 18th Edition, M. A. H. Franson (Managing Editor), Prepared and published jointly by: American Public Health Association (APHA), American Water Works Association (AWWA) and Water Environment Federation (WEF), Washington, DC.

ASTM, (1976), "Test method for pore size characteristics of membrane filters", *Am. Soc. Testing Materials*, Washington, DC.

Bacchin, P., Aimar, P. and Sanchez, V., (1995), "Model for colloidal fouling of membranes", *AIChE Journal*, Vol. 41, No. 2, 368-376.

Bacchin, P., Aimar, P. and Sanchez, V., (1996), "Influence of surface interaction on transfer during colloid ultrafiltration", *J. Membr. Sci.*, **115**, 49.

Bailey, J. E. and Ollis, D. F., (1990), *Biochemical engineering fundamentals*, 2nd Edition, McGraw-Hill, Inc., New York.

- Barella, S. R., Cui, Z. F. and Pepper, D. S., (1996), "Gas sparging to enhance permeate flux in ultrafiltration using hollow fibre membranes", *J. Membr. Sci.*, **121**, 175-184.
- Belfort, G., (Ed.) (1984), *Synthetic membrane processes: Fundamentals and water applications*, Academic Press Inc., London.
- Bemberis, I. and Neely, K., (1986), "Ultrafiltration as a competitive unit process", *Recent advances in separation techniques-III, AIChE Symposium Series*, No. 250, Vol. 82, 65-77.
- Bertram, C. D., Hoogland, M. R., Li, H., Odell, R. A. and Fane, A. G., (1993), "Flux enhancement in crossflow microfiltration using a collapsible-tube pulsation generator", *J. Membr. Sci.*, **84**, 279-292.
- Bird, R. B., Stewart, W. E. and Lightfoot, E. N., (1976), *Transport phenomena*, John Wiley & Sons, New York.
- Botes, J. P., (1995), "Ultrafiltration as a single-step clarification and disinfection process for potable water supply to rural or farming communities", *Final year undergraduate project report*, Department of Chemical Engineering, University of Stellenbosch, Stellenbosch, South Africa.
- Botes, J. P.*, Jacobs, E. P., Saayman, H. M. and Bradshaw, S. M., (2-5 September 1996), "Membrane filtration for the effective supply of water to rural and peri-urban communities", *Poster presentation at the 2nd African Water Conference, Midrand, South Africa*.
- Botes, J. P.*, Jacobs, E. P., Bradshaw, S. M. and Saayman, H. M., (20-24 October 1997), "Long-term evaluation of a UF pilot plant for potable water production", *Oral presentation at the 2nd Water Institute of Southern Africa - Membrane Technology Division Workshop, Industrial Applications Session, Badplaas, South Africa*.
- Botes, J. P., Jacobs, E. P. and Bradshaw, S. M., (1998), "Long-term evaluation of a UF pilot plant for potable water production", *Desalination*, **115**, 229-238.
- Botes, J. P.*, (29 May 1998), "Membrane filtration for the effective supply of water", *Oral presentation at: 3rd Annual Post-graduate Chemical and Metallurgical Engineering Conference '98, Department of Chemical Engineering, University of Stellenbosch, Stellenbosch, South Africa*.
-

- Botes, J. P.*, (8 July 1998), "Membrane filtration technology in potable water treatment", *Oral presentation at: Department of Natural Sciences Winter School '98, University of Stellenbosch, Stellenbosch, South Africa.*
- Botes, J. P.*, (27 August 1998), "Flux enhancement in capillary membrane ultrafiltration: Design and optimization", *Oral presentation at: Post-graduate Seminar, Department of Chemical Engineering, University of Stellenbosch, Stellenbosch, South Africa.*
- Botes, J. P.*, Jacobs, E. P., Bradshaw, S. M. and Pillay, V. L., (26-29 September 1999), "4½ Years of capillary UF membrane operation: the Mon Villa case study", *Oral presentation at: 3rd WISA-MTD Workshop, Drakensville Resort, South Africa.*
- Brinkert, L., Paris, P., Rennar, M., Espenan, J M. and Aptel, P., (1994), "Pressure drops in radial flow membrane modules for ultrafiltration hollow fibres", *J. Membr. Sci.*, **92**, 131-139.
- Brock, T. D. and Brock, K. M., (1978), *Basic microbiology with applications*, Prentice-Hall, Englewood Cliffs, New Jersey.
- Cabassud, C., Laborie, S. and Lainé, J. M., (1997), "How slug flow can improve ultrafiltration flux in organic hollow fibres", *J. Membr. Sci.*, **128**, 93-101.
- Carman, P. C., (1938), "Fundamental principles of industrial filtration", *Trans. Inst. Chem. Eng.*, **16**, 168-188.
- Cheryan, M., (1986), *Ultrafiltration Handbook*, Technomic Publishing Company Inc., Lancaster, U.S.A.
- Cheryan, M., (1998), *Ultrafiltration and Microfiltration Handbook*, Technomic Publishing Company Inc., Lancaster, U.S.A.
- Clifton, M. J., Abidine, N., Aptel, P. and Sanchez, V., (1984), "Growth of the polarization layer in ultrafiltration with hollow-fibre membranes", *J. Membr. Sci.*, **21**, 233-246.
- Crozes, G. F., Jacangelo, J. G., Anselme, C. and Lainé, J. M., (1997), "Mimpact of ultrafiltration operating conditions on membrane irreversible fouling", *J. Membr. Sci.*, **124**, 63-76.
- Cui, Z. F. and Wright, K. I. T., (1996), "Flux enhancements with gas sparging in downward crossflow ultrafiltration: performance and mechanism", *J. Membr. Sci.*, **117**, 109-116.
-

- Delgrange, N., Cabassud, C., Cabassud, M., Durand-Bourlier, L. and Lainé, J. M., (1998), "Modelling of ultrafiltration fouling by neural network", *Desalination*, **118**, 213-227.
- Department of Water Affairs and Forestry, (DWAFF, 1996), *South African water quality guidelines for domestic use*, 2nd Edition, Pretoria.
- De Villiers, H. A.*, Jacobs, E. P. and Botes, J. P., (8 November 1996), "Using filtermembranes to clear water of pathogens", *Oral presentation at: the Association for Vegetables under Protection, Symposium and Workshop, Welgevallen, Stellenbosch, South Africa*.
- Doetsch, R. N. and Cook, T. M., (1973), *Introduction to bacteria and their ecobiology*, University Park Press, Baltimore.
- Doshi, M. R., Dewan, A. K. and Gill, W. N., (1971), "The effect of concentration dependent viscosity and diffusivity on concentration polarization in reverse osmosis flow systems", *AIChE Symposium Series*, No. 68, Vol. 124, 323-339.
- Fane, A. G. and Fell, C. J. D., (1987), "A review of fouling and fouling control in UF", *Desalination*, **62**, 117-137.
- Finnigan, S. M. and Howell, J. A., (1989), "The effect of pulsatile flow on ultrafiltration fluxes in a baffled tubular membrane system", *Chem. Eng. Res.Des.*, **67**, 278-282
- Futselaar, H., Zoontjes, R. J. C., Reith, T. and Rácz, I. G., (1993), "Economic comparison of transverse and longitudinal flow hollow fibre modules for reverse osmosis", *Desalination*, **90**, 345-361.
- Geankoplis, C. J., (1993), *Transport Processes and Unit Operations*, 3rd Edition, Prentice-Hall, Englewood Cliffs, New Jersey.
- Gelman, C. and Williams, R. E., (1983), "Ultrafiltration", Chapter 12 in *Liquid Filtration*, Cheremisinoff, N. P. and Azbel, D. S. (Eds.), Ann Arbor Science Publishers, Woburn, Massachusetts.
- Genthe, B. and du Preez, M., (1995), "Evaluation of rapid methods for the detection of indicator organisms in drinking water", *WRC Project Report No. 610/1/95*.
- Genthe, B and Kfir, R., (1995), "Studies on microbiological drinking water quality guidelines", *WRC Project Report No. 469/1/95*.
-

- Gill, W. B. and Bansal, B., (1973), "HFRO systems: Analysis and design", *AIChE J.*, **19**, 823.
- Glucina, K., Lainé, J. M. and Durand-Bourlier, L., (1998), "Assessment of filtration mode for the ultrafiltration membrane processes", *Desalination*, **118**, 205-211.
- Grangeon, A., Lenoir, J. and Pelissier, R., (1991), "Procédé et module perfectionnés de filtration en milieu de liquide sous flux tangentiel instationnaire", *French Patent 01655*.
- Gupta, B. B., Blanpain, P. and Jaffrin, M. Y., (1992), "Permeate flux enhancement by pressure and flow pulsations in microfiltration with mineral membranes", *J. Membr. Sci.*, **70**, 257-266.
- Gupta, B. B., Blanpain, P. and Jaffrin, M. Y., (1993), "Scaling up pulsatile filtration flow methods to a pilot apparatus equipped with mineral membranes", *J. Membr. Sci.*, **80**, 13-20.
- Hadzismajlovic, D. E. and Bertram, C. D., (1998), "Flux enhancement in laminar cross-flow microfiltration using a collapsible-tube pulsation generator", *J. Membr. Sci.*, **142**, 173-189.
- Hillis, P., Padley, M. B., Powell, N. I. and Gallagher, P. M., (1998), "Effects of backwash conditions on out-to-in membrane microfiltration", *Desalination*, **118**, 197-204.
- Human, C., (1998), "Automation of an ultrafiltration plant for potable water production, with generic comments on the conceptualization of discrete logic control systems", *Final year undergraduate project report*, Department of Chemical Engineering, University of Stellenbosch, Stellenbosch, South Africa.
- Incropera, F. P. and De Witt, D. P., (1985), *Fundamentals of Heat and Mass Transfer*, 2nd Edition, John Wiley & Sons Inc. New York.
- Higgo, J. J. W., Kinniburgh, D., Smith, B. and Tipping, E., (1993), "Complexation of Co^{2+} , Ni^{2+} , UO_2^{2+} , and Ca^{2+} by humic substances in groundwaters", *Radiochimica Acta*, **61**, 91-103.
- Himmelblau, D. M., (1982), *Basic principles and calculations in Chemical Engineering*, 4th Edition, Prentice-Hall International, London, U.K.
- Howell, J. A. and Nyström, M., (1993), "Fouling phenomena", Chapter 6 in *Membranes in Bioprocessing: Theory and Applications*, Howell, J. A., Sanchez, V. and Field, R. W. (Eds.), Chapman & Hall, London, U.K.
-

REFERENCES

- Howell, J. A. and Velicangil, O., (1982), "Theoretical considerations of membrane fouling and its treatment with immobilized enzymes for protein ultrafiltration", *J. Appl. Polym. Sci.*, **27**, 21-32.
- Howell, J. A., Sanchez, V. and Field, R. W. (Eds.), (1993), *Membranes in Bioprocessing: Theory and Applications*, Chapman & Hall, London, U.K.
- Jacangelo, J. G., Aieta, E. M., Carns, K. E., Cummings, E. W. and Mallevalle, J., (1989) "Assessing hollow-fibre ultrafiltration for particulate removal", *J. AWWA*, 68-75.
- Jacobs, E. P., Sanderson, R. D., Olivier, D. M., Domröse, S. E. and Koen, D. J., (1993), "The development and production of membrane systems", *WRC Report No. K5/387*, Water Research Commission of Southern Africa, Pretoria, South Africa.
- Jacobs, E. P., Botes, J. P.*, Sanderson, R. D., Domröse, S. E., Saayman, H. M. and Edwards, W., (11-13 September 1995), "Ultrafiltration in potable water production", *Poster presentation and pilot plant demonstration at International Water Supply Association Conference, Durban, South Africa*.
- Jacobs E. P. and Botes J. P., (November 1995), "Mon Villa rural watercare project", *WRC Report No. KV79/95*, Water Research Commission of Southern Africa, Pretoria, South Africa.
- Jacobs E. P. and Leukes W. D., (1996), "Formation of an externally unskinned polysulphone membrane", *J. Membr. Sci.*, **121**, 149-157.
- Jacobs, E. P., Botes, J. P., Burton, S. G., Edwards, W. and Saayman, H. M.*, (16-17 February 1996), "Novel capillary membranes for wastewater remediation or potable water production", *Oral presentation at: XIV National Symposium on Membranes in Chemical and Biochemical Industries, Indian Institute of Technology, Delhi, India*.
- Jacobs, E. P., Botes, J. P.*, Saayman, H. M., Bradshaw, S. M. and Sanderson, R. D., (20-23 May 1996), "Cross-flow ultrafiltration: A single-step approach to small and medium scale rural watercare", *Oral presentation at: the Water Institute of Southern Africa Biennial Conference and Exhibition, Port Elizabeth, South Africa*.
- Jacobs, E. P., Botes, J. P., Bradshaw, S. M. and Saayman, H. M.*, (18-23 August 1996), "Membrane filtration in potable water production", *Oral presentation at: the 1996 International Congress on Membranes and Membrane Processes, Yokohama, Japan*.
-

- Jacobs, E. P.*, Pillay, V. L., Bradshaw, S. M. and Botes, J. P., (12-24 November 1996), "New low-pressure UF membranes in aqueous applications", *Oral presentation at: the International Membrane Science and Technology Conference, University of Sydney, Sydney, Australia.*
- Jacobs, E. P. and Barnard, J. P., (January 1997), "Investigation to upgrade secondary treated sewage effluent by means of ultrafiltration and nanofiltration for municipal and industrial use", *WRC Report No. 584/1/97*, Final report to the Water Research Commission of Southern Africa, Pretoria, South Africa.
- Jacobs, E. P., Botes, J. P., Bradshaw, S. M. and Saayman, H. M., (1997), "Ultrafiltration in potable water production", *Water SA*, Vol. 23, No. 1, 1-6.
- Jacobs, E. P., Pillay, V. L.*, Botes, J. P., Swart, P., Maartens, A., Konig E. and Pryor, M., (4-7 May 1998), "Ultrafiltration - A process for quality potable water treatment?", *Oral presentation at: Water Institute of Southern Africa Biennial Conference and Exhibition, Cape Town, South Africa.*
- Jacobs, E. P.*, Pillay, V. L., Swart, P., Bradshaw, S. M., Maartens, A., Botes, J. P. and Pryor, M., (2 November 1998), "Ultrafiltration, a new but accepted technology for potable water production", *Oral presentation at: Chemical and Engineering R&D Conference '98, SAICE, Western Cape Branch, Stellenbosch, South Africa.*
- Jacobs, E. P.*, Pillay, V. L., Swart, P., Bradshaw, S. M., Maartens, A., Botes J. P. and Pryor, M., (12-18 June 1999), "UF, a new but acceptable technology for potable water", *Oral presentation at: International Congress on Membranes and Membrane Processes, ICOM'99, Toronto, Canada.*
- Jaffrin, M. Y., Gupta, B. B. and Paullier, P., (1994), "Energy saving pulsatile mode cross-flow filtration", *J. Membr. Sci.*, **86**, 281-290.
- Johnson, G. and Wenten, I. G., (1994), "Control of concentration polarization, fouling and protein transmission of microfiltration processes within the agro based industry", Presented at the *Workshop on Membrane Technology in Agro Based Industry*, Kuala Lumpur.
- Jucker, C. and Clark, M. M., (1994), "Adsorption of aquatic humic substances on hydrophobic ultrafiltration membranes", *J. Membr. Sci.*, **97**, 37-52.
- Kabadi, V. N., Doshi, M. R. and Gill, W. N., (1979), "Radial flow HFRO, Experiments and theory", *Chem. Eng. Sci.*, **3**, 39.
-

- Kempster, P. L. and Smith, R., (1985), "Proposed aesthetic/physical and inorganic drinking-water criteria for the republic of South Africa", *CSIR Research Report No. 628*, National Institute for Water Research, Pretoria, South Africa.
- Kempster, P. L., van Vliet, H. R. and Kühn, A., (1997), "The need for guidelines to bridge the gap between ideal drinking-water quality and that quality which is practically achievable and acceptable", *Water SA*, Vol. 23 No. 2, 163-167.
- Kesting, R. E., (1971), *Synthetic polymeric membranes*, McGraw-Hill, New York.
- Knight, C. A., (1975), *Chemistry of viruses*, 2nd Edition, Springer-Verlag, New York.
- Koros, W. J., (1995), "Membranes: learning a lesson from nature", *Chem. Eng. Progress*, **10**, 68-81.
- Koros, W. J., Ma, Y. A. and Shimidzu, T., (1996), "Terminology for membranes and membrane processes", © IUPAC, *Pure and Applied Chemistry*, **68**, 1479-1489.
- Kreyszig, E., (1988), *Advanced Engineering Mathematics*, 6th Edition, John Wiley & Sons Inc., New York.
- Lacey, R. E. and Loeb, S., (1972), *Industrial Processing with Membranes*, John Wiley & Sons Inc., New York.
- Leenheer, J. A., (1993), "Chemistry of dissolved organic matter in rivers, lakes and reservoirs", *American Chemical Society*, 196-221.
- Lloyd, D. R., (1985), "Materials science of synthetic membranes", in Sourirajan, S., and Matsuura, S. (Eds.), *American Chemical Society Symposium Series 269*, Washington, DC.
- Loeb, S. and Sourirajan, S., (1960), "Seawater demineralization by means of a semi-permeable membrane", *UCLA Water Resources Center Rep. WRCC-34*.
- Loeb, S. and Sourirajan, S., (1962), "Seawater demineralization by means of an osmotic membrane", *Advan. Chem. Ser.*, **38**, 117-132.
- Leung, W. F. and Probstein, R. F., (1979), "Low polarization in laminar ultrafiltration of macromolecular solutions", *Ind. Eng. Chem. Fundam.*, No. 3, Vol. 18, 274-278.
-

REFERENCES

- Maartens, A., Swart, P. and Jacobs, E. P, (1996), "Characterization techniques for organic foulants adsorbed onto flat-sheet UF membranes used in abattoir effluent", *J. Membr. Sci.*, **119**, 1-8.
- Maartens, A., Swart, P. and Jacobs, E. P, (1998), "Humic membrane foulants in natural brown water: characterization and removal", *Desalination*, **115**, 1-14.
- Matsumoto, K., Katsuyama, M. and Ohya, H., (1987), "Separation of yeast by cross-flow filtration with back-washing", *J. Ferment. Technol.*, **65** (1) 77.
- Matsumoto, K., Katsuyama, M. and Ohya, H., (1988), "Cross-flow filtration of yeast by microporous ceramic membrane with backflushing", *J. Ferment. Technol.*, **62** (2) 199.
- Mercier, M., Fonade, C. and Lafforgue-Delorme, C., (1997), "How slug flow can improve the ultrafiltration flux in mineral tubular membranes", *J. Membr. Sci.*, **128**, 103-113.
- Merry, A. J., (1996), "Membrane equipment and plant design", Chapter 3 in: *Industrial Membrane Separation Technology*, Scott, K. and Hughes, R. (Eds.), Chapman & Hall, London, U.K.
- Milicic, V. and Bersillon, J. L., (1986), "Anti-fouling techniques in cross-flow microfiltration", *Proc. 4th World Filtration Congress*, Vanbrabant, R., Hermia, J. and Weiler, R. A. (Eds.), Ostend, Belgium, Vol. 8, 19-24.
- Miller, R. W., (1989), *Flow Measurement Engineering Handbook*, 2nd Edition, McGraw-Hill, Inc., New York.
- Mulder, M., (1991), "Polarization phenomena and membrane fouling", Chapter 7 in: *Basic Principles of Membrane Technology*, Kluwer Academic Press,.
- Mulder, M., (1993), "Nature of membranes", in: *Membranes in bioprocessing: Theory and applications*, Howell, J. A., Sanchez, V. and Field, R. W. (Eds.), Chapman & Hall, London, U.K.
- Nikolov, N. D., Mavrov, V. and Nikolova, J. D., (1993), "Ultrafiltration in a tubular membrane under simultaneous action of pulsating pressures in permeate and feed solution", *J. Membr. Sci.*, **83**, 167-172.
-

REFERENCES

- Nyström, M. and Howell, J. A., (1993), "Flux enhancement", Chapter 7 in *Membranes in Bioprocessing: Theory and Applications*, Howell, J. A., Sanchez, V. and Field, R. W. (Eds.), Chapman & Hall, London, U.K.
- Nyström, M., Ruohomäki, K. and Kaipia, L., (1996), "Humic acid as a fouling agent in filtration", *Desalination*, **106**, 79-87.
- Pryor, M.*, Jacobs, E. P., Pillay, V. L., and Botes, J. P., (21-24 September 1998), "A low pressure ultrafiltration membrane separation system for potable water supply to developing communities in South Africa", *Oral presentation at: Membranes in Drinking and Industrial Water Production Conference, Amsterdam, The Netherlands*.
- Pryor, M., Jacobs, E. P., Pillay, V. L., and Botes, J. P., (1998), "A low pressure ultrafiltration membrane system for potable water supply to developing communities in South Africa", *Desalination*, **119**, 103-111.
- PTB, (1971), "Die dichte des wasser im internationalen einheitensystem und der internationalen praktischen temperaturskala von 1968", *PTB Mitt.*, Vol. 81, No. 6, 412-414.
- Rashid M. A., (1971), "Role of humic acids of marine origin and their different molecular weight fractions in complexing di- and trivalent metals", *Soil Science*, **111**, 298-306.
- Rautenbach, R. and Albrecht, R., (1989), *Membrane Processes*, John Wiley & Sons Inc., New York.
- Redkar, S. G. and Davis, R. H., (1993), "Cross-flow microfiltration of yeast suspensions in tubular filters", *Biotechnol. Prog.*, **9**, 625.
- Redkar, S. G. and Davis, R. H., (1995), "Cross-flow microfiltration with high-frequency reverse filtration", *AIChE J.*, **41**, 501-508.
- Redkar, S. G., Kuberkar, V. and Davis, R. H., (1996), "Modeling of concentration polarization and depolarization with high-frequency backpulsing", *J. Membr. Sci.*, **121**, 229-242.
- Reid, R. C., Prausnitz, J. M. and Poling, B. E. (Eds.), (1977), *The properties of gases and liquids*, 3rd Edition, McGraw Hill, New York.
- Rosa, M. J. and de Pinho, M. N., (1997), "Membrane surface characterization by contact angle measurements using the immersed method", *J. Membr. Sci.*, **131**, 167-180.
-

REFERENCES

- Rodgers, V. G. J. and Sparks, R. E., (1991), "Reduction of protein fouling in protein ultrafiltration", *AIChE J.*, **37**, 1517-1528.
- Rodgers, V. G. J. and Sparks, R. E., (1992), "Effect of transmembrane pressure pulsing on concentration polarization", *J. Membr. Sci.*, **68**, 149.
- Rodgers, V. G. J. and Sparks, R. E., (1993), "Effect of solution properties on polarization redevelopment and flux in pressure pulsed ultrafiltration", *J. Membr. Sci.*, **78**, 163-180.
- Rodgers, V. G. J. and Miller, K. D., (1993), "Analysis of steric hindrance reduction in pulsed ultrafiltration", *J. Membr. Sci.*, **85**, 39-58.
- Scott, K. and Hughes, R., (1996), "Introduction to industrial membrane processes", Chapter 1 in: *Industrial Membrane Separation Technology*, Scott, K. and Hughes, R. (Eds.), Chapman & Hall, London, U.K.
- South African Bureau of Standards, (SABS, 1999), *Specification for water for domestic supplies*, South African Standard SABS 241-1999, Pretoria.
- South African Pump Manufacturers Association, (SAPMA, 1996), *Pumps: Principle and Practise*, 3rd Edition, Published by Myles, K, and Associates cc, Northcliff, Republic of South Africa.
- Spiazzi, E., Lenoir, J. and Grangeon, A., (1993), "A new generator of unsteady-state flow regime in tubular membranes as an anti-fouling technique: a hydrodynamic approach", *J. Membr. Sci.*, **80**, 49-57.
- Stairmand, J. W. and Bellhouse, B. J., (1985), "Mass transfer in a pulsating turbulent flow with deposition onto furrowed walls", *Int. J. Heat Mass Transfer*, **27**, 1405-1408.
- Stefanova, M., Velinova, D., Marinov, S. P. and Nikolova, R., (1993), "The composition of lignite humic acids", *Fuel*, Vol. 72, No. 5, 681-684.
- Strohwald, N. K. H. and Jacobs, E. P., (1992), "An investigation into UF systems in the pre-treatment of seawater for RO desalination", *Wat. Sci. Tech.*, Vol. 25, No. 10, 69-78.
- Swart, P., Maartens, A., Allie, Z., Engelbrecht, J. and Jacobs, E. P., (1999), "The development and implementation of biological cleaning techniques for ultrafiltration and reverse osmosis membranes fouled by organic substances", *WRC Report No. 660/1/99*, Final report to the Water Research Commission of Southern Africa, Pretoria, South Africa.
-

REFERENCES

- Tate, C. H. and Arnold, C. F., (1990), "Health and aesthetic aspects of water quality", Chapter 2 in: *A handbook of community water supplies (AWWA)*, Pontius, F. W. (Ed.), 4th Edition, McGraw-Hill, New York.
- Tchnobanoglous, G. and Schroeder, E. D., (1985), *Water quality – Characteristics, modelling, modification*, Addison-Wesley, Reading, Massachusetts.
- Toyomoto, K. and Higuchi, (1992) "Microfiltration and Ultrafiltration", Chapter 8 in: *Membrane Science and Technology*, Osada, Y. and Nakagawa, T. (Eds.), Marcell Dekker Inc., New York.
- Wankat, P. C., (1994), *Rate-controlled separations*, Chapman & Hall, London, U.K.
- Water Research Commission, (1993), "Flow arrangements", by: Jacobs, E. P., Domröse, S. E. and Sanderson, R. D., *South African Patent No. 93/0309*.
- Water Research Commission, (1996a), "Capillary membrane module potting and encapsulation method", by: Domröse, S. E., Jacobs, E. P., Koen, D. J. and Sanderson, R. D., *South African Patent No. 96/1580*.
- Water Research Commission, (1996b), "Method of making hollow fibre membranes", by: Jacobs, E. P. and Sanderson, R. D., *South African Patent No. 96/7520*.
- Water Research Commission, (1999), "Reverse-pressure pulse generator", by: Jacobs, E. P., Botes, J. P., Koen, D. J. and Pillay, V. L., *South African Patent No. 99/4620*.
- Wetterau, G. E., Clark, M. M. and Anselme, C., (1996), "A dynamic model for predicting fouling effects during the ultrafiltration of a ground water", *J. Membr. Sci.*, **109**, 185-204.
- White, F. M., (1994), *Fluid mechanics*, 3rd Ed., McGraw-Hill Inc., New York.
- World Health Organization, (WHO, 1984), *Guidelines for drinking-water quality Vol. 2: Health criteria and other supporting information*, World Health Organization, Geneva.
- World Health Organization, (WHO, 1993), *Guidelines for drinking-water quality Vol. 1: Recommendations*, 2nd Edition, World Health Organization, Geneva.
- Xu, Y., Dodds, J. and Leclerc, D., (1995), "Optimization of a discontinuous microfiltration backwash process", *Chem. Eng. J.*, **57**, 247.
-

Appendix A: INDICATOR ORGANISMS

A.1 Heterotrophic Bacteria

Heterotrophic bacteria are *naturally occurring organisms* that are used to indicate the general microbial quality of water. Bacteria are single-cell organisms, but may exist in four basic morphological forms, namely *spirilla* (spirals), *bacilli* (rods), *vibrios* (curved-rods) and *cocci* (spheroids) [Bailey and Ollis, 1990]. Bacteria range in size from 0.15 to 4 μm [Doetsch and Cook, 1973]. Analysis for heterotrophic bacteria does not indicate the total number of bacteria present or possible faecal pollution, but only those bacteria able to grow under the specific conditions (incubation at 35 °C for 48 hours) of the test. Heterotrophic plate counts are reported as counts (number of colonies/ml) and high plate counts in treated water are indicative of inadequate treatment, post-treatment contamination or bacterial aftergrowth in the distribution system.

A.2 Total Coliform Bacteria

Total coliform bacterial counts are used to assess the general hygienic quality of water, to evaluate the efficiency of potable water treatment and the integrity of the distribution system. Total coliform bacteria includes all bacteria which produce colonies with a typical metallic sheen after incubation for 24 h at 35 °C on m-Endo agar, including bacteria of faecal origin from the genera *Escherichia*, *Citrobacter*, *Enterobacter*, *Klebsiella*, *Serratia* and *Rahnella*. Examples of such bacterial pathogens are *Salmonella spp.*, *Shigella spp.*, *Vibrio cholerae*, *Camphylobacter jejuni*, *C. coli*, *Yersinia enterocolitica* and pathogenic *E. coli*. Diseases caused by these organisms include gastroenteritis, salmonellosis, dysentery, cholera and typhoid fever.

A.3 Faecal Coliform Bacteria

Indicator organisms in the faecal coliform bacteria group are used to evaluate the quality of waste water effluents, river water, sea water at bathing beaches, raw water for drinking supplies, treated drinking water and water used for recreation, irrigation and aquaculture. *Escherichia coli* (*E. coli*) usually comprises about 97 % of coliform bacteria in human faeces, and are thus the most commonly used indicator of faecal pollution by humans. Faecal coliform bacteria are all bacteria that produce typical blue colonies after incubation for 24 h at 44.5 °C, while *E. coli* are considered to be all faecal coliforms which test indole-positive at 44.5 °C.

A.4 Coliphages

Coliphages are *bacterial viruses* that infect and replicate in *E. coli* and may infect related coliform bacteria. Two broad groups are identified, namely somatic coliphages and male-specific coliphages. Coliphage counts are usually reported as counts per 10 mL and are detected in water by their ability to form visible plaques in a plaque assessing an *E. coli* host under incubation conditions of 16 h at 35 °C.

A.5 Enteric Viruses

Viruses are *sub-microscopic inert particles* of protein and nucleic acid that are unable to replicate or adapt to environmental conditions outside a living host. Enteric viruses are usually transmitted by the *faecal-oral route* (such as faecally-contaminated water or food) and include enteroviruses (polio, coxsackie A and B and echo viruses), enteric adenoviruses, reoviruses, rotaviruses, hepatitis A and E viruses, calciviruses (Norwalk virus) and astroviruses. Although the size and shape of viruses vary considerably, viruses as a group range in size from about 10 to 300 nm [Knight, 1975]. Health effects include paralysis, meningitis, hepatitis, respiratory illness and diarrhoea. Although free-chlorine concentrations of 0.5 mg/L will inactivate viruses, it is still difficult to monitor viral presence [Brock and Brock, 1978].

A.6 Protozoan Parasites

Giardia and *Cryptosporidium* are protozoan parasites with several lifecycle stages, of which the cysts (*Giardia lamblia*) or oocysts (*Cryptosporidium parvum* and *Entamoeba histolytica*) are extremely infective to humans. Diseases associated with ingestion of the cysts or oocysts include gastroenteritis, diarrhoea, and vomiting. Chlorination also has a minimal effect on their activity.

Appendix B: HEAD VS. CAPACITY PUMP CURVES

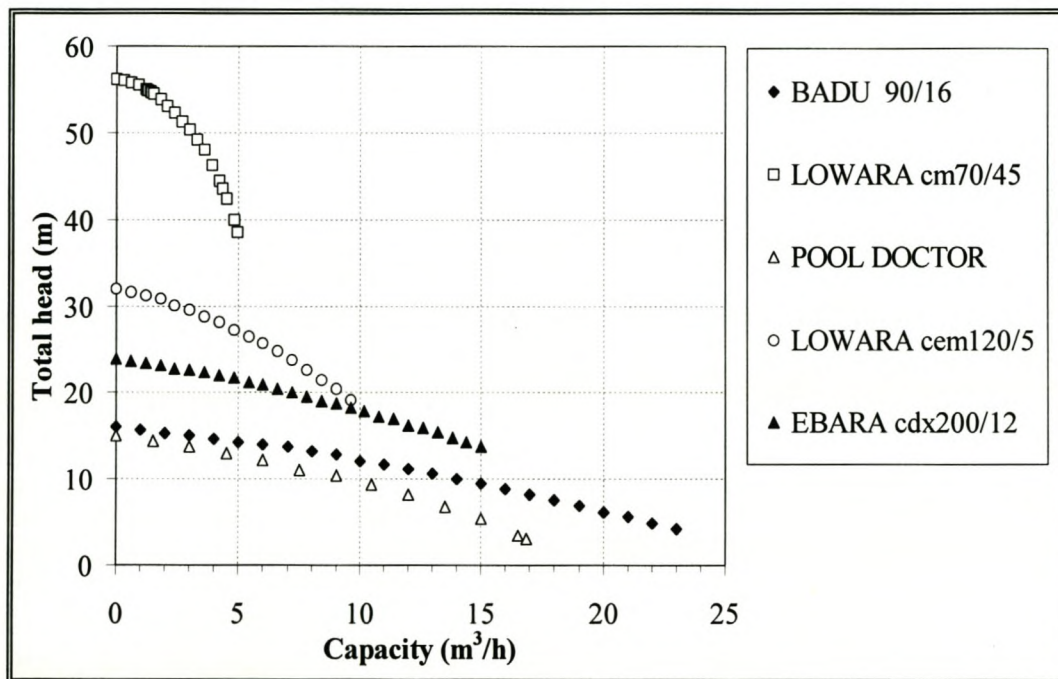


Figure 47: Characteristic curves of total head vs. capacity for the centrifugal pumps used during the course of this investigation.

Appendix C: ADDITIONAL RESULTS FROM CASE STUDY 1

C.1 Design Considerations

The system was designed to supply 10 m³/d potable water for domestic use to the Mon Villa Seminar Centre. The only other supply of potable water on the farm was a bore hole, but during the summer months the water table dropped considerably, water shortages were frequent and the quality of this water supply decreased severely. It was therefore essential that the UF system should be able to produce a steady supply of potable water for the centre. In this regard, the system was a complete success. Figure 48 shows that the daily production rates at Mon Villa exceeded 10 m³/d, which during most of the operation satisfied the desired design capacity.

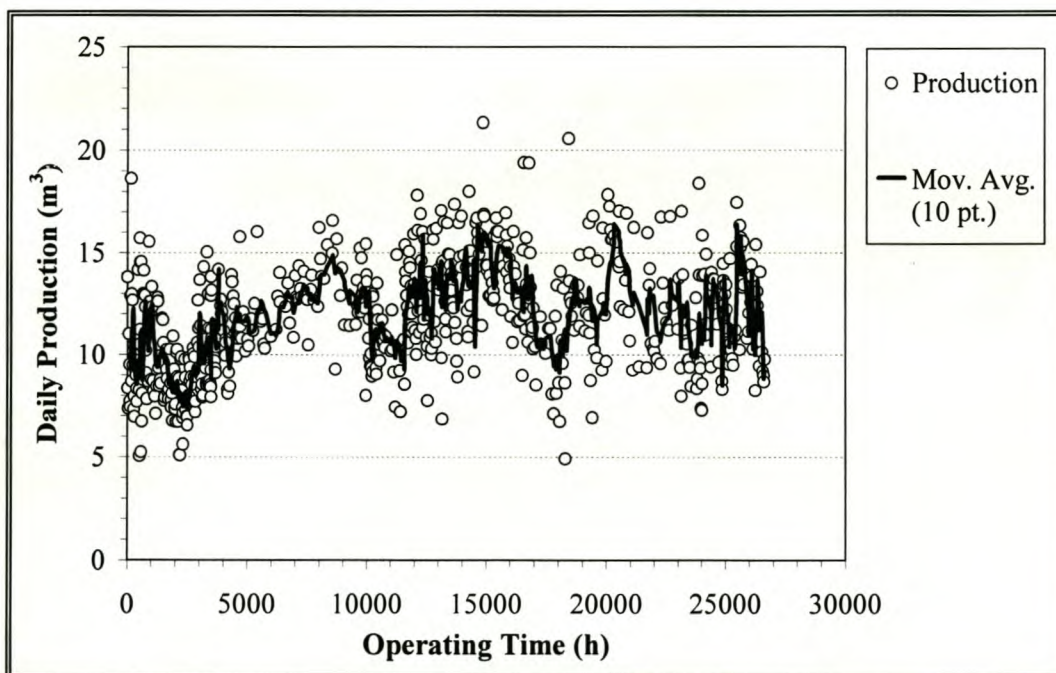


Figure 48: Daily production at Mon Villa.

C.2 Temperature Correction

In Figure 49 the seasonal variation in the operating temperature is plotted versus system operating time for the entire 27 000 h investigation period.

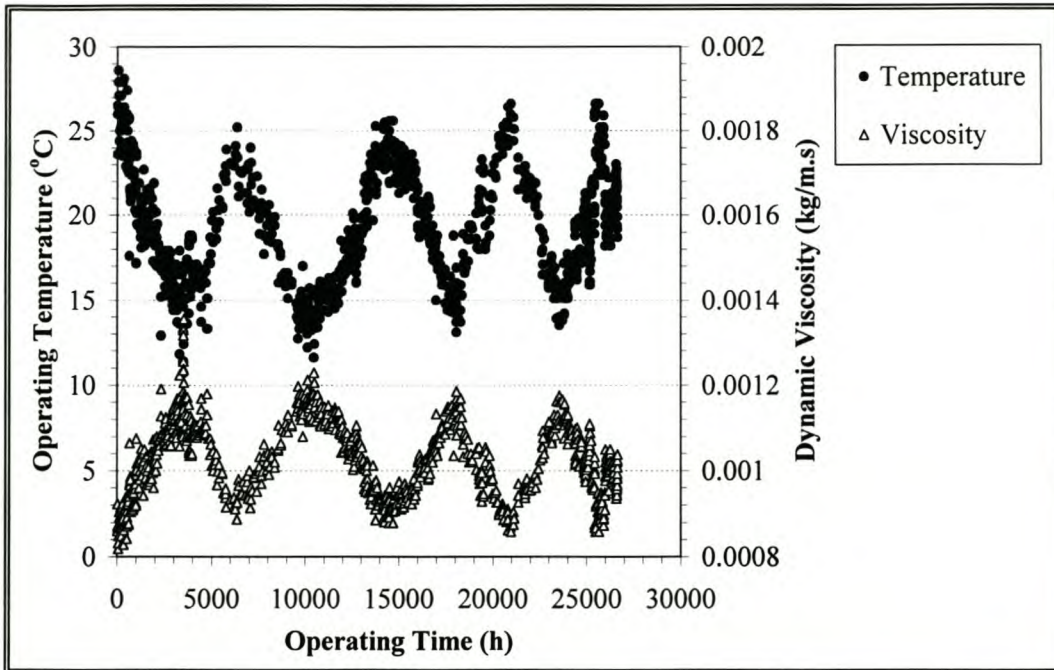


Figure 49: Operating temperature and viscosity at Mon Villa.

The secondary y-axis shows that an increase of 10 °C from minimum (*ca* 15 °C) to maximum (*ca* 25 °C), decreased the calculated pure-water viscosity by about 30 %. The viscosity was calculated from eq. (2.38). As the system was operated continuously without heat exchange, the measured process flux was corrected to an (averaged) standard temperature of 20 °C. It was, however, not possible to account for pressure and concentration dependent viscosity changes in the boundary layer.

C.3 Microbial Indicators

A number of analyses were also conducted to determine the level of microbiological contamination in the feed, and to evaluate the reduction efficiency of the membranes. In Table 23 the results of a typical grab sample are listed, near the end of a filtration run when the concentrate was recycled to the feed tank. The samples were taken on-site by the author on 27 September 1995 and analysed the same day by the CSIR, Stellenbosch. The SABS 241 (1984, 1999) guidelines are included for comparison. Although no *E. Coli* bacteria were present in the samples, it is evident that the fresh irrigation feed water did not comply with the SABS

guidelines for potable water. Although the plate count of the raw and recycled feed had reached excessive levels at the time of sampling, the heterotrophic plate count of the permeate before chlorination was significantly reduced. The membranes were also able to remove all the faecal and other coliform bacteria present in the feed water.

Table 23: Grab samples of microbial indicators

Potable Water Standard	SABS-241 (1984)	Source	Recycled Feed	Permeate before Chlorination
Total Coliforms per 100 mL	0	96	70	0
Faecal Coliforms per 100 mL	0	10	40	0
Plate Count per 1 mL	100	188	34 500	44
E. Coli per 100 mL	0	0	0	0

C.4 Colour Reduction

A portable HACH DR2000 spectrophotometer was acquired to determine the colour of water samples in Hazen ($^{\circ}\text{H}$). Figure 50 shows the apparent (unfiltered) colour reduction over the latter period of the investigation. Although values of between 100 and 350 $^{\circ}\text{H}$ were recorded for the total feed, the colour of the permeate was reduced to 8-20 $^{\circ}\text{H}$. This translated to a reduction of 92 to 97 %.

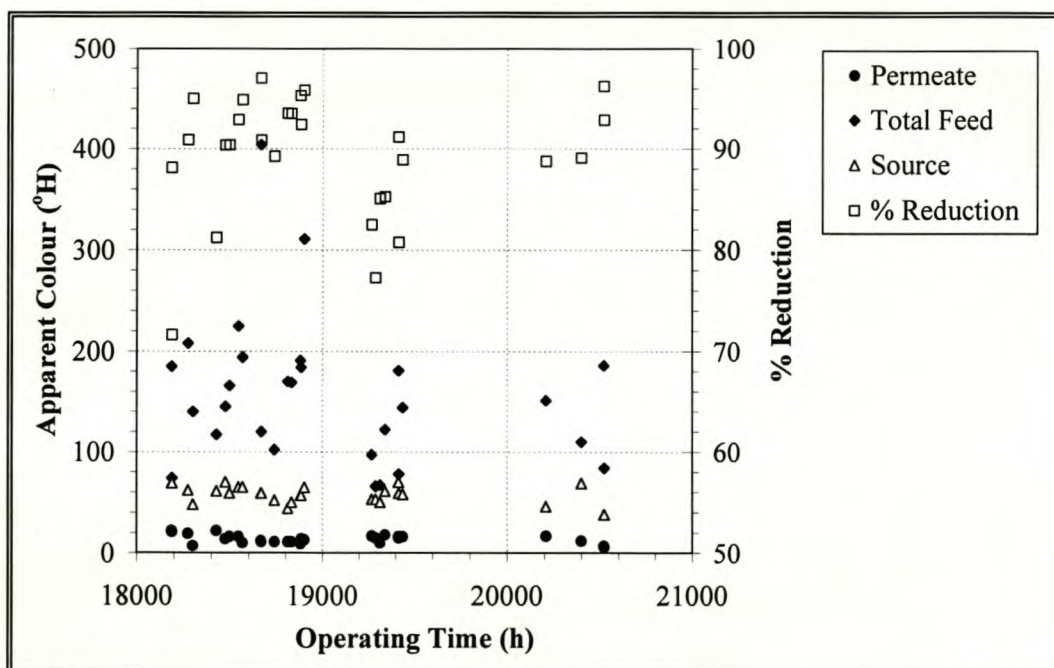


Figure 50: Apparent colour reduction at Mon Villa.

C.5 Iron and NOM Reduction

Low concentrations of iron (*ca* 0.3 mg/L) were also present in the fresh feed water, as indicated in Figure 51. Because the system was operated with concentrate being recycled to the feed tank and the process, the result was that the iron concentration in the total feed could increase steadily as high as 2.5 mg/L. Nevertheless, the filtration process was still able to reduce the iron content to less than 0.02 mg/L, resulting in a 97 to 99 % removal of the total iron content in the feed.

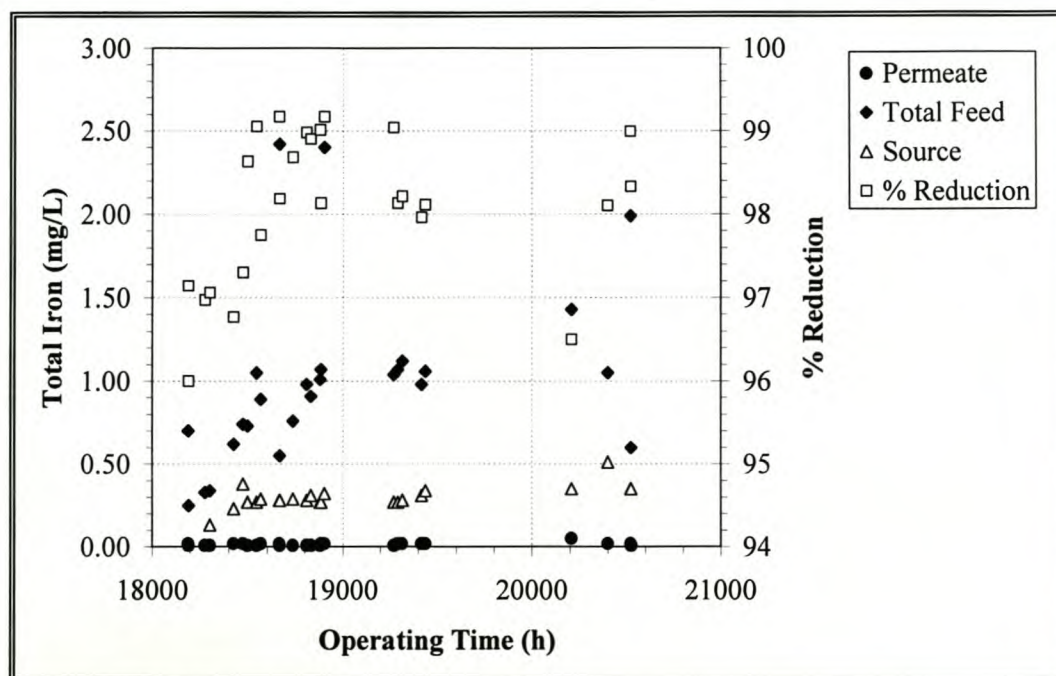


Figure 51: Iron reduction at Mon Villa.

The iron was in the ferrous (Fe^{2+}) or ferric (Fe^{3+}) ionic states, which are known to form water-insoluble complexes with NOM present in aquatic environments. NOM is also known to adsorb more divalent than trivalent metal ions [Rashid, 1972].

These metal-organic complexes are adsorbed onto PSf membranes, both on the surface and in the pores, and may cause irreversible flux loss as a result of pore plugging if not removed regularly with complexing agents. Throughout the investigation period, the productivity of the membranes could be regenerated to an acceptable value only if a complexing agent such as EDTA was included in the CIP solution.

Maartens [Swart *et al.*, 1999] recently developed a simple method to characterize NOM present in some aquatic systems in the Southern Cape, South Africa. The method consisted of freeze drying an amount of raw water, making up a stock solution of 90 mg/L NOM and adjusting the

pH to 8.0 to ensure total solubility of the NOM. The stock solution was then diluted to a range of concentrations and the absorbency of each solution measured at 254 nm in a UV-VIS spectrophotometer.

A calibration curve (Figure 52) constructed through the origin with concentration (mg/L) on the y -axis and absorbency on the x -axis yielded the slope of the plot as a constant, which could then be used to calculate the NOM concentration from absorbency for subsequent samples.

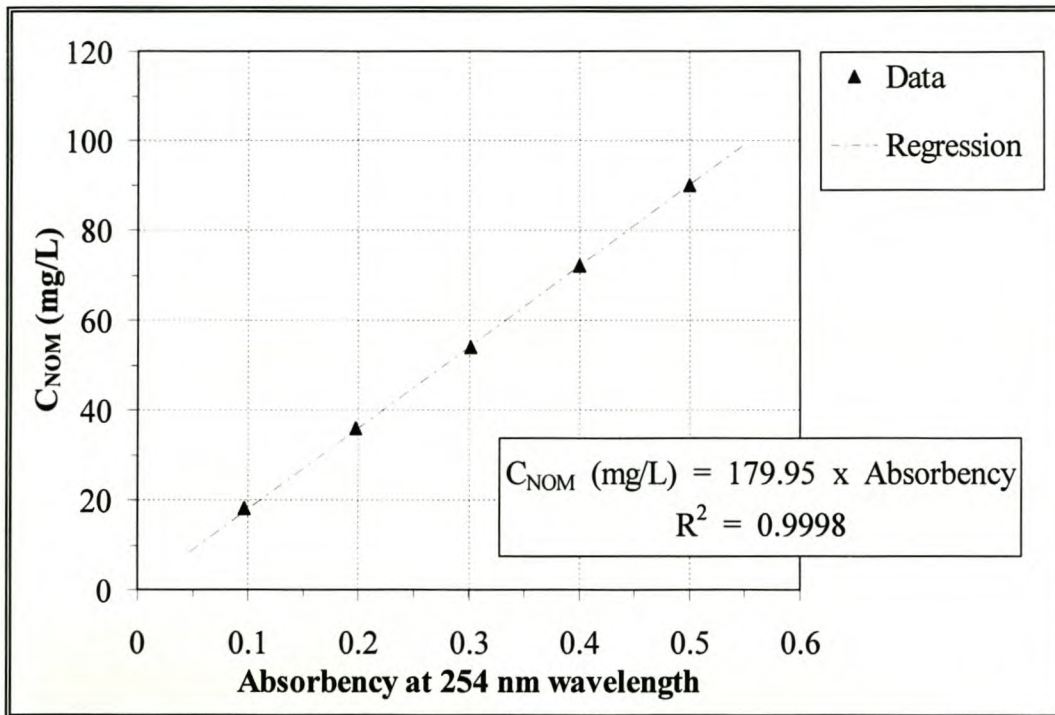


Figure 52: Calibration curve for the Theewaterskloof NOM.

Figure 53 shows the removal of NOM from the Mon Villa combined feed during one typical filtration run. The concentrate was returned to the feed tank. During the last two days of the run, the quality of the fresh feed water deteriorated significantly and NOM concentrations greater than 40 mg/L were recorded. The NOM concentration in the recycled feed stream increased to above 110 mg/L.

Despite this, the NOM concentration in the permeate remained below 20 mg/L. It was also evident that as the concentration in the feed tank increased steadily, the reduction increased from 60 % to 85 %. This could be ascribed to the fact that the fouling layer was acting as a filter aid.

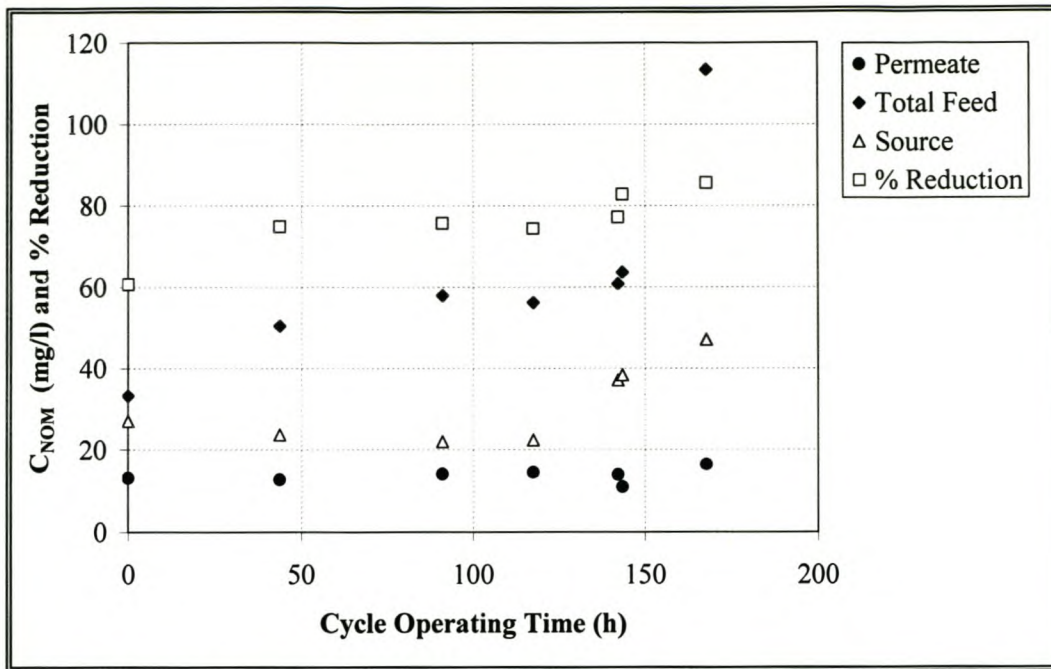


Figure 53: NOM reduction at Mon Villa.

C.6 Analysis of Variance Tables for B/F Experiments

Table 24: Summary of statistics for individual and combined experiments

Groups	Count	Sum	Average (%)	Variance (%) ²
A1	13	139	10.69	12.86
A2	13	56.4	4.34	6.52
A1 + A2	13	195.4	15.03	32.20
B1	8	25.3	3.16	2.90
B2	8	56.3	7.04	4.40
B1 + B2	8	81.6	10.2	12.84

Table 25: ANOVA Table for Experiments A1 and B1

Source of Variation	SS	df	MS	F _{calc}	P-value (%)	F _{crit,0.05}
Between Groups	280.7901	1	280.79011	30.55773	0.0025	4.3808
Within Groups	174.588	19	9.1888411			
Total	455.3781	20				

From Table 25 $F_{\text{calc}} > F_{\text{crit},0.05}$, thus the null hypothesis H_0 is rejected at the 0.05 significance level, and it can be concluded that there is a significant difference between experiments A1 and B1. The P-value indicates a 0.0025 % probability of a *type-1 error*, i.e. rejecting a true H_0 .

Table 26: ANOVA Table for Experiments A1 and B2

Source of Variation	SS	df	MS	F_{calc}	P-value (%)	$F_{\text{crit},0.05}$
Between Groups	66.15202	1	66.152019	6.790762	1.737	4.3808
Within Groups	185.088	19	9.7414727			
Total	251.24	20				

From Table 26 $F_{\text{calc}} > F_{\text{crit},0.05}$, thus the null hypothesis H_0 is rejected at the 0.05 significance level, and it can be concluded that there is a significant difference between experiments A1 and B2. The P-value indicates a 1.7 % probability of a *type-1 error*, i.e. rejecting a true H_0 .

Table 27: ANOVA Table for Experiments A1 and A2

Source of Variation	SS	df	MS	F_{calc}	P-value (%)	$F_{\text{crit},0.05}$
Between Groups	262.4138	1	262.41385	27.08788	0.0025	4.2597
Within Groups	232.5	24	9.6875			
Total	494.9138	25				

From Table 27 $F_{\text{calc}} > F_{\text{crit},0.05}$, thus the null hypothesis H_0 is rejected at the 0.05 significance level, and it can be concluded that there is a significant difference between experiments A1 and A2. The P-value indicates a 0.0025 % probability of a *type-1 error*, i.e. rejecting a true H_0 .

Table 28: ANOVA Table for Experiments B1 and B2

Source of Variation	SS	df	MS	F_{calc}	P-value (%)	$F_{\text{crit},0.05}$
Between Groups	60.0625	1	60.0625	16.45628	0.118	4.6001
Within Groups	51.0975	14	3.6498214			
Total	111.16	15				

From Table 28 $F_{\text{calc}} > F_{\text{crit},0.05}$, thus the null hypothesis H_0 is rejected at the 0.05 significance level, and it can be concluded that there is a significant difference between experiments B1 and B2. The P-value indicates a 0.1 % probability of a *type-1 error*, i.e. rejecting a true H_0 .

Table 29: ANOVA Table for Experiments A2 and B1

Source of Variation	SS	df	MS	F_{calc}	P-value (%)	$F_{\text{crit},0.05}$
Between Groups	6.848576	1	6.848576	1.320917	26.469	4.3808
Within Groups	98.50952	19	5.1847115			
Total	105.3581	20				

From Table 29 $F_{\text{calc}} < F_{\text{crit},0.05}$, thus the null hypothesis H_0 is true at the 0.05 significance level, and it can be concluded that there is *not* a significant difference between experiments A2 and B1. The P-value indicates a 26.5 % probability of a *type-1 error*, i.e. rejecting a true H_0 .

Table 30: ANOVA Table for Experiments A2 and B2

Source of Variation	SS	df	MS	F_{calc}	P-value (%)	$F_{\text{crit},0.05}$
Between Groups	36.07715	1	36.077147	6.288128	2.139	4.3808
Within Groups	109.0095	19	5.7373431			
Total	145.0867	20				

From Table 30 $F_{\text{calc}} > F_{\text{crit},0.05}$, thus the null hypothesis H_0 is rejected at the 0.05 significance level, and it can be concluded that there is a significant difference between experiments A2 and B2. The P-value indicates a 2.1 % probability of a *type-1 error*, i.e. rejecting a true H_0 .

Table 31: ANOVA Table for combined Experiments (A1+A2) and (B1+B2)

Source of Variation	SS	df	MS	F_{calc}	P-value (%)	$F_{\text{crit},0.05}$
Between Groups	115.5704	1	115.5704	4.610124	4.490	4.3808
Within Groups	476.3077	19	25.068826			
Total	591.8781	20				

From Table 31 $F_{\text{calc}} > F_{\text{crit},0.05}$, thus the null hypothesis H_0 is rejected at the 0.05 significance level, and it can be concluded that there is a significant difference between experiments A2 and B2. The P-value indicates a 4.5 % probability of a *type-1 error*, i.e. rejecting a true H_0 .

Appendix D: ADDITIONAL RESULTS FROM CASE STUDY 2

D.1 Marker Outputs and Durations for Experiments 1 to 14

Table 32: Outputs activated by markers (M) and duration (Δt) of R/P events for Experiments 1 to 4

Outputs	M 1	M 2	M 3	M 4	M 5	M 6
Recycle pump	S	S	S	S	R	R
ProdV	R	R	S	S	R	S
UpflowV1		R	S	R	R	R
Feed pump		R	R	R	S	S
Prodfwd Pump		R	R	R	R	R
ConcV2		S	R	S	S	R
Experiment	Δt (s)	Δt (s)	Δt (s)	Δt (s)	Δt (s)	Δt (s)
1	2	5	30	2	2	300
2	1	5	35	2	1	300
3	1	5	35	2	1	300
4	5	8	35	5	2	300

Table 33: Outputs activated by markers (M) and duration (Δt) of R/P events for Experiments 5 to 9

Outputs	M 1	M 2	M 3	M 4	M 5	M 6
Recycle pump	R	S	S	S	R	R
ProdV	R	R	S	S	R	S
UpflowV1		R	S	R	R	R
Feed pump		R	R	R	S	S
Prodfwd Pump		R	R	R	R	R
ConcV2	S	S	R	S	S	R
Experiment	Δt (s)	Δt (s)	Δt (s)	Δt (s)	Δt (s)	Δt (s)
5	5	8	35	5	2	900
6	3	10	35	5	2	600
7	3	10	35	5	2	600
8	3	10	35	5	2	600
9	3	10	35	5	2	600

Table 34: Outputs activated by markers (M) and duration (Δt) of R/P events for Experiments 10 to 11

Outputs	M 1	M 2	M 3	M 4	M 5	M 6	M 7	M 8
Recycle pump	R	R	S	S	S	R	S	R
ProdV	R	R	R	R	S	R	R	S
UpflowV1	R	R	R	S	S	R	R	R
Feed pump	S	R	R	R	R	R	S	S
Prodfwd Pump	R	R	R	R	R	R	R	R
ConcV2	S	S	R	R	R	S	S	R
Experiment	Δt (s)	Δt (s)	Δt (s)	Δt (s)	Δt (s)	Δt (s)	Δt (s)	Δt (s)
10	8	5	2	10	20	2	2	900
11	8	5	2	10	20	2	2	600

Table 35: Outputs activated by markers (M) and duration (Δt) of R/P events for Experiment 12

Outputs	M 1	M 2	M 3	M 4	M 5	M 6	M 7	M 8
Recycle pump	R	R	S	S	S	S	S	R
ProdV	R	R	R	R	S	R	R	S
UpflowV1	R	R	R	S	S	R	R	R
Feed pump	S	R	R	R	R	S	S	S
Prodfwd Pump	R	R	R	R	R	R	R	R
ConcV2	S	S	R	R	R	S	S	R
Experiment	Δt (s)	Δt (s)	Δt (s)	Δt (s)	Δt (s)	Δt (s)	Δt (s)	Δt (s)
12	8	8	1	6	29	1	2	600

Table 36: Outputs activated by markers (M) and duration (Δt) of R/P events for Experiments 13 to 16

Outputs	M 1	M 2	M 3	M 4	M 5	M 6	M 7	M 8
Recycle pump	S	S	S	S	S	S	S	R
ProdV	R	S	R	S	R	S	R	S
UpflowV1	R	S	R	S	S	S	R	R
Feed pump	R	R	R	R	R	R	R	S
Prodfwd Pump	R	R	R	R	R	R	R	R
ConcV1	S	R	S	R	R	R	S	S
ConcV2	R	R	R	R	R	R	R	R
Experiment	Δt (s)	Δt (s)	Δt (s)	Δt (s)	Δt (s)	Δt (s)	Δt (s)	Δt (s)
13 to 16	2	15	2	15	2	15	2	600

During experiments 13 to 16 the R/P cycle was looped inside a 12 000 s filter cycle, followed by a 120 s backflush. For experiment 13 the B/F was in the downward direction, while for the remainder the B/F was in the upward direction.

D.2 Additional dP and Flux Responses

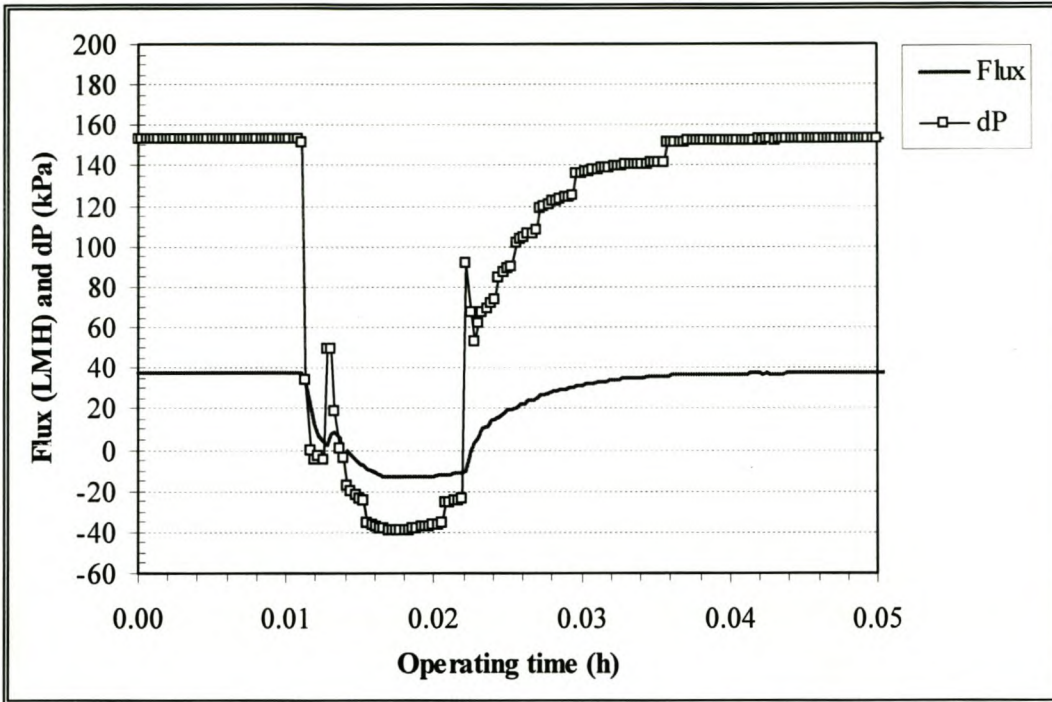


Figure 54: R/P flux and dP response for experiment 2.

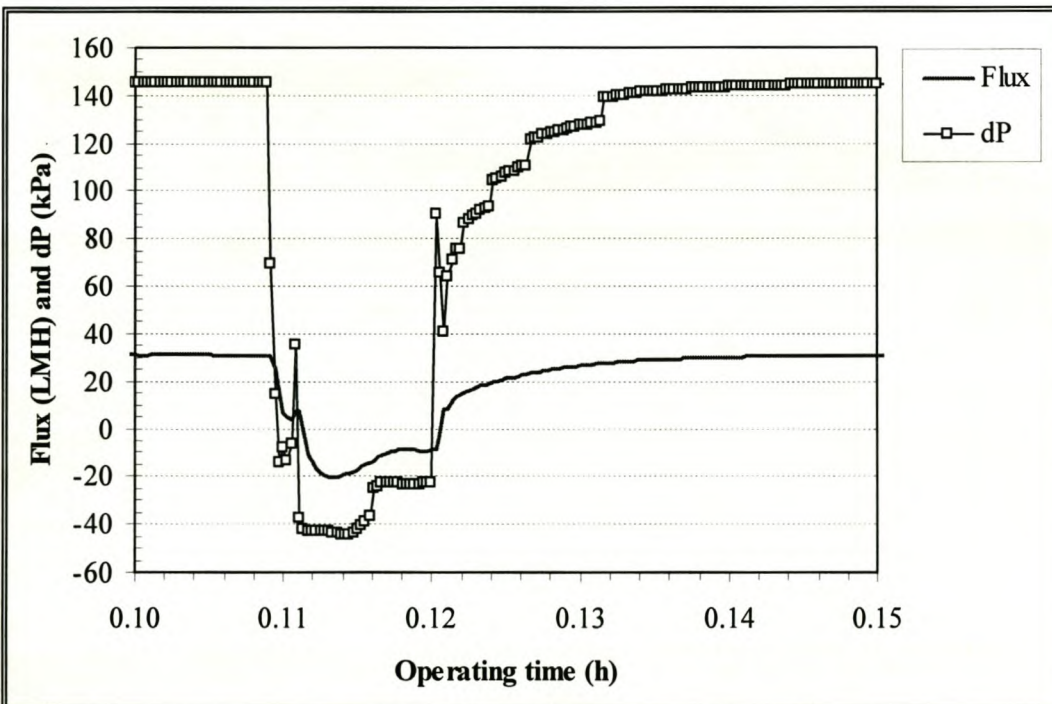


Figure 55: R/P flux and dP response for experiment 3.

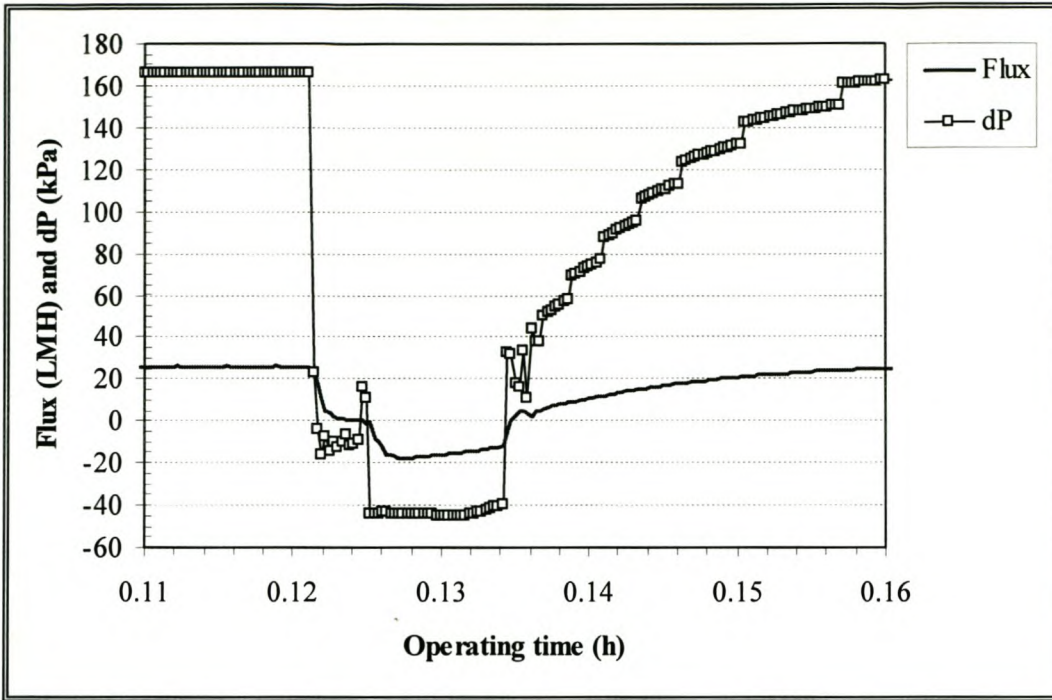


Figure 56: R/P flux and *dP* response for experiment 5.

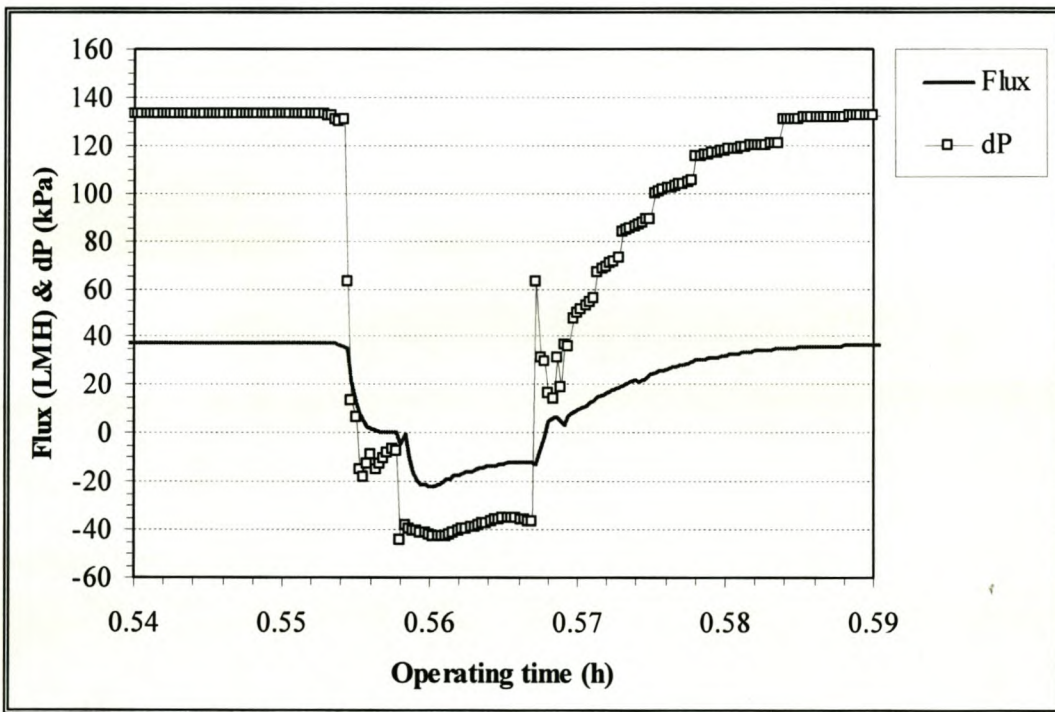


Figure 57: R/P flux and *dP* response for experiment 8.